




12-2021

## **ANALYTICAL CONSIDERATIONS AND METHODS FOR COMPREHENSIVE ANALYSIS OF BACTERIAL PHOSPHOLIPIDOMICS USING HILIC-MS/MS**

David Thomas Reeves  
dreeves4@vols.utk.edu

Follow this and additional works at: [https://trace.tennessee.edu/utk\\_graddiss](https://trace.tennessee.edu/utk_graddiss)

 Part of the [Analytical Chemistry Commons](#), [Bioinformatics Commons](#), [Structural Biology Commons](#),  
and the [Systems Biology Commons](#)

---

### **Recommended Citation**

Reeves, David Thomas, "ANALYTICAL CONSIDERATIONS AND METHODS FOR COMPREHENSIVE ANALYSIS OF BACTERIAL PHOSPHOLIPIDOMICS USING HILIC-MS/MS. " PhD diss., University of Tennessee, 2021.  
[https://trace.tennessee.edu/utk\\_graddiss/7008](https://trace.tennessee.edu/utk_graddiss/7008)

This Dissertation is brought to you for free and open access by the Graduate School at TRACE: Tennessee Research and Creative Exchange. It has been accepted for inclusion in Doctoral Dissertations by an authorized administrator of TRACE: Tennessee Research and Creative Exchange. For more information, please contact [trace@utk.edu](mailto:trace@utk.edu).

To the Graduate Council:

I am submitting herewith a dissertation written by David Thomas Reeves entitled "ANALYTICAL CONSIDERATIONS AND METHODS FOR COMPREHENSIVE ANALYSIS OF BACTERIAL PHOSPHOLIPIDOMICS USING HILIC-MS/MS." I have examined the final electronic copy of this dissertation for form and content and recommend that it be accepted in partial fulfillment of the requirements for the degree of Doctor of Philosophy, with a major in Energy Science and Engineering.

Robert L. Hettich, Major Professor

We have read this dissertation and recommend its acceptance:

Francisco Barrera, James G. Elkins, Todd Reynolds, Timothy J. Tschaplinski

Accepted for the Council:

Dixie L. Thompson

Vice Provost and Dean of the Graduate School

(Original signatures are on file with official student records.)

**ANALYTICAL CONSIDERATIONS AND METHODOLOGICAL  
DEVELOPMENT FOR COMPREHENSIVE CHARACTERIZATION  
OF BACTERIAL CELL MEMBRANE MODIFICATION IN  
RESPONSE TO SOLVENT STRESS**

**A Dissertation Presented for the  
Doctor of Philosophy  
Degree  
The University of Tennessee, Knoxville**

**David Thomas Reeves  
December 2021**

Copyright © 2021 by David Thomas Reeves  
All rights reserved.

## ACKNOWLEDGEMENTS

Firstly, I would like to thank my advisor, Dr. Robert Hettich, for being willing to take me under your wing and give me a chance to transition into a field I have always been interested in. Ever since college and my first real exploration into science, I have had troubles finding ways to properly engage in research, and working in your laboratory was the first time I really felt like I had a solid support system with which to properly grow as a researcher. Despite a lot of growing pains, I truly feel like I have advanced so much as a scientist under five-plus years under your tutelage, and I cannot express my gratitude enough for that.

A sincere thank you to my committee, Drs. Francisco Barrera, Jim Elkins, Todd Reynolds, and Tim Tschaplinski, for their willingness to assist me in my PhD journey and provide constructive feedback on both my dissertation as well as experimental design. I know that participating on a PhD committee can sometimes be a significant time drain, especially with the added challenges of a pandemic on top of it, and I appreciate that you were willing to sacrifice your time to support me and help me get to the finish line.

I never knew that a program with as many ties and interdisciplinary opportunities could realistically exist within a university system, but the unique relationship between the University of Tennessee and Oak Ridge National Laboratory has enabled all manner of collaborative work, and as such, I have an immense amount of gratitude towards Dr. Lee Riedinger and everyone (past and present) who is a part of the Bredesen Center for

championing such an innovative program. I sincerely hope that the program continues to evolve and flourish with more brilliant young scientists moving forward.

To everyone I've met during this PhD, either as a part of the Bredesen Center or as a fellow member of the Hettich lab, you will never know how much just being around was a blessing in disguise. Your presence, either as a mentor, associate, or just a friend, was invaluable to me, and for that I am grateful. I want to give a special thanks to the various collaborators that I worked alongside throughout my dissertation – Kyle Bonifer, Sanjeev Dahal, Enzo Dinglasan, Ray Henson, Hugh O'Neill, and Brian Sanders.

It would not be proper to ignore the small things that got me through some of the hardest days of this PhD. Fantasy football with the 4A crew, League of Legends with the NGL boys, rediscovering my love for Yu-Gi-Oh, and (many, many) trips to Sonic all helped to keep me sane. I cannot express enough how critical it is to not lose yourself in your work. Always find time in your day to take a break – you will thank yourself later.

Finally, I want to save a special spot for family. While having two parents who have both obtained PhDs has, at times, has at times led to feelings of pressure or unrealistic expectations, my appreciation for their experience and guidance as well as their willingness to just listen to me vent or have dinner for a brain drain cannot truly be put into words. To my mom and dad, Mark and Linda Reeves, as well as my grandma Irene Pocratsky (having you local now is such a blessing), Peanut (god rest your soul), and Envy (even if you treat me as a chew toy), I love you all.

## ABSTRACT

Omics technologies have rapidly evolved over the last half century through vast improvements in efficient extraction methodologies, advances in instrumentation for data collection, and a wide assortment of informatics tools to help deconvolute sample data sets. However, there are still untapped pools of molecules that warrant further analytical attention. As the frontline defense of the cell against exterior influences, the phospholipid membrane is key in structure, defense, and signaling, but current omics studies are only just now catching up to the potential hidden within cellular lipid profiles. Examination of shifts in phospholipid speciation and character could provide researchers with a wealth of information about how a cell attempts to adapt and survive when faced with adverse conditions. Application of such information could be valuable to the production of industrially relevant specialized bacterial strains, capable of processing large amounts of waste or feedstock as an affordable and renewable method. Using a flexible lipid extraction method using methyl *tert*-butyl ether (MTBE) combined with nanoscale hydrophilic interaction chromatography (HILIC) and nano-electrospray (nESI) tandem mass spectrometry (MS/MS), shifts in the lipidomes of several bacteria under consideration as industrial workhorses were investigated under variable growth conditions induced by introduction of toxic chemicals. Specific lipidome shifts were linked to specific growth conditions, which could lead to the production of bacterial strains designed to survive rough environments through genetic modification of phospholipid production.

## TABLE OF CONTENTS

CHAPTER 1: A BRIEF INTRODUCTION ON BIOLOGICAL APPLICATIONS AND ANALYTICAL CONSIDERATIONS OF BACTERIAL LIPIDOMICS .....	1
Lipidomics as a tool for monitoring industrially relevant bacteria .....	6
Approaching lipidomics from an analytical viewpoint .....	7
Liquid chromatography-mass spectrometry as a tool for lipidomics research .....	7
Building blocks of the membrane – a brief introduction to phospholipids .....	8
Membrane fluidity and lesser reported phospholipid perturbations .....	11
Membrane damage .....	15
Membrane modifications .....	16
Attempting to solve the issues in lipidomics .....	18
Dissertation overview .....	20
CHAPTER 2: FUNDAMENTALS OF SAMPLE EXTRACTION, MEASUREMENT, AND DATA-MINING FOR MS/MS-BASED LIPIDOMICS .....	24
Abstract .....	25
Considerations for mass spectrometry-based lipidomics .....	25
Brief considerations prior to sample analysis .....	27
Cell culture preparation .....	27
Chemicals and supplies .....	28
MTBE extraction as an alternative to traditional chloroform-methanol methods .....	30
LC-MS/MS Analysis .....	32
Setup of HILIC-based liquid chromatography methods .....	32
Quality Control .....	38
Operation and methods for tandem mass spectrometry using the LTQ-Orbitrap Velos Pro .....	39
Fundamentals of nano-electrospray ionization .....	39
A brief discussion of mass analyzers .....	43
Instrument quality control .....	48
On internal standards .....	49
Approaching the difficult task of processing MS-MS lipidomics data .....	50
Bulk processing of raw MS/MS files using MZmine .....	50
Leveraging tandem MS data using LIQUID .....	55
Manual spectral interpretation using Xcalibur .....	58
Statistical analysis using MetaboAnalyst .....	58
Conclusions .....	60
CHAPTER 3: DEVELOPMENT AND OPTIMIZATION OF A FLEXIBLE LC-MS ANALYSIS PLATFORM FOR LIPIDOMICS MEASUREMENTS .....	61
Abstract .....	62
Introduction .....	62
Lipid extraction .....	63
A brief consideration about sample preparation .....	63
Selection of optimal extraction solvent .....	64
Approaching cell lysis for lipidome access .....	67



Lipidome analysis – proper selection of analytical parameters .....	68
Effect of injection solvent choice .....	68
Importance of proper stationary phase selection .....	71
Polarity selection in lipidomics.....	80
Identification of key phospholipid species using MS spectra.....	85
Phosphatidylglycerol and phosphatidylethanolamine.....	85
Cardiolipin .....	90
Phosphatidylserine and phosphatidic acid .....	93
Use of isotopic labeling in lipidomics .....	97
Tracking the efficiency of label incorporation into the bacterial cell membrane .....	97
Processing lipidomics data – selected tools and techniques .....	101
Data processing programs .....	101
Conclusions .....	104
<b>CHAPTER 4: PROBING OF THE LIPIDOME OF THE MODEL ORGANISM</b>	
<b><i>BACILLUS SUBTILIS</i> ACROSS DIFFERENT GROWTH CONDITIONS REVEALS</b>	
<b>SHIFTS IN PHOSPHOLIPID COMPOSITION .....</b>	<b>105</b>
Abstract .....	106
Introduction.....	107
Experimental Approach .....	109
Preparation of <i>B. subtilis</i> cell cultures .....	109
MTBE-based extraction of <i>B. subtilis</i> lipidome .....	110
LC-MS/MS lipidomics analysis.....	110
Lipidomics data analysis.....	111
Results and Discussion .....	120
Unmodified <i>Bacillus subtilis</i> phospholipidomics are in line with previous studies	120
Comparison of fatty acid feeding conditions confirms effectiveness of genetic	
modifications to fatty acid metabolism.....	126
The effect of solvent present during growth on phospholipid composition .....	135
A brief examination across all conditions.....	142
Phospholipid derivatives and other lipid species .....	146
Aminoacylated phospholipids.....	146
Lipoteichoic acid.....	151
Discussion/Conclusions .....	156
<b>CHAPTER 5: <i>PSEUDOMONAS PUTIDA</i> GROWTH IN SIMULATED</b>	
<b>WASTEWATER CONDITIONS REVEALS SHIFTS IN PHOSPHOLIPID PROFILE</b>	
<b>INDICATIVE OF MEMBRANE DAMAGE.....</b>	<b>158</b>
Abstract .....	159
Introduction.....	160
Experimental Approach .....	163
Preparation of <i>P. putida</i> cell cultures .....	163
MTBE-based extraction of <i>P. putida</i> lipidome .....	167
LC-MS/MS lipidomics analysis.....	167
Lipidomics data analysis.....	168
Results and Discussion .....	179

The lipids of the gene-reduced strain <i>Pseudomonas putida</i> EM42 align similarly to the commonly researched strain <i>P. putida</i> KT2440 .....	179
A high-level view of <i>P. putida</i> phospholipid speciation and characteristics .....	184
p-Cresol shows notable relative increases in fully saturated fatty acid content .....	187
The mystery of odd-numbered fatty acids appearing within <i>P. putida</i> phospholipids within sodium acetate-grown cultures .....	191
Vanillin reveals increased presence of lysophospholipids.....	200
A brief examination of the lipid profiles of the mock wastewater solution.....	203
A brief look across all phospholipid profiles.....	203
Phospholipid derivatives and other lipid species .....	206
Aminoacylated phospholipids.....	206
Discussion/Conclusions .....	208
CHAPTER 6: OVERVIEW AND OUTLOOK ON UTILIZATION OF LIPIDOMICS IN BIOLOGICAL RESEARCH .....	212
Dissertation in summary .....	213
What challenges remain in lipidomics? .....	215
Where does lipidomics go from here? .....	219
REFERENCES .....	222
VITA .....	249

## LIST OF TABLES

Table 1. Inventory of lipid standards purchased from Avanti Polar Lipids used in testing and quality control of lipidomics experiments.....	29
Table 2. Gradient conditions for nano-LC-MS separations using ZIC-pHILIC stationary phase. ....	37
Table 3. Comparison of elution quality between C5 and HILIC stationary phases across positive and negative ionization mode using Avanti's Ion Mobility standard mix. .	75
Table 4. Comparison of elution quality between C5 and HILIC stationary phases across positive and negative ionization mode using Avanti's LightSPLASH standard mix. ....	76
Table 5. Peak areas of PG(14:1/14:1), PE(14:1/14:1), and CL(14:1/14:1/14:1/14:1) in the Avanti Ion Mobility standard mix, as well as ratios of the peak areas. ....	79
Table 6. Preferred ionization polarities for major classes of phospholipids.....	82
Table 7. Compiled master list of selected phospholipid species with averages across triplicate MZmine-aligned peak areas in <i>B. subtilis</i> 168 samples grown in normal media.....	112
Table 8. Compiled master list of selected phospholipid species with averages across triplicate MZmine-aligned peak areas in <i>B. subtilis</i> 168 samples grown in varying concentrations of butanol.....	114
Table 9. Compiled master list of selected phospholipid species with averages across triplicate MZmine-aligned peak areas in <i>B. subtilis</i> 168 samples grown in varying concentrations of isobutanol. ....	116
Table 10. Compiled master list of selected phospholipid species with averages across triplicate MZmine-aligned peak areas in <i>B. subtilis</i> 168 samples grown in varying concentrations of THF. ....	118
Table 11. Summary of a selection of previous studies on <i>Bacillus subtilis</i> lipidomics, demonstrating general proportions of major expected phospholipid species .....	123
Table 12. Chemical classes and origins of chemicals used to simulate various wastewater streams .....	165
Table 13. Composition of the mock wastewater solution.....	166
Table 14. Compiled master list of phospholipid species validated by MS2 spectra in LIQUID with MZmine-aligned peak areas in <i>P. putida</i> EM42 samples grown in the two glucose control conditions. ....	169
Table 15. Compiled master list of phospholipid species validated by MS2 spectra in LIQUID with MZmine-aligned peak areas in <i>P. putida</i> EM42 samples grown in 2-cyclopentenone and formaldehyde. ....	172
Table 16. Compiled master list of phospholipid species validated by MS2 spectra in LIQUID with MZmine-aligned peak areas in <i>P. putida</i> EM42 samples grown in <i>p</i> -cresol and sodium acetate. ....	175
Table 17. Compiled master list of phospholipid species validated by MS2 spectra in LIQUID with MZmine-aligned peak areas in <i>P. putida</i> EM42 samples grown in vanillin and the mock wastewater solution. ....	177

Table 18. Previous phospholipid profiling studies performed on several strains of <i>Pseudomonas putida</i> , as well as representative <i>P. aeruginosa</i> profiles to exemplify the differences within a genus.....	181
Table 19. GC-MS data of the fatty acid composition of <i>Pseudomonas putida</i> EM42 ..	197

## LIST OF FIGURES

Figure 1. Major omics fields, along with a brief description of what each aims to examine. ....	3
Figure 2. General characteristics of phospholipids. A) Phosphate backbone, where R1 and R2 indicate fatty acids and R3 indicates head group. B) Examples of structures of saturated and unsaturated fatty acids. C) Phospholipid head groups.....	9
Figure 3. A brief demonstration of membrane fluidity. A) A largely rigid membrane, composed of tightly packed phospholipids with saturated fatty acids. B) A more fluid membrane, consisting of phospholipids with bent, unsaturated fatty acids that cannot pack as tightly.....	13
Figure 4. Mechanics of analyte elution on columns using A. RP (C18) stationary phase and B. HILIC (ZIC-pHILIC) stationary phase, along with schematics of the stationary phases. ....	35
Figure 5. Fundamentals of electrospray ionization, demonstrating A. ion formation through the Coulomb explosion generating dry charged ions that are left to be pulled via vacuum into the mass spectrometer, as well as the B. the Taylor cone, an observable demonstration of this phenomenon.....	42
Figure 6. Schematic of the LTQ Orbitrap Velos Pro mass spectrometer (ThermoFisher Scientific) [150]. ....	44
Figure 7. Image of the LTQ Orbitrap Velos Pro mass spectrometer (photo taken by the author). ....	44
Figure 8. Example LIQUID output, showing the interface and customizable search options and an example sample run and matching of MS2 peaks to the database. ..	56
Figure 9. Comparison of lipidomics extraction methods. A. MTBE-based extraction, with the organic lipid layer present at the top of the extraction and the protein pellet settling at the bottom of the vial. B. CME extraction, with the organic lipid layer at the bottom of the vial and the protein pellet lying at the interface between the aqueous and organic layers. ....	65
Figure 10. Extracted ion chromatograms of A. PG(28:2), B. PE(28:2), and C. CL(56:4), each shown shown diluted in methyl tert-butyl ether (top), chloroform (middle), and methanol (bottom).....	70
Figure 11. Issues using C18-based stationary phases in RP-LC-MS lipidomics. A: A commonly observed phospholipid within the cell membrane, PG(34:0). B: Example of how the non-polar interactions of the long fatty acid chains can interact with each other and create strong interactions that are hard to separate without the use of an incredibly strong nonpolar solvent.....	72
Figure 12. Comparison of lipid associations between a generic long fatty acid chain phospholipid and A: a C18 column and B: a C5 column. ....	74
Figure 13. Comparison of eluted lipid profiles in <i>Pseudomonas putida</i> EM42, EM42-cti, KT2440, and KT2440-cti between HILIC and C5 RP columns, both performed in negative ionization mode. ....	78

Figure 14. Extracted ion chromatograms of the PG, PE, and CL standards within a 25 $\mu\text{g/mL}$ dilution of the Avanti Ion Mobility standard mix in A) positive ionization mode and B) negative ionization mode. ....	83
Figure 15. Comparison of eluted lipid profiles in a selection of <i>Pseudomonas putida</i> samples (KT2400/EM42 and KT2440-cti/EM42-cti, strains with an overexpressed cis-trans isomerase, cti) run on a HILIC column in positive and negative ionization modes, along with total lipid species observed in each sample. ....	84
Figure 16. General structures of A. PG and B. PE. ....	87
Figure 17. Extracted ion chromatogram (top) and MS2 spectrum (bottom) of PG(14:1/14:1) along with annotated fragment peaks. ....	88
Figure 18. Extracted ion chromatogram (top) and MS2 spectrum (bottom) of PE(14:1/14:1) along with annotated fragment peaks. ....	89
Figure 19. General structure of cardiolipin. ....	91
Figure 20. Extracted ion chromatogram (top) and MS2 spectrum (bottom) of CL(14:1/14:1/14:1/14:1) along with annotated fragment peaks. ....	92
Figure 21. General structures of A. PS and B. PA. ....	94
Figure 22. Extracted ion chromatogram (top) and MS2 spectrum (bottom) of PS(14:1/14:1) along with annotated fragment peaks. ....	95
Figure 23. Extracted ion chromatogram (top) and MS2 spectrum (bottom) of PA(14:1/14:1) along with annotated fragment peaks. ....	96
Figure 24. Comparison of lipid profiles across various deuteration levels within the fatty acids of <i>E. coli</i> . ....	99
Figure 25. Comparison of lipid profiles across various deuteration levels within the PE species of <i>E. coli</i> ....	99
Figure 26. Comparison of lipid profiles across various deuteration levels within the PG species of <i>E. coli</i> ....	100
Figure 27. Comparison of lipid profiles across various deuteration levels within the CL species of <i>E. coli</i> ....	100
Figure 28. Comparison of the observed phospholipids (0-1 double bonds and FAs ranging from 14-17 carbons in length) for the no fatty acid feeding control of <i>B. subtilis</i> 168. ....	121
Figure 29. KEGG pathway for fatty acid degradation in <i>Bacillus subtilis</i> 168 [236], with the highlighted gene FadN knocked out in the $\Delta\text{yusL}$ strain to prevent the cell from being able to efficiently recycle fatty acids into energy or back into new lipids [237]. ....	125
Figure 30. Comparison of A) chain length and B) degree of unsaturation of the fatty acids within phospholipids extracted from each feeding condition applied to <i>B. subtilis</i> 168. Stars indicate groups deemed significantly different from the no feeding control by the Student's t-test. ....	127
Figure 31. KEGG pathway for fatty acid biosynthesis in <i>Bacillus subtilis</i> 168, with the highlighted gene FabF being knocked down in samples fed fatty acid mixtures [238]. ....	128
Figure 32. KEGG pathway for glycerophospholipid metabolism in <i>Bacillus subtilis</i> 168 [239]. ....	129

Figure 33. Generic view of the two forms of fatty acid synthases (FAS) observed in most organisms. Type I FAS are largely observed in animals and fungi, while Type II FAS is the one observed in <i>B. subtilis</i> . FabF, the gene encoding the enzyme crucial for fatty acid elongation, is once more highlighted [238].....	131
Figure 34. Comparison of fatty acid feeding conditions in <i>B. subtilis</i> 168. Relative phospholipid content in the A) control cultures with no fatty acid supplementation, B) cultures fed a native mixture of fatty acids commonly observed in <i>B. subtilis</i> , and C) cultured fed a more restrictive mixture of fatty acids. D) Heatmap showing fold change differences of the 38 most significantly variable features (as determined by ANOVA). E) Principal component analysis (PCA) plot showing the degree of separation across the replicates of each feeding condition with a 95% confidence region. ....	134
Figure 35. Comparison of A) chain length and B) degree of unsaturation of the fatty acids within phospholipids extracted from each solvent growth condition applied to <i>B. subtilis</i> 168. Stars indicate groups deemed significantly different from the no feeding control by the Student's t-test. ....	138
Figure 36. Comparison of fatty acid solvent growth conditions in <i>B. subtilis</i> 168. Relative phospholipid content in the A) control cultures, B) cultures grown in butanol, C) cultures grown in isobutanol, and D) cultures grown in THF. D) Heatmap showing fold change differences of the 42 most significantly variable features (as determined by ANOVA). E) Principal component analysis (PCA) plot showing the degree of separation across the replicates of each solvent growth condition with a 95% confidence region. ....	141
Figure 37. Individual phospholipid speciation comparisons across each <i>B. subtilis</i> 168 sample, with rows showing solvent growth conditions and columns showing fatty acid feeding conditions. ....	143
Figure 38. Comprehensive analysis of all combinations of fatty acid feeding and solvent growth conditions in <i>B. subtilis</i> 168. ....	145
Figure 39. Summary of observed aminoacylated phospholipids observed in select <i>B. subtilis</i> 168 cultures with no fatty acid modification. A) Control, B) Butanol, C) Isobutanol, D) THF.....	149
Figure 40. Summary of observed lipoteichoic acid species observed in select <i>B. subtilis</i> 168 cultures with no fatty acid modification. A) Control, B) Butanol, C) Isobutanol, D) THF E) Generic structure of DAG-Glc2-P-Gro. F) Generic structure of DAG-Glc2-P-Gro-Ala.....	154
Figure 41. Individual wastewater components being examined. ....	165
Figure 42. Phospholipid composition by peak area of <i>P. putida</i> EM42 cultures grown in glucose to A) mid exponential phase and B) late exponential phase.....	180
Figure 43. KEGG pathway of glycerophospholipid metabolism within <i>Pseudomonas putida</i> KT2440 [369] .....	182
Figure 44. KEGG pathway for fatty acid biosynthesis in <i>Pseudomonas putida</i> KT2440. [377].....	185

Figure 45. Ratio of PE to PG across all sampling conditions of <i>P. putida</i> EM42. Stars indicate species deemed significantly different from the mid exponential glucose control by the Student's t-test. ....	186
Figure 46. Average fatty acid chain length of phospholipids across all sampling conditions of <i>P. putida</i> EM42. Stars indicate species deemed significantly different from the mid exponential glucose control by the Student's t-test. ....	188
Figure 47. Average degree of unsaturation of phospholipids across all sampling conditions of <i>P. putida</i> EM42. Stars indicate species deemed significantly different from the mid exponential glucose control by the Student's t-test. ....	189
Figure 48. A) Heatmap, B) PCA plot (with 95% confidence regions), and C) volcano plot (left indicating preference to the control and right indicating preference to the sampling condition) comparing the lipid profiles of p-cresol to the mid exponential glucose control in <i>P. putida</i> EM42. ....	190
Figure 49. Heatmap of the fully saturated phospholipids compared between the glucose control and p-cresol samples in <i>P. putida</i> EM42.....	192
Figure 50. A) Heatmap, B) PCA plot (with 95% confidence regions), and C) volcano plot (left indicating preference to the sampling condition and right indicating preference to the control) comparing the lipid profiles of sodium acetate to the mid exponential glucose control in <i>P. putida</i> EM42. ....	193
Figure 51. Comparison of the mass-equal palmitoleic acid (top) and the cyclopropane variant 8-(2-pentylcyclopropyl)octanoic acid (bottom).....	195
Figure 52. Comparison of the mass-equal palmitic acid (top) and the branched fatty acid 14-methylpentadecanoic acid (bottom).....	195
Figure 53. Heatmap of the cardiolipin species compared between the glucose control and p-cresol samples in <i>P. putida</i> EM42. ....	198
Figure 54. Ratio of PE to CL across all sampling conditions of <i>P. putida</i> EM42. Stars indicate species deemed significantly different from the mid exponential glucose control by the Student's t-test. ....	199
Figure 55. A) Heatmap, B) PCA plot (with 95% confidence regions), and C) volcano plot (left indicating preference to the sampling condition and right indicating preference to the control) comparing the lipid profiles of vanillin to the mid exponential glucose control in <i>P. putida</i> EM42. ....	201
Figure 56. A) Heatmap, B) PCA plot (with 95% confidence regions), and C) volcano plot (left indicating preference to the sampling condition and right indicating preference to the control) comparing the lipid profiles of the mock wastewater solution to the mid exponential glucose control in <i>P. putida</i> EM42 .....	204
Figure 57. Full comparison of the phospholipid profiles across all conditions. A) Heatmap. B) PCA plot. General phospholipid profiles for C) the mock wastewater solution, D) 2- cyclopentenone, E) formaldehyde, F) p-cresol, G) sodium acetate, and H) vanillin in <i>P. putida</i> EM42.....	205
Figure 58. Ala-PG species observed within <i>P. putida</i> EM42 strains inoculated with different wastewater simulated conditions. Stars indicate species deemed significantly different from the mid exponential glucose control by the Student's t-test. ....	207

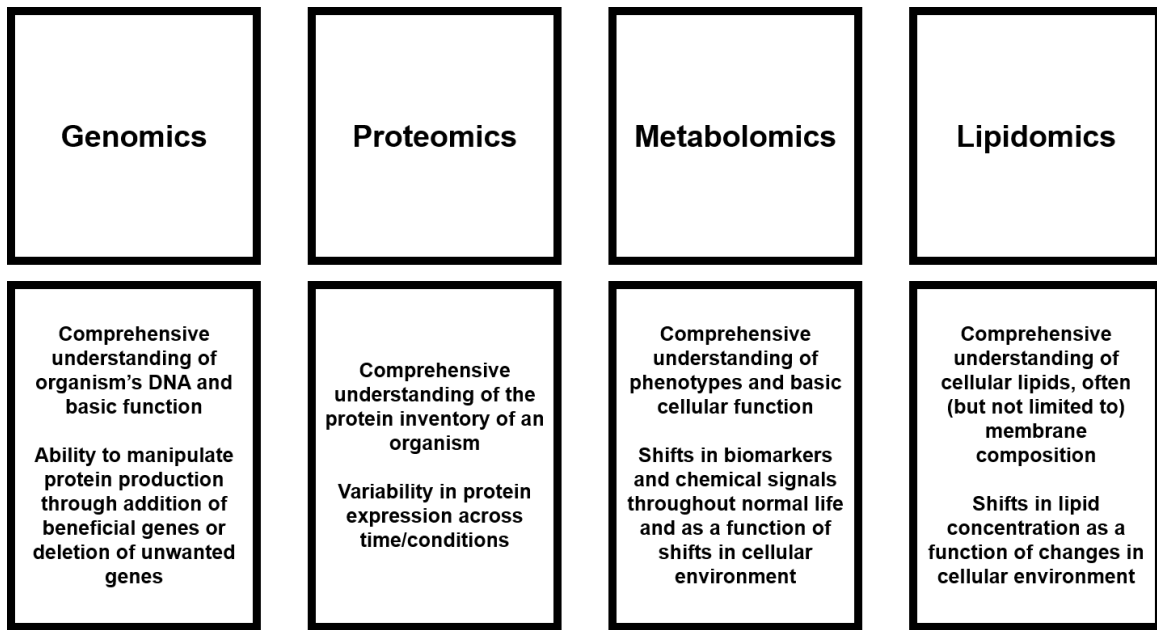


Figure 59. Genes of interest for future engineered strains of *P. putida* encoding A) regulation of fatty acid cis double bonds (FabA and FabB) and B) production of PS and PE production (pssA) and cardiolipin (ClsA), as well as those regulating trans unsaturated fatty acids (Cti) and cyclopropane fatty acids (cfaB) (unshown) [377, 414] ..... 210

# **CHAPTER 1: A BRIEF INTRODUCTION ON BIOLOGICAL APPLICATIONS AND ANALYTICAL CONSIDERATIONS OF BACTERIAL LIPIDOMICS**

As approaches to biological research have grown more advanced with the development of increasingly versatile and sensitive instrumentation, more focused lines of research, and better understanding of biological questions that remain to be answered, the importance of robust omics technologies becomes more valuable. Comprehensive exploration of specific classes of macromolecules can help to deconvolute ongoing biological questions [1], and the rising interest of systems biology [2] to tie together multiple different aspects of cellular function means that robust measurements across several molecular categories are crucial. However, this is not an easily achievable goal upon consideration of the cell as a complicated, multidimensional unit. Deoxyribonucleic acid (DNA), the building block of life itself, drives cellular propagation. Transformation of that data into proteins via ribonucleic acid (RNA) and assembly of amino acids in specific orders helps to create the machinery that keeps the cell alive. Those proteins drive basic cellular functions by creation, conversion, and transportation of a plethora of small molecules that can be collectively referred to as metabolites, itself a broader categorization with several different subgroups.

This central dogma is further described within Figure 1, which shows the main branches of omics technologies. While genomics, proteomics, and metabolomics are generally considered to be comprehensive measurement platforms, subcategories do exist. Research areas focusing on transcriptomics [3, 4] and peptidomics [5, 6] have arisen as scientists have gradually begun digging deeper into genomics and proteomics data. Likewise, subsets of metabolomics have focused on sugars (glycomics [7, 8]), lipids (lipidomics), or even more systems-level studies like metabolic flux (fluxomics [9, 10]).



**Figure 1. Major omics fields, along with a brief description of what each aims to examine.**

Still, even at this broad level of observation, it becomes very clear that comprehensive examination and understanding of all facets of the cell is not a task that can be accomplished with just a singular analysis, and even understanding within a given category likely requires careful consideration of all potential molecular subclasses and modifications.

Delving into shifts in lipid composition specifically has a lot of untapped potential, especially in the context of single cell organisms that are not subject to the level of cellular differentiation within eukaryotic organisms. While manipulation of genetic material and proteins have widespread implications in multiple cellular processes, lipids are often uniquely localized within the cell membrane, contributing heavily to cellular structure [11], energy storage [12, 13], and propagation of the cell cycle [14-17], and this level of specialization can be incredibly useful for answering very specific questions about cellular function. In addition to natural shifts in phospholipid speciation and fatty acid modifications to modulate the permeability of the membrane [18, 19], specialized lipid species such as complexes with sugars and amino acids (peptidoglycan), glycerol (teichoic and lipoteichoic acids), and proteins (lipoproteins) all contribute to cellular response to exterior stimuli [20].

The complexity of these datasets can quickly escalate even within the simplest of organisms across all omics experimental designs, and lipidomics is no different. As of September 2021, the LIPID MAPS Structure Database contained 46,150 unique lipid structures, 24,205 of which were experimentally determined and/or mined from literature reports and 21,945 of which were generated through computer modeling. While this may

appear to be a large number, it is important to understand that this is somewhat misleading. For example, consider the phosphatidylglycerol (PG) species PG(32:2). This phospholipid contains fatty acids (FA) whose carbon chains total to 32 carbons and have a total of two double bonds contained within them. However, there are many different variations of PG(32:2) – this could be the result of many different fatty acid combinations such as 16:1/16:1, 20:0/12:2, 17:2/15:0, or 18:0/14:2, just to name a few. Additionally, many databases or informatics packages fail to comprehensively report generic lipids as well as all possible alterations that can be observed. These can include oxidation [21], addition of amino acids [22, 23], and modification of the fatty acid content of the phospholipid [24]. While databases are generally robust when it comes to generic lipid coverage, the depth of measurements is often just limited to variations in fatty acid composition and isomerization issues (often the result of headgroups), so many of these modifications are left to be studied in more focused studies instead of being present in databases [25].

Despite this, the functional building blocks of phospholipids afford a certain level of predictability within lipidomics. While deep dives into each and every member and perturbation of the phospholipid membrane are intriguing, it is often more than sufficient to start with basic lipidomics questions about phospholipid head groups and fatty acid character, and that alone can be an incredibly powerful tool for analytical chemists to utilize for research and industrial experiments. Combined with a highly sensitive, robust analysis platform, fluctuations in phospholipid profile can be identified and probed to elucidate how organisms modify the structure of their cell membrane in response to

various challenges and conditions. To that end, execution of a tandem mass spectrometry platform combined with effective separations and a workable informatics approach should enable comprehensive analysis of lipids as well as observation of trends across variance in cellular environment.

### **Lipidomics as a tool for monitoring industrially relevant bacteria**

Currently, humanity faces several challenges that are not easily or quickly solved. As changes to the environment continue to be an ongoing problem in the world, many different solutions have been proposed to try to circumvent the cost, danger, and/or investment required to approach these issues. Increasing interest in biofuels has been driven as a current alternative and future replacement for fossil fuels and is primarily driven by relative increases in energy yield, decreased pollutant dispersion and reduction of greenhouse gas emission [26]. Cleanup of waste sites [27, 28] and contaminant spills [29] has proven to be difficult to completely solve by conventional means. Additionally, many common household, medical, and industrial products come at a heavy cost of production [30, 31], requiring a large material and monetary investment.

All these can potentially be addressed by bacteria, which offer a renewable, efficient, and cost-effective platform that can be manipulated to address a wide array of systematic issues [32-36], and utilization of lipidomics can offer a unique approach to assessing how bacteria respond to these various conditions [37, 38]. While production of medically important bioproducts such as insulin [39] may not place much stress on bacteria, forced production of ethanol [40] or biodiesel [41] or exposure to waste streams for bioremediation [42, 43] can lead to decreased productivity over time or even cell

death. However, observation of how the cell attempts to remodel the composition of its cell membrane, the first line of defense against the environment, is a key area of focus for researchers in ongoing research to develop optimized bacteria strains for widespread industrial applications [44-46].

### **Approaching lipidomics from an analytical viewpoint**

#### ***Liquid chromatography-mass spectrometry as a tool for lipidomics research***

While researchers have attempted to approach lipidomics with nuclear magnetic resonance (NMR) [47] and matrix-assisted laser desorption/ionization (MALDI) [48] mass spectrometry, an ongoing challenge endemic to omics as a field is the issue of balancing complex sample extracts with comprehensive analysis. Both NMR and MALDI-MS struggle to measure complex mixtures in such a way that they are easily deconvoluted during analysis, which is why mass spectrometry methods directly coupled to efficient chromatography separations have become the primary method for omics-based analyses in recent years.

Application of electrospray ionization (ESI) alongside tandem mass spectrometry was first proposed in 1994 [49] as a possible approach to large scale comprehensive lipidomics, with nESI methods quickly rising to popularity in the coming years [50]. From there, multiple different approaches to mass spectrometry-based lipidomics have been developed, including wholesale shotgun lipidomics for full sample analysis [51] and multiple reaction monitoring (MRM) for quick characterization of known lipids [52].

Mass analyzers have also advanced over the years to help researchers more thoroughly annotate lipid extracts. Time of flight (TOF) instruments have moderate



resolution and high mass accuracy coupled to fast scan rates, but often the limited dynamic range of the mass analyzer restricts measurement depth [53]. Fourier transform ion cyclotron mass spectrometry (FT-ICR-MS) offers upside in tandem mass spectrometry analysis, with hybrid mass analyzers allowing for detection of precursor masses as well as fragmentation spectra, and extremely high mass accuracy and resolution aid in efficient identification of lipids, but low scan speeds can be a hindrance in increasingly complex samples [54]. This has led to the coupling of the linear ion traps seen in FT-ICR-MS instruments with the orbitrap analyzer, which helps to balance slightly lower resolution and mass accuracy with increased scan speed, allowing for scans of precursor and fragmentation spectra at respectable resolution and low mass error while not significantly compromising the speed at which measurements are made, which is of critical importance for complex lipidomics samples [55, 56].

### ***Building blocks of the membrane – a brief introduction to phospholipids***

With an understanding of how to approach lipidomics, it is also essential to understand the targets of analysis. Within bacterial lipidomics, the most prominent category of lipids is mainly the phospholipids comprising the cell membrane. As shown in Figure 2, even fundamental phospholipids can carry a wide array of variability. While the backbone of phospholipids remains largely consistent across all phospholipids (Figure 2A), variation in fatty acid chain length and/or saturation (Figure 2B) as well as head groups that can be key modifiers in membrane chemical properties (Figure 2C) can create wildly variable cell membranes.

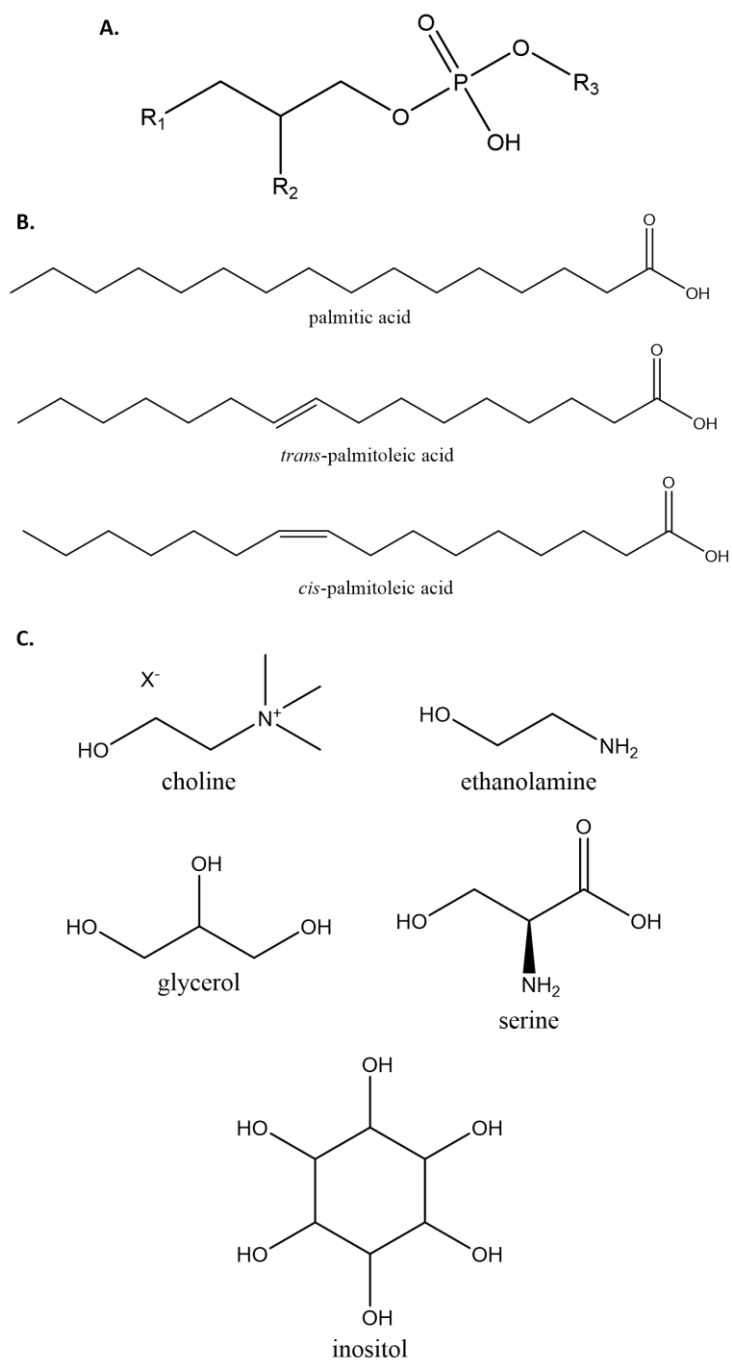


**Figure 2. General characteristics of phospholipids. A) Phosphate backbone, where R1 and R2 indicate fatty acids and R3 indicates head group. B) Examples of structures of saturated and unsaturated fatty acids. C) Phospholipid head groups.**

Understanding the importance of each phospholipid, as well as how each individual phospholipid species differs in head group and fatty acid character, is a key component of crafting lipidomics experiments. Without a firm approach to obtaining the complete lipidome of a given sample set, it is readily possible to end up with data sets that are lacking in depth and quality.

Specifically in the context of bacterial lipidomics, it is important to also understand whether the bacteria in question is Gram-negative or Gram-positive, as specified by the process of Gram staining to determine the retention of Gram stain (Gram-positive) within the cell or lack of retention (Gram-negative). While not a strict rule, generally Gram-negative bacteria prefer larger proportions of PE within their cell membranes, while Gram-positive bacteria often prefer PG, though the latter is much more variable than the former in terms of PE/PG ratio [57, 58]. Additionally, the Gram-staining class of bacteria can also lead to further questions such as the presence and/or absence of other lipid derivatives such as teichoic and lipoteichoic acids, aminoacylated phospholipids, and lipid A, among others, which can help drive the determination of more thorough lipid profiles [57]. This can help to narrow potential targets and streamline analysis.

Despite the relative predictability across phospholipid construction thanks to the modular character of this molecular class, it is important to consider proper selection of chromatography when executing LC-MS experiments. This is largely driven by the proposed goals of the study – while RP analyses can help to provide excellent separation of phospholipids by the length of fatty acid tails, HILIC is highly efficient at separating

phospholipids by head group chemical character [59]. This results in experiments being designed around whether the head group or fatty acid tails of the phospholipid are more desirable, but this also leads to complementary experiments being a viable path forward for comprehensive experiments. However, issues can arise without careful consideration of how lipids will interact with each stationary phase (which will be described further in Chapters 2 and 3). Deciding whether separation quality or complete elution of samples is an important aspect of experimental design, and improper selection and deployment of LC-MS/MS methods and instruments could block complete acquisition of lipidomes from sample sets.

### ***Membrane fluidity and lesser reported phospholipid perturbations***

While understanding how to obtain robust lipidomics data sets is important, it is also critical to have a thorough grasp on how to interpret changes in the context of biology. In addition to reporting the general phospholipid or fatty acid composition of a given lipidome, recognizing how those components influence the level of fluidity or rigidity of the membrane is a vital aspect of understanding lipidome trends. The concept of membrane fluidity is driven by several different extracellular effects, including shifts in pH [60-62], temperature [63, 64], electrostatics [65, 66], solute permeability [67], and salinity [68], which then drives changes in the character of the cell membrane by way of modifications to phospholipid speciation [69, 70] and degree of unsaturation of fatty acids [71, 72]. However, it is not reasonable to expect that every organism will have the same response to every type of environmental change, nor is it reasonable to expect that a specific shift in cellular condition will have the same effect across all organisms.

In general, membrane fluidity can be narrowed down to very specific metrics (Figure 3). Membrane rigidity is often conferred by the presence of phospholipids containing longer fatty acids with little to no unsaturation [73] (Figure 3A). This allows the membrane to pack more tightly together and reduce how easily molecules can diffuse through the membrane due to increased thickness. On the other hand, introduction of kinks by way of fatty acid unsaturation or a general thinning of the membrane because of shorter fatty acids leads to increased gaps and increased liquid and metabolite permeability (Figure 3B). The modulation of membrane rigidity and fluidity is a key factor in prolonged survival of the cell, and careful observation of how the cell attempts to change membrane character by way of fatty acid length and saturation as well as modifications to phospholipid head group character and proportion can be incredibly informative to researchers attempting to craft new bacterial strains that can better withstand the pressures of potentially harmful environments.

However, there is still much to learn about membrane fluidity, even amongst traditionally accepted metrics, including what exactly controls the action of membrane fluidity and rigidity. While there are methods to quantitate membrane fluidity, often through fluorescence polarization measurements [74-76] or through observation of other related metabolic processes that may have an influence on membrane properties [77], these measurements are very topical and do not really help to explain how the membrane changes in terms of actual membrane composition.

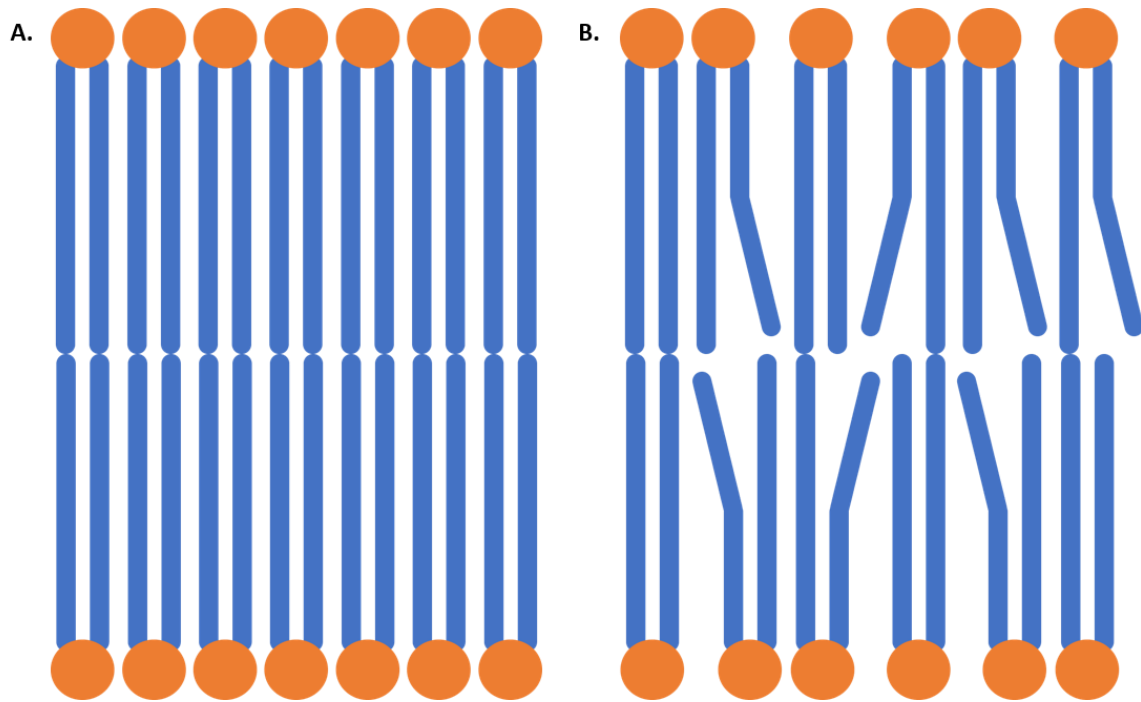


**Figure 3. A brief demonstration of membrane fluidity. A) A largely rigid membrane, composed of tightly packed phospholipids with saturated fatty acids. B) A more fluid membrane, consisting of phospholipids with bent, unsaturated fatty acids that cannot pack as tightly.**

There can also be conflict in experimental data depending on the construction of the experiment – often times, it is possible to observe completely opposite trends in membrane fluidity in an organism despite being exposed to environments which would theoretically drive membrane fluidity in a similar fashion. This was observed within this dissertation, where it almost seemed like cells were caught in the middle of transition from one membrane condition to another one, indicating that perhaps the time needed to adapt to a new environment or cellular growth stage could have an impact on membrane fluidity as well.

Membrane fluidity is also driven by the presence of membrane proteins and other molecules such as sugars that can interact with membrane phospholipids to stabilize or fluidize the membrane. Expanding this understanding further, bacteria are often characterized as having a cell envelope, which is considered to include everything that binds the cytoplasm, including the membrane as well as other structures that help to offer a level of protection and structural integrity. While proteins are often embedded within the membrane and act as solid rafts in a sea of phospholipids, other structures such as lipopolysaccharides, teichoic acids, and peptidoglycan extend past the membrane and confer a level of structural integrity to the cell. With the right tools, these can also be probed using lipidomics given that many are either derived from or contain lipids, and many often contribute, at least partially, to the fluidity of the cell membrane [78]. Additionally, studies on lipid rafts, which are enriched regions of specific lipid within the membrane, have increased in recent years, as they were previously thought to be a eukaryotic feature but have been shown to be present in bacteria as well. Regions of

singular phospholipids would also have a notable effect on membrane fluidity, though perhaps the effect of lipid rafts on membrane fluidity may be more localized to specific membrane regions than across the entire cell. Additionally, lipid rafts are not as readily analyzed through the means described later here and are more easily detected through the use of visualization tools such as fluorescence microscopy [79]. Nevertheless, it is important to note that phospholipids in isolation are not necessarily the only factors driving membrane fluidity.

To address what exactly is driving the fluidity or rigidity of the cell membrane, more thorough measurements are needed to probe the phospholipid profiles of sample sets and assess how phospholipid head groups and fatty acid composition change as a function of applied sample conditions. Mass spectrometry can be incredibly powerful in this regard, with LC-MS being a powerful tool for analysis of lipid speciation by head group composition [80] and GC-MS having a long history in characterization of fatty acids using the fatty acid methyl ester (FAME) method [81]. Comprehensive analysis of phospholipid character and thorough understanding of the relationship between membrane fluidity and lipid modifications can greatly help in understanding a cell's response to environmental changes.

### ***Membrane damage***

While membrane fluidity does offer a window into how bacteria remodel the cell membrane, it is often more of a concerted response to environmental shifts or changes through manipulation of phospholipid species and fatty acid properties. Membrane damage, a much more uncontrollable phenomenon, is the other possible result of this.



However, this can still be detectable through lipidomics, just with slightly different approaches. Currently, known pathways of membrane damage include inhibition of phosphatidic acid production as well as shifts in fatty acid profile, the latter of which being somewhat more niche [82]. There are also less observable effects – with knowledge that phospholipids can arrange in bundles in the membrane for various biological purposes, the loss of that phospholipid localization can also be interpreted as a type of membrane damage [83]. This is often how antimicrobial peptides damage cell membranes through simple forced incorporation into the membrane [84]. Additionally, membrane damage can simply be observed through spectroscopic and microscopic approaches – this can often be observed through warping of the shape of the cell and observation of pockmarks across the membrane [82]. While not a primary focal point within a mass spectrometry-based bacterial lipidomics analysis, it is important to note that it is possible to observe damage visually, and the coupling of mass spectrometry to neutron scattering could also yield valuable information about physical membrane damage using isotope labels specifically targeting phospholipids and/or fatty acids of interest [85-87].

### ***Membrane modifications***

As mentioned earlier, one of the big analytical challenges associated with lipidomics is the ability to detect and accurately identify how basic phospholipids are modified to adapt to changing cellular conditions. This is most often centered within modification of the fatty acids comprising the phospholipids, as any kind of bend or kink in the fatty acids can begin to introduce voids, decreasing the ability of membrane

phospholipids to pack as tightly as they could in an ideal scenario with fully saturated, unmodified fatty acids.

Cell can also modify membrane phospholipid fatty acids to modulate membrane fluidity; these include modification of the double bonds in unsaturated fatty acids into cyclopropane or oxidized products. These transformations can have unique effects on the property of the membrane. In the case of cyclopropane fatty acids, while the addition of a protruding carbon in the middle of the fatty acid has a negative impact on the ability of the membrane to pack tightly, they do confer a moderate upgrade in stabilization due to the rigid cyclopropane ring heavily restricting bond rotation, leading to the odd combination of promotion of membrane fluidity and increased membrane stability [88]. Oxidized double bonds within the membrane often result in the same effect [89]. Cells can also modulate the conformation of double bonds to swap between cis and trans double bonds – cis double bonds create disorder and loosen the rigid character of the membrane, much like what is shown in Figure 3B, while trans double bonds often mimic the character of fully saturated fatty acids and encourage better overall packing of the phospholipids, leading to relatively rigid membrane structures [90, 91].

There are also changes associated with the head group of the phospholipid – aminoacylation of the head group of phospholipids is a common membrane modification within bacteria, allowing bacteria to better control the electronic potential of the membrane and resist potentially deadly cationic antimicrobial agents through the addition of negatively charged amino acids (such as lysine and alanine) to the head groups of specific phospholipid species, most often phosphatidylglycerol [92, 93].

All of these changes have differing effects on the fluidity and permeability of the cell membrane and arise from different scenarios, but it is important to understand not only that they do exist but also to have methods of detection so as to account for their influence within the membrane. This ensures that lipidomics analyses are as comprehensive as possible and can adequately answer any relevant biological questions being probed.

### **Attempting to solve the issues in lipidomics**

Analytical challenges in lipidomics range from efficient and complete extraction of lipid profiles from samples [94], selection of a proper stationary phase for quality separations (in the case of mass spectrometry) [59], and approaching backend data analysis. However, of the previously described issues, none is more vital to solve than the issue of current lipidomics informatics. Lipidomics is not lacking in open-source programs that can process lipidomics data sets to varying degrees; examples include LipidFinder 2.0 [95], LipidXplorer [96], Lipostar [97], and LIQUID [98]. Additionally, generic omics data processing programs such as MZmine [99], XC-MS [100], and MAVEN [101] all offer an excellent combination of data processing power and access to lipidomics databases. However, testing with actual data has shown that there are several issues associated with current lipidomics informatics approaches.

The first issue is balancing the efficiency of data processing power with the depth of lipid database searching. Most of the programs described above are incredibly powerful with specific tasks, such as proper utilization of mass spectrometry data for lipid annotation, filtering of unwanted or duplicate peaks, or alignment of broad sample

sets, but most lack the ability to fully perform all of those tasks. To properly assess the lipidome of a sample set measured using tandem mass spectrometry, it is essential to have all three of those metrics present within the analytical protocol of the experiment, and currently many programs just do not have those capabilities.

The other is the depth of current lipid databases. Current lipid search tools are incredibly robust when it comes to determination of general phospholipid head group and fatty acid character, especially when those tools have access to methods for using fragmentation spectra, many of them are woefully deficient in helping to determine modifications within sample sets. While lipid variants such as aminoacylated phospholipids [92], teichoic and lipoteichoic acids [102], lipid A [103], oxidized lipids and fatty acids [104], and cyclopropane fatty acids [88] are well reported in literature, they are not necessarily well represented in many mass-spectrometry-based lipid databases. Given that many of those are simple lipid modifications, they could easily be incorporated into databases as a possible search option, much like how proteomics search tools have begun to add post translational modifications to search algorithms [105].

Unfortunately, there is no easy solution to any of these problems. While the obvious approach would be to combine many of these complaints or deficiencies alongside an existing robust platform and create a new program, most of these open-source programs were designed with specific needs in mind, not for more widespread applications, and as such there is not necessarily a significant need for a more generally applicable program. Additionally, databases such as LIPID MAPS would greatly benefit from development of increased annotation for lipids containing head group modifications

or fatty acid variants, either through better incorporation of lipids reported in literature or tools to help analyze datasets and predict the occurrence of these modifications through identification of characteristic peaks within fragmentation spectra. Understanding how organisms modify their membranes through changing lipid character can have important implications in future experimental design, and as such it is important to push the boundaries of current lipid analysis tools to help advance the field.

### **Dissertation overview**

While bacteria are relatively simplistic organisms, there is still a wide range of value that can be gleamed from omics analyses when exposing cells to controlled conditions of interest. Additionally, with selection of the proper species, bacteria can be highly customizable to fit any number of industrial, medical, or experimental niches, modified to eliminate harmful characteristics, emphasize beneficial traits, or improve production of desired natural products through careful genetic engineering. Lipidomics can offer a unique perspective on these questions through a much more simplistic view of cellular health than what is normally observed in genomics, proteomics, and metabolomics while simultaneously giving insights about how the cell immediately reacts to shifts or drastic changes in the cellular environment, which can then drive future experiments in genomics and proteomics to engineer more efficient organisms or better responses to those cellular stressors.

To that end, this dissertation aims to address two main research questions: 1) What is needed to construct a robust analytical platform combining multiple aspects of high throughput, high sensitivity mass spectrometry analyses to perform comprehensive

lipidomics on bacteria species? and 2) What are the trends that can be observed within bacteria that are indicative of shifts in the membrane phospholipid profile as a function of several controlled applications of exterior growth conditions? Described here is a comprehensive lipidomics platform built using several different methodologies tested for optimal use alongside each other, involving thorough examination of potential parameters for sample preparation, lipid extraction, mass analysis, and lipid annotation. Specific focus was placed upon balancing methodological efficiency with a sufficient thoroughness and depth of measurements such that inference of specific phospholipid shifts can be observed using a high-performance LC-MS/MS platform and an informatics pipeline crafted to answer relevant biological research questions.

After a brief expose of the state of the field of lipidomics described here in Chapter 1, Chapter 2 will delve into an in-depth explanation of the materials and methods associated with the selected lipidomics pipeline approach - methyl *tert*-butyl ether lipid extraction, successful execution of nanoscale HILIC chromatography, nESI tandem mass spectrometry, and phospholipid characterization using a combination of several open-source programs and manual spectral interpretation. Chapter 3 will expand further on Chapter 2, focusing more on the rationale behind each module from sample creation to annotation, as well as optimization steps and testing to ensure robust operation and measurements. Each step will contain further explanation of why it was deemed to be the optimal approach, supported by experimental data and potential concerns.

Chapters 4 and 5 will apply the comprehensive lipidomics platform designed and described in Chapters 2 and 3 to relevant sample sets and examine how bacteria modify

their membrane in response to environmental challenges, as well as consideration of the concept of membrane fluidity and how bacteria attempt subvert solvent presence causing the softening of the bacteria membrane. Chapter 4 explores changes induced in the model organism *Bacillus subtilis* from genetic alterations to fatty acid biosynthesis and degradation as well as exposure to solvents characteristic of conditions commonly seen in biofuel reactors. Lipidomics will be used to examine phospholipid speciation trends to potentially identify targets for improved production of more rugged *B. subtilis* strains for use in industry, as well as whether manipulation of fatty acid metabolism can be used as a possible vector for improved strain creation as well. Chapter 5 will explore the lipidome of *Pseudomonas putida*, a commonly observed Gram-negative microbe within wastewater streams and a major target for bioremediation studies. Lipidomics will examine how *P. putida* attempts to modify membrane composition as a function of exposure during growth to several chemicals commonly observed in wastewater streams, as well as a composite mock wastewater solution. The dissertation is concluded by a summary of the conducted research, as well as perspectives on the field of lipidomics and possible routes for future research.

This dissertation will demonstrate the development, optimization, and execution of a comprehensive lipidomics platform to characterize phospholipid trends and changes in bacteria as a function of induced challenges during growth. While none of the individual components of this dissertation are necessarily novel in isolation, the simultaneous execution of an untargeted, nanoscale HILIC, nESI-MS/MS analysis of bacterial phospholipids extracted with MTBE and critically analyzed with MS2

validation is one of the first of its kind and will hopefully aid in streamlining future lipidomics studies. Furthering the understanding of how bacteria respond to specific environmental challenges will enable genetic modification of fatty acid and phospholipid synthesis to emphasize beneficial membrane characteristics that show evidence of sustained resistance to toxic conditions, leading to development of bacterial strains that can better survive and propagate for experimental and industrial applications.



## **CHAPTER 2: FUNDAMENTALS OF SAMPLE EXTRACTION, MEASUREMENT, AND DATA-MINING FOR MS/MS-BASED LIPIDOMICS**

## **Abstract**

Omics platforms require delicate planning and execution to fully capture and visualize molecular classes of interest. This is no different with lipidomics; while traditional reversed-phase (RP) methods are prevalent in lipidomics literature, in practice they can be difficult to set up properly, and complete elution of all desired analytes within an extract is not always possible without customized solvent conditions. As a result, an alternative approach using HILIC was crafted with a focus on complete lipid elution over separation quality in order to capture the lipid profiles more fully within the experiments described in Chapters 4 and 5. Presented here is a lipidomics platform utilizing methyl tert-butyl ether (MTBE) extractions and nanoscale HILIC separations alongside nESI ionization and tandem mass spectrometry, with a combination approach to lipidomics informatics and annotation validation. Perspectives on each of the decisions made here will be presented later in Chapter 3.

## **Considerations for mass spectrometry-based lipidomics**

With all omics measurements, it is of critical importance to construct an experimental design that enables the most efficient method of extracting, isolating, and analyzing the target group of molecules for the study being performed. These steps include proper sample preparation, an effective method for cell lysis and extraction of desired analytes, a robust system for data collection, and an informatics approach that allows for efficient use of data and highly accurate annotations. While a certain level of overlap is possible, particularly with chromatography and mass detection, it is important to keep the desired pool of analytes at the forefront of research design.

To that end, a workflow was developed, tested, and executed that aimed to capture and detail the full lipidome of a given sample set. Important analytical metrics were considered along each step of the pathway, including extraction efficiency, matching chromatography conditions to the analytes, and key analytical figures of merit that drove selection of mass spectrometry parameters. To sufficiently capture the information captured within a sample lipidome, it is critical to consider and optimize each of these metrics for both the sample as well as the analyte of interest. Automatic assumption of similarity between lipidomics experimental setups and those used for metabolomics or proteomics could work, but there is no guarantee that it would yield optimal results, and there is an equal likelihood of failure, which is why it is important to select parameters specifically for lipidomics.

For a lipidomics experiment using bacterial samples, it is crucial to understand how to approach construction of a proper protocol. Omics studies have long been subject to the question of how to accurately capture detected features and sample hits within a desired pool of similar analytes that are detected by robust analysis techniques and validated by appropriate informatics packages [106, 107]. This is always the goal for omics platforms, but each pool of analytes presents different challenges and considerations. Metabolomics is possibly the most difficult – potential annotations can come from a massive pool of classes such as sugars, amino acids, nucleotides, and energetics, as well as difficulties introduced by varying chromatography affinities between metabolite classes and shared isomers [108-110]. Genomics and proteomics are made slightly easier by well-defined backbones (nucleotides and amino acids,

respectively) giving a level of predictability to analysis as well as benefiting for a greater length of time in the research spotlight [111]; lipidomics operates in a similar manner, especially in phospholipidomics, where lipids can be characterized and sorted by headgroup and fatty acid chain character (length and level of saturation).

Finally, while not always applicable depending on the sample in question, literature review of previous studies can help to focus analytical targets. Studies are available that have previously characterized normal cultures of the bacteria that were used for the experiments described in Chapters 4-5, which is useful for providing a framework for expected lipid profile composition. This enables studies to focus on how the lipidomes shifts as the cell either changes internally due to genetic modifications or is forced to adapt to changing exterior conditions by using known lipids as a base and then expanding into other potential matches as well as lipid derivatives that are known to exist within the bacteria of interest. Literature is also the best source for most of the novel lipid derivatives or modifications that are of rising interest to researchers, which can help to flesh out the depth of lipidomics measurements.

### **Brief considerations prior to sample analysis**

#### ***Cell culture preparation***

Samples were prepared with experimental design in mind. In Chapters 4 and 5, both bacterial sample sets involved modification of growth conditions specifically for analysis via lipidomics to test the strain and changes that the cell membrane would undergo to attempt to adapt to those changing conditions. Chapter 4 also involved genetic modifications specifically to test how bacteria can adapt when the ability to inherently

produce, modify, and process fatty acids has been stripped away. Samples were delivered in the form of whole cell pellets so that the period of time between cell lysis and analysis was kept as short as possible to prevent degradation or alteration of lipid extracts. Each sampling condition was also delivered in biological triplicate to monitor fluctuations due to experimental design as well as help with statistical validation.

For experiment-specific sample preparation, including cell culturing, genetic modifications, and customized growth conditions, please refer to Chapters 4 and 5.

### ***Chemicals and supplies***

Methanol (MeOH), water (H<sub>2</sub>O), chloroform (CHCl<sub>3</sub>), isopropanol (IPA), and acetonitrile (ACN), all LC-MS grade, were purchased from MerckMillipore (OmniSolv, Burlington, MA, USA). The ionization agent ammonium acetate (NH<sub>4</sub>Ac) and extraction solvent MTBE were purchased from Sigma-Aldrich (St. Louis, MO, USA). Acetic acid (used in preparation of calibration solutions) and nitric acid (used in cleaning of metal LC-MS components) were purchased from Sigma-Aldrich. Calibration solutions for positive and negative ionization modes were obtained from ThermoFisher Scientific (Waltham, MA, USA). Standards were purchased from Avanti Polar Lipids (Alabaster, AL, USA); these include the LightSPLASH LIPIDOMIX Quantitative Mass Spec Primary Standard, the Differential Ion Mobility System Suitability Synthetic Standard Mixture, and standards for individual phospholipids (Table 1). Phospholipid standards were stored in glass vials at -20°C when not in use; dilutions were prepared with a 50/50 solution of methanol and chloroform and stored in glass autosampler vials for analysis. All chemicals were used as supplied, without further purification.

**Table 1. Inventory of lipid standards purchased from Avanti Polar Lipids used in testing and quality control of lipidomics experiments**

LightSPLASH LIPIDOMIX Quantitative Mass Spectrometry Standard (each @ 100 µg/mL)	Differential Ion Mobility System Suitability LipidoMix Kit (each @ 1 mg/mL)	Other Standards
18:1 Cholesterol Ester	19:0 Cholesterol Ester	CL(16:0/18:1/16:0/18:1)
	Cholesterol	CL(16:1/16:1/16:1/16:1)
		CL(18:1/18:1/18:1/18:1)
C15 Ceramide (d18:1/15:0)	Ceramide (18:1/18:1)	
		PC(15:0/15:0)
MG(18:1)	DG(14:1/14:1)	
SM(d18:1/18:1)	SM(18:1/18:1)	PE(16:1/16:1)
TG(15:0/18:1/15:0)	TG(18:1/18:1/18:1)	PE(18:0/18:0)
		PE(18:1/0:0)
PC(15:0/18:1)	CL(14:1/14:1/14:1/14:1)	PE(18:1/18:1) (Δ9-Cis) (DOPE)
PC(18:1/0:0)	PA(14:1/14:1)	PE(18:1/18:1) (Δ9- Trans)
PE(15:0/18:1)	PC(14:1/14:1)	
PE(18:1/0:0)	PC(18:1/0)	PG(18:1/0:0)
PG(15:0/18:1)	PE(14:1/14:1)	PG(18:1/18:1) (Δ9-Cis)
PG(15:0/18:1)	PG(14:1/14:1)	PG(18:1/18:1) (Δ9- Trans)
PI(15:0/18:1)	PI(14:1/14:1)	
PS(15:0/18:1)	PS(14:1/14:1)	

### **MTBE extraction as an alternative to traditional chloroform-methanol methods**

While most traditional approaches to cellular lipid extraction rely on decades-old chloroform/methanol solvent systems [112, 113], the use of MTBE as the organic solvent for lipid extraction has risen in popularity in recent years because of a significantly lower density, resulting in separations that have the organic layer lying on top of the extraction mixture instead settling to the bottom. The generic outline of an extraction using MTBE as the primary organic solvent for trapping lipids was first published by Matyash in 2008 [114], with solvent amounts scaled down to match smaller sample sizes while retaining published solvent ratios.

After receipt of the cell pellets and any required washing steps, cell samples were kept at -80°C for storage as recommended for long term lipid viability [115]. dried cell pellets (typically around 10-50 milligrams each and around 10% of the dry weight of bacterial cells [116]) were left in 1.5 mL Eppendorf centrifuge tubes for extraction and stored on ice whenever possible. Once samples were dried and isolated as dry cell pellets, it is often advisable to keep track of dry cell weights, both to help with data normalization as well as allowing for percentage weight calculations of the lipid extract from the cell.

To begin, 150 µL of methanol were added to each sample, after which the samples were each vortexed for approximately 10 seconds to ensure cell dispersion. 500 µL of MTBE was then added to each sample. A Branson 450 digital sonifier (Branson, CT, USA) fitted with an upright adaptor was used to mechanically lyse cells; the sonicator top was rinsed with a 70% ethanol solution before and after each cycle of cell lysis. Samples were pulsed for 10 seconds at 20% amplitude, followed by 10 seconds of

rest, for a total of 2.5 minutes of sonication and a total lysis cycle length of 5 minutes. Samples were suspended in a room temperature water bath during sonication for cooling.

After cell lysis, samples were lightly shaken on ice for 1 hour. To induce phase separation, 125  $\mu$ L of water was added to each sample and briefly sonicated. Samples were centrifuged for 15 minutes at 4°C at 20000 x g to confirm phase separation. The upper MTBE organic phase containing the nonpolar lipids was removed for drying, and the lower aqueous layer (containing polar metabolites and DNA) and protein pellet were retained in case further analysis using metabolomics, proteomics, and/or genomics. Each 500  $\mu$ L organic partition was concentrated to 100  $\mu$ L using a nitrogen air stream, and all samples were stored in a -20°C freezer until analysis, the recommended temperature by Avanti Polar Lipids for storage of their standard mixes [117]. Previous literature reports storage at -80°C being appropriate [115], though Avanti does warn against long term storage at extremely low temperatures. Total lipid mass or concentration was not measured, but there are methods [118] using ultraviolet-visible spectroscopy (UV-Vis) [119, 120], Fourier transform infrared spectroscopy (FTIR) [121-123], and nuclear magnetic resonance spectroscopy (NMR) [47, 124, 125] that can accomplish this if desired, as well modified mass spectrometry (MS) methods such as those described here in tandem with standards [50, 126, 127]. The experiments in Chapters 4-5 were targeted at assessing relative shifts within phospholipid profiles, so more quantitative measurements using dry cell weights and standard dilution curves were not as necessary.



## LC-MS/MS Analysis

### *Setup of HILIC-based liquid chromatography methods*

Liquid chromatography (LC) separations were performed using a Dionex UltiMate 3000 HPLC pump and autosampler (ThermoFisher Scientific), coupled to an LTQ Orbitrap Velos Pro mass spectrometer (ThermoFisher Scientific) for mass detection. Described here is the preparation, upkeep, and use of the liquid chromatography segment of sample analysis, as well as the basic principles of chromatography and why it is an effective tool to couple to mass spectrometry for both general omics analyses as well as the uses and considerations in lipidomics.

Chromatography is a very simple but powerful approach for achieving highly customizable separations. The technique relies on equilibrium partitioning involving three separate entities – the stationary phase, the mobile phase, and the analyte. Experiments utilizing chromatography must take stock of a few things. Of primary importance is the analyte of interest – this could be as simple as a single class of molecules largely sharing chemical properties or as complicated as a generic cellular extract containing anything soluble in the extraction solvent. As mentioned earlier, most omics studies focus on a specific class of molecules, with the notable exception of some untargeted metabolomics research. Knowledge of the general chemical characteristics of the sample in question drives the decision making in selection of the stationary and mobile phases. The stationary phase is the solid material to which the analytes adhere; optimal stationary phases will retain most/all analytes in a sample but not to such an extent that the mobile phase is unable to break the interactions between the analyte and

the column. The mobile phase, either a liquid or a gas, can be constructed in a variety of different ways. Depending on the interaction between the analyte and the stationary phase, the mobile phase can be as simple as a singular component or as complicated as a multi-step, multi-component gradient that forces elution of different analytes with solvents of varying chemical characteristics [128].

For a liquid chromatography setup coupled to a mass spectrometer, column selection is the first consideration. While micro-scale and capillary liquid chromatography methods have been used in mass spectrometry-based analyses for years with larger scale columns (inner diameters on the scale of millimeters and hundreds of micrometers), [129], reduction of the inner diameter of the column can grant significant analytical advantages, which is why the use of nanoscale chromatography methods (using columns with tens of micrometer inner diameters) has become more widespread in recent years [130, 131]. Use of nanoscale liquid chromatography offers several advantages when applied to LC-MS experimental designs [132, 133]. The decreased size of the column automatically reduces both the amount of solvent needed for analysis as well as the amount of sample needed to achieve similar analyses. This is automatically appealing to omics analyses, where sample amounts are often precious and limited - instrument failure no longer means restarting from the beginning because not all sample is necessarily expended in the first attempt at analysis.

The other consideration in column selection was stationary phase. Both RP and HILIC columns were considered for use with lipid extracts. While several RP columns (C5 and C18 being the most notable) were tested for their ability to elute lipids with

various mobile phase compositions, it was determined that lipids could not be disassociated from the highly nonpolar character of RP columns without a mobile phase composed of predominantly isopropanol. Isopropanol has issues as well when used as a major component of a chromatography gradient. When a chromatography gradient has upwards of 90% isopropanol content, the high viscosity of isopropanol can cause pressure spikes within the LC; while the UltiMate 3000 system is rated for high pressure chromatography systems, this is not universally applicable. Additionally, while the LC might be rated for higher pressure chromatography systems, this is not always applicable to the downstream fittings used to connect the LC to the column, as higher viscosity solvents can cause those fittings to rupture due to an increase in system pressure.

Therefore, the column of choice for untargeted lipidomics analysis was HILIC. HILIC and RP operate in complementary manners; while RP separations elute increasingly nonpolar analytes, HILIC separations start with the elution of hydrophobic analytes and end with elution of hydrophilic analytes (Figure 4). This complementary relationship has a unique dichotomy in lipidomics – RP separations tend to separate lipids based on fatty acid chain length, while HILIC separations are usually driven by lipid head groups. Here, the polymeric ZIC-pHILIC zwitterionic stationary phase was used (5  $\mu$ m, SeQuant, bulk stationary phase provided through special request via Merck Millipore), demonstrating efficient hydrophilicity-based separations (Figure 4B). Because of the specialized nature of the stationary phase being used here, special instructions for preparation, care, and use of a HILIC column are included; unless otherwise noted procedures described here are in accordance with SeQuant's provided direction [134].

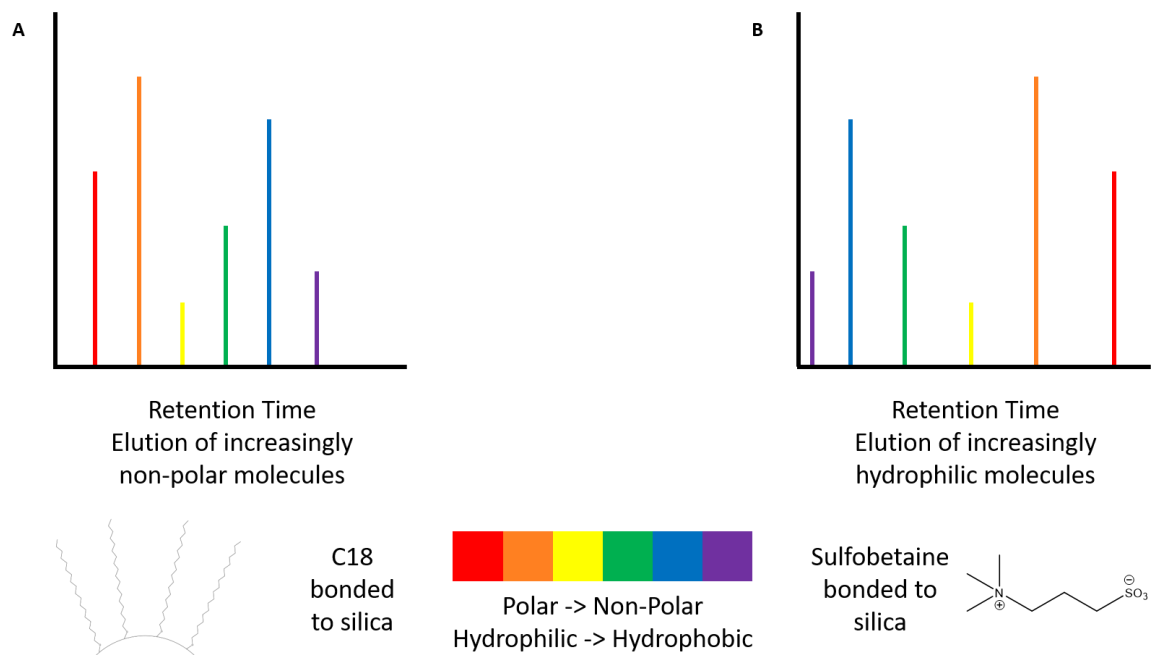


**Figure 4. Mechanics of analyte elution on columns using A. RP (C18) stationary phase and B. HILIC (ZIC-pHILIC) stationary phase, along with schematics of the stationary phases.**

Columns were prepared in-house using a laser tip puller and pressure cell. A P-2000 laser-based micropipette puller (Sutter Instrument) was used to create the electrospray tips on a length of 100  $\mu\text{m}$  inner diameter (i.d.) fused silica (Polymicro Technologies) sufficient to pack a 15 cm column with a small amount of void volume. The empty, fused silica tip was then packed with the HILIC stationary phase by use of a pressure cell driven by helium carrier gas. The stationary phase was delivered via a slurry composed of around 100 mg of the ZIC-pHILIC column material and 1 mL of 5 mM ammonium acetate in water. Columns were filled to approximately 15 cm on the pressure cell, usually erring on the side of excess in the case of further packing induced by the pressure exerted by the LC instrument.

The construction of the LC solvents and gradient is shown in Table 2. For HILIC columns, the gradient started with the strong organic component of the mobile phase and shifted towards the more aqueous component to elute increasingly hydrophilic compounds off the column. As with preparation of the column, there was a level of care needed to balance the amount of water that the column can take at any given time. Per the care and use instructions, the column always needs to have a minimum level of water exposure to keep the stationary phase hydrated. However, oversaturation of the column with water, overly steep gradients, or extreme flow rates can lead to a complete loss of column separation efficiency, making the preparation and upkeep of HILIC columns difficult without adequate experience. Those factors were taken under consideration during crafting and testing of the LC gradient to ensure that the column was operating properly.

**Table 2. Gradient conditions for nano-LC-MS separations using ZIC-pHILIC stationary phase.**

ZIC-pHILIC Gradient Conditions

Time, minutes	% B (97/3 ACN/H <sub>2</sub> O + 5 mM NH <sub>4</sub> Ac)	% A (5 mM NH <sub>4</sub> Ac in H <sub>2</sub> O)
0	100%	0%
1	100%	0%
20	40%	60%
25	100%	0%
35	100%	0%

The HPLC flow rate was set to 100  $\mu\text{L}/\text{min}$ ; this was the flow rate of the mixed solvent and sample flowing out of the LC. However, this was not the effective flow rate being delivered downstream at the tip of the column. Instead of a split less flow system where all solvent and sample are delivered directly to the ESI source of the mass spectrometer, this setup utilized a split flow system, discarding the majority of the LC output to waste and only delivering a small fraction of the total solvent/sample mixture to the mass spectrometer [135]. This is largely done to perform nanoflow LC-MS/MS measurements, where samples in nanoliters worth of liquid are ionized instead of microliters [136-138]. Estimates of the flow rate at the tip of the column were made via liquid collection with a capillary – typical columns tested throughout the course of later described experiments delivered flow rates of approximately 100-300 nL/min, meaning that over 99% of the original LC liquid flow was being discarded to waste.

### ***Quality Control***

Prior to runs, there were several checks and cleaning steps performed to ensure that the liquid chromatography setup was functioning optimally. Upon changing chromatography solvents and prior to a sample set, each line leading from the solvent bottle to the mixer within the instrument was purged to waste for 5 minutes to remove any lingering air bubbles from the solvent and solvent lines that may have been introduced during exchange or refilling of solvent bottles. Similar checks were made with the injection needle; sequential blank injections of a set volume of solvent B were performed to ensure that the autosampler is drawing the correct amount of liquid from a vial, and the injection needle is checked for any buildup of air pockets that could skew

the effective injection volume. For downstream checks, all plumbing past the exit line from the LC to the column was replaced and/or cleaned prior to a new sample set being run. Fused silica lines, including connective pieces between the LC and the column as well as the waste line, were replaced with clean fused silica, metal connective pieces were sonicated in a 35% nitric acid solution and rinsed with water and methanol, and plastic connective pieces were either cleaned with a 10% methanol solution or replaced for new ones if irreparably clogged.

After equilibration of a new column but before exposure to any sample sets, standard mixes (Avanti's Ion Mobility mix or their LightSPLASH mix) were run on the column in order to confirm that analytes were eluting off the column properly and that the retention quality of the stationary phase was in line with expected results. As mentioned later, this was also done sporadically within sample sets for spot checking as well as at the end of a sample set to confirm that there had not been any drift in retention time or degradation of column quality.

## **Operation and methods for tandem mass spectrometry using the LTQ-Orbitrap Velos Pro**

### ***Fundamentals of nano-electrospray ionization***

The first consideration needed when approaching an experiment in mass spectrometry is the method with which ions will be delivered to the mass spectrometer. The mass spectrometer can detect molecules as charged ions, not as neutral molecules, so it is important to use a technique that will efficiently convert analytes into charged ions. There are several approaches which can adequately do this – electrospray ionization (ESI), matrix-assisted laser desorption ionization (MALDI), and atmospheric pressure



chemical ionization (APCI) are the most common sources used in mass spectrometry. For the LTQ Orbitrap Velos Pro instrument used in later experiments, ESI-based methods were used.

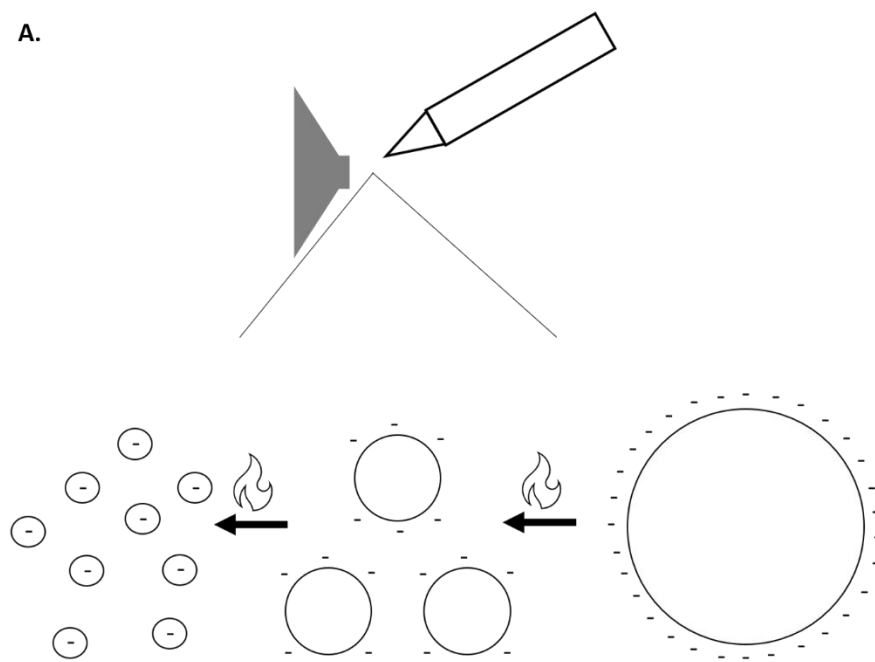
Electrospray ionization has long been known as a possible method for delivering molecules in a liquid medium by converting them into gaseous ions. Taylor [139] and Dole [140] both theorized that there was a way to use electrospray to create beams of molecules from a liquid source, but they were both limited by the technology of their day. Only in the 1980s did instrumentation finally catch up with theory, and Fenn and Mann discovered a way to convert proteins into gaseous ions in a way that did not destructively break them down [141]. Since then, ESI-based MS experiments have risen to prominence as reliable, sensitive methods for analyte detection.

Electrospray ionization operates on a relatively simple concept (Figure 5A). ESI starts with proper composition of the mobile phase using either an aliquot of liquid (for direct infusion approaches) or a liquid chromatography gradient infused with sample, combined with an ionization agent, usually a volatile weak acid (acetic or formic acid) or base (ammonium acetate) to have prepared charged ions present at the point of emission from the column tip. As the liquid stream approaches the column, an electric voltage is applied to the liquid, creating a stream of small, charged droplets that erupt from the tip of the column. This is achieved by creation of an electronic potential between the capillary and the tip of the column, usually around 1-5 kV and attuned before runs to create decent spray quality as well as ion transfer. As the charged droplets leave the tip of the column, the heat of the adjacent capillary in the instrument causes rapid evaporation

of the LC solvent. The shrinking size of the droplets creates a subsequent increase of charge density across the droplet, rapidly increasing the Coulomb repulsive force contained within the droplets. Once the droplets shrink enough and that force is powerful enough to overcome the adhesive force of the solvent mixture's surface tension, a Coulomb explosion occurs, causing fission events creating increasingly smaller droplets. This process continues to occur until all solvent has been fully evaporated and raw ions are being ejected and pulled into the heated capillary by the vacuum created within the mass spectrometer. This process of creating gas phase ions from the output of a liquid chromatography column creates a visible phenomenon known as the Taylor cone (Figure 5B) [142, 143].

While good in theory, there are some significant challenges that arise when analyzing samples instead of controlled standards. Complex mixtures, the purity of a sample, LC solvent composition, and the presence of salt within the sample can create significant issues with electrospray ionization [143]. Many of these problems can be overcome by using a separation technique prior to mass analysis, which is why chromatography methods are so often attached to mass spectrometry. Another approach is careful formulation and tuning of solvent compositions. The high surface tension of water makes it unappealing as a dominating component of an ESI-based LC-MS experiment, so more volatile organic solvents are often included to coax conditions to a state that is more amenable to ESI methods [144]. This is also why most mass spectrometry experiments only focus on one class of molecules; it reduces the variables needed both in extraction as well as fine tuning analysis.

A.



B.

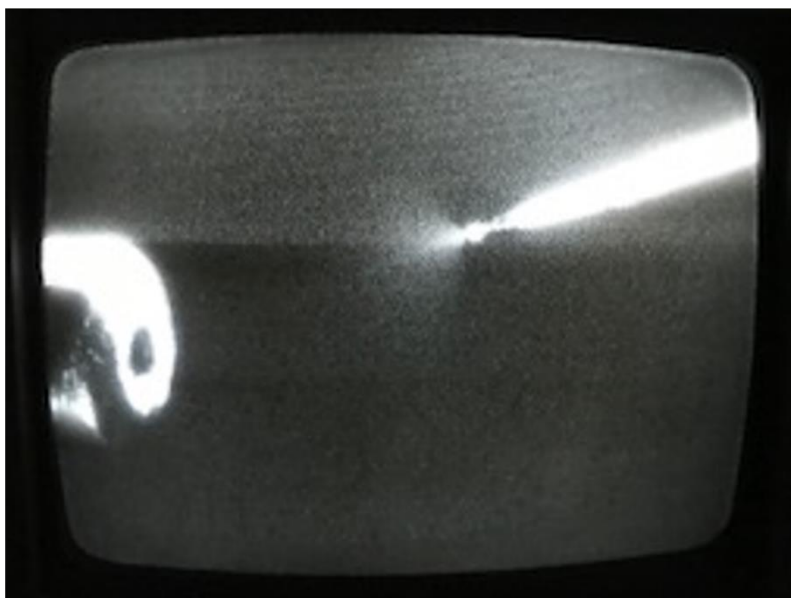


**Figure 5. Fundamentals of electrospray ionization, demonstrating A. ion formation through the Coulomb explosion generating dry charged ions that are left to be pulled via vacuum into the mass spectrometer, as well as the B. the Taylor cone, an observable demonstration of this phenomenon.**

However, the issue of salt interference is one that is not easily solved, especially when it comes to samples that end up being extracted within water or water-soluble solvents. The presence of salt within a sample can create significant interference once a voltage potential is applied at the column tip, leading to bad spray quality and poor ionization. Thankfully, increasing use of nESI has helped to alleviate this [145, 146]. The issues of salt intolerance and sample investment that plague normal ESI approaches can be significantly mitigated by using a narrower bore column, which also then lowers the solvent investment and LC flow rate requirements [147, 148]. The biggest advantage is an overall increased tolerance for salt present in the sample. With less injected sample volume and lower sample flowing through the column (on average an order of magnitude less), effective salt concentrations at the tip are much smaller, meaning there is less interference caused during ionization [149]. While this is not nearly as relevant in lipidomics, where samples are extracted in highly organic solvents, it does significantly help in aqueous extracts used in proteomics and metabolomics. Still, the lower sample injection investment is always beneficial, no matter which method is used.

### ***A brief discussion of mass analyzers***

The LTQ Orbitrap Velos Pro (schematic in Figure 6, instrument image in Figure 7) was used for mass analysis. This instrument contains two different mass analyzers, enabling MS/MS experiments that can capture both precursor scans and fragmentation of individual ions within that precursor scan. MS/MS approaches are incredibly valuable, enabling full cataloging of masses within a sample while also correlating masses with tentative annotations through characteristic fragmentation ions or patterns.

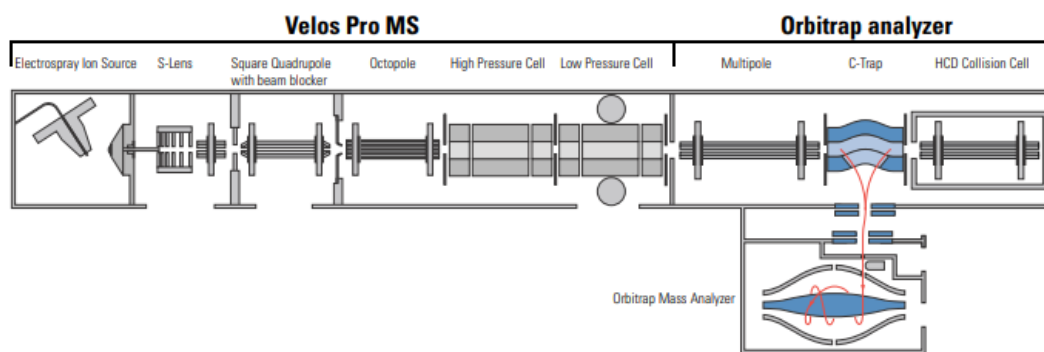


**Figure 6. Schematic of the LTQ Orbitrap Velos Pro mass spectrometer (ThermoFisher Scientific) [150].**

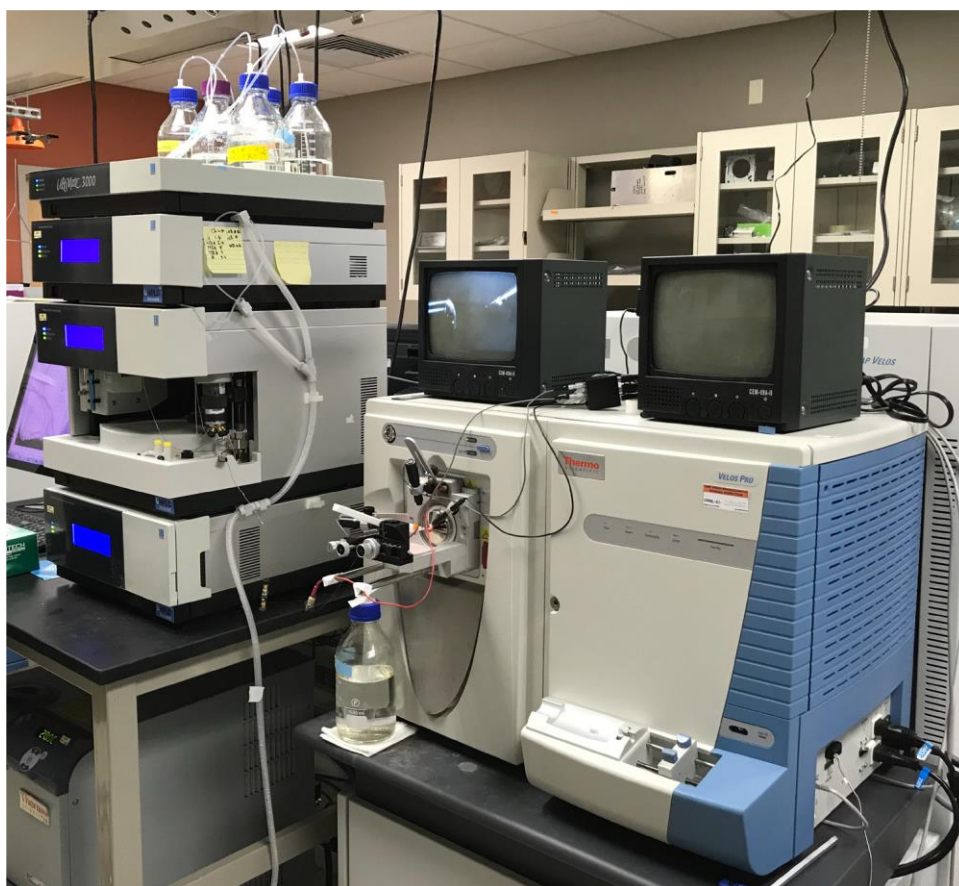


**Figure 7. Image of the LTQ Orbitrap Velos Pro mass spectrometer (photo taken by the author).**

In order to fully capture the data contained within a lipid extract, a method was created to not only detect the masses of precursor ions (defined as MS1 scans, the first and most basic level of mass spectrometry analysis) but also destructively fragment those precursor ions and record the fragmentation patterns of each precursor ion (defined as MS2 scans, as in the second and next deeper level) that can be used to more definitely confirm tentative annotations and provide an extra layer of validation that can be utilized by certain informatics packages. The methods by which these scans are recorded differ depending on experimental design and the desired level of resolution depth with which one wishes to capture data. Here, lipidomics runs were operated in a high-low scan mode, with precursor MS1 scans obtained within the high-resolution Orbitrap and 10 subsequent MS2 fragmentation scans were obtained within the low-resolution ion trap using the top 10 most intense unique ions from the MS1 scan.

The Orbitrap is an incredible piece of technology, dating back to theories in the 1920s stating that it was possible to trap ions within a metal can using only a charged wire [151]. While intriguing in theory, applications for mass spectrometry were nonexistent; trapping ions was great but there was no way to convert those trapped ions into tangible mass information. Despite attempts to couple a detector to the system, the simplistic design of the metal wire and can model made separation of complex samples nigh impossible [152]. This problem was finally alleviated thanks to the work of Makarov, who took the can and wire model and reengineered it such that the wire was now a large, machined electrode in the general shape of a football [153]. Further advancements led to the C-trap, which allowed efficient coupling to other mass analyzers

contained within one instrument and sequential injection of packets of ions into the Orbitrap [154]. This design enables injection of specific packets of ions into the trap, which are contained as oscillating rings around the central electrode that exert slightly different currents that can be detected by an amplifier and converted into  $m/z$  values. Here, the Orbitrap is utilized to capture high resolution precursor MS1 scans.

Once the instrument creates an MS1 scan with a given list of ions, a list of the top ions in terms of abundance is created depending on the desired number of fragmentation scans as well as exclusion list settings forcing ignorance of ions that have recently been fragmented (here, this was set to exclude ions observed within the previous 30 seconds and not to select them for fragmentation for the next 120 seconds). In the experiments described here, ten MS2 scans are created per MS1 precursor. These MS2 fragmentation scans are created using collision-induced dissociation (CID), where ions are excited through the application of an electrical potential and fragmented through collisions with an inert gas (here, helium). This data-dependent acquisition (DDA) method of high-resolution precursor scans created within the Orbitrap and subsequent lower-resolution fragmentation scans created by CID within the two-dimensional ion trap from the initial MS1 scan is repeated throughout the entirety of an LC-MS/MS run.

Finally, a brief examination of analytical figures of merit was necessary to fine-tune the MS/MS method. The first metric is quite simple – mass range is usually relatively easy to establish. For lipidomics, there are distinct groups of lipids and lipid components that lie within specific mass-to-charge ( $m/z$ ) values. Basic fatty acids are  $m/z$  200-400, lyso-phospholipids containing only one fatty acid chain are  $m/z$  400-600, most

basic phospholipids are  $m/z$  600-800, and cardiolipin species start at  $m/z$  1100-1200.

With that in mind, the mass range selected for the lipidomics experiments described here was  $m/z$  200-2000.

Next are mass accuracy, sensitivity, resolution, and duty cycle – key analytical figures of merit in mass spectrometry that warrant consideration when crafting a method for MS/MS analysis. Mass accuracy is perhaps the easiest to define as well as actively monitor – as described in the next section, frequent checks of mass calibration using specially crafted calibration solutions enables that the instrument accurately detects masses. Typically, calibration checks keep mass error below 1 ppm, while in practice Orbitrap instruments can reasonably retain a mass accuracy between 5-10 ppm.

Sensitivity is typically a bit more nebulous. Sensitivity refers to signal-to-noise ratio, which generally is a measure of how well the samples can be detected against the inherent background noise signal of a mass spectrometry run. This is typically achieved not through a specific setting but rather through testing and modification of several different parameters, including sample loading amounts, selection of an appropriate chromatography technique, testing and use of an optimal ionization voltage for a given setup, and avoidance of ion suppression agents within the mobile phase.

Resolution and duty cycle go hand in hand. Resolution is the ability of an instrument to be able to distinguish between two peaks whose  $m/z$  values are closely related, thus enabling accurate assignment of  $m/z$  values as well as efficient discrimination of between  $m/z$  values that are close in value. Orbitrap instruments can achieve resolutions as high as 100,000, but this is more relevant when applied to highly



complex samples that contain thousands of potential features processing at the same time. Lipidomics samples are far less complex, and as such, there is less need to examine samples quite that deep, so these runs were performed with a resolution of 30,000. Duty cycle is the amount of time it takes to accomplish one full “cycle” of scans, or the amount of time that it takes the mass spectrometer to complete detection of a singular MS1 scan and the 10 data dependent MS2 scans. Resolution and duty cycle share an inverse relationship – while slowing scan rate down will allow for better ion accumulation and increased mass accuracy, less ions can realistically be detected, and with the coupling of chromatographic separations, this can lead to lost features. Therefore, a balance must be struck between resolving power and being able to process ions in a timely, efficient manner.

### ***Instrument quality control***

As with the LC, the mass spectrometer does require a certain level of upkeep to maintain good working order. Weekly calibration checks were performed on the instrument to ensure that both the ion trap and the Orbitrap/FT analyzer were working as expected, using calibration solution containing compounds with masses that are recognized by the instrument for mass calibration and other checks. An ion optics charging evaluation was also done during those checks to discharge ion buildup on the instrument lenses by sequentially swapping the polarity of the electronic potential across each lens. In the case of a failure to pass, the merits of an inhouse instrument cleaning were considered, where the RF lenses and the top coverboard containing the quadrupole and octupole were removed and all accessible lenses and multipoles were cleaned using

multiple sonication-aided washes with soap, water, and methanol. The heated capillary, through which ions enter the mass spectrometer, was cleaned with a 35% nitric acid wash before sample sets were processed to remove any buildup. Because the mass spectrometer creates vacuum using heavy duty vacuum mechanical pumps, those pumps were frequently ballasted and checked for oil leaks, refilling if necessary.

### ***On internal standards***

Before discussing data analysis, it is worth mentioning the use of standards in analysis. While it has been mentioned that standards were regularly used for quality control purposes, no internal standards were explicitly used during the testing of bacterial lipidomics samples. Data normalization was and remains a key aspect of backend omics data processing, lipidomics not excluded [155], but often internal standards are much more useful for quantitative studies [156]. Many of the relevant research questions surrounding the bacterial lipidomics experiments described here involve relative comparisons instead of absolute quantification of all lipid species present in the samples, and as such, there is little need. Chapter 3 describes the use of standards to help normalize mass spectrometric response as a function of phospholipid headgroup, but this is largely the extent of any quantitative analysis performed with the samples analyzed in Chapters 4-5, and as such standards were largely reserved for quality control before and during mass spectrometric analysis of bacterial lipidomics sample sets. Additionally, the use of dry sample weights and statistical data normalization was deemed more than sufficient for the relatively qualitative analysis being performed in this dissertation.

### **Approaching the difficult task of processing MS-MS lipidomics data**

As with all omics-based analyses, it is important to choose informatics packages and approaches that are appropriate for the type of analysis that is being performed. There are several options for analyzing lipidomics data, with the choice being between free open-source programs and vendor-curated packages that can be used effectively, so it is crucial to test several potential options and select programs that best help in answering relevant research questions. For the projects and experiments described in Chapters 3-5, it was essential to have access to a way to consolidate multiple raw files into one dataset matched across detected masses, validation of annotations using MS2 data collected in each raw file, and methods for simple statistical analysis and comparison between sampling conditions. The following section describes the selection of programs and processes that were used to process raw lipidomics files, assign tentative annotations to lipid features, and perform basic statistical analysis, as well as why each choice was key in comprehensive analysis.

#### ***Bulk processing of raw MS/MS files using MZmine***

Raw LC-MS/MS files were first processed using the open-source software MZmine2 (version 2.53) [99]. The framework of the analysis performed here using MZmine was previously outlined [157] and modified for use with extracted lipid sample sets. After downloading, selected raw files were first uploaded into the program using the Raw data import option. For the experiments described here, all copies of the dataset raw files plus a few blanks from the beginning of the sample set to remove background peaks were uploaded to MZmine. To begin analysis, the MS/MS peak peaker was used to scan

each raw file and extract any chromatographic peaks that have MS2 scans associated with them. Metrics were selected in accordance with the method file used in Chapters 3-5 for lipidomics runs. For this and most subsequent modules, 10 parts per million (ppm) was used for the m/z window as that is generally considered to be the upper end of the mass error for the LTQ Orbitrap Velos Pro instrument used for mass analysis. This module specifically did not have an option for ppm error, so  $\pm m/z 0.05$  was used as an analogue for 10 ppm. The time window of 35 minutes was set to match the length of the LC gradient, and the polarity and spectrum types were similarly matched to the MS method of negative ionization and centroided spectra, respectively.

Having extracted peaks that contained MS2 hits, the next step was to transform and shape those single points into fully exploded extended peaks using the Peak Extender module. This was done by searching in both directions from a point found in the previous step and extending the peak shape through each scan until no valid data was found within the bounds of the selected m/z window and/or minimum peak height requirement. The mass tolerance here did have an option for both m/z window and ppm, so the same values were used as described earlier. This module also had a minimum peak height restriction; typically, this can be attuned to the noise threshold of the sample as demonstrated by blanks. In these lipidomics samples, the noise threshold is typically in the E4-E5 range, but for analysis it was intentionally kept it lower just to ensure that any relevant lipid species that were present at lower concentrations in the sample did not accidentally get removed from later analysis.

After regeneration of peaks from the raw data, the next step was to begin removing extraneous data and consolidating files. The first step was isolating isotope packets within the peak lists by identifying groups of peaks that formed an isotope packet using the Isotope peaks grouper module. This module would consolidate an entire isotope packet down and only retain the main, naturally occurring isotope peak for later steps. For metrics, retention time tolerance was kept tight to 1 minute; any peaks that would be within an isotope packet should elute near the parent peak. Because the expected features in these sample sets were only singly charged, the monotonic shape function was enabled, and the maximum charge was kept at 1. Finally, the  $m/z$  tolerance was kept the same as described previously. As a side note, when MZmine was employed for data consolidation of runs where isotope labeling was used, this step was not used to avoid removing any peaks that were of interest.

The next step of data filtering involved the removal of duplicate peaks within the datasets using the duplicate peak filter. This allows extraneous peaks to be removed in favor of the most abundant peaks for a given  $m/z$  value. Duplicate peaks can be a byproduct of overloading, poor column performance, or simply the presence of analytes that have a high affinity with the column, all of which are hopefully removed through column and system quality control testing but can still be a factor. For these lipidomics runs, the NEW AVERAGE filter mode was used, which considers peaks as duplicates if their  $m/z$  values and retention time differences are within the set tolerances. This filter created a consensus row using the lowest ID number, which is related to retention time; this accounted for peaks of analytes that are retained on the column for most/all of a

chromatography run. The  $m/z$  tolerance was kept the same as before; the retention time tolerance was kept wider at 5 minutes to account for long eluting peaks, which is a concern specific to potentially sticky and recalcitrant lipid samples.

Next, the retention time of samples was normalized using the retention time calibration module (this was referred to as the retention time normalizer module in previous versions of MZmine). As indicated by the name, the function of this module was to attempt to reduce the variability between retention times of a given  $m/z$  within a peak list. This module treated peaks (and their  $m/z$  values and retention times) shared across all files as standards and used them to adjust the retention times of all other peaks within the list of selected files. The  $m/z$  tolerance and minimum standard intensity were kept the same as with previous modules, and the retention time tolerance was kept relatively strict at 3 minutes because there was a low likelihood of peaks that escaped previous filters that fall well outside those bounds needing to be aligned using this tool. Finally, this module was only used on sets of similar samples, and never on blanks.

After application of relevant filtering steps, the next step was to align all the separate peak lists from the samples and blanks into one file. There are a few options contained within MZmine that can do this; the RANSAC aligner [158] was selected for this analysis. Samples were aligned by using a master peak list created by the alignment tool and through the creation of a model of deviation across all samples to align retention times. Previews provided within MZmine allowed for modification of parameters if the model did not perform well across most peaks. For metrics, the retention time tolerance was set to the length of the run as done previously, and the retention time tolerance post

correction narrows the range that the aligner can probe for correction. Here, this correction was set to approximately 2/3 of the full run length. RANSAC iterations indicates the number of times the module will search for the right model for use in alignment. Because that number is typically not known, a value of zero can be used to let the tool decide the number of necessary iterations needed, and that is what was used here. The minimum number of points needed to create a valid model is dependent on how strict the researcher desires the model to be; because these are somewhat rich sample sets, this value was set low at 10%. The same charge state is also required, simply because none of the desired samples should have variable charge states. Finally, the threshold value is like previous retention time tolerance values, indicating the window within which a data point can fit the created model; because these samples have already been processed, this window was set low at 1 minute.

Here, analysis can be somewhat divergent depending on what is desired. If there is a predetermined list of results that needs to be probed, the aligned file can be exported for analysis within Microsoft Excel using a list of masses. If automated search results are of interest, MZmine has built-in tools for searching LipidMaps as well as a relatively new in-house lipid search tool [159]. To have the search results in hand for comparison to later searches, the online database search module was used to search LipidMaps, while the lipid search module was used for the MZmine-based tool. LipidMaps bounds were kept within the boundaries of the LTQ Orbitrap Velos Pro's expected mass error, with the m/z tolerance kept at 10 ppm as described previously and the ionization type set to the

standard [M-H]<sup>-</sup> as well as [M-Ac]<sup>-</sup> to account for complexes formed as a byproduct of the ammonium acetate included in the mobile phase.

For the lipid search tool, constraints were kept wide simply because of the known presence of cardiolipin in the bacterial lipid extracts. The ionization methods searched were the same as with the LipidMaps search, and all possible lipids were probed.

### ***Leveraging tandem MS data using LIQUID***

MZmine's power lies largely in data analysis and refinement; however, in order to fully leverage the power of MS2 fragmentation spectra, LIQUID was chosen as an excellent complementary tool. LIQUID is another free, open-source program that uses a database of MS2 fragments to match to imported raw files and gives scored returns based on the level of overlap between MS2 peak and database as well as MS1 m/z matching [98]. LIQUID has a very simple and user-friendly interface (Figure 8). For a global analysis of a single file, as was done for the lipidomics samples acquired in Chapters 3-5, the mass errors were set to expected Orbitrap values of 10 ppm for precursor masses and 100 ppm for CID mass error. Lipid target libraries for both positive and negative mode are provided within the download of LIQUID; the library for the relevant ionization mode was loaded into the program. Raw files were uploaded and processed to output a list of tentative identifications, scored by the level of overlap with MS2 fragments stored within the database. A higher score indicates a higher level of overlap with the database.



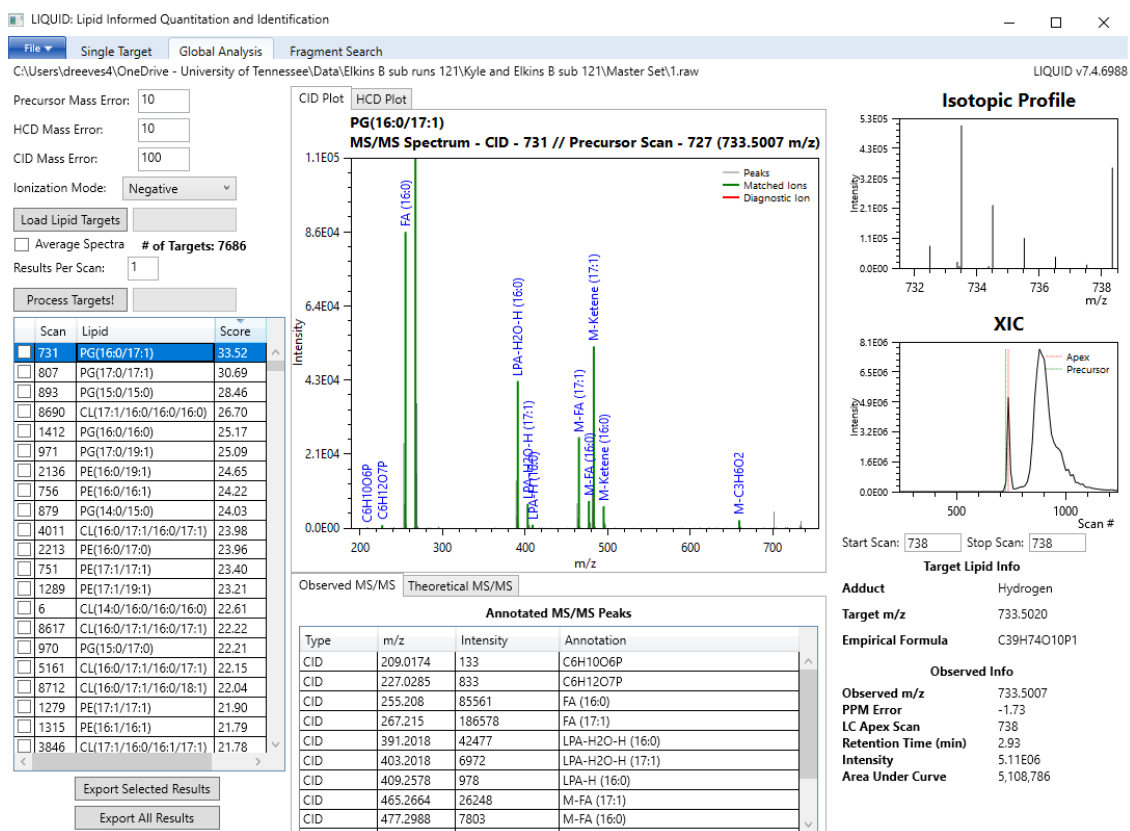


**Figure 8. Example LIQUID output, showing the interface and customizable search options and an example sample run and matching of MS2 peaks to the database.**

Each LIQUID output was then exported as a .csv file and further filtered in Microsoft Excel. Manual examination of outputs, such as the sample output shown in Figure 8, led to application of an arbitrary score cut off at 10 and above, which is (on average) where the quality and quantity of MS2 matches begin to drop. The resultant pool of potential hits was then manually filtered to remove duplicate m/z values to narrow down search results from hundreds of rows to around a few dozen. Finally, sample outputs were manually consolidated and aligned, with care taken to retain which annotations corresponded to which specific sample runs. For comparative analysis across an entire sample campaign, a tentative annotation was not removed within a specific sampling condition if it was present in at least 2 of the three triplicate sample runs; any annotations that only appeared once across a triplicate were removed. This method created robust lists of tentative annotations across several different sampling conditions that take full advantage of MS2-level validation.

Where LIQUID fails is where MZmine shines – LIQUID can only process one raw file at a time, and it also has no tools built into the program for data filtering or processing. As a result, there is a lot of manual processing needed to be able to fully utilize the output of a LIQUID file. Manual data filtering and alignment of files must be done by hand with the exported LIQUID outputs through Microsoft Excel, a task that can be increasingly tedious the larger the sample set is. However, it is a necessary step to obtain a focused list of tentative annotations with which to begin analysis. Despite these difficulties, MZmine and LIQUID are excellent when used in tandem. Cross validation of the highly processed aligned MZmine files and LIQUID outputs with validated MS2

scans gives rich peak lists from which inferences can be made about the biology of the system.

### ***Manual spectral interpretation using Xcalibur***

Manual interpretation of files was also necessary to characterize lipid derivatives and modified lipid species either known or theorized to be present in sample sets, including everything from fatty acid oxidation products to aminoacylated phospholipids. ThermoFisher's inhouse qualitative browser contained within the control software Xcalibur (version 3.0.63) was used to manually locate species of interest, such as the aminoacylated phospholipids described in Chapters 4-5. The qualitative browser allows manual exploration of raw files, with the ability to pull out peaks by  $m/z$  value or an  $m/z$  range and examine the MS2 spectra for presence and quality.

### ***Statistical analysis using MetaboAnalyst***

For statistical analysis and data visualization, there were a few options available. InfernoRDN (previously known as DAnTE) [160] was previously used to validate datasets and generate data-driven images for publications, but it has not been supported and updated frequently and contains modules for crucial steps that either break or are non-functional. As such, a different program was desired that could handle basic statistical analysis as well as being able to produce high quality images for data comparison. MetaboAnalyst provides both of those contained within a single, web-based, user-friendly package [161].

MetaboAnalyst's statistical analysis tool was used for Chapters 4-5.

MetaboAnalyst can accept several different forms of mass spectrometry data; to get robust lists of MS-validated, aligned features, combination of MZmine and LIQUID outputs was necessary. All features found by LIQUID over the score cutoff within at least two of a set of biological triplicates were retained; a master list of tentative MS-validated lipid annotations was constructed by combining those files from all conditions within a sample set. Simultaneously, lists of processed, aligned peak areas produced by the above methods in MZmine were exported, and peak areas were assigned tentative annotations using the LIQUID master list (in the case of multiple hits within an error range of  $m/z$  value, the maximum peak area within those possible features was retained for a given condition), resulting in a master list of tentative lipid annotations supported by peak areas. If data for normalization by raw cell pellet mass was available, this was performed by dividing the masses of each pellet by the mass of the heaviest pellet within the sample group; the peak areas of a given condition were divided by the mass ratio obtained for each pellet to normalize by raw cell mass.

For MetaboAnalyst analysis, a plain text file (.csv) of the above data was uploaded to the web module, with appropriate sample condition titles added as per the recommended settings, selecting the settings for unpaired data in columns and peak intensity table. Because the uploaded files did not contain wholly comprehensive, untargeted sample sets and instead selected based on MS2 validation from LIQUID no filtering was applied to the uploaded sample sets. Basic data transformation was performed by way of mean normalization, log transformation, and mean centering, which

enables use of several different data visualization tools. For sample sets that have corresponding sample weights, the normalization can be skipped in favor of normalization prior to statistical analysis.

For comparison of lipid sample sets between control samples and specific sampling conditions, the Student's t-test (one mean, two tailed). For comprehensive examination of all conditions, the analysis of variance (ANOVA) test was used. Heatmaps and principal component analysis (PCA) plots were generated with this online tool for data visualization and comparison. Heatmaps were constructed using only significantly variable features as indicated by ANOVA or t-test p-values under 0.05, with variance being indicated by relative fold change on a color gradient scale. PCA plots were generated with the including of 95% confidence regions. Volcano plots were constructed using a p-value threshold of 0.05 (from the Student's t-test) and a fold change threshold of 2.

## **Conclusions**

Presented here is the complete lipidomics platform used to undertake the experiments described in Chapters 4-5, with thorough explanation of each step and the relevant metrics involved. Having laid out the numerous parameters required for an untargeted lipidomics experiment, including selection of an optimal extraction method, chromatography setup, mass detection platform, and informatics software, the next step is to examine the available options for each step of the process and defend the use of the methods described here in Chapter 2 while also considering other options, which will be presented in Chapter 3.

### **CHAPTER 3: DEVELOPMENT AND OPTIMIZATION OF A FLEXIBLE LC-MS ANALYSIS PLATFORM FOR LIPIDOMICS MEASUREMENTS**

## **Abstract**

Preparing a robust analysis pipeline requires thorough understanding of relevant options, background research, difficult decisions about what approach to try for each individual step, and no shortage of testing to determine the best manner with which to proceed through analysis. Just as with all types of omics platforms, there have been many different modifications and improvements suggested over the years to try to fully optimize various techniques, but each advance comes with caveats specific to the sample, analysis, or desired outcome of the study. Additionally, conditions and issues related specifically to experimental design, samples, or accessible instrumentation can add an extra layer of complexity to parameter selection. Presented here is a systematic pipeline development explaining each step of the lipidomics analysis process utilized in later chapters, discussing each step from sample preparation to analysis and why specific choices were made in the context future plans experiments.

## **Introduction**

While Chapter 2 laid out the general mechanics behind each step of the lipidomics platform constructed here, there are still many other options available with which to approach lipidomics. Methods of sample preparation are highly variable depending on experimental design, extraction methodologies have slowly evolved over the years to allow for more optimized preparations, and there are constantly new programs with different functions and upgrades that attempt to solve previous issues in lipidomics. One of the biggest issues in lipidomics, the balancing act within chromatography sample elution off columns and adequate retention to allow for separation, required ample testing

of multiple different combinations of mobile and stationary phases to determine which system would work best to detect the range of lipids expected within bacterial lipid extracts. Described here is the process of how each step of the lipidomics analysis platform was established, discussing the choices made and the alternatives that have been reported previously in literature studies.

## **Lipid extraction**

### ***A brief consideration about sample preparation***

Before any extraction and analysis takes place, one needs to be mindful of what exactly they are going to be receiving from a collaborator. Depending on the organism, sampling conditions, and any special modifications that may have been incorporated into the experiment, it is possible to receive cell pellets or cultures in any number of different ways. Inconsistent concentrations/biomass amounts, the presence or lack of media and/or buffer, and whether the pellets are frozen or delivered as cell cultures are just several the issues that need to be considered before beginning extraction.

For the work in Chapters 4 and 5, bacterial cells were delivered as pellets in variable levels of dryness and size. Because the extraction methodology was designed to fully extract a lipidome using only tens of milligrams worth of cell material, pellets upwards of hundreds of milligrams or even grams would not only force a modification of procedure but also would waste precious sample material that could instead be kept frozen for possible later reanalysis if needed. There is also the matter of making sure pellets were washed as thoroughly as possible to remove anything that might remain from preparation. This was mainly done to avoid backend issues within the LC-MS analysis –



while not as much of a concern with nanoscale LC-MS setups, it is still always preferable to wash cultures before extraction with phosphate-buffered saline (PBS) to have access to clean extracts free from the high concentrations of salt that can cause irregular spray quality and signal suppression in LC-MS setups [143, 162, 163]. This wash step also allowed for partitioning of large pellets into smaller aliquots, half of which will usually be used for lipid extraction and the other half stored at -80°C as a backup for reruns or other analysis.

### ***Selection of optimal extraction solvent***

As outlined in Chapter 2, traditional lipidomics experiments have heavily preferred to use chloroform-based extraction procedures; however, in recent years MTBE has risen to prominence as a functional alternative to CME approaches. While both are functionally equivalent in terms of pure extraction efficiency, there are some practical applications that bear mentioning specifically for lipidomics experiments or multiomics experiments that have a lipidomics component to them.

Figure 9 outlines the differences between extractions using MTBE and chloroform as the primary organic component. For MTBE-based extractions (Figure 9A), the lower density of the MTBE layer results in the lipid-containing organic layer being at the top of the extraction, while the water and methanol aqueous layer, containing water-soluble metabolites and genetic material, sinks below, and the remaining solid protein and cellular waste pelleting at the bottom of the vial. With chloroform-based extractions (Figure 9B), the chloroform layer is much denser than water, and as such it sinks to the bottom of the vial.

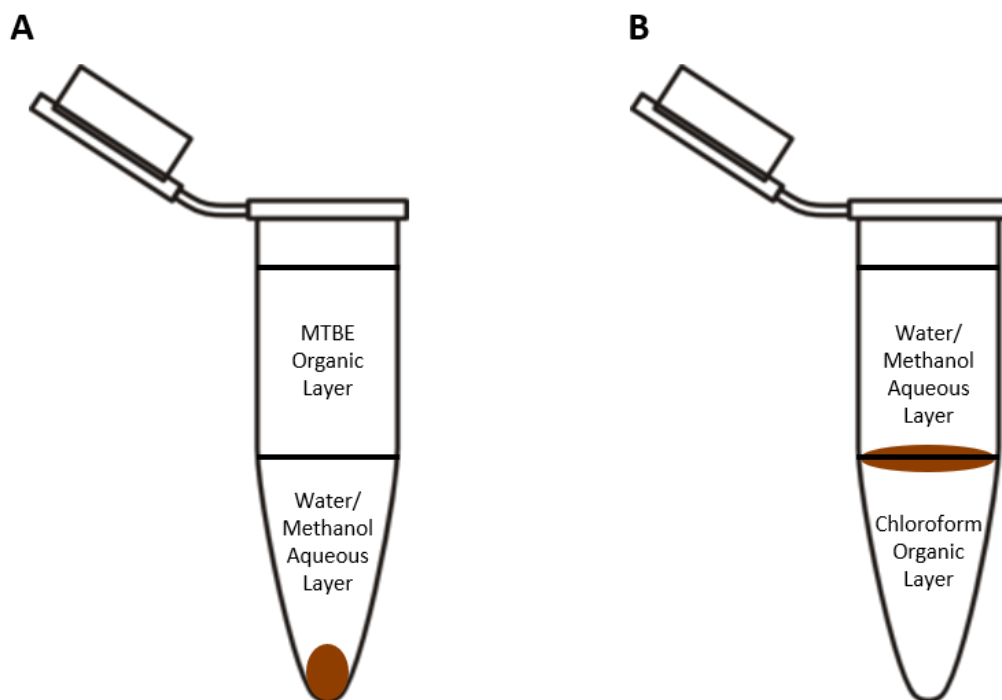


**Figure 9. Comparison of lipidomics extraction methods. A. MTBE-based extraction, with the organic lipid layer present at the top of the extraction and the protein pellet settling at the bottom of the vial. B. CME extraction, with the organic lipid layer at the bottom of the vial and the protein pellet lying at the interface between the aqueous and organic layers.**

In fact, chloroform is so dense that even the solid protein partition ends up turning into a semi-solid layer present between the aqueous and organic layers. The lipid-containing chloroform layer lying at the bottom of the extraction vessel is problematic if none of the other layers are of interest in a strictly lipidomics-only experiment and are effectively discarded to waste – in testing, it was found that there was a significant risk of contamination from one or both of the solid protein layer and aqueous metabolite partition that was not easily mitigated. MTBE extractions largely avoided that issue; any level of slight contamination from the aqueous layer could easily be removed thanks to the differences in solvent density, and there was no chance of contamination from the solid protein partition, so pure MTBE lipid extracts were much easier to acquire than with chloroform extractions, which is why MTBE was selected for this experimental design.

While it is easier to access lipids with MTBE in isolation, there are also implications when applied to one pot multiomics analyses, where one can theoretically perform some or all of genomics, proteomics, metabolomics, and lipidomics using a single extraction. While the focus of the experiments described in later chapters was solely on lipid analysis, there were considerations about exploring the other layers for metabolomics, proteomics, and genomics. Having easy access to both liquid layers and then availability of the solid layers as a leftover with the MTBE setup results in a much more streamlined procedure than having to avoid contamination of the liquid layers because of the solid protein lying at the liquid-liquid interface. While not applicable here, this was an important consideration for future experimental design.

### *Approaching cell lysis for lipidome access*

Another metric that bears a brief discussion is how to lyse cells. In lipidomics, this is particularly important because the main lysis target – the cell membrane – is also the target of extraction. Bursting cells for omics experiments to access the various pools of macromolecules contained within is not usually difficult – methanol alone (which many extraction methods use) is more than sufficient to denature membrane-bound proteins as well as increase the overall fluidity and permeability of the membrane, rendering it loose and/or broken [164, 165]. However, it is worthwhile to apply another method to ensure that the cell membrane is completely dispelled, an important consideration for lipidomics, and there are a number of mechanical disruption methods available to perform such a task. Bead beating and sonication are among the most popular mechanical lysis methods for omics studies, but as with all steps it is critical to consider which is going to provide the best results [166-168]. Physical disruption by way of the addition of plastic or metal beads of various sizes and high-speed shaking or vibration can create very thorough cell lysis. However, this is typically reserved for cells that have thick cell walls and require a level of physical disruption and simulation of tearing forces to get past the hard cell wall and access the weaker cell membrane. Bead beating also requires use of both beads (which may or may not be recoverable and/or recyclable) and an instrument with which to perform bead beating. Sonication is much more effective at more generic bacterial lysis, only requiring a probe and appropriate settings for the sonic waves applied to the sample as well as cooling.

The main drawback of sonication usually lies in overall efficiency - the method employed for the analysis in Chapters 4 and 5 uses a sonicator that can only process one sample at a time, and each run takes approximately as long as bead beating would take on an entire sample set [169]. While this was admittedly a significant detriment, sample sets were not usually large enough for this to be a significant problem, or samples were received and processed in waves, and as such it was more than sufficient for the experiments described here.

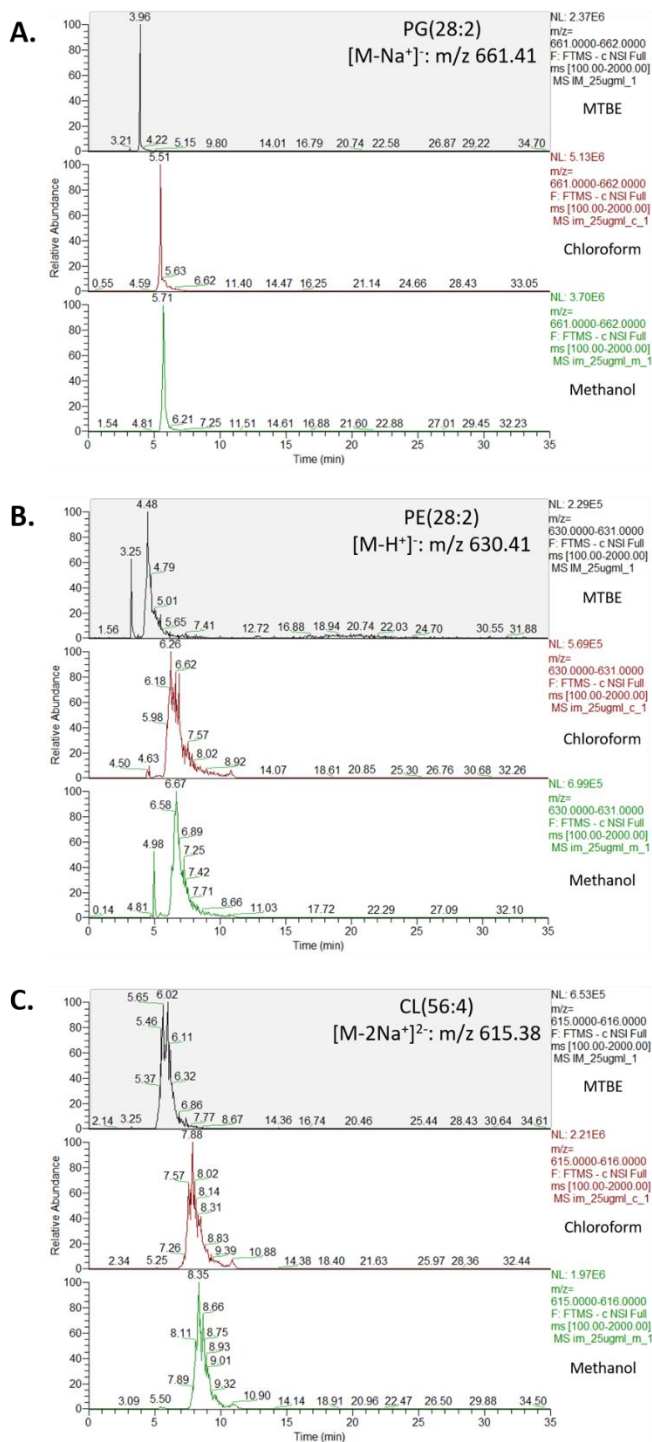
### **Lipidome analysis – proper selection of analytical parameters**

#### ***Effect of injection solvent choice***

Before discussing mass spectrometry parameters, it is worth discussing injection of samples once they have been prepared. Samples are delivered to the mass spectrometer within a solvent that can readily dissolve the analytes; however, this may not always be a solvent that is also present within the specific liquid chromatography setup being utilized. The interaction between injection solvent, mobile phase, and stationary phase is of critical importance to quality separations. Using injection solvents that do not sufficiently share similar chemical characteristics with the mobile phase can cause the analytes to not sufficiently interact with the column and coelute in a bundle at or near the void volume [170]. In the case of HILIC-MS/MS measurements, such as the ones being described here, the main mobile phase is composed primarily of acetonitrile, with a gradient towards an increasing amount of water content as well as a low concentration of ammonium acetate for ionization. This would generally dictate that the samples be dissolved in acetonitrile to match the LC solvents.

Preservation of samples is important, so it was not possible to directly test bacterial extracts with a variety of injection solvents. However, the possible effects of this on chromatographic separations can be observed using standards as a stand-in (Figure 10). While the standard mixtures used were prepared in a 1:1 mixture of chloroform/methanol, 1:4 dilutions in each of the major solvents enabled an adequate platform for comparison. MTBE was used because of the extraction procedure, and pure methanol and chloroform were used because of their use in prepared standards, both stand alone as well as in a mixture with each other. Because of the nature of lipids and how they interact specifically with a HILIC-based column, as will be described in the following section, there is not a reasonable expectation that changing the solvent in which a lipid extract is dissolved would cause a massive shift in retention times. However, there is a reason to believe that changing dissolution solvent could lead to a change in peak shape.

As can be seen, samples dissolved in MTBE generally led to quicker elution times, while methanol and chloroform solutions are generally more delayed. However, there was not much of a difference in retention time between the methanol and chloroform solutions across all samples, and there was also not a massive difference in gross retention time, as all three specified samples eluted over the span of about 2-2.5 minutes. This would indicate that while it is possible to manipulate retention time, there is not a massive gain in overall separation, and as such, there was no real need to dry samples and redissolve them in either methanol or chloroform.



### Standard Mix:

Differential Ion Mobility  
System Suitability  
Synthetic Standard  
Mixture  
(Avanti Polar Lipids)

1 mg/mL each diluted to  
25 µg/mL:  
PG(14:1/14:1)  
PE(14:1/14:1)  
CL(14:1/14:1/14:1/14:1)

**Figure 10. Extracted ion chromatograms of A. PG(28:2), B. PE(28:2), and C. CL(56:4), each shown shown diluted in methyl tert-butyl ether (top), chloroform (middle), and methanol (bottom).**

### ***Importance of proper stationary phase selection***

Chapter 2 introduced RP and HILIC as commonly used stationary phases for LC-MS based omics experiments. While both have been used successfully in literature for years, it was important to test them both within the context of the experiments described in Chapters 4-5. Described here is a brief explanation behind the thought and testing between RP and HILIC stationary phases.

The expected range of fatty acid length observed in *B. subtilis* [171] and *P. putida* [172] phospholipids is 14 to 18 carbons, with some minor variation observed depending on species and cellular environment. In traditional C18 columns, this is a major issue to consider and overcome (Figure 11). Lipids must migrate through many centimeters worth of packing material that holds a surprisingly similar amount of chemical character to the samples. The non-polar interactions between these 18 length carbon chains on the silica base of C18 and the 14-18 carbon long fatty acids are rather strong, rather hard to break without the presence of an extremely strong nonpolar solvent. The nonpolar component of the mobile phase in RP experiments is typically acetonitrile. While this can be overcome with isopropanol [173-176], as described in Chapter 2, operation of such a system can be unpredictable and unstable, and even with substantial amounts of isopropanol, it was found that very little phospholipid would elute. Often, the only species that would be observed would be lyso-phospholipids, which only have one fatty acid tail and as such would likely not create as strong of an association as a normal phospholipid with 2 or 4 fatty acids. This was like due to improper dissociation from the stationary phase, resulting in a shearing of sorts and loss of one fatty acid tail.



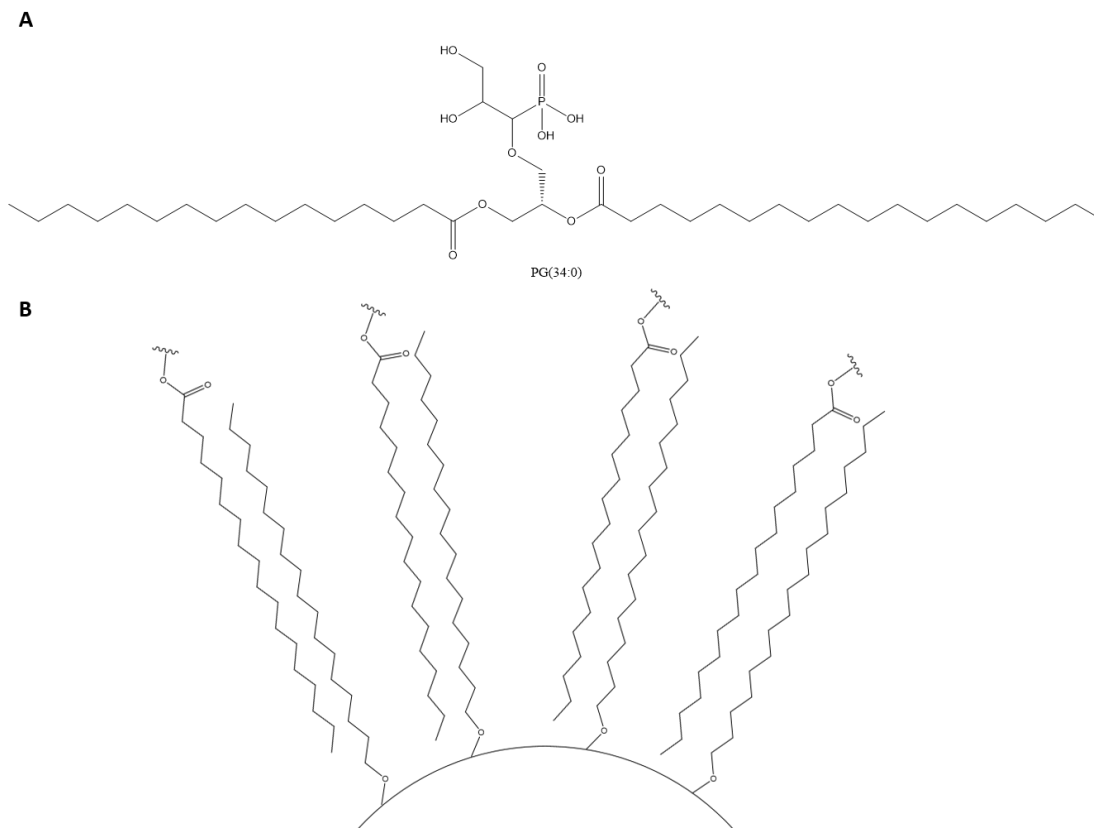


**Figure 11. Issues using C18-based stationary phases in RP-LC-MS lipidomics. A: A commonly observed phospholipid within the cell membrane, PG(34:0). B: Example of how the non-polar interactions of the long fatty acid chains can interact with each other and create strong interactions that are hard to separate without the use of an incredibly strong nonpolar solvent.**

One alternative is using an RP packing material that has shorter carbon chains attached to the silica base, such as C5 which has been shown to be largely successful in elution of most components of lipid standard mixes [177, 178]. C5 largely avoids the problems observed with C18 RP stationary phase (Figure 12A) because the carbon chains on C5 stationary phase are still nonpolar to enable retention but not long enough to create the near-irreversible interactions observed with C18 (Figure 12B).

In practice, the C5 column did perform well when analyzed using Avanti's standard lipid mixtures (Ion Mobility – Table 3; LightSPLASH – Table 4). A C5 column equipped with a 60-minute isocratic gradient primarily composed of isopropanol was successful in eluting most of the lipids contained within a lipid standard mix, but the issues associated with isopropanol were still present, which meant that moving away from RP-based column systems appeared to be a better direction. This led to HILIC-based separations, which have been popular in recent years in part due to elutions based more in hydrophilic interactions between column, solvent, and analytes [59, 179-181]. This also allowed for separations that focused on the more polar parts of the lipid, namely the headgroups, while RP was almost completely blind to headgroups and separated based on chain length when elution was possible.

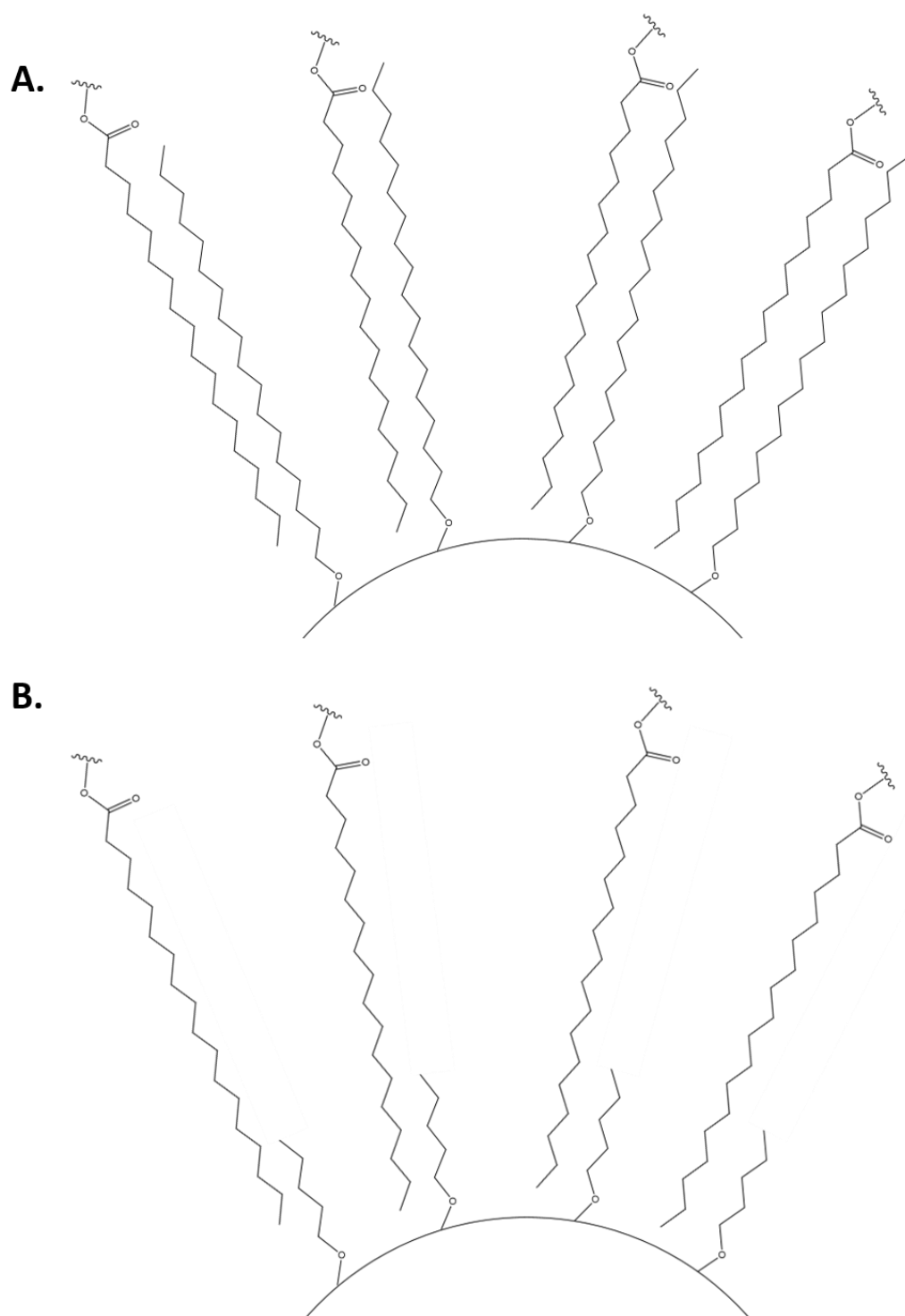


**Figure 12. Comparison of lipid associations between a generic long fatty acid chain phospholipid and A: a C18 column and B: a C5 column.**

**Table 3. Comparison of elution quality between C5 and HILIC stationary phases across positive and negative ionization mode using Avanti's Ion Mobility standard mix.**

<b>Lipid Species</b>	<b>C5 Column Positive Ionization</b>	<b>C5 Column Negative Ionization</b>	<b>HILIC Column Positive Ionization</b>	<b>HILIC Column Negative Ionization</b>
Ceramide (18:1)	Yes	Yes	No	Yes
CL(14:1) (Na salt)	No	No	No	Yes, [M-2Na] <sup>2-</sup>
Cholesterol	Yes, [M+H-H <sub>2</sub> O] <sup>+</sup>	No	No	No
Chol Ester (19:1)	No	No	No	No
DG(14:1)	Yes	No	No	No
Lyso- PC(18:1)	Yes	No	Yes	No
PA(14:1) (Na salt)	No	Yes, [M-Na] <sup>-</sup>	Yes	Yes, [M-Na] <sup>-</sup>
PC(14:1)	Yes	No	Yes	No
PE(14:1)	Yes	Yes	Yes	Yes
PG(14:1) (Na salt)	Yes	Yes, [M-Na] <sup>-</sup>	Yes	Yes, [M-Na] <sup>-</sup>
PI(14:1) (NH <sub>4</sub> salt)	Yes	Yes, [M-NH <sub>4</sub> ] <sup>-</sup>	Yes	Yes, [M-NH <sub>4</sub> ] <sup>-</sup>
PS(14:1) (Na salt)	Yes	No	Yes	Yes, [M-Na] <sup>-</sup>
SM(18:1)	Yes	No	No	No
TG(18:1)	Yes	No	No	No

**Table 4. Comparison of elution quality between C5 and HILIC stationary phases across positive and negative ionization mode using Avanti's LightSPLASH standard mix.**

<b>Lipid Species</b>	<b>C5 Column Positive Ionization</b>	<b>C5 Column Negative Ionization</b>	<b>HILIC Column Positive Ionization</b>	<b>HILIC Column Negative Ionization</b>
C15 Ceramide	Yes	Yes	Yes	Yes
Chol Ester (18:1)	No	No	No	No
DG(15:0/18:1)	Yes	No	No	No
Lyso-PC(18:1)	Yes	No	Yes	No
Lyso-PE(18:1)	Yes	Yes	Yes	Yes
MG(18:1)	Yes	No	No	No
PC(15:0/18:1)	Yes	No	Yes	No
PE(15:0/18:1)	Yes	Yes	Yes	Yes
PG(15:0/18:1) (Na salt)	Yes	Yes, [M-Na] <sup>-</sup>	No	Yes, [M-Na] <sup>-</sup>
PI(15:0/18:1) (NH <sub>4</sub> salt)	Yes	Yes, [M-NH <sub>4</sub> ] <sup>-</sup>	Yes	Yes, [M-NH <sub>4</sub> ] <sup>-</sup>
PS(15:0/18:1) (Na salt)	No	Yes, [M-Na] <sup>-</sup>	No	Yes, [M-Na] <sup>-</sup>
SM(d18:1/18:1)	Yes	No	No	No
TG(15:0/18:1/15:0)	No	No	No	No

Additionally, in testing of extracts from strains of *P. putida*, HILIC separations resulted in a wider variety of lipid samples than RP analyses, as can be observed in Figure 13. Not only were more lipid species detected in HILIC by head group, over double the individual lipid species were detected in most HILIC samples. Crucially, cardiolipin was not detected using the C5 RP column, while it was readily observed and one of many different expected lipid classes seen using the HILIC column. If cardiolipin was not a major component of the bacterial species being tested, it would have been much easier to approach the later described experiments with a complementary chromatography approach, but the known presence of cardiolipin within bacteria meant that HILIC was needed for a more complete analysis.

Another important observation is the disparity in intensities between lipid species. Specifically, while the relative proportion of PG to PE was around 2:1 in the HILIC separations, this widened significantly to at least 4:1 and maxed out at 8:1 in the RP separations, which is indicative of differing response rates of the analyte to the separation method. To track this, peak areas of equimolar standards of PG, PE, and CL within Avanti's Ion Mobility mix were extracted to observe the peak area ratios of PG, PE, and CL (Table 5). Despite equimolar concentrations of each lipid standard, the peak areas differed depending on the lipid class. Because this was done in a pure standard mix, matrix effects were assumed to be relatively low, which is not necessarily a logical assumption in a cellular lipid extract. Still, this can be a useful correction to be able to compare relative proportions of lipid within a sample, and this correction was applied in Chapters 4 and 5 when appropriate.

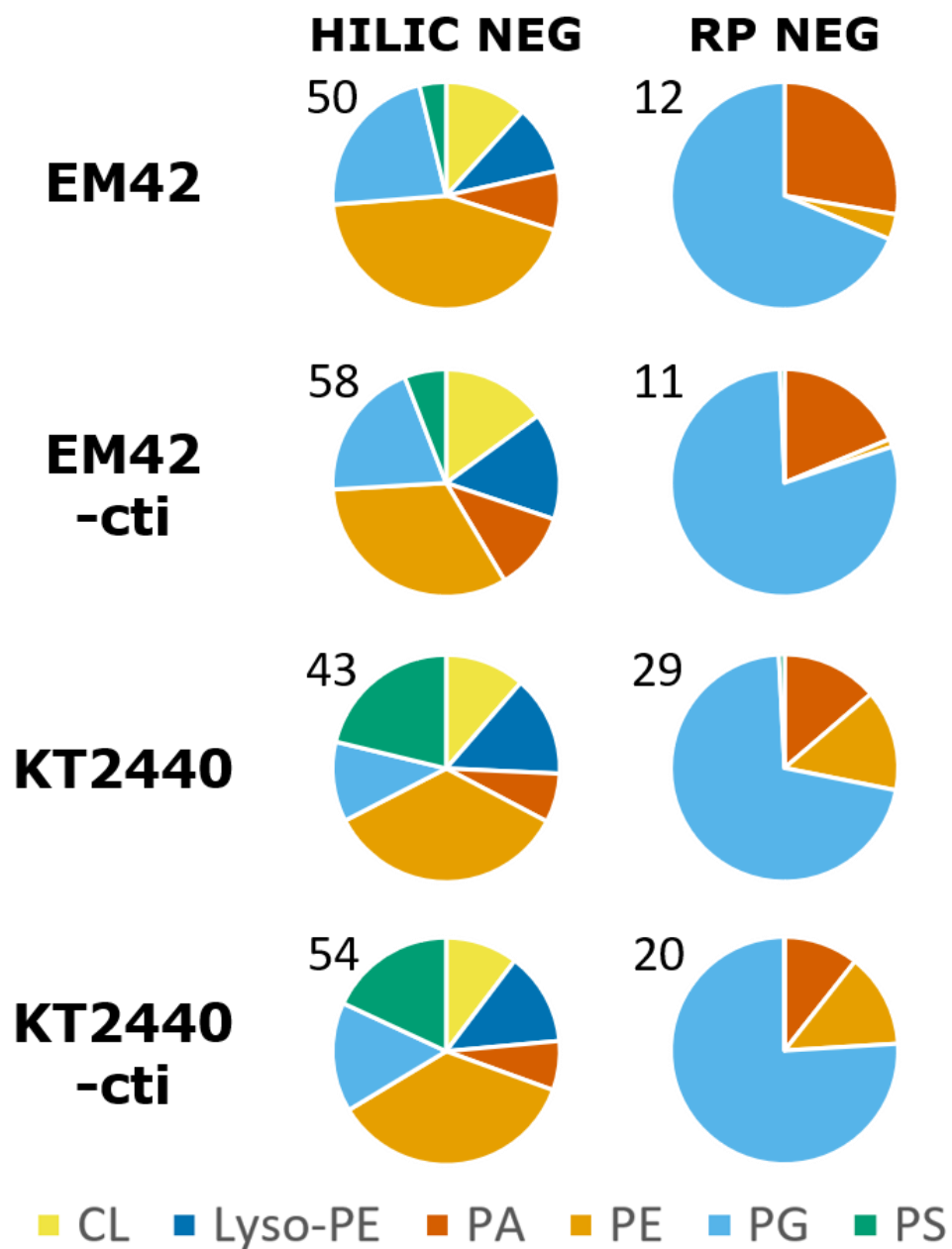


Figure 13. Comparison of eluted lipid profiles in *Pseudomonas putida* EM42, EM42-cti, KT2440, and KT2440-cti between HILIC and C5 RP columns, both performed in negative ionization mode.

**Table 5. Peak areas of PG(14:1/14:1), PE(14:1/14:1), and CL(14:1/14:1/14:1/14:1) in the Avanti Ion Mobility standard mix, as well as ratios of the peak areas.**

Concentration	10 ug/mL		25 ug/mL		Average Factor of PG/PE
Solvent	MTBE 1	MTBE 2	MTBE 1	MTBE 2	
PG(14:1/14:1)	$1.14 \times 10^7$	$7.65 \times 10^6$	$1.17 \times 10^7$	$1.34 \times 10^7$	
PE(14:1/14:1)	$4.36 \times 10^6$	$4.40 \times 10^6$	$7.41 \times 10^6$	$6.10 \times 10^6$	
PG/PE	2.62	1.74	1.59	2.20	2.04

Concentration	10 ug/mL		25 ug/mL		Average Factor of PG/CL
Solvent	MTBE 1	MTBE 2	MTBE 1	MTBE 2	
PG(14:1/14:1)	$1.14 \times 10^7$	$7.65 \times 10^6$	$1.17 \times 10^7$	$1.34 \times 10^7$	
CL(14:1/14:1/14:1/14:1)	$1.53 \times 10^7$	$1.55 \times 10^7$	$2.70 \times 10^7$	$2.31 \times 10^7$	
PG/CL	0.75	0.49	0.43	0.58	0.56

Concentration	10 ug/mL		25 ug/mL		Average Factor of PE/CL
Solvent	MTBE 1	MTBE 2	MTBE 1	MTBE 2	
PE(14:1/14:1)	$4.36 \times 10^6$	$4.40 \times 10^6$	$7.41 \times 10^6$	$6.10 \times 10^6$	
CL(14:1/14:1/14:1/14:1)	$1.53 \times 10^7$	$1.55 \times 10^7$	$2.70 \times 10^7$	$2.31 \times 10^7$	
PG/CL	0.28	0.28	0.27	0.26	0.28



With all these factors in mind, it was found that based on the proposed sample sets, expected range of lipids, and the limits of the instrumentation being used, HILIC was the stationary phase best suited for the needs of this lipidomics platform.

### ***Polarity selection in lipidomics***

Another major consideration for all mass spectrometry-based omics sciences is knowing which ionization polarity is effective for the specific sample set being tested. Proteomics utilizing mass spectrometry is strongly dominated by positive ionization studies, but given the variability of the electronic character of amino acids and the preference of post-translational modifications for negative ionization, comprehensive proteomics studies would be remiss without a thorough examination of a sample in both polarity modes [182]. Similarly, metabolomics has historically also followed a similar trend, given large classes of molecules tend to prefer positive or negative ionization modes [183], and even within lipidomics this still applies. Although the fundamental base of most phospholipids, phosphatidic acid, retains a strong negative charge thanks to the phosphate group, the addition of various headgroups can quickly modify that.

Specifically, in the case of lipidomics, it is possible to be somewhat more selective in how one chooses to approach an approach based in mass spectrometry. This becomes a key consideration in analysis of plant and animal cell-derived lipidomes, as phosphatidylcholine (PC) is a major component of the membranes in those organisms. However, PC is rarely observed in bacterial membranes, which allows a level of selectivity within bacterial lipidomics analyses. The major expected phospholipids in most bacterial species are PG, PE, and CL, with trace amounts of PA, PS, and PI

occasionally be present as either species-specific contributors or as intermediates of synthesis for the more common phospholipids. As such, use of a singular polarity mode where all of those species can be readily detected can greatly streamline analysis (Table 6). Standards of those specific phospholipid species (Figure 14) indicated that both PE and PG were readily visible in both positive and negative mode, while cardiolipin stands out as primarily visible within negative ionization mode only. As a result, negative ionization stands out as the polarity of choice for bacterial lipidomics studies (Figure 15).

While there are studies that have shown methods for using both modes with minimal effort [184, 185], they often use setups that can utilize both positive and negative ionization with minimal risk or downtime. Most modern instruments (such as the Thermo Q-Exactive instruments) can easily switch back and forth between polarities within a set of runs, but older instruments (like the LTQ Orbitrap Velos Pro used here) often need downtime in between runs of differing polarities. For experiments where both positive and negative polarity runs are performed, this is circumvented by placing several blanks in a run sequence that help to bridge the gap and allow sufficient time for the instrument to re-equilibrate to a different polarity. Still, if prior knowledge of expected phospholipids is known, the time investment into measuring samples using both polarities may not be worth the effort. Therefore, alongside testing of the LC-MS platform in general for metrics like spray quality and stability, negative ionization was determined to be a much more functionally useful ionization mode. While there is a possibility that positive mode could yield results for minor phospholipids, negative mode is the ionization mode of choice to comprehensively process bacterial lipidomes.

**Table 6. Preferred ionization polarities for major classes of phospholipids.**

<b>Phospholipid Species</b>	<b>Polarity (at neutral pH)</b>	<b>Preferred Ionization Mode</b>
Phosphatidic Acid (PA)	Anionic	Either
Phosphatidylglycerol (PG)	Anionic	Either
Phosphatidylethanolamine (PE)	Zwitterionic	Either
Phosphatidylcholine (PC)	Zwitterionic	Positive
Phosphatidylserine (PS)	Anionic	Either
Phosphatidylinositol (PI)	Anionic	Either
Cardiolipin (CL)	Anionic	Negative

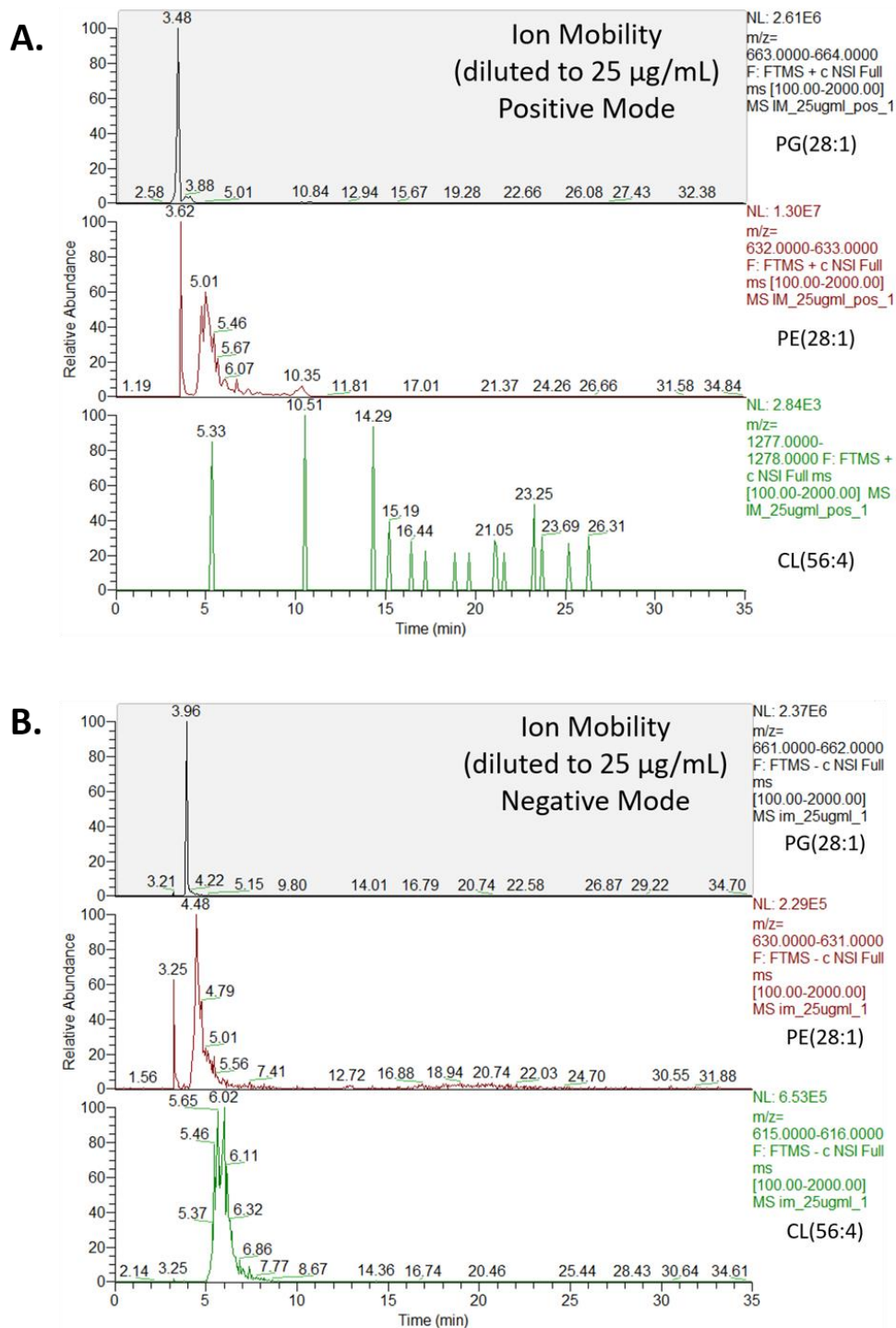


**Figure 14. Extracted ion chromatograms of the PG, PE, and CL standards within a 25 µg/mL dilution of the Avanti Ion Mobility standard mix in A) positive ionization mode and B) negative ionization mode.**

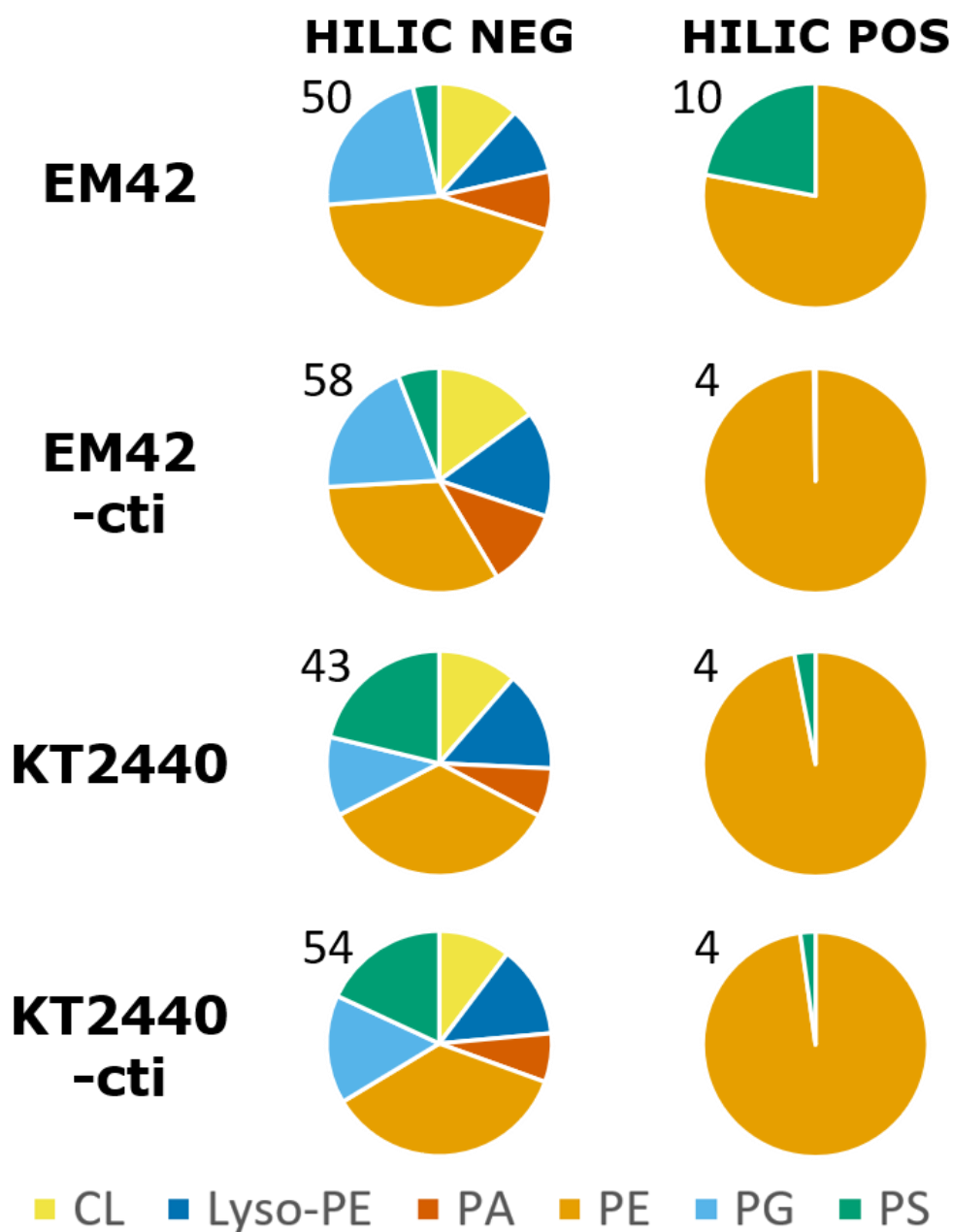


**Figure 15.** Comparison of eluted lipid profiles in a selection of *Pseudomonas putida* samples (KT2400/EM42 and and KT2440-cti/EM42-cti, strains with an overexpressed cis-trans isomerase, cti) run on a HILIC column in positive and negative ionization modes, along with total lipid species observed in each sample.

## **Identification of key phospholipid species using MS spectra**

Finally, before delving into applied lipidomics experiments, it is important to understand the general contents of the samples in question. Much like proteomics, lipidomics carries a significant advantage over metabolomics because of a level of predictability granted by a building block-like system of lipid construction. While this is not universally applicable to all lipids (sterols and acylglycerides have their own unique construction), for phospholipidomics this is incredibly powerful. Outlined here are brief descriptions of the major expected phospholipids for the experiments described within Chapters 4-5 along with additional species that were deemed relevant due to presence as intermediate species or as literature-reported lipid variants. Annotated mass spectra were extracted from runs using the Differential Ion Mobility System Suitability LipidoMix Kit from Avanti Polar Lipids.

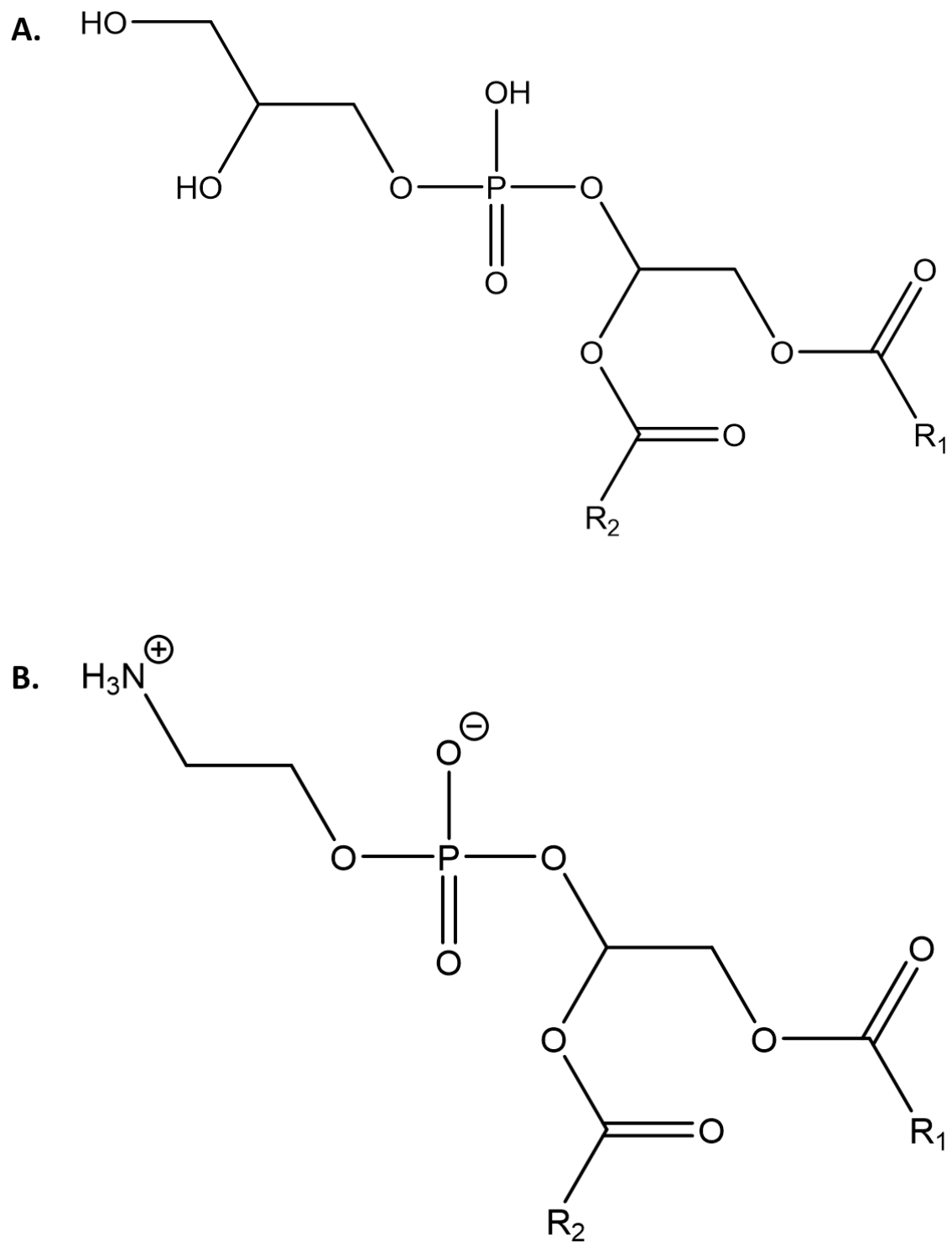
### ***Phosphatidylglycerol and phosphatidylethanolamine***

The cell membranes of most bacteria are primarily composed of phosphatidylglycerol (PG) and phosphatidylethanolamine (PE), with varying proportions depending on the species in question [186]. Both are produced from cytidine diphosphate-diacylglycerol (CDP-DAG), a derivative of the main phospholipid precursor phosphatidic acid (PA). For PG, CDP-DAG reacts with glycerol-3-phosphate to form an intermediate known as phosphatidylglycerol phosphate; the phosphate group is hydrolyzed to result in PG species. PE is synthesized by transformation of CDP-DAG into phosphatidylserine, a common phospholipid in other organisms but often only

fleetingly observed in bacteria as an intermediate, followed by a decarboxylation step to create PE species [57]. The structures of PG and PE are shown in Figure 16.

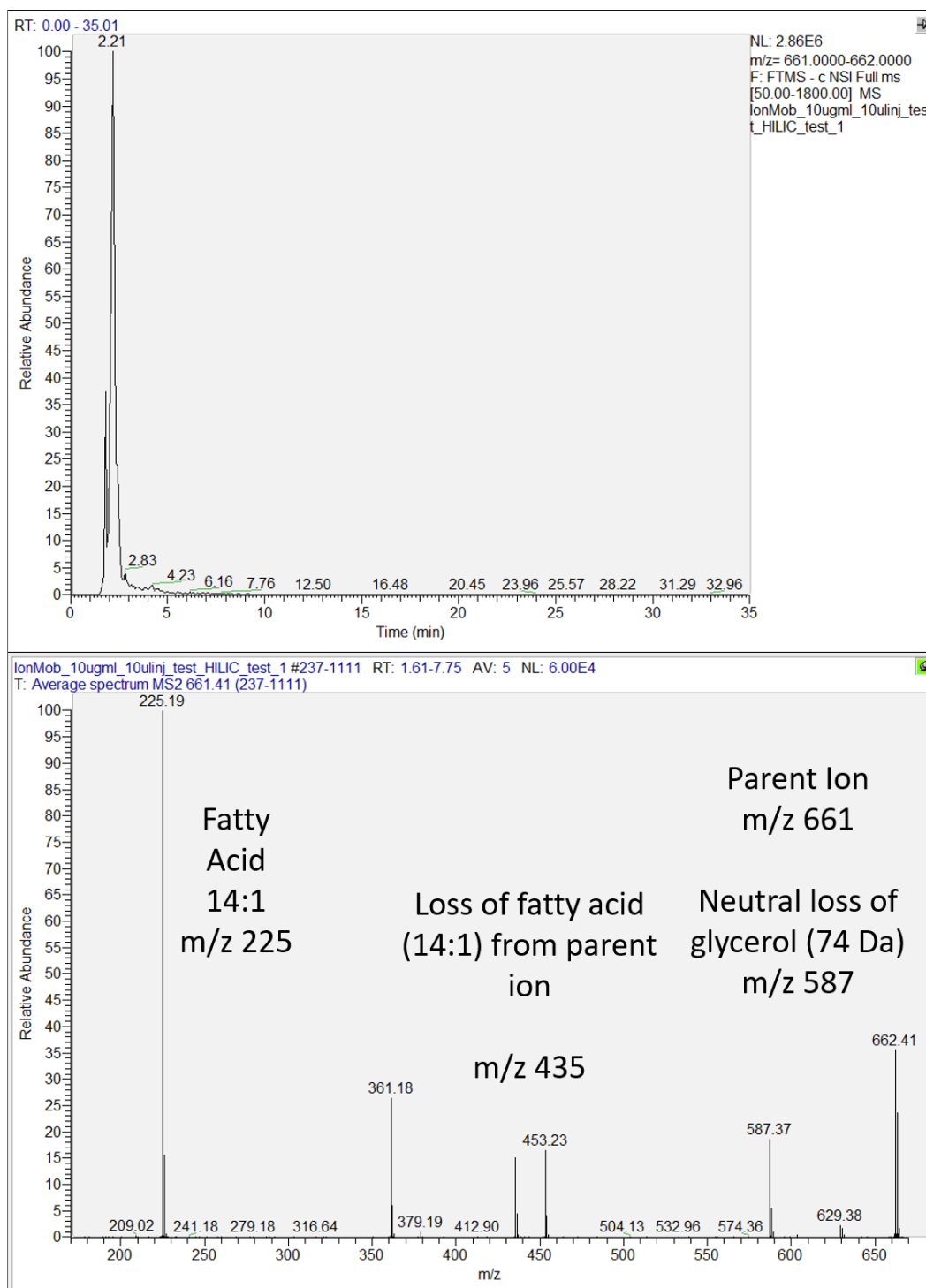
As mentioned earlier, mass-spectrometry based lipidomics is aided by a certain level of predictability in how lipids fragment. It is often very easy to obtain MS2 spectra with clear fatty acid traces as well as some type of peak or neutral loss that corresponds to the headgroup of a specific phospholipid species. Figure 17 shows a sample MS2 spectra of PG with characteristic fragmentation peaks. In negative ionization mode, while the glycerol head group is too low of a mass to be observed in the MS2 spectrum, the loss of the glycerol can be observed at  $m/z$  587 as a loss of 74 Da, which is the rearranged oxirane form of glycerol created through the loss of water. Additionally, PG generally follows the pattern of most phospholipid ionization, showing the fragmentation and loss of fatty acids through the base fragment peaks (here, shown at  $m/z$  225 since both fatty acid chains are identical) and the loss of the fatty acid (at  $m/z$  435) [187].

Figure 18 shows a sample MS2 spectra of PE with characteristic fragmentation peaks. PE is somewhat harder to pin down specifically by MS2 validation simply because the ethanolamine head group lies beneath the  $m/z$  range of the MS2 spectrum, and there is no discernable loss peak that can be connected to the head group, at least with the settings used in these experiments. There is a rearranged version of the headgroup involving an additional fragment of the phospholipid being retained as an epoxidized adduct; this ion appears at  $m/z$  196 and is visible within the mass spectrum, giving validation that this is in fact PE [188].



**Figure 16. General structures of A. PG and B. PE.**





**Figure 17. Extracted ion chromatogram (top) and MS2 spectrum (bottom) of PG(14:1/14:1) along with annotated fragment peaks.**

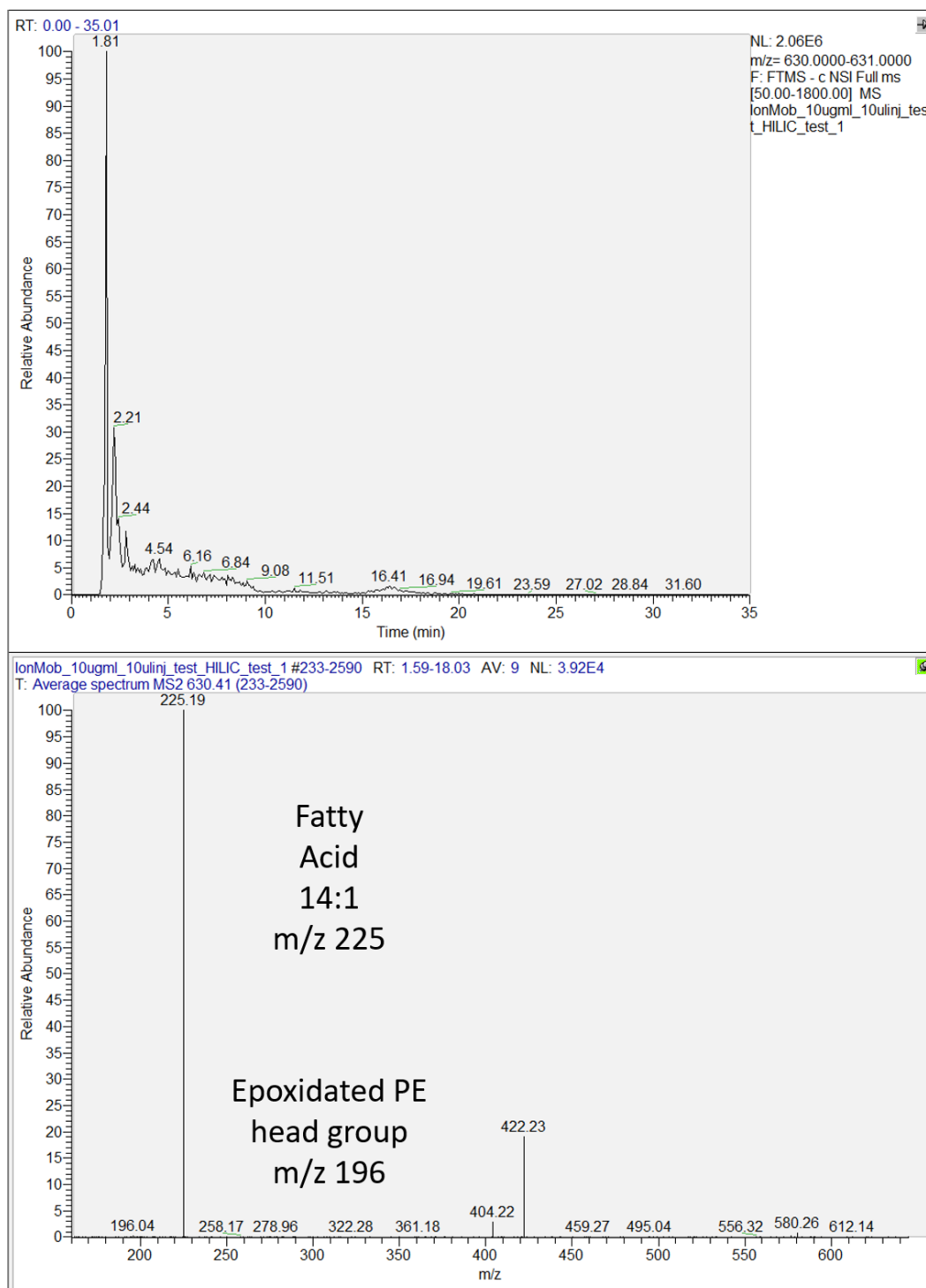


**Figure 18. Extracted ion chromatogram (top) and MS2 spectrum (bottom) of PE(14:1/14:1) along with annotated fragment peaks.**

Another issue with MS2 validation of PE is the issue of isomeric convolution with PC species [189]. However, this can be largely mitigated by which ionization mode is selected for analysis. As shown earlier, this setup did not detect PC species in negative ionization mode, and all This can also be somewhat avoided through prior research of the samples in question – both *B. subtilis* [171] and *P. putida* [172] do not have any reported presence of PC as a component of their membranes.

### ***Cardiolipin***

Cardiolipin (CL, structure shown in Figure 19, fragmentation of CL(14:1/14:1/14:1/14:1) shown in Figure 20) is also present in many bacterial cell membranes but at much lower concentrations as a structural aid. It is synthesized from PG as a dimer of sorts, creating a phospholipid that has one glycerol head group but with four fatty acid chains instead of two. Fragmentation of cardiolipin is somewhat dependent on the sample – cardiolipin can appear as a doubly charged ion, as shown earlier (Table 3), or as a singly charged ion, as is commonly observed within extracted lipidomes from samples. Doubly charged cardiolipin ions are relatively easy to decipher thanks to the presence of the singly charged parent ion (here, at  $m/z$  1230), as well as the loss of fatty acids from the singly charge parent ion ( $m/z$  1005) [190].

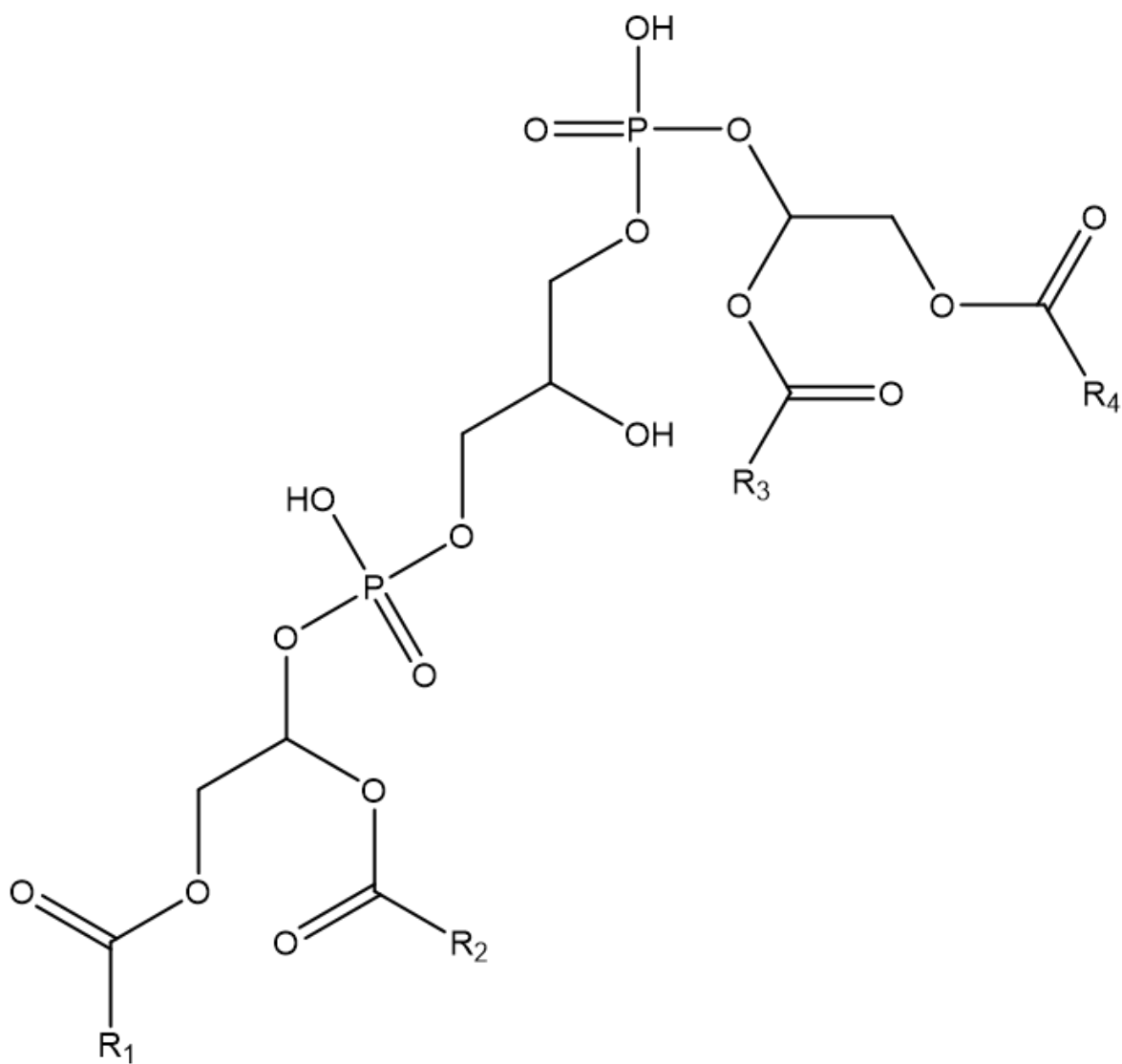


**Figure 19. General structure of cardiolipin.**

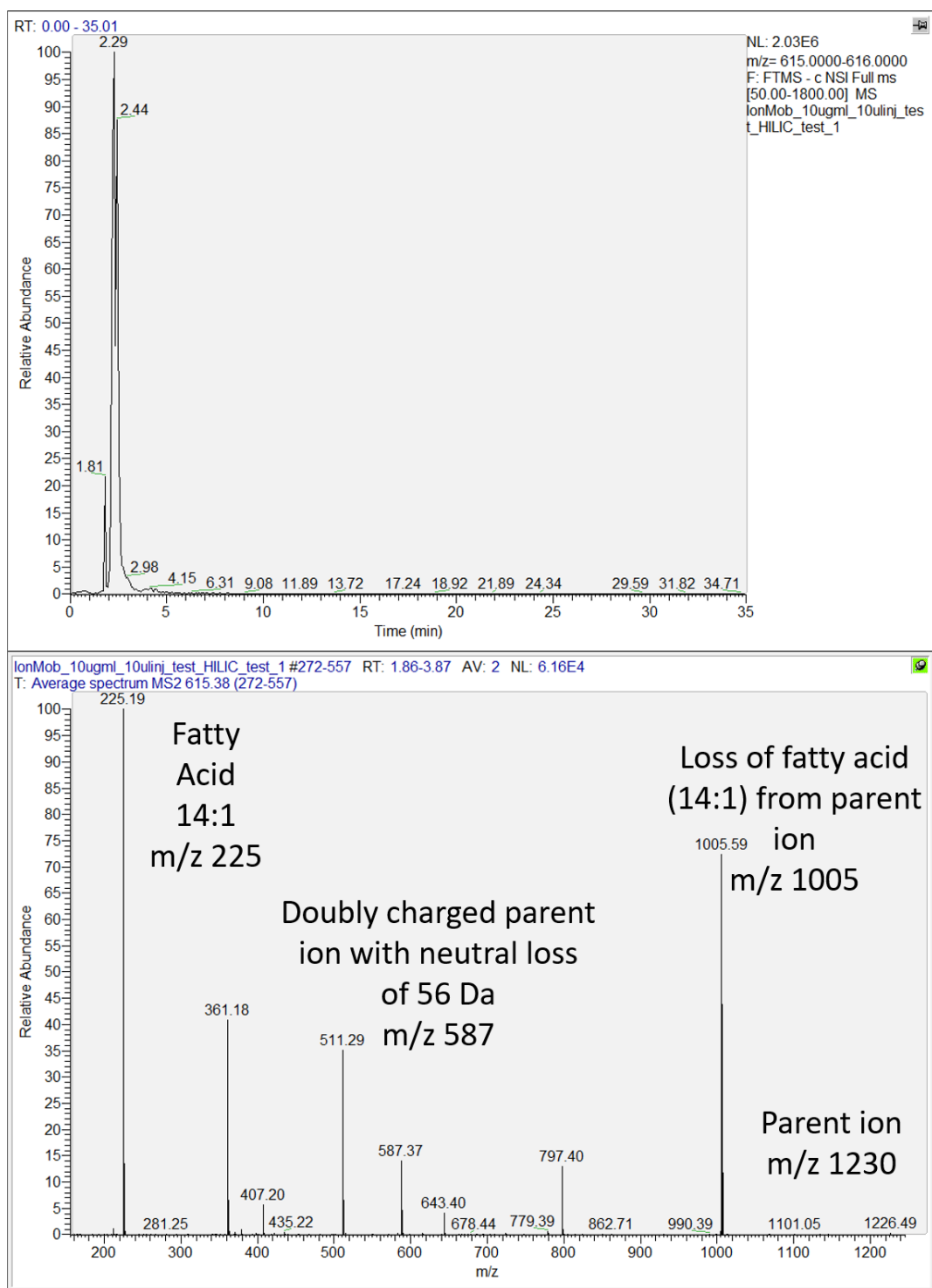


**Figure 20. Extracted ion chromatogram (top) and MS2 spectrum (bottom) of CL(14:1/14:1/14:1/14:1) along with annotated fragment peaks.**

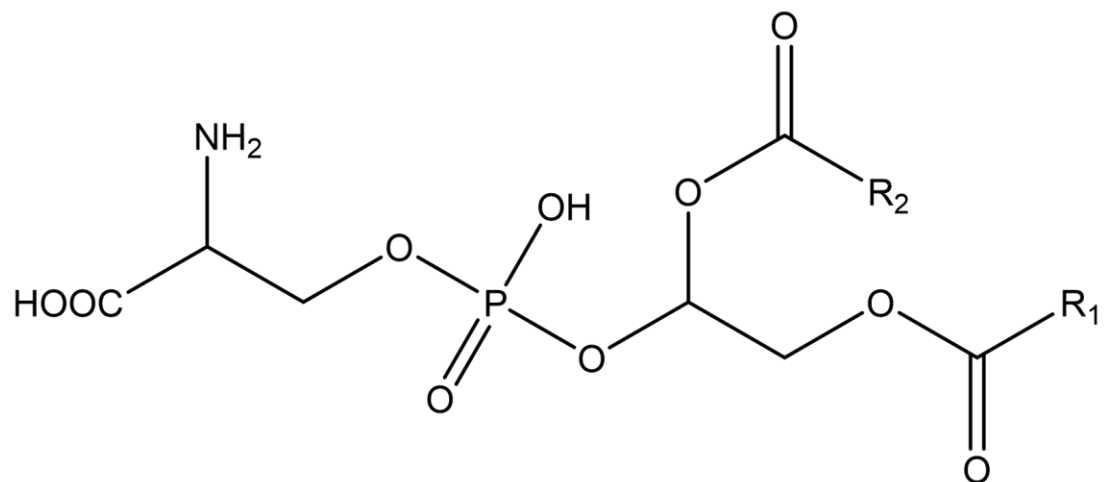
### ***Phosphatidylserine and phosphatidic acid***

As mentioned previously, PS and PA (structures shown in Figure 21, fragmentation of PS shown in Figure 22, fragmentation of PA shown in Figure 23) are only present as intermediates in bacteria and not as majorly abundant phospholipid species – PS is regularly observed as an intermediate in PE production, while PA is a universal precursor to most common phospholipids. However, it is still important to be able to identify them, as lysis of cell cultures will likely result in extraction of non-zero amounts of PS and PA due to interrupted metabolism and synthesis.

PS is readily identifiable by the neutral loss of the serine headgroup; this is visible at  $m/z$  587 (Figure 22) [188]. Additionally, normal fatty acid fragmentation can be observed as described earlier, with losses of fatty acids showing up as peaks along with the aforementioned neutral loss of serine. As the common precursor to most phospholipids, PA does not have a specialized head group, and as such, there is no head group to observe in fragmentation. The resultant fragmentation is very simple (Figure 23) – observation of the fatty acid fragment, as well as the losses from those fatty acids and the ketene forms of the fatty acids from the parent ion.

Using these known fragmentation patterns for each phospholipid species as well as the data mining tools afforded by programs such as MZmine and LIQUID, as will be described later, it is possible to create lists of high quality, high confidence annotations of lipid profiles.

A.



B.

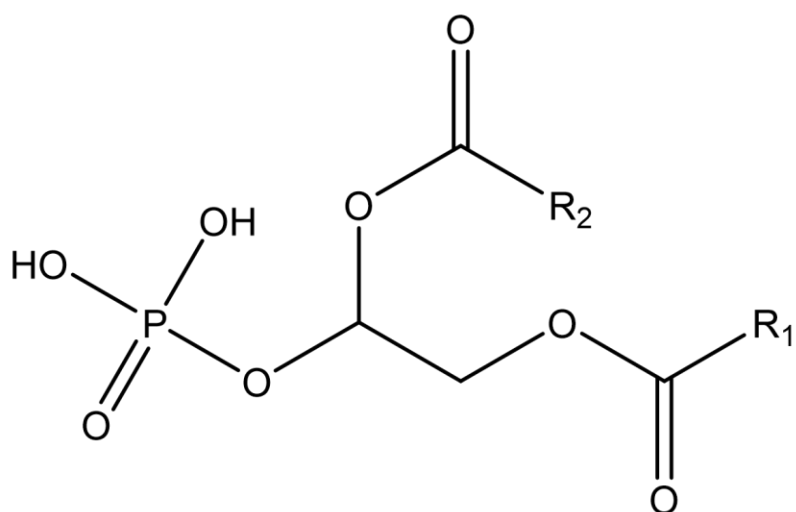


**Figure 21. General structures of A. PS and B. PA.**

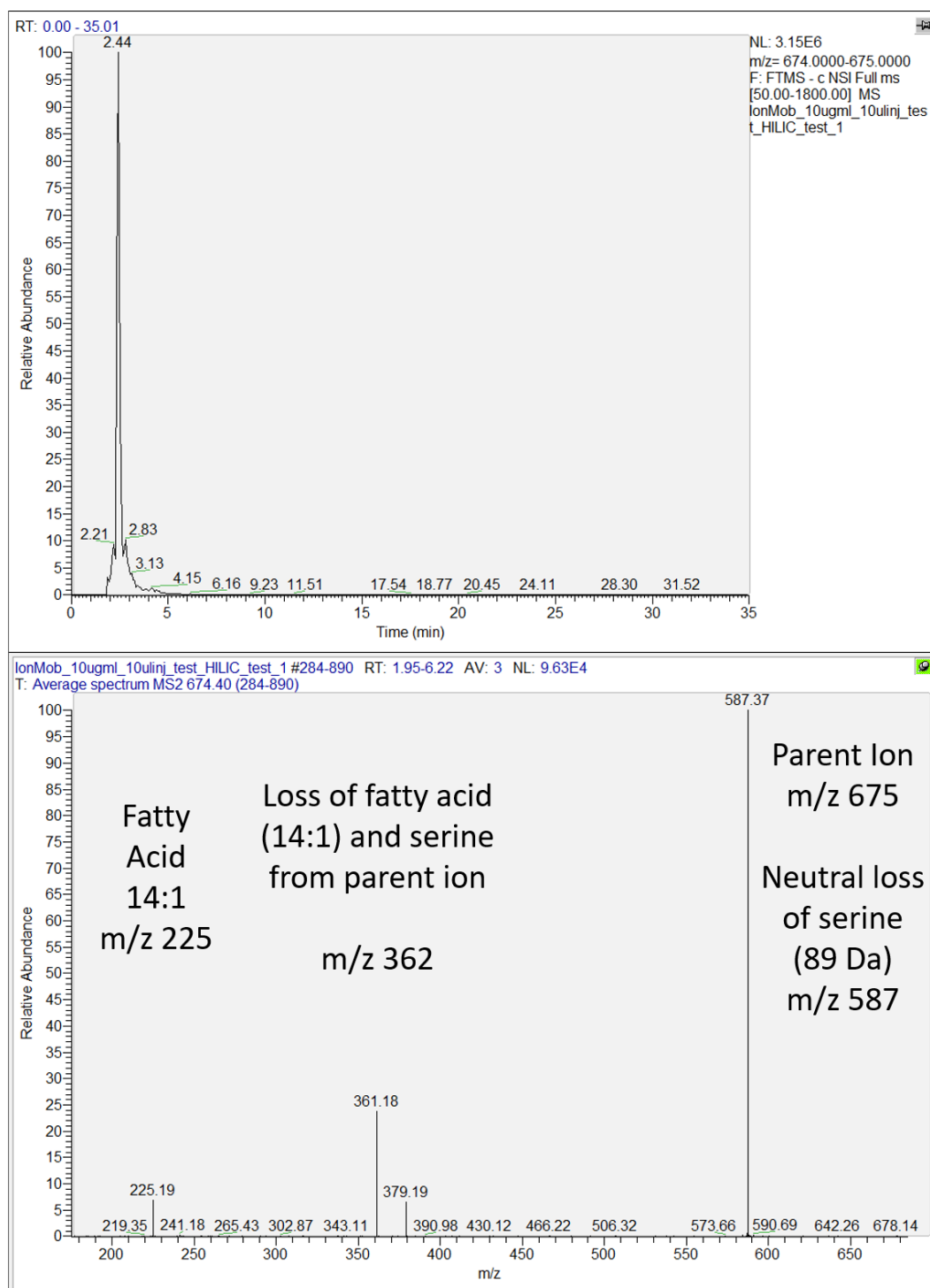


**Figure 22. Extracted ion chromatogram (top) and MS2 spectrum (bottom) of PS(14:1/14:1) along with annotated fragment peaks.**



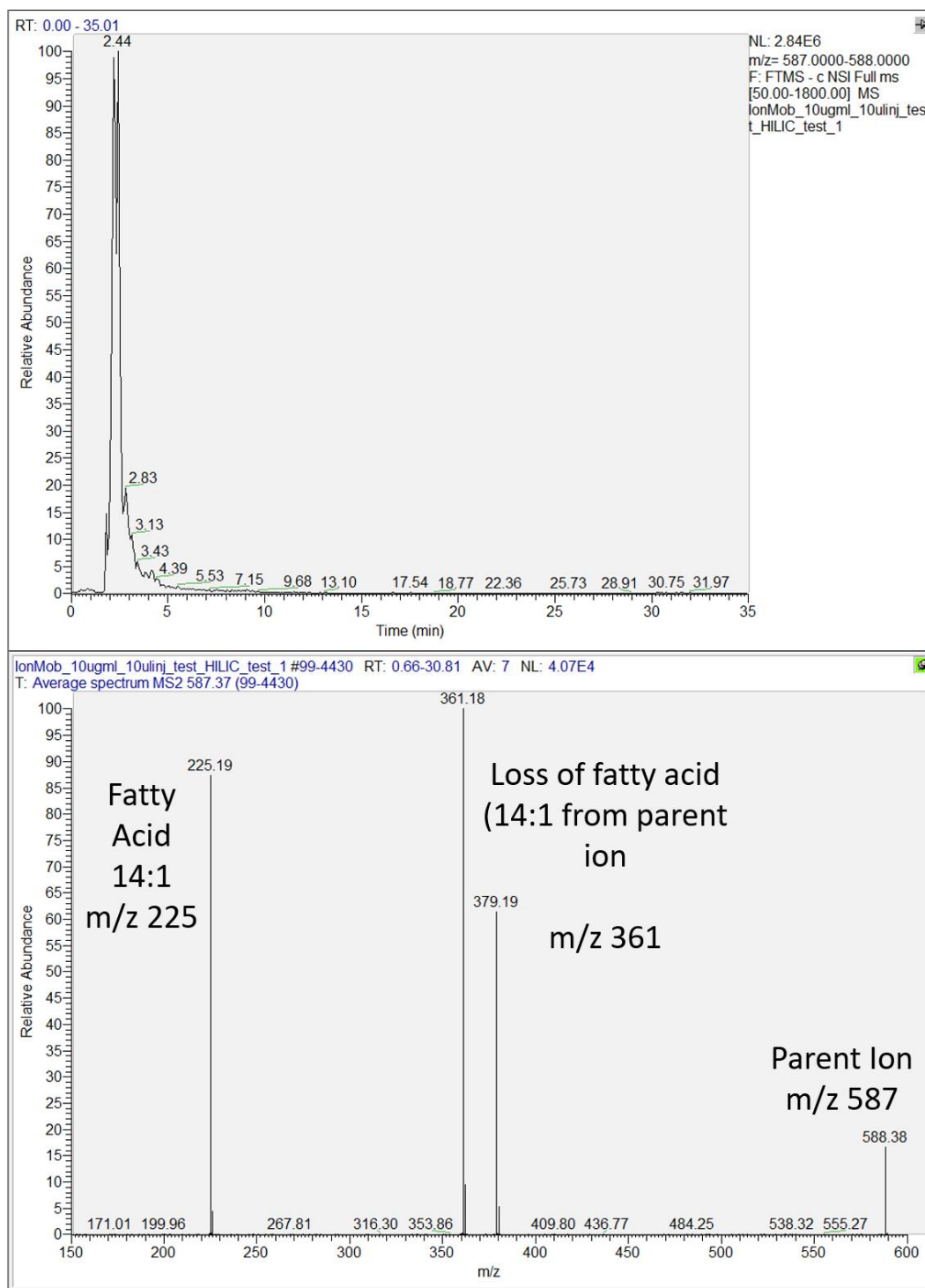


**Figure 23. Extracted ion chromatogram (top) and MS2 spectrum (bottom) of PA(14:1/14:1) along with annotated fragment peaks.**

## Use of isotopic labeling in lipidomics

While not a major component of the studies shown here, it is important to mention the utility that isotopic labeling can provide to an omics study [191-195]. While most untargeted studies aim to fully catalog as many of the components of a sample as possible, the incorporation of isotopic labeling into an organism and/or sample can reveal crucial insights into how molecules move within a system and are transformed into other molecules. In mass spectrometry-based omics, the simple mass difference between a labeled and unlabeled atom is more than enough to identify an added molecular isotope or a downstream derivative of a known added isotope, which can help to reveal the movement of molecules within a system and unlock new lines of targeted research.

### *Tracking the efficiency of label incorporation into the bacterial cell membrane*

Tracking the incorporation of deuterium into phospholipids can be a useful tool for researchers. While deuterium is an appealing labeling method in general due to the ease with which one can generate deuterated molecules, there are some discrepancies that need to be addressed when it comes to exchangeable hydrogens. When feeding a cell culture an aliquot of known percentages of deuterated water, a reasonable expectation for incorporation into the sample is that molecules will have deuterium incorporation that is comparable to the percentage of D<sub>2</sub>O fed to the sample. However, this is not generally observed, as the phospholipids in samples grown in 100% D<sub>2</sub>O never exceeded 85% incorporation, with the lower percentages of feedstock D<sub>2</sub>O following similar trends. Similarly, this has been observed in previous studies that have a setup not unlike what has been described here [196-198].

The cause of this is likely a very simple answer that can be quickly tested and reveal some interesting insights into how the cell synthesizes both phospholipids as well as the components (fatty acids and head groups). D<sub>2</sub>O is not the only component of the cell culture broth; there are also sugars and other molecules containing hydrogen that could just as easily be incorporated into a given phospholipid and affect the percentage of deuterium incorporation. To fully achieve a level of deuterium incorporation that is in line with the expected percentage of deuterium, it is necessary to regulate not only the D<sub>2</sub>O but also any other organic molecules in the media that the cell could incorporate. This generally means analyses such as this require media-relevant sugars to also be fully deuterated, which would then likely cover as many of the possible routes of exchangeable hydrogens into the cell as possible.

Despite these challenges, this type of analysis has shown some very promising preliminary results, with the fatty acids (Figure 24), PE species (Figure 25), PG species (Figure 26), and CL species (Figure 27) all showing distinct patterns of deuteration. Despite a certain level of necessary ambiguity about the exact number of labeled carbons per lipid species at each deuteration level, especially considering the previous concerns about unlabeled hydrogens managing to be incorporated into the phospholipids even at 100% deuterated water, there is clear evidence of a rising amount of deuteration within both the fatty acids and the phospholipids as the level of deuteration in the starting culture increases. Further testing to establish easier methods of identifying the level of deuterium incorporation is needed, but this is a promising start.

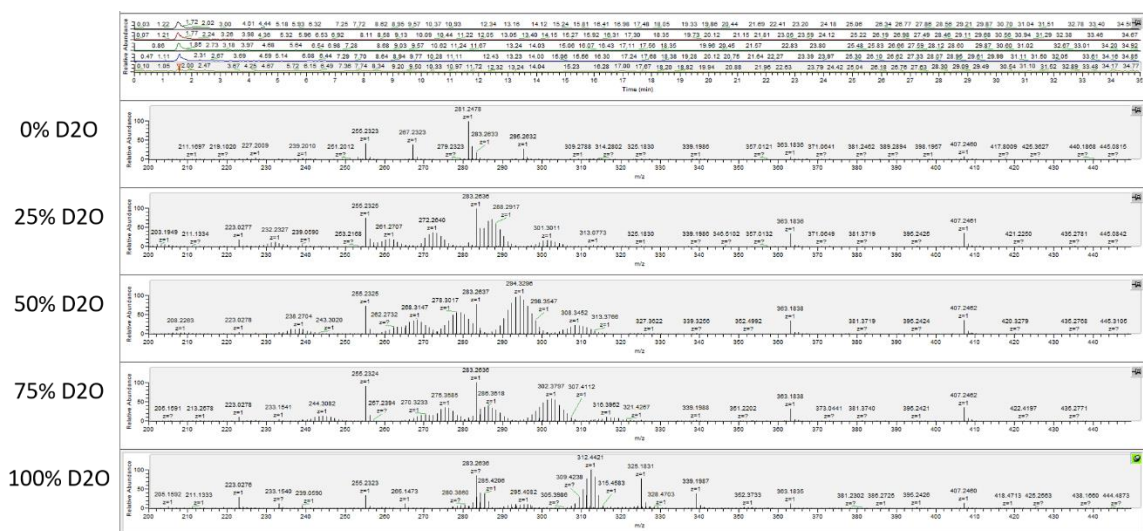


**Figure 24. Comparison of lipid profiles across various deuteration levels within the fatty acids of *E. coli***

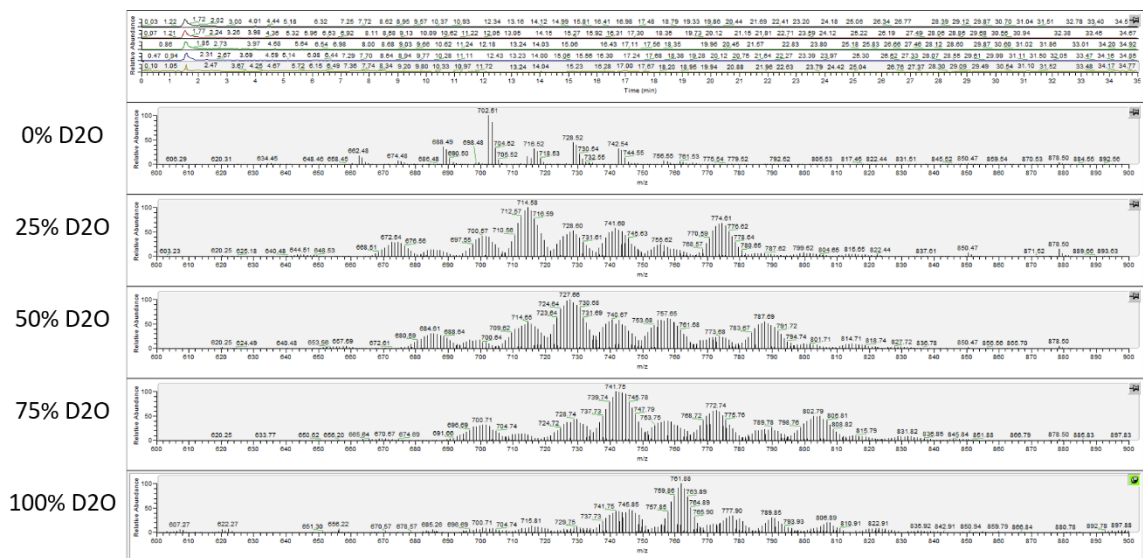


**Figure 25. Comparison of lipid profiles across various deuteration levels within the PE species of *E. coli***

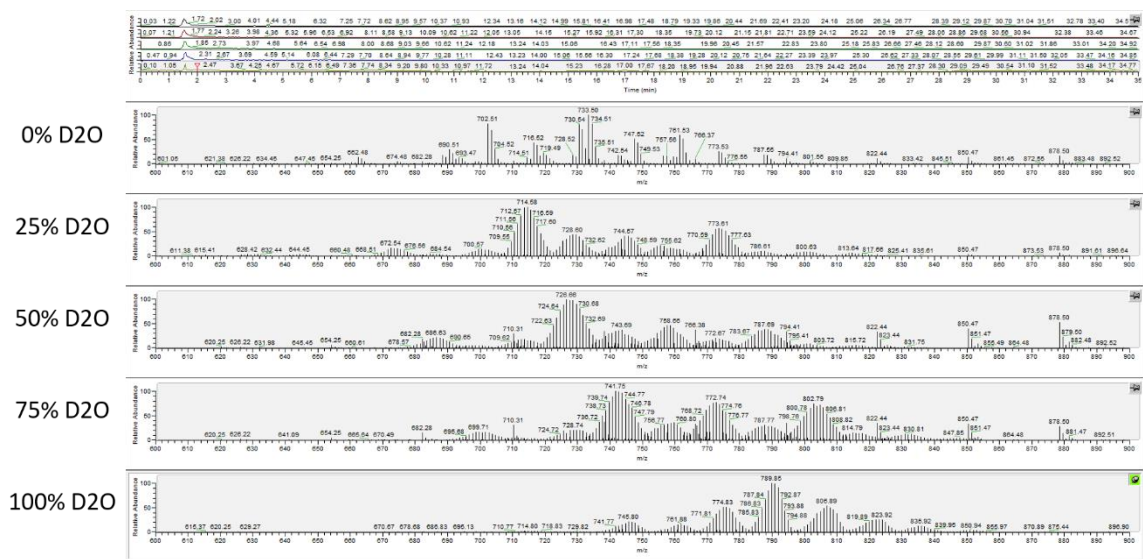


**Figure 26. Comparison of lipid profiles across various deuteration levels within the PG species of *E. coli***

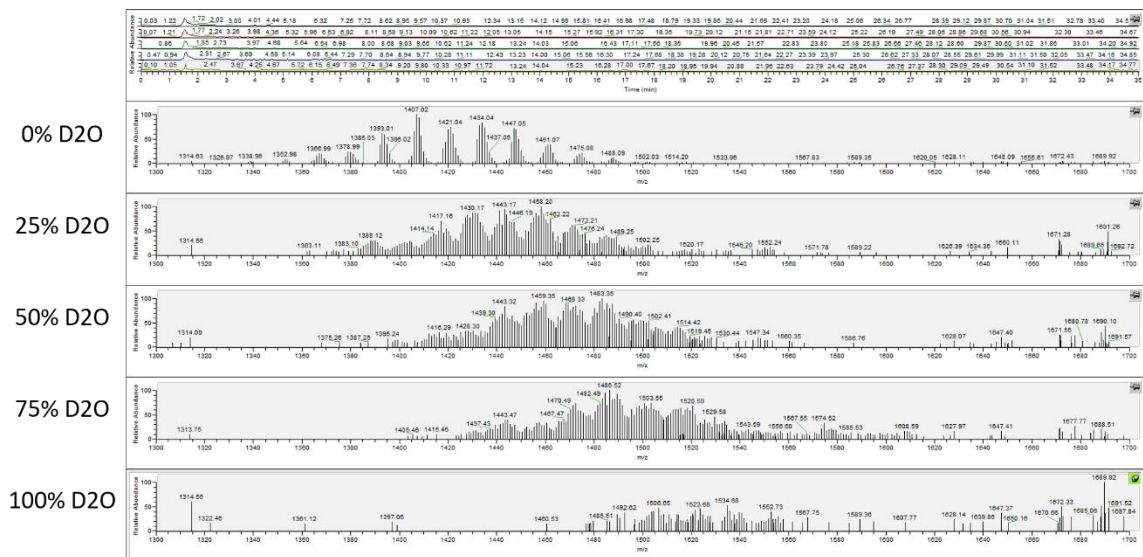


**Figure 27. Comparison of lipid profiles across various deuteration levels within the CL species of *E. coli***

## **Processing lipidomics data – selected tools and techniques**

Data processing is always a key consideration with omics analysis. Being able to full utilize all aspects of mass spectrometry-produced data as well as manipulating and filtering it properly means that it is necessary to explore all the possible options available that would be useful. While there are still many informatics packages locked behind paywalls or instrumentation-specific metrics, there are a wide variety of free, open-source programs available that can perform a more than sufficient analysis. Here, the selection and rationale behind approaching lipidomics with an informatics platform comprised of several methods and programs will be discussed.

### ***Data processing programs***

The first software package commonly used within metabolomics is MZmine, a frequently updated metabolomics data processing and annotation informatics package that provides a high level of data curation while also containing access to several different databases. Very user friendly and highly customizable to whatever experiment or dataset being examined, MZmine offers a fantastic platform for almost any type of omics analysis, modified to the demands of the researcher piloting it. As a brief overview, MZmine utilizes raw spectral files that can be transformed and enhanced in several different fashions, depending on the study in question. Spectral lists with information-rich peaks can be generated, which then can be modified, edited, and filtered using several modules to the level with which the researcher is comfortable, after which the files can be searched using databases that have MZmine plug-ins.

Outside of processing time for certain modules and database searches, MZmine is a relatively quick and intuitive program. Still, there is one notable downside, and that lies in the near complete lack of any level of MS2 validation. While MZmine does use MS2 scans to create pick lists, it does not utilize that data in any appreciable way, which means tentative annotations rely almost exclusively on high mass accuracy MS1 masses. This can lead to major issues specifically with isomers - metabolomics and lipidomics are rife with isomers that can quickly convolute analyses, and a lack of MS2 validation means the only way to approach a level of accuracy is to use context clues from the organism or system being examined. This can be used in lipidomics in select circumstances; the studies described later rely on the assumption that a lack of clarity between PC and PE is largely moot because of the species in question not possessing any discernable level of PC. However, metabolomics is much harder to deconvolute this issue. Take central metabolism as an example – with the abundance of sugars and sugar derivatives in glycolysis, interest may arise in being able to discriminate between forms of fructose and glucose. While there are labeling methods that can achieve this [199, 200], reliance on underivatized samples and MS1 measurements cannot fully achieve desired results.

To solve the issue of MS2 validation in lipidomics, LIQUID was explored as a possible alternative or complementary package to MZmine. On the surface, LIQUID appears to be an exceptional upgrade over MZmine. After processing a raw file with appropriate mass error boundaries, LIQUID generates an output file based on mass accuracy and MS2 fragment overlap, giving a score that is indicative of how well a given MS1 peak matches up to the database based on head group- and fatty acyl-specific MS2

fragmentation. However, the one major downside to LIQUID is a complete lack of any data consolidation or processing tools. Files can only be processed one by one, which eliminates any possibility of automated alignment and consolidation of files, and there are no filtering tools to eliminate duplicate peaks. As a result, despite the massive upgrade this program provides over MZmine in MS2 validation, LIQUID is still somewhat limited in applicability as a stand-alone application, though it does notably work very well as a very quick spot checker for simplified runs such as standards. Additionally, while LIQUID is very proficient at basic phospholipid identifications, LIQUID's provided databases appear to be limited to just that; examination of MZmine hits do reveal occasional lipid variants and fatty acid modifications, while LIQUID appears to be more restricted to basic, higher-level lipids.

New tools for lipidomics are also being produced every year, with LipidCreator [201] and lipidr [202] being just two promising programs released in the past 2 years that were considered as possible alternatives. There are also more traditional tools that have been available for years, such as LipidBlast [203] and the recently updated LipidFinder 2.0 [95], as well as instrument- or platform-specific programs like Thermo's LipidSearch and Sciex's LipidView. Each one offers slightly different levels of peak validation, data processing, and user viability, but the level of comfort with the programs selected as well as the scientific questions being probed meant that MZmine and LIQUID were the primary choices for later experiments.

It is also worth mentioning manual annotation as the most basic method of tentative annotation and species confirmation. Manual spectra examination remains the



best method for determination of lipid species, but it is an incredibly slow method. Still, in a field where variants and modifications are common and largely unrepresented in most databases, despite being reported in literature, knowing how to manually explore spectra for MS1 masses and figure out how a given molecule fragments to identify peaks within an MS2 spectrum is a crucial skill to have. In this manner, it is possible to fully validate tentative annotations with highly accurate precursor masses as well as identification of key fragment peaks, but it is preferable to only use this when database searching proves fruitless.

## Conclusions

Described here was a thorough exploration into each step of the lipidomics analysis outlined in Chapter 2, critically examining each step for validity and optimization as well as explaining the thought process behind selection of techniques used over possible alternatives. Having established both a methodology as well as robust testing of validation of the various steps within the procedure, the next step is to apply these principles to actual samples. In the following two chapters, lipidomics experiments are describe that have probed the lipid profiles of *Bacillus subtilis* and *Pseudomonas putida* samples under several conditions. These include growth in several solvents and solutions that are indicative of conditions that might be present where those bacterial species are expected to be of specialized industrial use in the future. By understanding the changes induced within the cell membrane by presence of specific conditions, it may become possible to engineer bacterial strains that can better adapt and survive under those conditions for large scale industrial applications.

**CHAPTER 4: PROBING OF THE LIPIDOME OF THE MODEL ORGANISM  
*BACILLUS SUBTILIS* ACROSS DIFFERENT GROWTH CONDITIONS  
REVEALS SHIFTS IN PHOSPHOLIPID COMPOSITION**

A version of this chapter is in preparation for publication:

Reeves, D.T., Bonifer, K.S., Elkins, J.G., Hettich, R.L. "Changes in membrane physiology of *Bacillus subtilis* from biofuel reactor conditions revealed by HILIC-MS/MS lipidomics (tentative title)." Manuscript currently in preparation.

### **Abstract**

Critical bottlenecks have emerged that require innovative solutions to overcome. As natural resources are drained and supply chains are stressed by ever growing needs, increasingly diverse methods are necessary to keep up with demand. *Bacillus subtilis* offers a unique research platform with which to design experiments based in biotechnology, as it has a long history of characterization as a model organism while also generating significant interest in medical, industrial, and biofuel applications. Utilization of the information provided by the *B. subtilis* lipidome, which has been thoroughly researched and published, can give crucial information about how the bacterial cell adapts and reacts to adverse growth conditions, from various solvent growth conditions characteristic of expected biofuel reactor conditions to genetic modifications and restrictions on cellular fatty acid access. Described here is a lipidomics platform that allows for comprehensive examination of the *B. subtilis* lipidome, probing differences induced by several experimental conditions as well as testing measurement depth through the exhibition of expected phospholipid profiles and lesser expected lipids. Additionally, lipid variants were characterized, such as aminoacylated derivatives of phosphatidylglycerol and cellular structural components like lipoteichoic acid, that are not always commonly reported as being present in generic lipidome extracts. The ability to pull out lipidome differences arising from known growth perturbations in conjunction

with the utilization of quality MS2 spectra for lipid characterization is encouraging to future lipidomics studies, and the implications of the results within the context of *B. subtilis*-driven studies will fuel endeavors to create bacterial strains optimized for future biotechnology applications.

## Introduction

*Bacillus subtilis* has long been used as a model organism for research projects in no small part due to thorough understanding of the genome and proteome compiled over the years and general ease in genetic manipulation, which lends itself to a certain amount of untapped potential for production of important bioproducts and even industrial goods with proper engineering [204]. This potential has intrigued scientists for years, raising the question of how to properly utilize *B. subtilis* in such a way that cells can efficiently produce natural products with minimal risk to the long-term viability of the cell.

This is critically important when engineering strains of *B. subtilis* for use in various large scale industrial biofuel operations that utilize lignin as a feedstock targeted for degradation. While bacteria have been shown to be a capable vector for lignin degradation [205], both the chemicals used to help soften lignin to a state that is processable as well as the expected products (short-chain alcohols) present a challenge for extended viability of the potential bacterial workhorses [206]. Therefore, it is critical to understand how the bacterial cell reacts when faced with the (often toxic) chemicals that would be expected to be present as desired products or waste. While downstream effects likely would be evident throughout all aspects of the cell, the cell membrane is particularly intriguing as it lies in direct contact with the exterior environment and would

theoretically be subject to more drastic and immediate changes than either the genome or proteome [207, 208]. With phospholipids comprising the main portion of the cell membrane, lipidomics has recently risen to prominence as a useful tool in assessing how a cell or system instantaneously reacts to the presence of a foreign substance or shift in cellular environment by modifying the construction and fluidity of the cellular membrane in an attempt to survive or adapt [209]. Because of the general interest in advancing understanding of human health, utilizing lipidomics often centers around how it can aid in the discovery of important biomarkers [210-212], but applications within bacteria [213], fungi [214], and plants [215, 216] have countless different applications as well.

The basic *B. subtilis* lipidome has been thoroughly investigated in the past [85, 171, 217, 218], but studies relating to how the membrane reconfigures as a function of exterior environment have largely been limited to common solvents such as methanol and ethanol [219]. While those two alcohols are highly desired products for use for industry and transportation [220, 221], the ability to efficiently mass produce longer chain alcohols would further embolden those fields. However, butanol and related isomers are not as easily produced, even though they challenge ethanol and acetone as highly prized chemicals that can be produced via microbe [222-225]. There are also considerations in the solvents required for the softening of lignocellulosic material; tetrahydrofuran (THF) is often used as a pretreatment that is effective in isolating lignin from the lignocellulosic biomass, and the active biomass would be exposed to significant levels of THF [226, 227]. However, THF has been shown to exhibit inhibitory effects on the microbial communities used in activated sludge used to treat wastewater [228, 229]. While there are

reports on genomic and proteomic consequences of prolonged exposure of bacterial cultures to these solvents, effects on the bacterial cell membrane are not well reported.

In this study, a comprehensive examination of the lipidome of *Bacillus subtilis* will be performed, with a focus on how the phospholipid profile shifts in response to growth within varying concentrations of butanol, isobutanol, and THF. Additionally, strains of *B. subtilis* that have been altered to remove significant portions of the fatty acid biosynthesis pathway will be examined, probing how the membrane composition of those strains shifts when exposed to fatty acid feed stocks of variable complexity. Finally, in addition to probing the generic phospholipid profile of *B. subtilis*, characterization of lesser reported phospholipid derivatives and phospholipid-adjacent molecules will be undertaken, such as expected aminoacylated phospholipids as well as cellular structural components like lipoteichoic acid, which are not always observed in general lipidomics extracts and analyses. Through this study, the goal is to demonstrate tangible shifts in the phospholipid profile, tied to specific experimental conditions, that can be used in future work to engineer workhorse microbial communities with phospholipid membranes that can withstand increasingly harsh environments while not sacrificing industrial efficiency.

## **Experimental Approach**

### ***Preparation of B. subtilis cell cultures***

Cultures of *Bacillus subtilis* 168 were prepared to examine an array of modifications to phospholipid speciation and responses to environmental challenges similar to those that might be observed within biofuel reactor conditions. Fatty acid access was modulated by introducing a knockdown of the FabF gene and then adding

mixtures of fatty acids to the resultant culture; all cultures (both the FabF knockdown strains and the control cultures with no modification to fatty acid biosynthesis) also contained a knockout for FadN to prevent fatty acid recycling within the cell. Fatty acid mixtures included a native mixture of six fatty acids commonly seen within *B. subtilis*, as well as a more restrictive non-native mixture of two fatty acids. Additionally, cultures were grown in butanol (2%) and isobutanol (2%), as relevant potential bioproducts, and THF (6%), as a commonly used chemical for lignocellulose degradation. In addition to isolated cultures, mixtures of the fatty acid feeding conditions and solvent growth conditions were performed as well.

#### ***MTBE-based extraction of *B. subtilis* lipidome***

Samples were delivered in biological triplicate as large, dried cell pellets grown to an optical density (OD) of 0.6-0.8 in 1.5 mL Eppendorf centrifuge tubes and were stored overnight at -20°C before processing, after which they were consistently kept on ice during extraction. For lipid extraction, a modified version of the Matyash method was used with MTBE, as previously described in Chapter 2 [114].

#### ***LC-MS/MS lipidomics analysis***

Before sample processing, samples were loaded into auto-sampler vials (10 µL of sample, 5 µL sample injection volume). No ionization agent was added to samples prior to injection, as the additive in the HILIC-specific chromatography solvents used here (specifically, 5 mM ammonium acetate) are sufficient for ionization, both in positive- and negative-ion mode. Samples were run in batches, with technical blanks added in between

similar sampling conditions for quality control as well as to monitor potential carry-over and standards run at frequent intervals to monitor consistency. Chromatographic separations and tandem mass spectrometry analysis were performed as previously described in Chapter 2 for HILIC separations in negative polarity mode.

### ***Lipidomics data analysis***

Bulk processing of the raw LC-MS/MS files was performed using the free, open-source software MZmine (version 2.53) [99, 159, 230] alongside manual annotation. Information regarding the purpose and rationale for each step of data analysis within MZmine can be found within Chapter 2.

Here, because a significant facet of the experimental design revolved around limiting the ability of the bacteria to have full access to fatty acid biosynthesis and degradation pathways, a specific range of lipids was created with prior studies and previously observed *B. subtilis* lipidomes in mind. References to literature indicated that the phospholipids of *B. subtilis* were relatively uniform and well known [231], though there is some debate on the presence of unsaturated fatty acids [171]. To that end, the masses of PE, PG, and PL species containing fatty acids of length 14-17, corresponding to the range of fatty acids including in the fatty acid mixtures fed to specific cultures in this experiment, as well as no greater than one double bond per 2 fatty acid chain phospholipid (max of 2 for cardiolipin species) were calculated, and the corresponding aligned peak areas from MZmine were assigned to each feature. The peak areas for those phospholipids are shown below for growth in normal media (Table 7), butanol (Table 8), isobutanol (Table 9), and THF (Table 10).



**Table 7. Compiled master list of selected phospholipid species with averages across triplicate MZmine-aligned peak areas in *B. subtilis* 168 samples grown in normal media.**

<b>Phospholipid Species</b>	<b>No Solvent/No FA Feeding</b>	<b>No Solvent/Native FA Mixture</b>	<b>No Solvent/Non-Native FA Mixture</b>
PE(28:1)	0	369225.3254	0
PE(28:0)	33183.3218	5871.184497	394377.8825
PE(29:1)	2194.391782	417287.7238	657462.568
PE(29:0)	366532.7018	5451.292518	136584.8929
PE(30:1)	28431.62967	2909427.806	24173431.13
PE(30:0)	2136151.637	732278.0842	606768.4296
PG(28:1)	3717.86891	2464915.964	9560.414528
PG(28:0)	2792027.246	359514.5503	1617658.276
PE(31:1)	436909.2763	13478662.11	272816.8093
PE(31:0)	486799.9432	31769.79694	21693711.69
PG(29:1)	25189.19157	1439643.299	125902.4741
PG(29:0)	4387951.214	941355.5651	3633778.806
PE(32:1)	3310826.019	3248181.025	60596.06377
PE(32:0)	46263269.86	29383.79354	53767.92449
PG(30:1)	513987.0254	28844310.53	5261984.52
PG(30:0)	31409040.75	13865534.04	77446021.8
PE(33:1)	502692023.5	10703834.94	354582.7977
PE(33:0)	29393737.11	199468.3808	0
PG(31:1)	10878309.5	59594507.86	25465999.64
PG(31:0)	3129830.913	24747963.14	465029977.6
PE(34:1)	32244649.53	54687.07425	1163.610792
PE(34:0)	389506.5341	0	0
PG(32:1)	22402794.18	40805100.9	200520.4248
PG(32:0)	129383933.1	9671369.196	10946565.83
PG(33:1)	1203863455	118007748.6	204927.8127
PG(33:0)	19176892.54	19210857.77	1022.947742
PG(34:1)	2545978.769	518032.8452	12280.26943
PG(34:0)	4206656.512	1205.162678	55326.89252
CL(56:0)	0	0	0
CL(57:0)	0	0	157132.3102
CL(58:0)	0	2522.812739	796795.1633
CL(59:1)	0	0	6710.39045
CL(59:0)	56873.65835	0	1549375.143
CL(60:1)	1144.330108	0	204836.049
CL(60:0)	261876.0316	5539.278829	3315032.717
CL(61:2)	2377.36184	0	62934.7493
CL(61:1)	0	1884.290161	2372873.409

**Table 7 Continued**

<b>Phospholipid Species</b>	<b>No Solvent/No FA Feeding</b>	<b>No Solvent/Native FA Mixture</b>	<b>No Solvent/Non-Native FA Mixture</b>
CL(61:0)	317517.864	5053.208832	36613965.79
CL(62:2)	2269.610872	6799.485589	173341.755
CL(62:1)	15518.72611	3248.435181	9893224.666
CL(62:0)	359039.1743	20969.13057	97520482.49
CL(63:2)	1584.250345	1675.199527	1355.478529
CL(63:1)	14160.04828	3230.997518	114870.7374
CL(63:0)	116924.257	1627.980228	1631774.289
CL(64:2)	4025.351023	7798.846141	10804.10292
CL(64:1)	62789.58228	10507.65306	2361.871341
CL(64:0)	83638.35224	3655.647765	23275.9076
CL(65:2)	0	0	0
CL(65:0)	81843.74808	2236.245177	0
CL(66:2)	6104739.989	22323.96358	32405.96719
CL(66:1)	2391589.231	24986.79573	18140.266
CL(66:0)	84120.10663	5142.88952	1943.589582
CL(67:2)	1192730.488	9732.876378	126138.5157
CL(67:1)	449242.7496	3636.56685	2083.415598
CL(67:0)	1433886.991	1695.81638	0
CL(68:2)	4631907.729	850261.3061	670483.0541
CL(68:1)	8649206.933	29216.61671	1259.523691
CL(68:0)	131480.3624	0	0

**Table 8. Compiled master list of selected phospholipid species with averages across triplicate MZmine-aligned peak areas in *B. subtilis* 168 samples grown in varying concentrations of butanol.**

<b>Phospholipid Species</b>	<b>Butanol @ 2%/No FA Feeding</b>	<b>Butanol @ 2%/Native FA Mixture</b>	<b>Butanol @ 2%/Non-Native FA Mixture</b>
PE(28:1)	0	0	0
PE(28:0)	3455.359	31433.95	647836.3
PE(29:1)	3183.052	3016907	53813.33
PE(29:0)	9218.614	1817080	10024
PE(30:1)	41213.84	5790066	16438121
PE(30:0)	362804.8	89419344	58289.5
PG(28:1)	6385.345	68464.84	13031.11
PG(28:0)	189394.8	72319.07	167890.1
PE(31:1)	1545874	1292099	12856.95
PE(31:0)	105694.6	38029664	6452957
PG(29:1)	2457522	1539332	163924.3
PG(29:0)	1312094	15803263	531371.9
PE(32:1)	25808389	102521.4	24037.85
PE(32:0)	24863410	58808148	626235.4
PG(30:1)	4275486	8160213	12722105
PG(30:0)	6008363	1.75E+08	59363270
PE(33:1)	2.47E+08	12105.2	8926.025
PE(33:0)	16023907	83105.22	1746.954
PG(31:1)	332310.2	6416434	9230995
PG(31:0)	15388280	1.19E+08	3.03E+08
PE(34:1)	2972643	991.0627	1330.766
PE(34:0)	421925.2	0	0
PG(32:1)	8976626	12982460	47013.6
PG(32:0)	9300852	2.49E+08	2526142
PG(33:1)	14385267	4099.572	5315.308
PG(33:0)	1136120	1586933	21021.18
PG(34:1)	676299	29782.57	1577.762
PG(34:0)	307179.4	84087.82	22645.27
CL(56:0)	0	0	0
CL(57:0)	0	0	0
CL(58:0)	0	297423.6	1285.562
CL(59:1)	0	282779	0
CL(59:0)	18658.11	6913208	40100.75
CL(60:1)	1720.881	2450703	62729.39

**Table 8 Continued**

<b>Phospholipid Species</b>	<b>Butanol @ 2%/No FA Feeding</b>	<b>Butanol @ 2%/Native FA Mixture</b>	<b>Butanol @ 2%/Non-Native FA Mixture</b>
CL(60:0)	79853.73	33049056	2403358
CL(61:2)	5226.289	0	9886.6
CL(61:1)	6497.846	2571888	1337158
CL(61:0)	64209.05	24792770	45721275
CL(62:2)	0	4363.1	0
CL(62:1)	5447.933	3686812	1716296
CL(62:0)	310629.9	32001060	1.07E+08
CL(63:2)	1243.305	6109.086	2486.92
CL(63:1)	110990.3	1010209	21943.71
CL(63:0)	236746	17977424	283318.5
CL(64:2)	45385.35	16671.71	13145.16
CL(64:1)	163021.9	1285712	7068.758
CL(64:0)	197092.1	22998950	1348.719
CL(65:2)	3377040	0	0
CL(65:0)	230157.1	82113.72	7944.025
CL(66:2)	62843715	63500.63	1038.921
CL(66:1)	20868002	0	17290.4
CL(66:0)	77048.37	981.1345	0
CL(67:2)	5862908	397243.7	7690.919
CL(67:1)	2831287	15814.61	0
CL(67:0)	337789.2	1139.617	0
CL(68:2)	11303277	449054.7	251510.9
CL(68:1)	1920356	0	997.0182
CL(68:0)	1228836	2114.543	0

**Table 9. Compiled master list of selected phospholipid species with averages across triplicate MZmine-aligned peak areas in *B. subtilis* 168 samples grown in varying concentrations of isobutanol.**

<b>Phospholipid Species</b>	<b>Butanol @ 2%/No FA Feeding</b>	<b>Butanol @ 2%/Native FA Mixture</b>	<b>Butanol @ 2%/Non-Native FA Mixture</b>
PE(28:1)	0	0	0
PE(28:0)	88681.98	22920.07	124004
PE(29:1)	16060.34	43523.12	951.6202
PE(29:0)	575850	356867.4	147820.5
PE(30:1)	30066.44	2058225	210533.1
PE(30:0)	4087494	18518012	9276673
PG(28:1)	7931.904	62211.01	101002.3
PG(28:0)	1307605	48022.75	6125.438
PE(31:1)	37539.73	118036.7	16882.68
PE(31:0)	4690131	30171038	1.03E+08
PG(29:1)	90111.72	2018740	135423.4
PG(29:0)	7214106	14275437	31837.11
PE(32:1)	203023.2	197819.3	34521.33
PE(32:0)	8787904	28581686	941679.6
PG(30:1)	424768.5	1903172	2558364
PG(30:0)	45081214	1.69E+08	20565235
PE(33:1)	1624362	102510	158400.7
PE(33:0)	24837.15	15764.39	6950.741
PG(31:1)	349846.9	1380529	392038.4
PG(31:0)	33826234	1.31E+08	1.1E+08
PE(34:1)	0	1149.018	0
PE(34:0)	0	0	0
PG(32:1)	224798	201946.8	588706.7
PG(32:0)	32084016	98237981	680256.3
PG(33:1)	374243.6	147899	149695.3
PG(33:0)	442837.9	332922.7	8283.131
PG(34:1)	8953.018	65414.1	4680.28
PG(34:0)	82528.87	3033.733	2777.628
CL(56:0)	0	0	0
CL(57:0)	0	0	0
CL(58:0)	141575.3	322244.7	7065.146
CL(59:1)	1722.041	11007.95	6767.186
CL(59:0)	878101.2	3101968	6305.94
CL(60:1)	6808.397	777474.8	10765.17

**Table 9 Continued**

<b>Phospholipid Species</b>	<b>Butanol @ 2%/No FA Feeding</b>	<b>Butanol @ 2%/Native FA Mixture</b>	<b>Butanol @ 2%/Non-Native FA Mixture</b>
CL(60:0)	2104205	52795456	1980644
CL(61:2)	0	29473.88	10404.97
CL(61:1)	32565.18	294512.6	23644.45
CL(61:0)	1869504	57004234	18023752
CL(62:2)	0	988.6198	1089.754
CL(62:1)	36467.58	73810.47	125952.5
CL(62:0)	6595169	49468729	69474968
CL(63:2)	0	5080.482	3887.81
CL(63:1)	8400.446	33588.98	5984.15
CL(63:0)	4804776	25920196	43258.84
CL(64:2)	0	26975.21	18917.09
CL(64:1)	5269.045	11987.9	2843.565
CL(64:0)	1431652	8332866	8321.577
CL(65:2)	0	0	0
CL(65:0)	123710.9	115335.7	7535.365
CL(66:2)	242697.6	14133.16	2469.03
CL(66:1)	133054.3	2471.504	3034.468
CL(66:0)	0	0	150823.8
CL(67:2)	20165.88	179256.7	6324.368
CL(67:1)	160180.2	1451.542	5142.529
CL(67:0)	54165.12	1051.971	16471.02
CL(68:2)	219061.3	131951.1	49429.5
CL(68:1)	0	1730.313	263228.8
CL(68:0)	0	995.2207	1207.655

**Table 10. Compiled master list of selected phospholipid species with averages across triplicate MZmine-aligned peak areas in *B. subtilis* 168 samples grown in varying concentrations of THF.**

<b>Phospholipid Species</b>	<b>THF @ 6%/No FA Feeding</b>	<b>THF @ 6%/Native FA Mixture</b>	<b>THF @ 6%/Non-Native FA Mixture</b>
PE(28:1)	0	0	0
PE(28:0)	9139550	35793.56	31521.66
PE(29:1)	7250.224	702441.8	3725.714
PE(29:0)	39094041	3215731	4379.504
PE(30:1)	161931.8	1159493	58857997
PE(30:0)	1.15E+08	70076925	290080.4
PG(28:1)	456696.4	202590.1	4186.08
PG(28:0)	23221180	233718.6	21984.09
PE(31:1)	676401.5	168596.1	29301.53
PE(31:0)	1.21E+08	52198368	13803786
PG(29:1)	2971259	2460956	64376.21
PG(29:0)	1.36E+08	26241119	14065.04
PE(32:1)	371773.1	49922.46	7449.387
PE(32:0)	77418738	32249269	67575.38
PG(30:1)	5074697	5986384	2041203
PG(30:0)	5.57E+08	2.99E+08	12265830
PE(33:1)	195959.4	6851.178	20798.73
PE(33:0)	891880.4	35939.27	2731.946
PG(31:1)	5872737	6596172	31679292
PG(31:0)	6.03E+08	2.37E+08	2.69E+08
PE(34:1)	0	0	0
PE(34:0)	144046.8	0	0
PG(32:1)	4959648	3339953	1362006
PG(32:0)	5.46E+08	1.7E+08	9174173
PG(33:1)	104279.7	2183.747	21454.24
PG(33:0)	18169813	1086736	11888.25
PG(34:1)	296208.4	153264	8072.067
PG(34:0)	3660594	5221.21	1092.83
CL(56:0)	0	0	0
CL(57:0)	325788.9	0	0
CL(58:0)	1934977	116386.7	4635.392
CL(59:1)	0	8358.592	6007.111
CL(59:0)	4486822	7173426	6885.485
CL(60:1)	3437.499	591394.2	1715.765

**Table 10 Continued**

<b>Phospholipid Species</b>	<b>THF @ 6%/No FA Feeding</b>	<b>THF @ 6%/Native FA Mixture</b>	<b>THF @ 6%/Non-Native FA Mixture</b>
CL(60:0)	11242015	48990584	9082.161
CL(61:2)	1202.391	8203.671	4232.763
CL(61:1)	73526.19	781615	722241.8
CL(61:0)	28351203	56567725	6325972
CL(62:2)	29469.43	3805.132	708678.4
CL(62:1)	106989.7	644972.8	16682636
CL(62:0)	39143723	39675936	54413784
CL(63:2)	22596.49	41843.12	0
CL(63:1)	87147.35	124521.6	30587.36
CL(63:0)	20497428	22796240	460525.6
CL(64:2)	4848.915	17906.61	5156.106
CL(64:1)	49055	9918.969	0
CL(64:0)	7631046	9734290	4139.545
CL(65:2)	0	0	0
CL(65:0)	210751.9	5832.173	0
CL(66:2)	885068.5	275021.8	4041.21
CL(66:1)	18731.61	1165.368	2422
CL(66:0)	2875.987	0	2818.574
CL(67:2)	2839581	2194636	9439.939
CL(67:1)	26394.04	109628	5791.713
CL(67:0)	14148.07	1153.91	13600.3
CL(68:2)	4547642	3057167	39246.24
CL(68:1)	0	0	1110.827
CL(68:0)	0	0	1061.127



## Results and Discussion

### *Unmodified Bacillus subtilis phospholipidomics are in line with previous studies*

To begin, the basic phospholipid profile of *B. subtilis* was examined. Figure 28 shows the raw sum peak areas for the major *B. subtilis* phospholipids PE, PG, and CL as detected in the main control sample of this study, with no major genetic modifications outside of the FadN knockout and no solvent modifications or fatty acid enrichments to growth and the cell culture. As mentioned previously, the phospholipids in this study contained a specific range of fatty acids, in line with previous studies using strains with modifications like what was used here, as well as head groups of the major expected phospholipid species in *B. subtilis* [231]. Additionally, because later experiments in this study explored the influence of fatty acid supplements to the composition of the lipidome, the range of expected phospholipids was further narrowed, resulting in a semi-targeted lipidome containing PG, PE, and CL species of fatty acid chain length 14-17 (corresponding to total fatty acid chain lengths of 28-34 in PG and PE and 56-68 in CL) were considered, alongside fully saturated and monounsaturated chains. This ensured that adequate comparison across sample conditions could be performed, though this could certainly lead to the exclusion of phospholipids with shorter fatty acid chains as a result of membrane damage or any potential lysophospholipid species present in the sample.

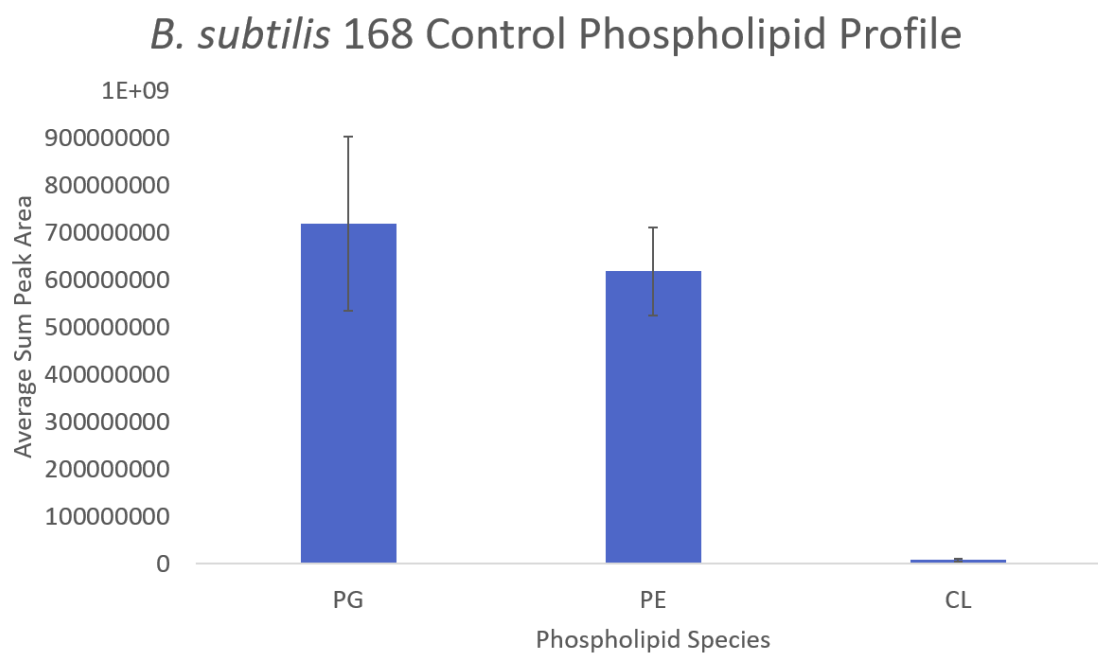


**Figure 28.** Comparison of the observed phospholipids (0-1 double bonds and FAs ranging from 14-17 carbons in length) for the no fatty acid feeding control of *B. subtilis* 168.

Previously reported ratios for the general *B. subtilis* lipidome, across several commonly used strains, are shown below in Table 11. Generally, *B. subtilis* and other Gram-positive bacteria (*Bacillus*, *Staphylococcus*, and *Streptococcus* species) trend towards relatively even proportions of PG or PE, with some species even pushing towards PG being the dominant phospholipid, while Gram-negative bacteria (*Escherichia coli* and *Pseudomonas* species, among others) are traditionally driven by high ratios of PE [58, 186]. Both classes of bacteria trend towards low proportions of cardiolipin, though this occasionally increases within certain species where PE is not normally observed [58, 186]. There are also other lipids that can appear, including PS as a precursor/intermediate in PE production and PA as a more generic precursor to most other phospholipids, as well as acylglycerols, but they are not commonly viewed as main membrane structural components in bacteria specifically [57].

While the observed phospholipids were generally in line with previous studies, it is worth mentioning that *B. subtilis* 168 (the final row of Table 11) specifically has been previously reported to have lipid profiles contrary to what most other studies have reported for other *B. subtilis* strains. Older research has indicated that the phospholipid profile of *B. subtilis* was driven more by the presence of PG than the presence of PE. However, Nickels [231] showed the exact opposite, with PE being by far the most abundant phospholipid species across several sampling conditions. Here, while the general proportions would be more in line with older studies with increased levels of PG, the error bars of both PG and PE are within range of each other, and it bears mentioning the possibility of variable PG to PE ratios given prior research on the strain used here.

**Table 11. Summary of a selection of previous studies on *Bacillus subtilis* lipidomics, demonstrating general proportions of major expected phospholipid species**

Previously Reported <i>B. subtilis</i> Phospholipid Ratios				
Source	PG	PE	CL	Other (if any)
Op den Kamp, et al (1969) [217] <i>B. sub</i> (Marburg) Analysis: TLC; Percentage using dry weight	58% in pH 7 medium (36% PG + 22% lysyl-PG)  60% in pH 5.5 medium (18% PG + 42% lysyl-PG)	30% in pH 7 medium  27% in pH 5.5 medium	12% in pH 7 medium  13% in pH 5.5 medium	N/A
Clejan, et al (1986) [232] <i>B. sub</i> BD99 Analysis: TLC and phosphorus analysis [233]	70%	12%	4%	Others: 14%
Kawai, et al (2004) [234] <i>B. sub</i> 168 Analysis: 2D TLC; fluorescence	Log: 55% (39.4% PG + 15.6% lysyl-PG)	Log: 24.4%	Log: 1.4%	Log: acylglycerols 10.6%, others 8.6%
	T <sub>2</sub> : 63.8% (47.1% PG + 16.7% lysyl-PG)	T <sub>2</sub> : 26.5%	T <sub>2</sub> : 2%	T <sub>2</sub> : acylglycerols 7.5%, others 1.4%
	T <sub>4</sub> : 49.7% (47% PG + 2.7% lysyl-PG)	T <sub>4</sub> : 22.9%	T <sub>4</sub> : 5.4%	T <sub>4</sub> : acylglycerols 9%, others 13%
Bernat, et al (2016) [171] <i>B. sub</i> I'1a Analysis: MS/MS; signal intensity normalization	55-58%	33-37%	5-8%	PA: >1%
Nickels, et al (2020) [231] <i>B. sub</i> 168, ΔyusL strain Analysis: MS/MS, mole fraction	15%	75%	>1%	Digalactosyl-diacylglycerol (DGDG): 10% PA: >5%

It is important to also understand that these *B. subtilis* samples contained genetic modifications in order to be able to understand fatty acid metabolism more fully within the cell and how it can be manipulated for future strain development. All samples analyzed in this study were  $\Delta yusL$  strains of *Bacillus subtilis*; these strains contain a knockout of the FadN gene (Figure 29) which belongs to a family of bacterial genes associated with fatty acid degradation and related processes such as  $\beta$ -oxidation [235]. Without access to a fatty acid recycling pathway that can convert excess or waste fatty acids into more basic CoA molecules or other energy sources, this strain is forced to produce fatty acids only from scratch, not from recycled molecules of spent lipids, which becomes important in later analyses where cultures are also deprived of a natural way to produce fatty acids and must rely on exogenous feedstocks to supply fatty acids for their membranes. This not only empowers downstream research by theoretically improving comprehensive lipidome extractions due to a lack of any efficient way of removing fatty acids from the cell but should also fully prevent cells with the FabF knockdown (which is described later) from having access to anything but the fatty acids provided to them. This type of basic genetic manipulation could prove to be extremely powerful if lipidomics trends are discovered that would benefit from depletion or enhancement of a specific set of fatty acids or even certain species of phospholipids.

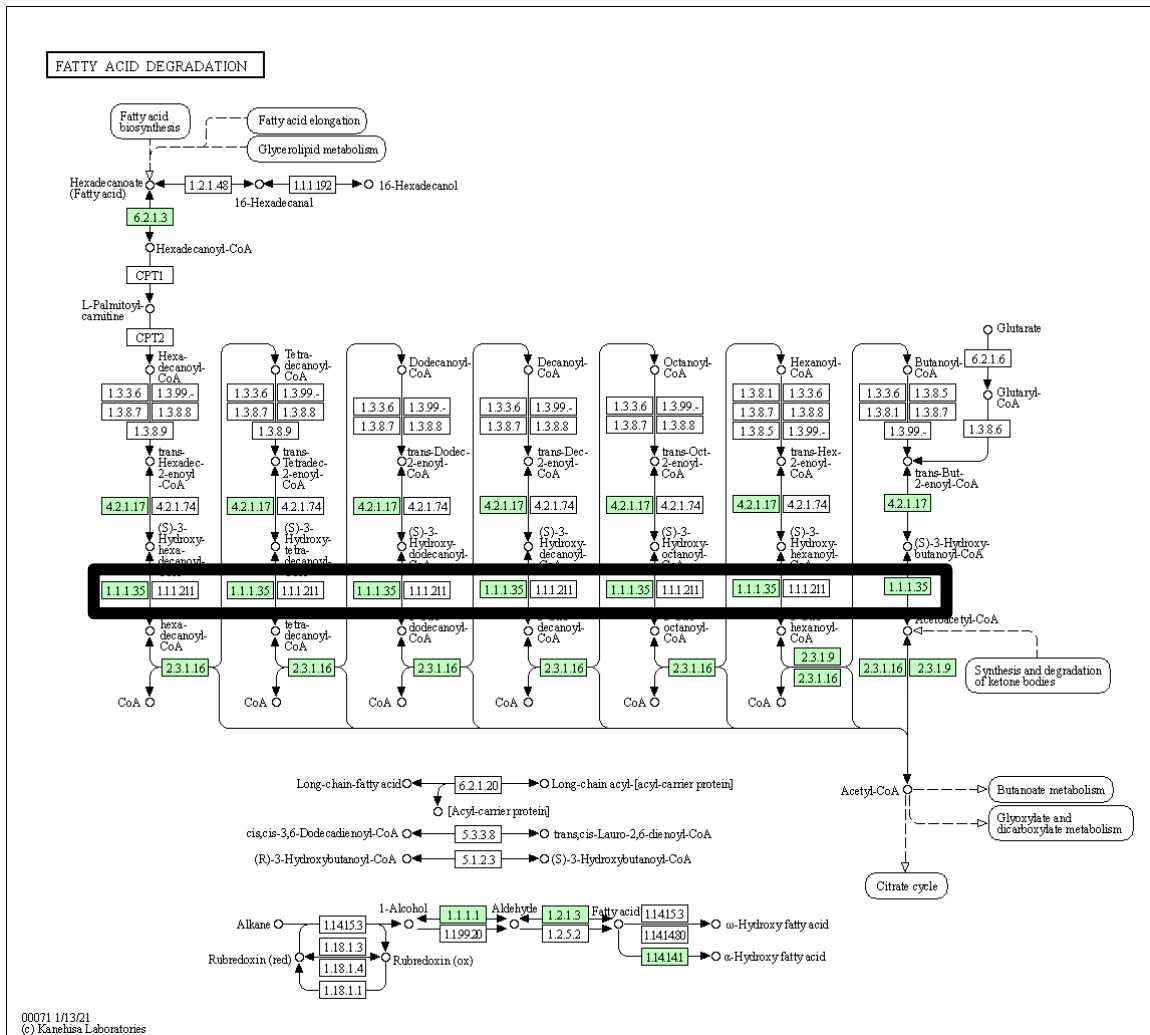


**Figure 29. KEGG pathway for fatty acid degradation in *Bacillus subtilis* 168 [236], with the highlighted gene FadN knocked out in the ΔyusL strain to prevent the cell from being able to efficiently recycle fatty acids into energy or back into new lipids [237].**

***Comparison of fatty acid feeding conditions confirms effectiveness of genetic modifications to fatty acid metabolism***

The first perturbation that was tested was how *B. subtilis* responds to modifications in pathways regarding fatty acid biosynthesis, a key chokepoint in phospholipid development. To begin, a general comparison of phospholipid composition was performed across each of the *B. subtilis* fatty acid feeding conditions (Figure 30). It was not especially surprising to observe that the control samples, with intact fatty acid biosynthesis pathways and no additional fatty acid supplementation, trended towards similar fatty acid composition to the cultures with impaired fatty acid biosynthesis pathways that were fed the native mixture of fatty acids commonly observed within *B. subtilis*. In a similar manner, it was also not surprising to observe that the modified cultures fed the more restrictive non-native fatty acid mixture were much more limited in chain length (Figure 30A) and also had a much lower degree of unsaturation (Figure 30B). The former is expected given a lower overall average chain length of the fatty acids being provided to the cultures, but the drastic drop off in double bond presence was not.

The variability between feeding conditions is a result of the manipulation of the fatty acid biosynthesis pathway (Figure 31). *B. subtilis* synthesizes fatty acid precursors by a stepwise process, starting with acetyl-CoA obtained from the citric acid cycle and converting it into a precursor attached to an acyl carrier protein (ACP), known as acetyl-ACP. This initial precursor is successively elongated through several steps until it is transformed into hexadecanoyl-ACP, which is then used for phospholipid synthesis (Figure 32).

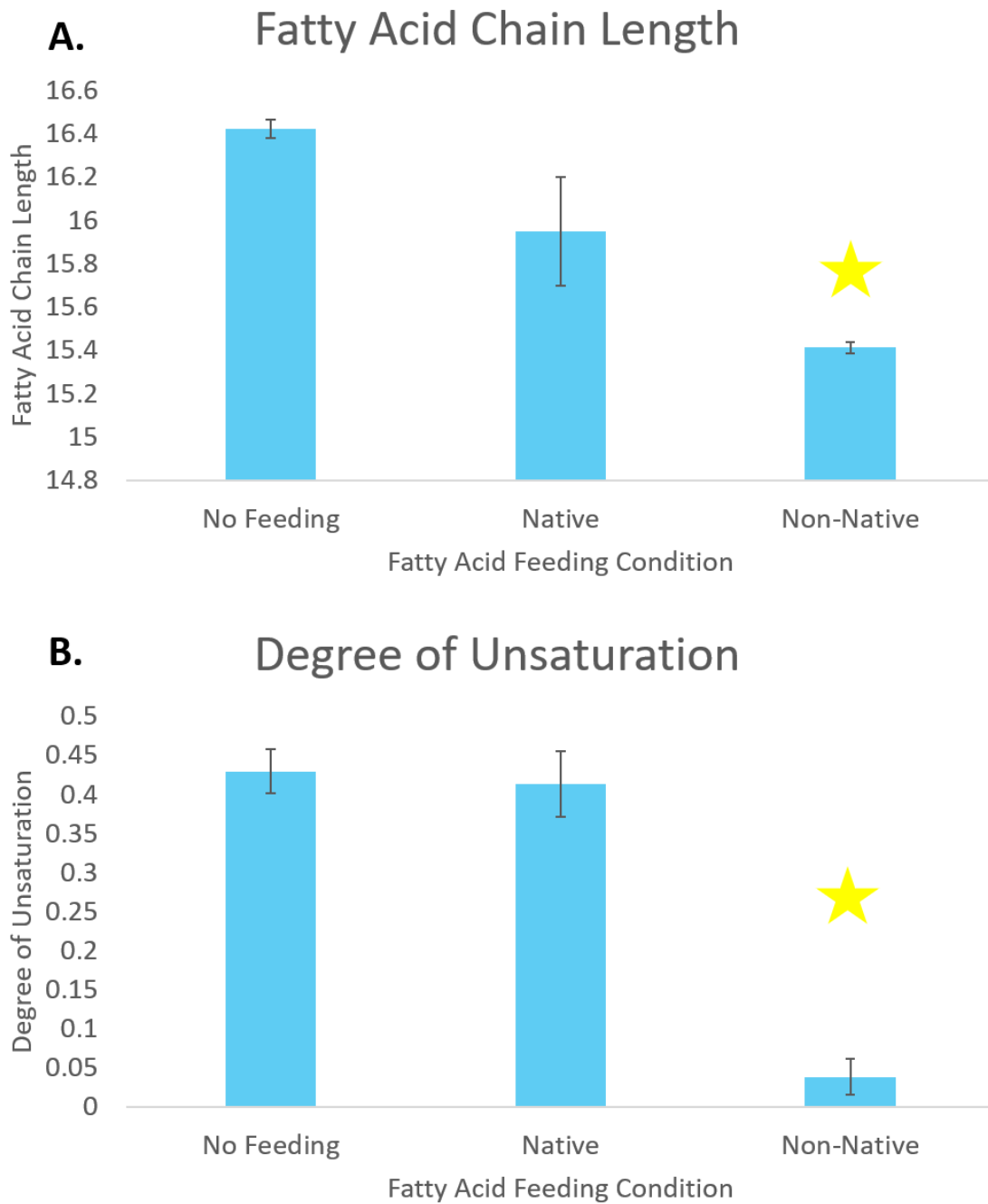


**Figure 30. Comparison of A) chain length and B) degree of unsaturation of the fatty acids within phospholipids extracted from each feeding condition applied to *B. subtilis* 168. Stars indicate groups deemed significantly different from the no feeding control by the Student's t-test.**





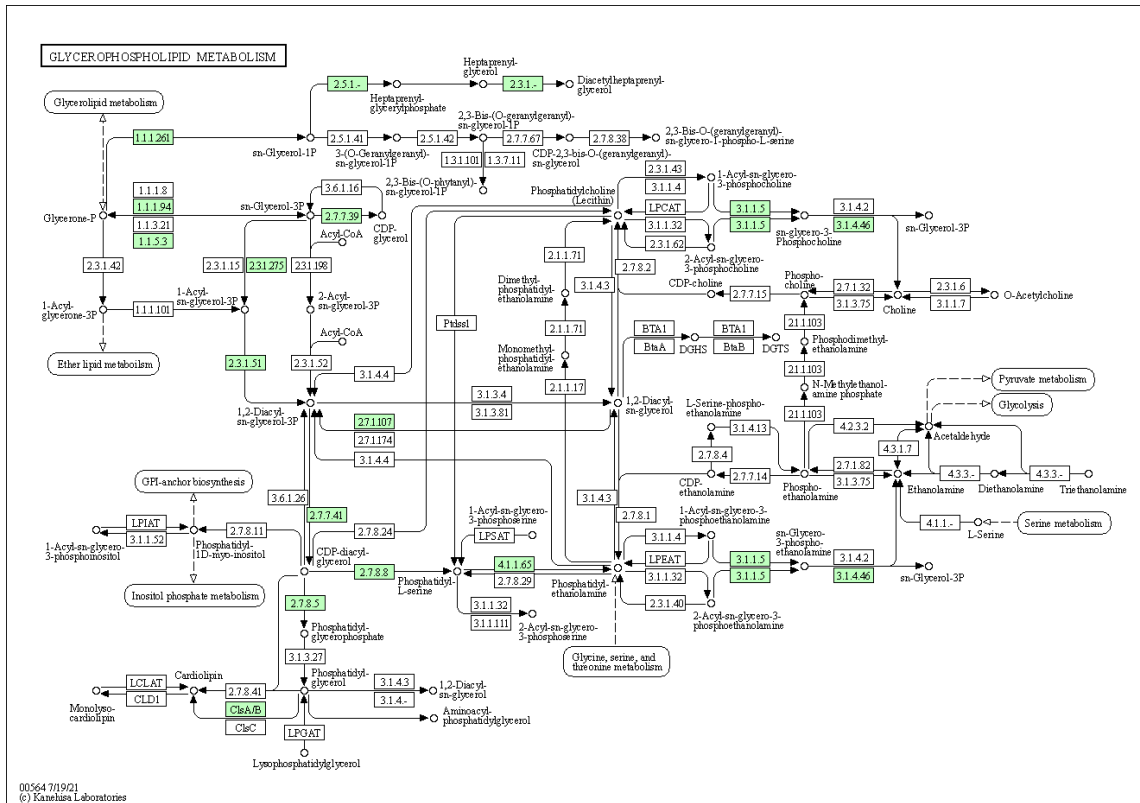
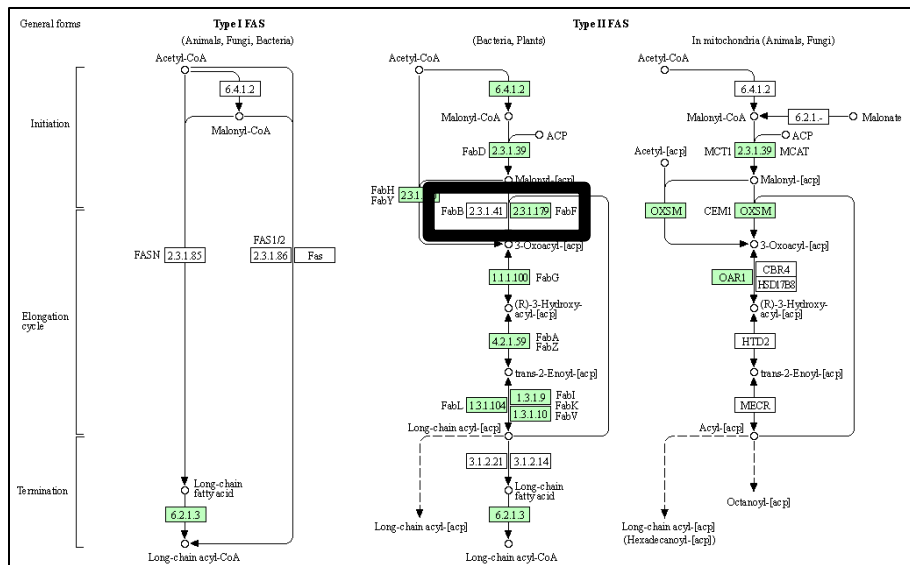


**Figure 32. KEGG pathway for glycerophospholipid metabolism in *Bacillus subtilis* 168 [239].**

The key enzyme in this precursor formation is FabF, which encodes the Type II fatty acid synthase (FAS) 3-oxoacyl-ACP synthase 2 (Figure 33). FabF is crucial for enabling the elongation of acyl-ACP species via a transfer of two carbons from malonyl-ACP to the acyl-ACP species being elongated, and it has previously been shown to be upregulated in transcription in response to environmental antimicrobial agents such as cerulenin [240], implying that FabF could be a key gene in modulation of the fluidity of the cell membrane in *B. subtilis*.

The ability of a cell to control the composition of the cell membrane is quite crucial, especially when faced with shifts in temperature, salinity, pH, and environmental composition. For example, bacteria cell membranes often contain higher proportions of phospholipids with shorter fatty acid chains and more degrees of unsaturation, as long and fully saturated fatty acids lead to compressed, rigid, and brittle membranes that are prone to cracking [241]. An increase in unsaturation within a given fatty acid corresponds to a subsequent decrease in freezing point compared to a fully saturated fatty acid of identical chain length, so an increased ratio of unsaturated to saturated fatty acids at colder temperatures works to lower the freezing point of the cell.

Conversely, higher temperatures showed a preference for saturated fatty acids, desiring a more compact and rigid membrane [242]. A shift from shorter saturated fatty acids to longer, monounsaturated fatty acids has been shown to be a symptom of increasingly acidic growth conditions [243], and salinity shows very subtle trends pointing towards saline concentration breakpoints causing increased ratios of C18/C16 and unsaturated/saturated fatty acids [244].



While many of these variables were not tested in this experiment specifically, it is important to understand that the cell membrane is a constantly changing element of the cell, readily changing in response to shifts in the extracellular environment.

Eliminating or interfering with the cell's capacity to easily modify the membrane would significantly affect the viability of the cell in challenging environments without easy access to other fatty acids, but potentially even more intriguing is the ability to force the cell to only use a selection of fatty acids that are supplied to it and then observe how the ratio of those fatty acids shifts as a function of growth condition. Here, strains of *B. subtilis* with no FabF knockdown and no additional fatty acid supplementation were tested against two different cultures with the FabF knockdown, one that was fed a mixture of six commonly observed fatty acids (iso-14:0, iso-15:0, anteiso-15:0, 16:0, iso-16:0, and iso-17:0) in *B. subtilis* and the other fed a more limited pool (only anteiso-15:0 and 16:0). This limitation of fatty acid access is the basis for the shifts observed in Figure 30, where significant changes in fatty acid length can be directly tied to limited natural fatty acid biosynthesis and restricted access to exogenous fatty acids in the culture.

Following fatty acid analysis was a broader look at phospholipid speciation across fatty acid feeding conditions (Figure 34). Phospholipid speciation follows most of the previous trends observed in older studies of *B. subtilis* (Figure 34A-C), with PG largely present as the dominant phospholipid species and PE present at lower quantities. Both of the cultures with impaired capabilities to self-produce fatty acids had notable relative drops in PE abundance compared to PG, possibly indicating that the FabF knockdown may have implications on phospholipid production outside of just biosynthesis of fatty

acids. Notably, the cultures fed the non-native mixture of fatty acids showed a relative increase in the cardiolipin composition of their lipidome (Figure 34C), again potentially indicating that specific phospholipid genesis may not be as isolated from fatty acid biosynthesis as metabolic pathways would indicate. Simple rerouting of bacterial access to fatty acids did seem to have a relevant effect on the overall composition of the *B. subtilis* lipidome, even with the assumption being that there theoretically is no difference in major fatty acid composition outside of the origin of the molecule.

Given a drastic shift towards PG and/or away from PE after manipulation of fatty acid biosynthesis pathways, as well as earlier observations of shifting fatty acid character, it is important to recognize the effects this could have on the permeability and stability of the membrane. Based on melting point alone, it can be inferred that increased PG (melting point of PG(28:0) is 23°C) and/or decreased PE (melting point of PE(28:0) is 50°C) within the membrane could be a sign of a more fluid, less stable membrane [245]. Therefore, there may be a correlation between alteration of the fatty acid composition of the membrane through forced feeding methods and the fluidization of the membrane.

Variance in phospholipid speciation and fatty acid composition led to the mostly unsurprising observation of distinct phospholipid profiles across each feeding condition (Figure 34A). The unmodified, unfed cultures showed a lipid profile favoring phospholipids with a mixture of saturated and unsaturated fatty acids, trending towards longer carbon chains. Similarly, the cultures fed the native fatty acid mixture showed a range of phospholipids in line with expected carbon count, though the lipidome of these samples appeared to be slightly more favored towards unsaturated fatty acids.

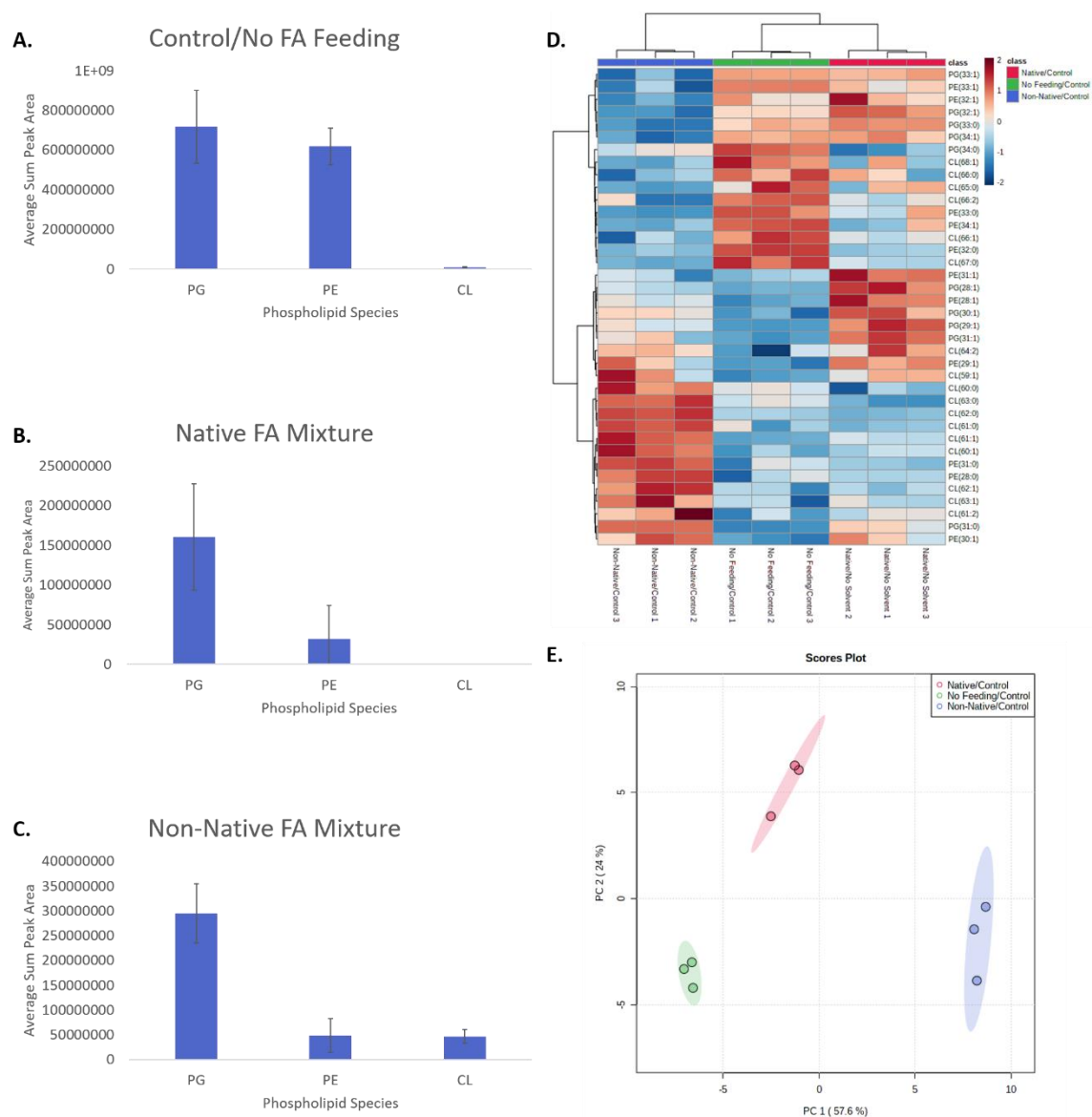


**Figure 34. Comparison of fatty acid feeding conditions in *B. subtilis* 168. Relative phospholipid content in the A) control cultures with no fatty acid supplementation, B) cultures fed a native mixture of fatty acids commonly observed in *B. subtilis*, and C) cultured fed a more restrictive mixture of fatty acids. D) Heatmap showing fold change differences of the 38 most significantly variable features (as determined by ANOVA). E) Principal component analysis (PCA) plot showing the degree of separation across the replicates of each feeding condition with a 95% confidence region.**

The cultures fed the non-native fatty acid mixture were confirmed to have a significant presence of fully saturated phospholipids, with most of those species coming from cardiolipin, confirming the observations from Figure 30B and Figure 34C. Finally, while there were significant areas of overlap seen within individual analyses, the phospholipid profiles of the unfed and native fed cultures were confirmed to be relatively distinct from each other as well as from the non-native fed cultures (Figure 34E).

### ***The effect of solvent present during growth on phospholipid composition***

Potentially even more key for biofuels research is understanding the effect of organic compounds when the cell is grown in different environments. In addition to the desired biofuel products, which can be increasingly toxic at high concentrations [246], biofuel reactors are full of other chemicals that are necessary for breaking down raw cellulosic material into a state that can be processed by the microbial cultures. These can range from sodium hydroxide solutions [247] and sulfuric acid hydrolysis [248] to mixtures of tetrahydrofuran and water [249] and pyrolysis and Kraft reactions driven by metal catalysts [250]. While some methods may allow for removal of the lignin softening agents, it may not be possible to separate that step from the microbial processing step, which would lead to the microbes being exposed to unnatural environments. Combined with the assumed biofuels that would also be present within the reactor as they are being produced, this can quickly create a lethal environment for cells that are unprepared for such a challenge.

The effects of alcohol on the cell have been studied quite thoroughly, with over 50 omics studies testing the effect of various alcohols, including ethanol, isopropanol,



and n-butanol, on *E. coli*, *C. acetobutylicum*, and *Synechocystis* strains with different modifications to increase tolerance to the alcohol stress condition [246]. Increasing concentrations of alcohol does impart an inhibitory effect on the growth rate of a given bacterial cell culture, as well as forcing a shift away from unsaturated fatty acids and towards saturated fatty acids [208]. This does make sense upon consideration of the chemical properties of shorter-chained alcohols such as methanol and ethanol; as smaller molecules that share properties with water (polarity and the ability to hydrogen bond), there is a certain level of similarity with how they interact with the cell membrane, as they can freely diffuse across the membrane [251]. Under lethal concentrations of alcohol, it does follow that the cell would attempt to shift towards saturated fatty acids within the membrane in an attempt to increase membrane rigidity and lower permeability.

Studies of this nature have also been done with *Bacillus subtilis*. As to be expected, the presence of alcohol has a significant effect on the growth rate of the cultures, as well as blocking the cell's ability to sporulate at higher concentrations. The phospholipid inventory showed a noticeable effect as well, with increasing concentrations of ethanol resulting in a similar increase in phospholipid inhibition. Fatty acid composition was also affected; while methanol did not induce noticeable changes, ethanol did force the cell away from odd numbered fatty acids and towards even numbered fatty acids. These results were mirrored in a similar study with *E. coli*, indicating that alcohols can have a profound effect on membrane fluidity [219], though the effect is not always consistent among variable types of alcohols [252].

Some of these effects were observed across the several solvent conditions applied during growth of *B. subtilis* (Figure 35). The most profound changes were apparent in both the isobutanol and THF samples, where the fatty acid composition of the phospholipids showed noticeably shorter fatty acids with less overall unsaturation. Curiously, the cultures grown in butanol were generally similar in composition to that of the control samples, with only the chain length showing significant differences from that of the controls ample (and only very slightly). Given that both butanol and isobutanol are known to be toxic to bacteria [253], there would be an expectation of similarity in fatty acid profiles between the alcohols, but not between the unaltered control and the butanol cultures. There have been several reports on the effects of butanol and isobutanol on bacterial cells specifically in the context of lipids or lipid-derived structures [254-256], but many of those reports refer to a shift towards phospholipids with longer, saturated fatty acids, characteristic of an increased level of membrane rigidity to counteract toxic environments.

Still, the drastic shift in fatty acid profile in both isobutanol and THF away from unsaturated fatty acid could be indicative of the bacterial cultures attempting to increase the rigidity of its membrane to attempt to keep those solvents from being able to diffuse through the membrane into the cell. The overall shortening of the fatty acid chains somewhat contradicts this, but the effect of straighter fatty acids is likely more relevant on membrane fluidity than a loss of one or two carbons in the fatty acid chain.

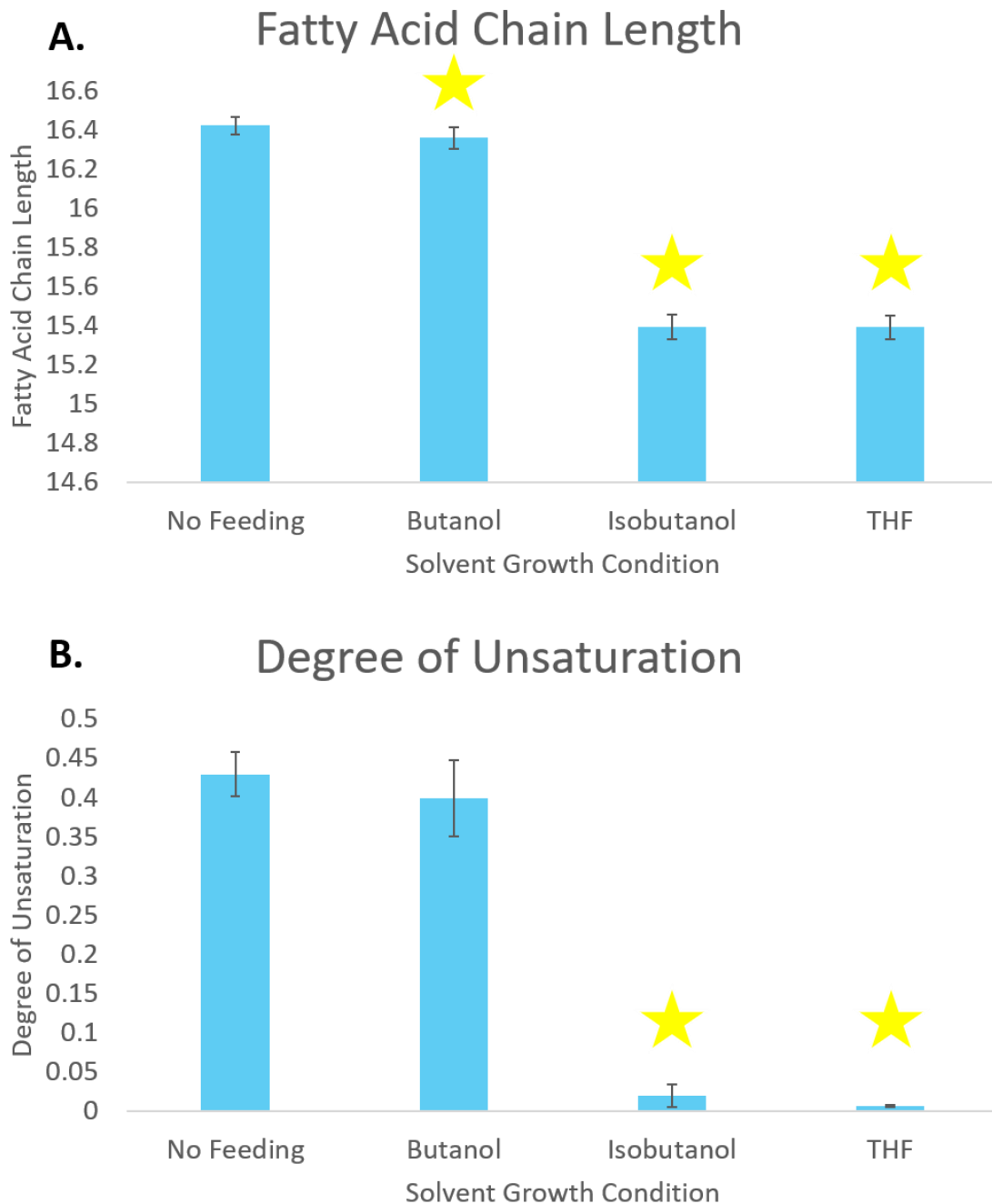


**Figure 35. Comparison of A) chain length and B) degree of unsaturation of the fatty acids within phospholipids extracted from each solvent growth condition applied to *B. subtilis* 168. Stars indicate groups deemed significantly different from the no feeding control by the Student's t-test.**

Other studies have been done with *B. subtilis* that have indicated that different alcohols have noticeably different responses to the membrane as a function of the chain length of the alcohol; as a relatively polar alcohol, the shorter methanol and ethanol tend to localize near the polar headgroups [257], while increasingly longer alcohols settle deeper within the nonpolar fatty acid tails within the membrane [258]. Regardless, this was indicative of alcohol disruptive effects being focused on the outer edges of the bilayer as opposed to deep within, which further validates a shift towards longer fatty acids and thicker membranes in an attempt to keep any forced increases in fluidity somewhat isolated in a specific part of the membrane [259].

Understanding the response of the cell membrane and lipidome to various solvent conditions is critically important for future applications in biofuels and biotechnology. Being able to leverage specially crafted strains of bacteria to produce natural products for use in industry is fantastic in theory, but that level of mass production quickly creates toxic accumulations of alcohol, not to mention the chemicals and catalysts used for lignin degradation that are also present in noticeable concentrations within these biofuel reactors. Observation of trends that arise because of growth within a given solvent could provide insight into how to genetically engineer future strains that emphasize solvent resistances.

A summary of the results of growth within butanol, isobutanol, and THF are shown below, along with a control for comparison (Figure 36). Interestingly, upon examination of the general phospholipid profiles of each solvent growth condition, the butanol sample once again stands out, this time for either a lack of expected PG or more

PE than expected (or a combination of both) (Figure 36B). While the control (Figure 36A), isobutanol (Figure 36C), and THF (Figure 36D) samples are largely in line with previous studies of *B. subtilis*, the butanol sample showed trends indicative of the Nickels study, though it bears mentioning that once again, the error bars for those samples indicate relative levels of PG and PE that are closer than the raw peak areas show.

Inspection of phospholipids that exhibited significant fold change differences across conditions helped to deconvolute why the profile of butanol looked out of place, as well as confirm earlier observations from the fatty acid data (Figure 36E). A combination of heavy relative abundances in PE species as well as equally large drops in PG species led to the lipid speciation seen in Figure 36B. Closer inspection of the isobutanol and THF samples revealed phospholipids with fatty acid compositions in line with prior observations, with significant increases in shorter, saturated fatty acids. The control sample showed significant decreases those same phospholipids, potentially indicating a lower priority of the cell to maintain membrane fluidity in the lack of any sort of environmental threat. Finally, the full profile comparisons showed that the isobutanol and THF samples correlated highly with each other, while the control and butanol samples were more isolated both from each other and from the other samples (Figure 36F). These trends support previous studies which emphasize the preference of a shift away from unsaturated fatty acids and towards saturated fatty acids, with an especially strong preference in both the isobutanol- and THF-grown samples.

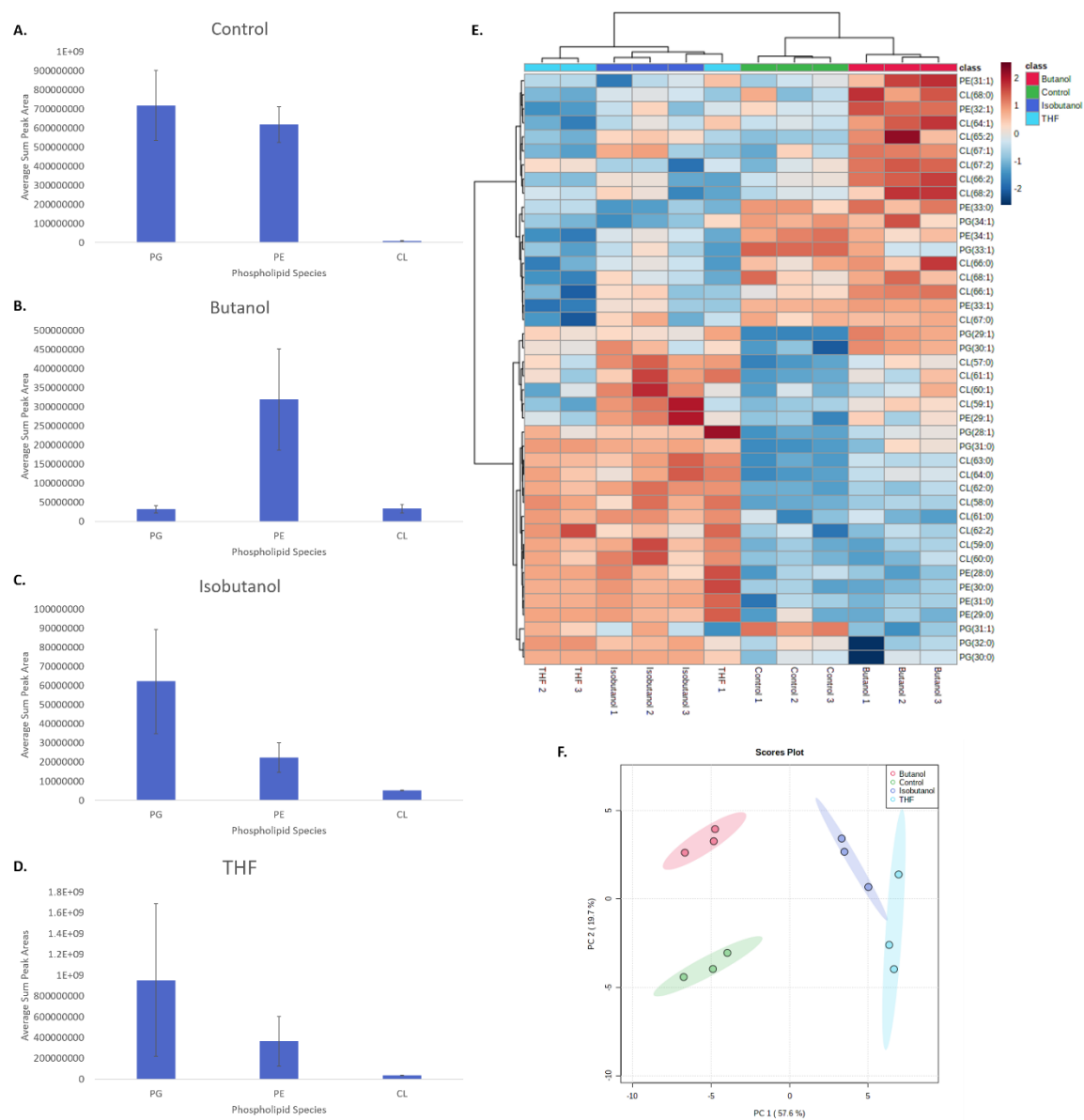


**Figure 36. Comparison of fatty acid solvent growth conditions in *B. subtilis* 168. Relative phospholipid content in the A) control cultures, B) cultures grown in butanol, C) cultures grown in isobutanol, and D) cultures grown in THF. D) Heatmap showing fold change differences of the 42 most significantly variable features (as determined by ANOVA). E) Principal component analysis (PCA) plot showing the degree of separation across the replicates of each solvent growth condition with a 95% confidence region.**

However, the shift away from longer fatty acids is not necessarily supported by previous studies [219]. Shorter, more unsaturated fatty acid chains would be indicative of lower efficiency interactions between the phospholipid tails and a subsequent increase in membrane fluidity. This would indicate that the cells are not trying to adapt and bolster their cell membranes but rather the membranes are becoming more porous, possibly an indication of damage. Still, previous studies have indicated that membrane fluidity is not the sole response to solvent tolerance and that the problem is multi-dimensional [260], and the presence of more saturated fatty acids could be more important than a slight shortening of chain length. That being said, visualization of membrane compositional shifts in line with expected membrane fluidity trends may help to inform future studies about how to engineer strains that can be more resistant to these solvent challenges.

#### ***A brief examination across all conditions***

Next, after examination of the fatty acid feeding experiments and solvent challenges in isolation, the phospholipid profiles were compared with all combinations of fatty acid and solvent feeding (Figure 37). Generally, samples that were not augmented with fatty acid mixtures during growth showed higher relative proportions of PE, while PG was often present in relatively higher amounts in the feeding conditions. Cardiolipin was also much more prevalent in samples that were fed fatty acid mixtures, as well as in samples that were exposed to solvent during growth.

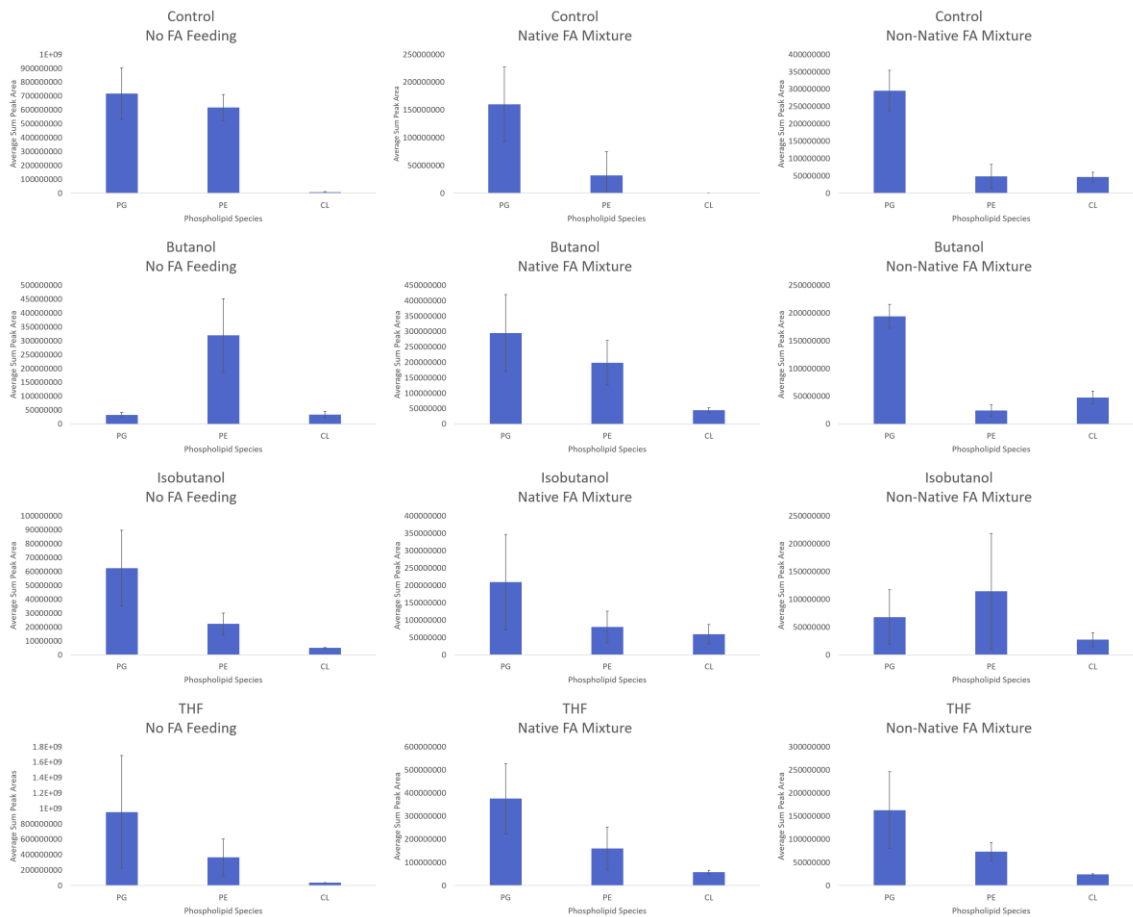


**Figure 37. Individual phospholipid speciation comparisons across each *B. subtilis* 168 sample, with rows showing solvent growth conditions and columns showing fatty acid feeding conditions.**



The cardiolipin shifts were especially interesting. Previous studies have shown that increased levels of cardiolipin within the membrane can have a negative effect on the stability of the membrane, indicating a more fluid structure [261]. This is more in line with the observation of increased relative levels of PG that also point towards increased membrane fluidity. It would stand to reason that *B. subtilis* would likely attempt to harden its membrane to protect the cell, but there have been studies showing that ethanol can force increased membrane fluidity [262], and butanol has been shown to be even more compromising to the cell due to increased penetration into the membrane and disruption of lipid hydrogen bonding. As a result, it may not be a complete surprise to observe increased fluidity of membranes stressed by organic solvents. Finally, persistent observation of increased ratios of PE continued across several conditions – while this is somewhat strange, it can be buoyed somewhat by the fact that in both the isobutanol and THF sample sets, both PG and PE abundances have large error, which is likely an indication of a membrane in transition.

Figure 38 shows a heatmap demonstrating comparison of all conditions across all observed phospholipids. Three large clusters of samples are visible – the largely baseline samples with little modification to the fatty acid composition of the membrane, the collective of samples fed only the non-native mixture of fatty acids, and the rest of the samples within solvent growth conditions. The baseline samples were characterized by increased levels of phospholipids with longer, unsaturated fatty acids, which is in line with fatty acid feeding condition being the main driver behind association of those samples.

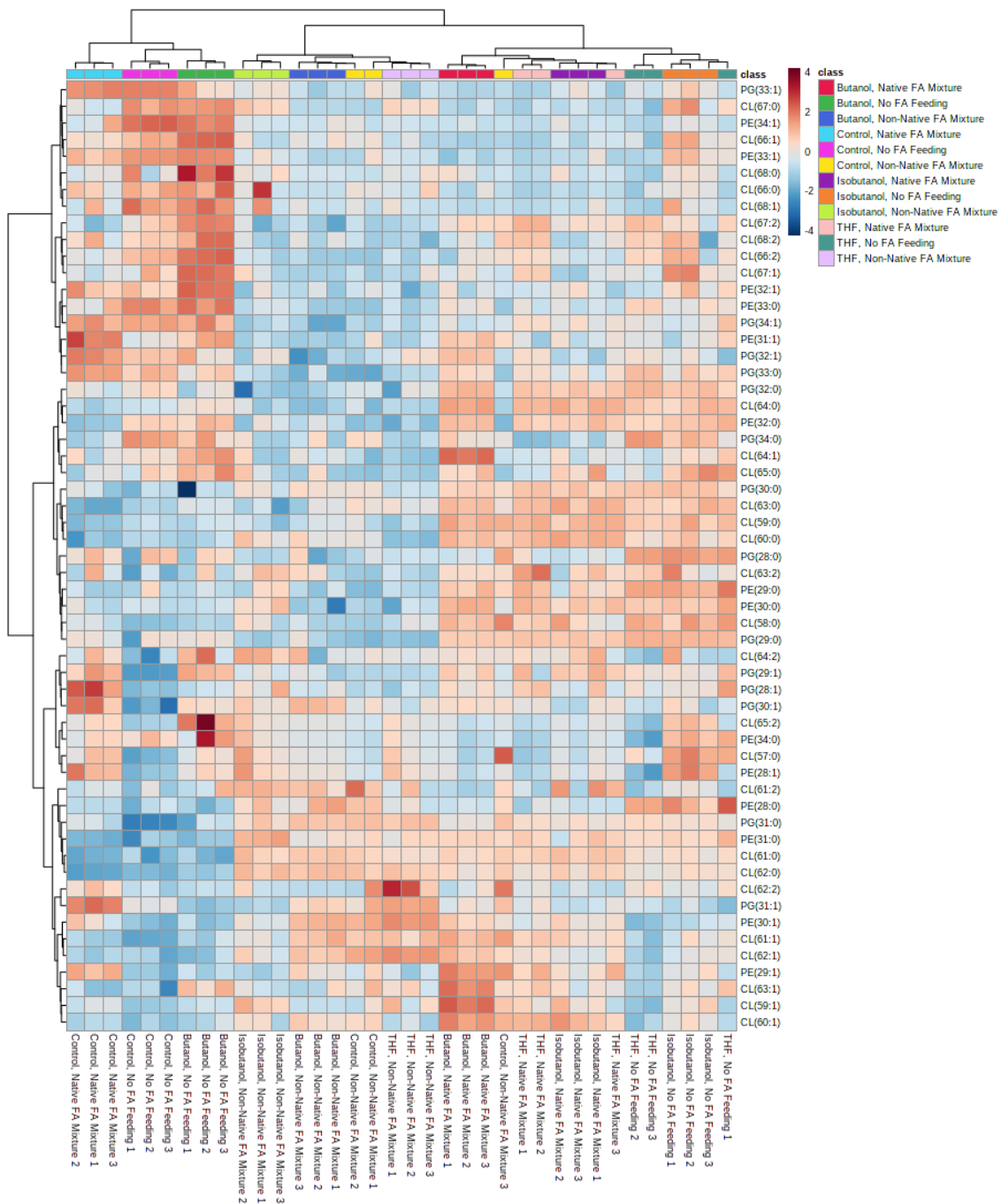


**Figure 38. Comprehensive analysis of all combinations of fatty acid feeding and solvent growth conditions in *B. subtilis* 168.**

Likewise, the cluster of samples fed the non-native fatty acid mixture were characterized by a more limited range of fatty acids, as well as phospholipids with fatty acids that would, in theory, be shorter than the provided fatty acids within the non-native mixture, possibly indicating the cell's ability to do slight modifications to the fatty acids despite not being able to synthesize them. Finally, the other cluster, primarily composed of the solvent growth conditions of the native and non-feeding fatty acid samples, was primarily characterized by a notable presence of phospholipids with fully saturated fatty acids, alongside notable increases in cardiolipin compared to the other two clusters.

### **Phospholipid derivatives and other lipid species**

#### ***Aminoacylated phospholipids***

One of the more intriguing aspects about phospholipids that often goes overlooked is the influence they have on the electronic nature of the membrane and the cell. The presence of phosphate ions within the structure of all phospholipids imparts an inherent negative charge to the membrane, which the cell can mask and neutralize through several different methods. In bacteria, this is often governed by whether the cell is Gram-negative or Gram-positive. Gram-negative bacteria often contain high concentrations of PE, and the zwitterionic character of that phospholipid is usually more than enough to keep a relative electric balance. Gram-positive bacteria are much lower in relative PE concentration, so their method of balancing out the negative phosphate charge involves the addition of amino acids to the head group of PG species within the membrane [93, 217]. Being able to maintain a more neutral charge in the membrane is vital to the survival of many microorganisms – the primary target of attacks by cationic

antimicrobial peptides (CAMPs) released by other bacteria is the primarily negatively-charge cell membrane of other nearby bacteria, driven by the heavy presence of anionic PG and CL and zwitterionic PE. Being able to maintain a more balanced charge distribution across the cell's surface aids in preventing attraction of such antimicrobials, which is why bacteria have evolved to modify their membrane phospholipid with cationic and zwitterionic amino acid residues [263].

Outside of antimicrobial resistance, there is not much else known about the function of aminoacylated phospholipids or the conditions necessary for the cell to produce them. Acidic environments are notable, with multiple studies showing that levels of both alanine- and lysine-modified phospholipids are increased when the cellular environment grows acidic [264, 265], and there are also studies showing that proportions of aminoacylated phospholipids are somewhat dependent on the growth phase of the cell [266, 267]. In *Bacillus subtilis* specifically, the presence of Lys-PG and Ala-PG leads to shifts in a number of physical characteristics of the cell, including production of more durable spores [268].

Variety within aminoacylated phospholipids is surprisingly diverse – there are multiple different aminoacylated variants for PG and CL, and there are even reports of aminoacylated PE species as well [92, 269]. In terms of the amino acids that have been observed as adducts to phospholipids, lysine and alanine are by far the most common, but arginine, ornithine, glycine, and serine variants have also been observed, and there have even been reports of N-succinylation in species that contain the lysine adducts of PG, similar to modifications withing bacterial proteins [270, 271].

Basic analysis of aminoacylated phospholipids by mass spectrometry has previously been reported [218, 269, 272, 273], with Atila and Luo demonstrating this specifically within *Bacillus subtilis*. Reported studies have used extraction procedures in line with most traditional lipidomics studies, with the chloroform-methanol method being the most common method [112, 272, 274, 275]. Thus, the MTBE method utilized here for comprehensive phospholipid extraction should be sufficient to extract aminoacylated phospholipids, if they were present within the samples. In brief, in addition to the range of commonly observed bacterial membrane phospholipids, the lipidomics analysis performed here was successful in enabling characterization of both the lysine and alanine PG variants that are expected within *B. subtilis*. Fully saturated lysine- and alanine-PG species were detected of fatty acid length 28-31, with lysine-PG species generally exhibiting higher abundance, as was previously reported (Figure 39) [269].

Lysine- and alanine-PG species did not appear in all samples. While there were traces of lysine-PG in all solvent conditions, alanine-PG was almost non-existent in both the isobutanol and THF-grown samples. Additionally, there was a noticeable trend correlating to fatty acid chain length; longer chain lengths were by far the more abundant lysine-PG species observed in the isobutanol- and THF-grown samples, while shorter chain lengths were generally favored among the alanine-PG species within the control and butanol-grown samples.

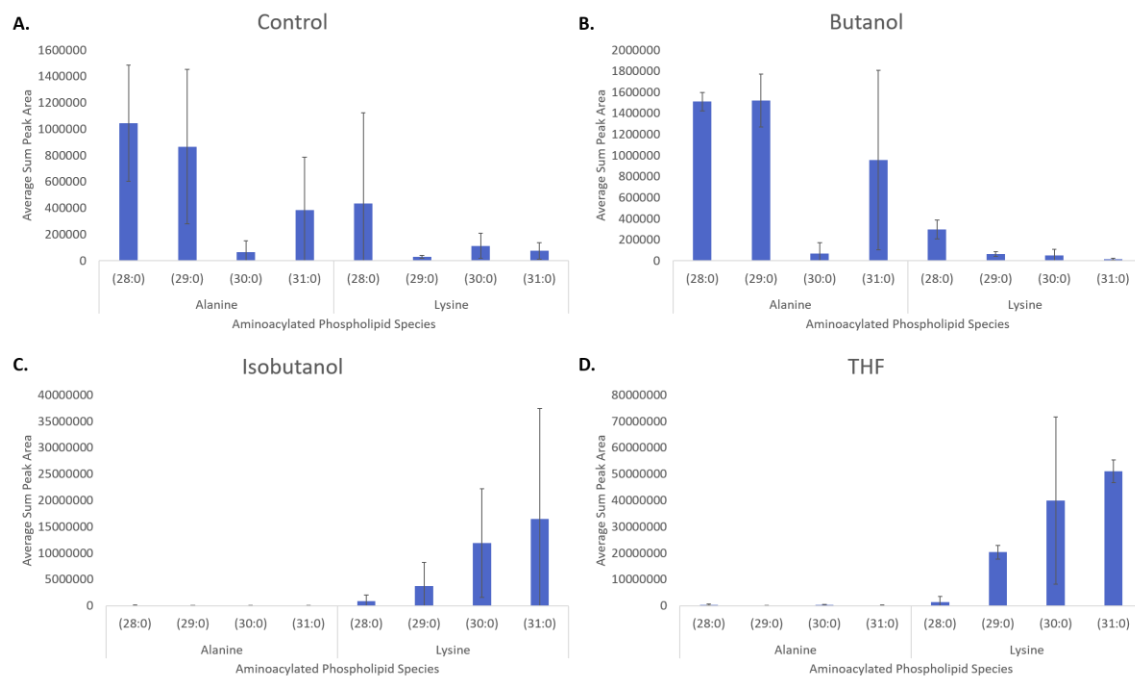


**Figure 39. Summary of observed aminoacylated phospholipids observed in select *B. subtilis* 168 cultures with no fatty acid modification. A) Control, B) Butanol, C) Isobutanol, D) THF**

The noticeable increase in abundance of lysine-PG species specifically within isobutanol- and THF-grown samples is curious. This would normally indicate the presence of CAMPs; a noticeable increase in lysine-PG should primarily point to the cell attempting to shift the electronic potential of the membrane in a positively charged direction [276, 277], but there is very little in previously reported literature about why these trends might be observed under conditions ignorant and devoid of antimicrobial agents, as the physiological causes behind the production of specific aminoacylated phospholipids and modifications to their fatty acid chain composition are not well understood. Ala-PG has been shown to affect membrane permeability, not only in the presence of CAMPS but also in response to other environmental challenges such as temperature, pH, and shifts in osmolarity [93]. Klein showed that in the case of a potent bactericidal molecule and weak acid in lactate, increased amounts of Ala-PG can decrease the permeability of the membrane, which could point to Ala-PG being important in the repelling of mildly acidic molecules. Similarly, links between increased concentrations of Lys-PG within the bacterial membrane and acidic growth conditions have also been reported previously [278].

With that context in mind, this might help to begin to explain some of the observed trends, even though this study does not deal as much with growth conditions with measured or adjusted pH so much as the composition of the growth media and environment. Generally, even though the physical properties of these aminoacylated phospholipids lead to decreased packing within the membrane, they are still quite effective at repelling strongly charged ions present within the cellular environment [278].

Examination of the fatty acid chain trends within the lysine-PG species trend well with what was previously observed within the generic lipidomes earlier, with longer chain lengths becoming increasingly prevalent within the isobutanol- and THF-grown species. Conversely, the alanine-PG species have a slight preference for shorter fatty acid lengths. Observation of these species, despite not being able to pull them out using the informatics methods described here, allows for further understanding of how *B. subtilis* attempts to remodel its membrane in order to face specific environmental challenges.

### ***Lipoteichoic acid***

Another key modification that occurs specifically within the cell envelope of Gram-positive bacteria is the presence of a much thicker cell wall because of not possessing an outer membrane. The cell wall is composed of layers of peptidoglycan, and the presence of teichoic acids (TA) bound to either the cell membrane via glycolipid (lipoteichoic acids, LTA [279]) or peptidoglycan (wall teichoic acids, WTA [280]) helps to act as an additional stabilization through a scaffold-like construction [281]. Both LTA and WTA are important factors in not only cellular shape but also with providing a level of antimicrobial resistance, though there is still a decent amount of uncertainty regarding their exact function [102, 282]. There are also implications involving human health, with lipoteichoic acids showing inflammatory [283, 284] and immunomodulatory [285, 286] effects while interacting with human cells. As a common member in the human gut microbiome, characterization of *B. subtilis*-derived lipoteichoic acid species could lead to better understanding of the mechanics behind inflammation of the human digestive tract. Additionally, as a key structural component of *B. subtilis*, shifts in composition or



abundance of specific lipoteichoic acid species under certain conditions could help guide the future engineering of more effective strains for bioindustrial applications.

Lipoteichoic acid in *Bacillus subtilis* is most observed as a series of glycerol-phosphate units, with scattered modifications of D-alanine and various sugars, that is free at one end to extend through the thick peptidoglycan cell wall to the exterior of the cell and anchored at the other end in the cell membrane by a glycolipid [287]. Of the five major types of lipoteichoic acid, the most basic Type I is the one most commonly observed, one of the varieties known to have D-alanine esterification sites [288], and the one being characterized here [102]. Thanks specifically to the presence of D-alanylation sites on these molecules, lipoteichoic acid functions not only as a key structural component of the cell but also yet another way for PE-deficient Gram-negative bacteria to neutralize the otherwise strongly negative charge of the cell surface through cationic accumulation, such as divalent  $\text{Ca}^{2+}$  and  $\text{Mg}^{2+}$ , at those sites [288].

Traditional lipoteichoic acid extraction procedures follow an approach similar to methods used for lipid A extraction through the use of a hot phenol/water mixture [289] or, in more recent studies, a multistep extraction using butanol and a cell lysis technique (either lyophilization or sonication) [290, 291], though more generic lipid extraction approaches utilizing the CME methods of Bligh-Dyer have also been shown to be effective [292]. Here, the Matyash MTBE extraction was sufficient to provide extraction of lipoteichoic acid species within the same organic partition as a large scale lipidome.

Luo demonstrated a thorough framework for LC-MS/MS analysis of the various components of lipoteichoic acid using *B. subtilis* strain 168. In their study, a complete

dissection of *B. subtilis* lipoteichoic acid components was performed, showing off the membrane anchor point, the core backbone of the lipoteichoic acid molecule, and how alanylation occurs, as well as what these various forms look like through the lens of an LC-MS/MS measurement. A similar examination was applied to regions of the MS1 spectra of tested *B. subtilis* samples to determine whether these lipoteichoic acid species were extracted using MTBE and if they could be analyzed via HILIC-MS/MS.

In brief, while these measurements were not able to identify the glycolipid anchor of lipoteichoic acid (DAG-Glc<sub>2</sub>) or the bis-alanylated primer DAG-Glc<sub>2</sub>-P-Gro-Ala<sub>2</sub>, two series of lipoteichoic acid primers were detected, the base form DAG-Glc<sub>2</sub>-P-Gro and the mono-alanylated form DAG-Glc<sub>2</sub>-P-Gro-Ala, with total fatty acid chain lengths ranging from 28:0 to 32:0 (for the base form) and 33:0 (for the mono-alanylated form) as seen below (Figure 40).

The base, unmodified Type I LTA was most observed across all solvent conditions, with the D-alanyl esterification being expressed in lower abundances. In general, both the base LTA as well as the D-alanyl variant were more abundant in the isobutanol- and THF-grown cultures; LTAs showed some level of presence in the control as well, but the butanol-grown samples only contained very low abundances of LTAs. This may be a direct result of the growth environment – the potential challenges caused by an increasingly toxic organic environment are known to cause shifts in the composition of the cell membrane, so it stands to reason that there may be downstream modifications or side effects that would influence the other exterior structural components of *Bacillus subtilis* to help the cell survive such an environment.

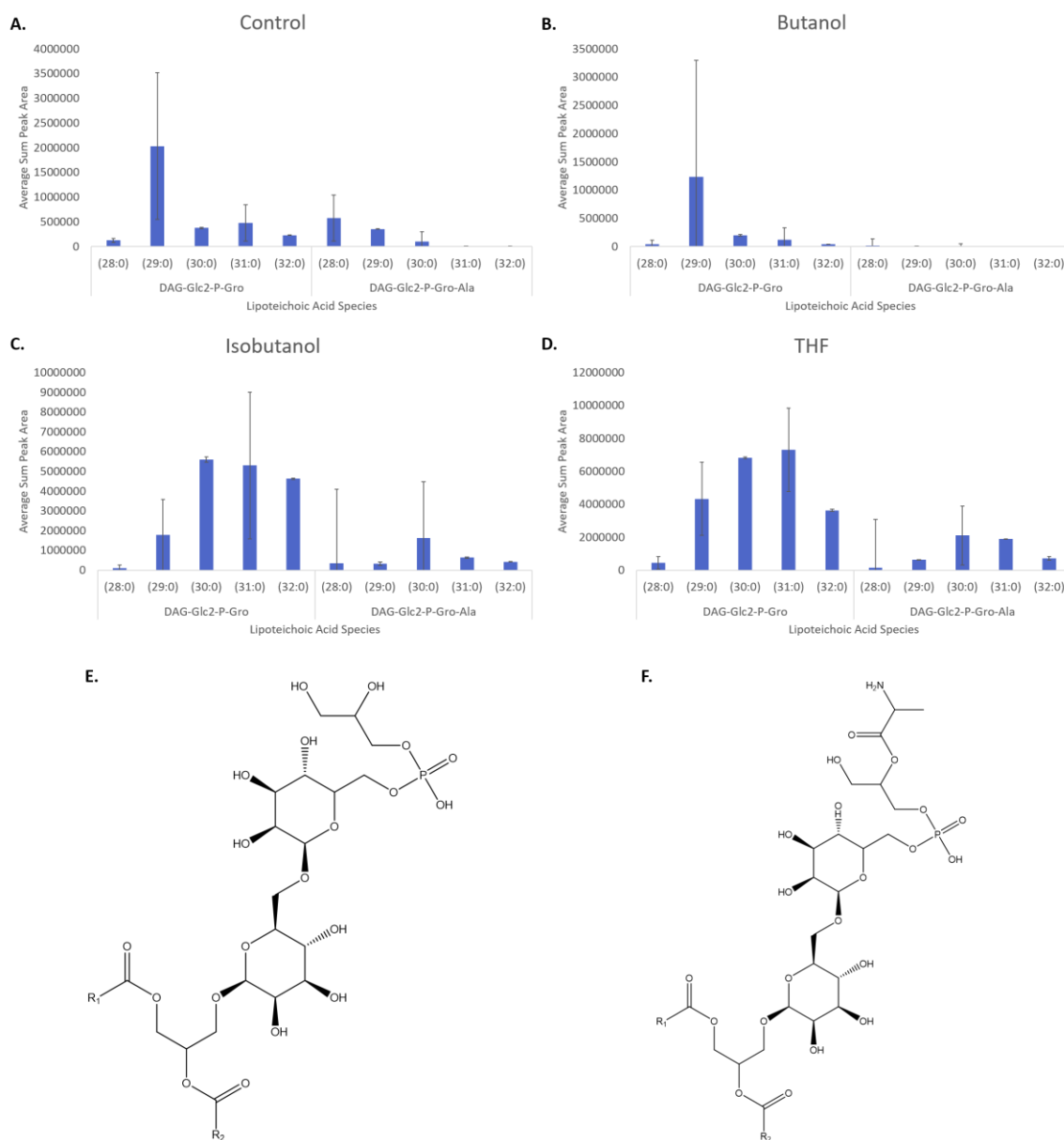


**Figure 40. Summary of observed lipoteichoic acid species observed in select *B. subtilis* 168 cultures with no fatty acid modification. A) Control, B) Butanol, C) Isobutanol, D) THF E) Generic structure of DAG-Glc2-P-Gro. F) Generic structure of DAG-Glc2-P-Gro-Ala.**

Perhaps more interesting was the trend of total fatty acid chain length observed across the different growth conditions (Figure 40B and C). LTAs in both the control and butanol-grown samples were only significantly present at lower fatty acid chain lengths, with both the control and butanol-grown samples showing a strong preference towards the 29:0 variant of the base LTA and a steady decline in abundance with increasing chain length. The D-alanyl variant was even more restrictive, with the butanol-grown samples showing next to no extraction at all. Conversely, the isobutanol- and THF-grown samples followed very similar trends to each other, with significant presence at all observed fatty acid chain lengths but showing much higher abundances at comparatively longer chain lengths than the control and butanol-grown samples.

The noticeable drop in LTAs in butanol-grown samples is particularly interesting, but a potential answer for why that set of samples specifically was deficient in LTAs may lie within common TA extraction protocols. As mentioned earlier, the most prevalent methods for extracting LTAs are either a mixture of hot phenol and water [289, 293] or, more recently, the use of butanol [290]. It was noted that the butanol extraction procedure was generally much more effective than the hot phenol/water method at extracting more intact LTAs, as well as retaining any substitutions (like D-Ala) that may have been present, which may explain why the washed cell pellets that were used for this analysis may have been deficient in LTAs. For the butanol-grown cultures specifically, it is entirely possible that a significant number of LTAs were simply lost during preparation of the bacteria because of the high reported efficiency of butanol as a method for LTA extraction.

## Discussion/Conclusions

Application of various fatty acid feeding conditions and solvent challenges, both in isolation and in tandem, to cultures of *B. subtilis* with genetic modifications forcing priority of phospholipid synthesis to be largely controlled by experimental design allowed for thorough probing of how *B. subtilis* adapts to increasingly difficult growth conditions through modification of its cellular membrane. Observation of phospholipid shifts show that *B. subtilis* will generally prefer shorter, saturated fatty acids as a part of the phospholipids comprising the cell membrane as increasingly harsher solvents are applied, while phospholipid speciation generally remains consistent across all sampling conditions, with some minor variation in PE and CL relative proportions. Probing across all sampling conditions indicated that relative increases in PG and CL could have a negative impact on membrane fluidity, possibly indicating targets for genetic manipulation to help aid in strengthening the membrane. Additionally, inspection of various phospholipid derivative species show that *B. subtilis* actively works to counteract imbalances in the electronic character of the cell and membrane through the use of amino acid augmentation.

However, one of the biggest findings here was confirmation that manipulation of the bacterial cell membrane by customization and restriction of fatty acids was possible without significant risk to the cell. While there are still many questions that remain unanswered about how the genetic manipulation of fatty acid biosynthesis affects other aspects of phospholipid synthesis, the general concept has been shown to be successful. Applying this further, the ability to customize bacteria with isotope-labeled phospholipids

will enable advanced neutron scattering studies to better understand the mechanics behind membrane assembly as well as track how specific phospholipids or fatty acids localize within the membrane [85]. The utility of customizable membranes will help to guide future studies, potentially targeting not only the fatty acid mechanisms of the cell shown here but also specific phospholipid species that may be enriched or downregulated in specific circumstances.

Comprehensive analysis showed that *B. subtilis* has a high level of specificity within its ability to reorganize, recharacterize, and remodel its membrane to adapt to a wide variety of shifts in cellular environment. Manipulation of the relative ratios between the major phospholipids PG, PE, and CL were indicative of a concerted cellular effort to maintain a high level of control over the fluidity of the cell membrane, as well as through modification of both the phospholipid head groups as well as modulation of the length and saturation of the fatty acid tails of the phospholipids. Even more fascinating was that while there were noticeable effects when *B. subtilis* was put under a heavy amount of stress, not every stressor affected the cell in the same manner, even across stressors that are close in chemical character (as was the case with butanol and isobutanol). These types of sensitive responses to changing conditions could be key to isolating specific trends in membrane change and composition for later experiments to leverage in order to help attune future *B. subtilis* strains to have increased tolerance to these harsh environments.

**CHAPTER 5: *PSEUDOMONAS PUTIDA* GROWTH IN SIMULATED  
WASTEWATER CONDITIONS REVEALS SHIFTS IN PHOSPHOLIPID  
PROFILE INDICATIVE OF MEMBRANE DAMAGE**

A version of this chapter is in preparation for publication:

Reeves, D.T., Henson, W.R., Borchert, A.J., Beckham, G.T., Hettich, R.L.  
“Reverse engineering of *Pseudomonas putida* lipid membrane composition alters microbial fitness for diverse substrates and products (tentative title).” Manuscript currently in preparation; target journal is Applied and Environmental Microbiology.

### **Abstract**

*Pseudomonas putida* has been shown to be surprisingly resilient, versatile, and effective in catabolizing chemicals contained within several different wastewater streams towards biological upgrading to valuable fuels, chemicals, and materials. Observing how chemicals in various wastewater streams impact the phospholipid inventory of the cell membrane could provide a glimpse into how *P. putida* attempts to adapt and survive in complex chemical mixtures found in aqueous waste streams. To this end, a lipidomics platform was deployed to examine differences in the lipidome of the gene-reduced *P. putida* strain EM42 in different compounds commonly observed in various types of wastewater, as well as a mock wastewater stream. Significant membrane remodeling was observed in response to different compounds, particular in the phospholipid profile and potential changes in fatty acid moieties. Lipid variants specific to *P. putida*, such as alanylated phosphatidylglycerol and lipid A, were also considered. The observation of membrane trends such as the rise of possible cyclopropane fatty acids and shifts in phospholipid composition offer a template from which to build reverse engineer *P. putida* for increased toxicity tolerance towards wastewater streams and other potential bioremediation applications.



## Introduction

*Pseudomonas putida* has long been known as a versatile microbe for research. While not directly useful for any type of medicinal research in human beings, the preferred soil and water habitats of *P. putida* make it a tantalizing target for environmental research. With rapid acquisition of the genome sequencing [294, 295] and metabolic modeling [296, 297] information over the last 60 years since it was discovered, *P. putida* is a well understood organism from which to build creative experiments, with slight tweaks of key synthetic pathways providing the possibility of dozens of potentially valuable natural products for industry [298].

One of the most impressive functionalities of *P. putida* lies in its potential in bioremediation. This microbe specifically has been shown to be incredibly effective and versatile when it comes to the sheer variety of molecules that have been shown to be able to be broken down by the microbe, which has enabled researchers to test out *P. putida* as a microbial cleaner for all types of environmental hazards. These include fossil fuels [299-302], aromatic compounds [303-305], halogenated organic compounds [306, 307], metals [308-311], environmentally hazardous waste streams [312-314], and lignin [315], among others. Often, the compounds lingering around in wastewater streams can be hazardous to the environment and/or human life, with many halogenated hydrocarbons [316-318] and phenolic compounds [319-321] having been shown to be either carcinogenic or toxic to animal and human life. Similarly, large spills of oil [322, 323] or other chemicals [324, 325] can pollute and cripple the spill site for years to come, potentially with no way to feasibly remediate the area.

*P. putida* KT2440 is commonly reported as a flexible cellular factory [294, 326], and it can easily be modified for renewable production of industrially relevant chemicals from a variety of sugars and waste streams [327, 328]. However, there are bottlenecks involved that hamper the feasibility in practice. One major drawback is toxicity tolerance towards compounds found in lignocellulosic hydrolysate and other waste streams. This issue is found in many microorganisms, and its investigation provides an important area of research that can provide significant general benefits for industrially relevant microbial hosts.

*P. putida* EM42, a heavily gene-reduced variant of *P. putida* KT2440, was constructed to remove several genes that are largely irrelevant in research and industrial settings but are sinks for reducing equivalents such as ATP and NAD(P)H [329]. *P. putida* EM42 was made through the deletion of eleven chromosomal regions that contain 300 genes, including the entirety of the cellular machinery comprising the flagella [330], the primary motility tool of *P. putida*, as well as all regions encoding for prophages [331] and several deoxyribonucleases that have been shown to make incorporation of plasmids more difficult [332]. The combined removal of all these genes resulted in the formation of a highly manipulable cell-factory in *P. putida* EM42 that can efficiently route energy into whatever cellular processes a researcher desires to explore.

While in theory leverage of bacteria as a cheap, renewable agent of bioremediation is a fantastic idea, the health of the bacteria needs to be recognized. Constant exposure to the very compounds the bacteria is attempting to decompose or transform can be incredibly harmful over long periods of time; studies have shown that

sustained growth is often only viable for a few days and no longer than around a week after introduction barring adaptations to survive [333]. This has led to the development of bacterial strains that have been optimized to both transform waste chemicals with increased tolerance to those same chemicals [334]. This has proven to be a major area of research, involving efforts in genetic engineering, modeling, and a plethora of potential targets for bioremediation [335].

These efforts are not limited to genetics – there has been a rising interest in utilizing the information provided by shifts in the composition of the cell membrane to better engineer efficient microbes [336]. Lipidomics can offer a unique look at how the microbe directly reacts to environmental molecules [38, 337]. Potentially hazardous organic molecules can directly interact with the membrane [338], and as the first contact of the cell with the environment, it stands to reason that the lipid composition of the membrane could be influenced by extracellular contact, either in a positive way (through reconstruction to better adapt to the environment) or negative way (membrane damage). Because these environmental contaminants often come from several different classes of molecules, often wildly varying in chemical characters, two different conditions could have drastically different effects on the membrane of a microbe that is a target for potential bioremediation use.

In this study, a thorough investigation of the lipidome response of *Pseudomonas putida* to several known wastewater contaminants was performed. A selection of compounds spanning a variety of classes of organic compounds as well as a variety of different waste streams were selected to test the response of the bacteria to exposure. The

organic compounds were selected to cover multiple different compound classes that would be expected within various wastewater streams, though compounds like halogenated organic compounds and heavy metals were largely ignored for safety reasons. A mock wastewater solution was also formulated, containing not only the compounds listed below but also several others within those organic classes. Untargeted lipidomics was performed on *P. putida* cultures grown in these samples, targeting the major classes of phospholipids known to exist in *P. putida* and examining how each compound affects the composition of the cell membrane, both in isolation as well as compared to each other and the composite mock wastewater solution. Additionally, as done with the prior study in *B. subtilis*, regions of interest that contained phospholipids and lipid derivatives that are under-reported in databases, such as aminoacylated phospholipids and the potential of lipid A, were explored and characterized. This study aims to identify shifts and changes in the lipid membrane of *P. putida* that can be linked to the growth conditions of the bacteria, which could lead to potential targets for future genetic modification of fatty acid and phospholipid-producing enzymes that aid in cellular survival.

## **Experimental Approach**

### ***Preparation of P. putida cell cultures***

Cultures of the gene-reduced variant of *P. putida* KT2440, EM42 [329], were prepared within a selection of chemicals to simulate growth in several different wastewater conditions. For cell culture, glycerol stocks of EM42 were inoculated in 5 mL of Luria Broth (LB) media for approximately 16 hours at 30°C, shaken at 225 rpm. Cells

were centrifuged at 4000 rpm for 5 mins, the supernatant was discarded, and the cells were resuspended within 1 mL of M9 salts with 20 mM glucose. The OD600 was measured before cells were subcultured within shaker flasks with an initial OD600 of 0.1.

For each wastewater simulated condition, 300 mL of M9 medium with 20 mM glucose was prepared for each condition. The pH of the media was adjusted to 7.2 and filter sterilized before use. Into each 300 mL bottle was added the simulated wastewater conditions as follows (Table 12, Figure 41): 0.1622 g of p-cresol to make a 5 mM solution, 48.7  $\mu$ L of formaldehyde to make a 0.75 mM solution. 125.6  $\mu$ L of 2-cyclopentenone to make a 2 mM solution, 0.6847 g of vanillin to make a 15 mM solution, and 3.6915 g of sodium acetate to make a 150 mM solution. Additionally, 25 mL of mock wastewater solution was prepared as per Table 13; to obtain a 3% mock wastewater solution for cultures, 10 mL of the stock was added to 290 mL of the M9 medium, the pH adjusted to 7.2, and the resultant solution filter sterilized.

Cells were centrifuged at 4000 rpm for 5 minutes, after which the supernatant was removed and discarded, and the cells were resuspended in 1 mL of M9 salts with 20 mM glucose. The OD600 was measured prior to analysis, and cells were shaken in flasks with a starting OD600 of 0.05. The OD600 was measured every 3 hours for 12 hours, and samples were saved once they reached an approximate OD600 of 1.0. 100 mL of cell culture were split and stored in four, 50 mL centrifuge tubes and centrifuged at 3000 x g for 10 minutes. The supernatant was removed and discarded, and cells were stored at -80°C for transportation.

**Table 12. Chemical classes and origins of chemicals used to simulate various wastewater streams**

Compound	Organic class	Removal Methods/Origin
Sodium acetate/acetic acid	Carboxylic acid	General treatment [339-341] Sugar processing [342] Recovery from waste streams [343, 344]
<i>p</i> -Cresol	Phenol derivative	General treatment [345-347]
Formaldehyde	Aldehyde	Removal/treatment [348-350]
2-cyclopentenone	Ketone	Pyrolysis plant wastewater [351-353] Derivatives also appear in waste from kraft mills [354, 355], olive mills [356], coal coke [357]
Vanillin	Phenolic aldehyde	Lignin waste converted to vanillin [358-360] <i>E. coli</i> previously shown to be capable of creating it [361]

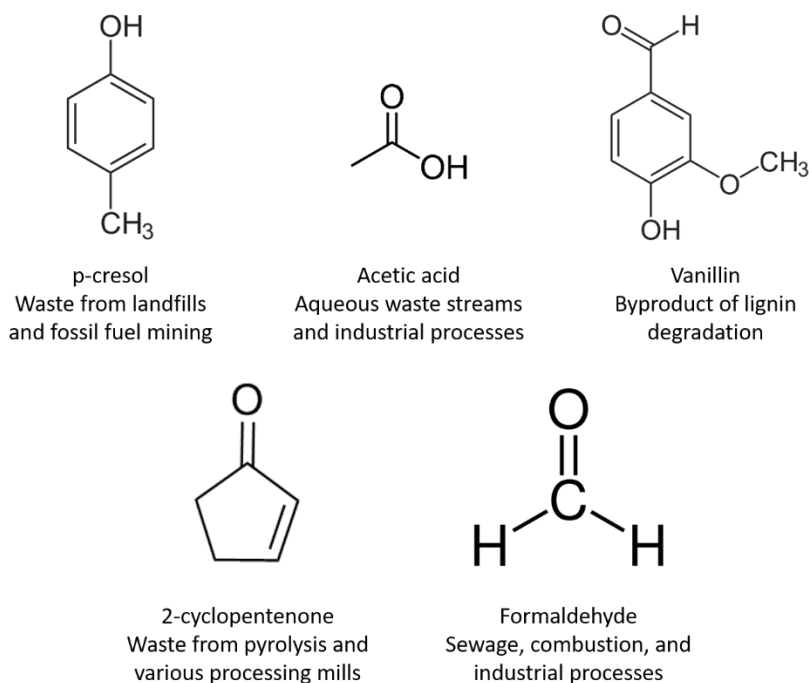


**Figure 41. Individual wastewater components being examined.**

**Table 13. Composition of the mock wastewater solution**

Substrate	Representative Chemical Class	Medium Composition	
		g/L	mM
Acetic acid	Organic Acid	4.14	68.94
Formic acid		0.98	21.29
Formaldehyde	Aldehyde	1.07	35.63
Furfural		1.39	14.47
Acetone	Ketone	2.06	35.47
Catechol	Phenol	4.57	41.51
Phenol		2.94	31.24
<i>o</i> -cresol		0.92	8.51
<i>m</i> -cresol		2.14	19.79
<i>p</i> -cresol		0.72	6.66
3-methyl catechol		1.14	9.18
4-methyl catechol		0.96	7.73
Methanol	Alcohol	1.14	35.58
Propan-1-ol		0.25	4.16
Butan-1-ol		0.29	3.91

### ***MTBE-based extraction of *P. putida* lipidome***

Samples were delivered as frozen cell pellets (on average, 50-200 mg in weight) in 50 mL centrifuge tubes. Cultures were thawed and washed with 1 mL phosphate-buffered saline (PBS). Because the cell cultures were large, each pellet was split approximately in half, the resultant dissolved pellets were centrifuged, and the PBS supernatant was removed, with sample weights of the pellets being recorded. For lipid extraction, a modified version of the Matyash method was used with MTBE, as previously described in Chapter 2 [114].

### ***LC-MS/MS lipidomics analysis***

Before sample processing, samples were loaded into auto-sampler vials (10  $\mu$ L of sample, 5  $\mu$ L sample injection volume). No ionization agent was added to samples prior to injection, as the additive in the HILIC-specific chromatography solvents used here (specifically, 5 mM ammonium acetate) are sufficient for ionization, both in positive- and negative-ion mode. Samples were run in batches, with technical blanks added in between similar sampling conditions for quality control as well as to monitor potential carry-over and standards run at frequent intervals to monitor consistency. Chromatographic separations and tandem mass spectrometry analysis were performed as previously described in Chapter 2 for HILIC separations in negative polarity mode, utilizing the same equipment (HPLC pump and mass spectrometer) and settings (chromatography runs and tandem MS analysis).



### *Lipidomics data analysis*

Bulk processing of the raw LC-MS/MS files was performed using the free, open-source software packages MZmine (version 2.53) [99, 230] and LIQUID (version 7.4.6988) [98] alongside manual annotation. MetaboAnalyst was used for statistical analysis and generation of figures; peak area lists created from LIQUID features and MZmine-aligned files were used for this. For comparison of phospholipid species, the sum average peak areas of PG and CL were normalized to the sum average peak area of PE as described in Chapter 3. Peak areas of phospholipid features were normalized by sample weight prior to statistical analysis. The methodology behind each of these steps is further explained in Chapter 2.

**Here, files for each sample within a biological replicate were generated in LIQUID; after filtering to remove low-scoring features and duplicates, any feature that was observed in at least two of the three biological replicates was retained. The lists for each triplicate across all sampling conditions were compiled into one master list, which was then annotated with aligned peak areas generated by MZmine. The results of that are shown in Table 14 (both glucose conditions),**

**Table 15 (2-cyclopentenone and formaldehyde), Table 15 Continued**

<b>Phospholipid Species</b>	<b>2-Cyclopentenone</b>			<b>Formaldehyde</b>		
PS(P-33:0)	6E+07	5E+07	8E+07	7E+05	1E+07	7E+05

Table 16 (*p*-cresol and sodium acetate) and Table 17 (vanillin and the mock wastewater solution).

**Table 14. Compiled master list of phospholipid species validated by MS2 spectra in LIQUID with MZmine-aligned peak areas in *P. putida* EM42 samples grown in the two glucose control conditions.**

Phospholipid Species	Glucose (Mid Exponential)			Glucose (Late Exponential)		
CL(64:1)	8E+06	3E+06	7E+06	2E+06	6E+05	9E+05
CL(64:2)	2E+07	2E+07	2E+07	6E+07	6E+07	5E+07
CL(64:3)	7E+05	1E+06	6E+05	1E+07	1E+06	1E+07
CL(65:1)	0	0	0	0	0	0
CL(65:2)	2E+05	3E+05	3E+05	1E+06	5E+05	4E+05
CL(66:2)	3E+07	4E+07	4E+07	8E+06	6E+06	5E+06
CL(66:3)	2E+07	3E+07	2E+07	2E+08	2E+08	2E+08
CL(67:2)	7E+05	3E+05	3E+05	0	0	0
CL(67:3)	8E+05	1E+06	8E+05	6E+06	6E+06	3E+06
CL(67:4)	0	0	0	9E+05	4E+05	4E+05
CL(68:0)	7E+05	1E+06	2E+06	6E+06	1E+06	7E+06
CL(68:1)	5E+06	3E+06	6E+06	5E+06	9E+06	4E+06
CL(68:2)	1E+07	4E+07	5E+06	5E+07	3E+07	5E+07
CL(68:3)	2E+07	3E+07	3E+07	1E+08	2E+08	1E+08
CL(68:4)	2E+07	2E+07	2E+07	2E+08	2E+08	1E+08
CL(69:3)	3E+05	0	0	4E+05	3E+05	3E+05
CL(69:4)	5E+05	3E+05	5E+05	4E+06	1E+06	0
CL(70:2)	2E+07	3E+06	6E+06	6E+06	1E+07	6E+06
CL(70:3)	4E+06	6E+06	6E+06	4E+07	6E+07	5E+07
CL(70:4)	4E+06	6E+06	5E+06	4E+07	4E+07	3E+07
CL(71:3)	0	0	0	0	2E+05	0
CL(71:4)	0	0	0	0	0	0
CL(72:2)	5E+05	7E+05	1E+06	2E+06	2E+06	5E+05
CL(72:3)	1E+06	4E+05	7E+05	2E+06	2E+06	9E+05
CL(72:4)	0	4E+05	2E+05	1E+06	1E+06	7E+05
PA(34:1)	3E+06	9E+06	4E+06	3E+05	1E+06	3E+06
PA(35:2)	3E+07	5E+06	6E+06	8E+06	2E+06	1E+06
PA(36:2)	1E+06	2E+05	3E+05	2E+05	1E+05	3E+05
PE(16:1)	6E+07	3E+07	5E+07	1E+08	1E+08	2E+08
PE(18:1)	9E+07	1E+08	1E+08	3E+08	3E+08	2E+08
PE(32:0)	1E+08	5E+07	5E+07	4E+07	1E+07	1E+07
PE(32:1)	1E+09	1E+09	1E+09	2E+09	9E+08	1E+09
PE(32:2)	8E+07	7E+07	9E+07	4E+08	9E+08	7E+08

**Table 14 Continued**

Phospholipid Species	Glucose (Mid Exponential)			Glucose (Late Exponential)		
PE(33:1)	2E+06	1E+06	2E+06	4E+06	3E+06	1E+07
PE(33:2)	9E+07	8E+07	7E+07	1E+08	9E+07	9E+07
PE(34:0)	2E+07	3E+06	1E+07	1E+07	1E+07	3E+06
PE(34:1)	7E+08	8E+08	7E+08	1E+09	6E+08	6E+08
PE(34:2)	9E+08	1E+09	1E+09	2E+09	1E+09	2E+09
PE(36:0)	0	5E+05	0	0	0	0
PE(36:1)	1E+07	2E+07	7E+06	9E+06	3E+06	2E+07
PE(36:2)	2E+08	2E+08	2E+08	3E+08	2E+08	2E+08
PE(37:2)	0	0	2E+05	0	0	0
PE(38:1)	0	0	0	0	0	0
PE(38:2)	2E+05	7E+05	5E+05	9E+05	6E+05	2E+05
PG(30:0)	6E+06	5E+06	3E+06	3E+06	8E+05	3E+05
PG(30:1)	7E+06	1E+07	7E+06	6E+06	5E+06	7E+05
PG(32:0)	3E+06	1E+06	1E+06	2E+05	0	0
PG(32:1)	1E+09	2E+09	2E+09	1E+09	1E+09	8E+08
PG(32:2)	6E+05	3E+07	9E+07	9E+07	9E+07	4E+07
PG(33:0)	2E+06	1E+06	0	6E+05	2E+06	5E+05
PG(33:1)	3E+07	4E+07	3E+07	3E+07	2E+07	3E+07
PG(33:2)	8E+06	1E+07	8E+06	7E+06	7E+06	1E+07
PG(34:0)	2E+05	3E+05	3E+05	0	0	0
PG(34:1)	9E+08	1E+09	1E+09	1E+09	7E+08	6E+08
PG(34:2)	2E+09	3E+09	2E+09	2E+09	2E+09	1E+09
PG(34:3)	0	4E+05	2E+06	7E+05	8E+05	0
PG(35:1)	8E+05	7E+05	9E+05	6E+05	8E+05	0
PG(35:2)	3E+07	5E+07	3E+07	4E+07	3E+07	2E+07
PG(36:0)	3E+06	1E+07	5E+06	3E+06	3E+06	2E+06
PG(36:1)	7E+07	1E+08	7E+07	6E+07	2E+07	4E+07
PG(36:2)	3E+08	5E+08	3E+08	4E+08	3E+08	2E+08
PG(37:2)	0	0	0	2E+05	0	0
PG(38:1)	3E+05	4E+05	6E+05	7E+05	3E+05	0
PG(38:2)	5E+06	8E+06	5E+06	6E+06	5E+06	2E+06
PS(34:1)	1E+06	7E+05	6E+05	1E+06	8E+05	2E+06
PS(34:2)	0	0	0	0	2E+05	0
PS(35:1)	9E+06	1E+07	9E+06	3E+07	3E+07	3E+07
PS(35:2)	2E+06	2E+07	4E+06	6E+07	5E+07	6E+07

**Table 14 Continued**

Phospholipid Species	Glucose (Mid Exponential)			Glucose (Late Exponential)		
PS(36:2)	0	0	0	0	0	3E+05
PS(O-35:1)	0	0	0	0	0	0
PS(P-33:0)	3E+07	2E+07	1E+07	6E+06	1E+06	4E+05

**Table 15. Compiled master list of phospholipid species validated by MS2 spectra in LIQUID with MZmine-aligned peak areas in *P. putida* EM42 samples grown in 2-cyclopentenone and formaldehyde.**

Phospholipid Species	2-Cyclopentenone			Formaldehyde		
CL(64:1)	0	8E+06	1E+07	1E+06	1E+06	2E+06
CL(64:2)	3E+07	3E+07	3E+07	5E+07	4E+07	4E+07
CL(64:3)	1E+06	0	2E+06	7E+06	8E+06	1E+06
CL(65:1)	6E+05	1E+06	7E+05	0	0	0
CL(65:2)	6E+06	6E+06	4E+06	2E+06	0	5E+05
CL(66:2)	8E+07	8E+07	7E+07	6E+06	2E+06	8E+07
CL(66:3)	6E+07	5E+07	6E+07	1E+08	1E+08	9E+07
CL(67:2)	0	1E+07	4E+06	0	0	0
CL(67:3)	1E+07	1E+07	8E+06	5E+06	3E+06	1E+06
CL(67:4)	0	0	0	3E+05	0	2E+05
CL(68:0)	5E+06	2E+06	3E+06	2E+06	3E+05	1E+07
CL(68:1)	5E+06	2E+07	1E+07	2E+07	4E+07	5E+06
CL(68:2)	2E+07	4E+07	4E+07	5E+06	8E+07	5E+07
CL(68:3)	8E+07	8E+07	7E+07	1E+08	1E+08	9E+07
CL(68:4)	3E+07	3E+07	4E+07	7E+07	8E+07	6E+07
CL(69:3)	3E+06	8E+06	4E+06	3E+05	0	0
CL(69:4)	4E+06	4E+06	4E+06	2E+06	0	2E+05
CL(70:2)	2E+07	1E+07	2E+07	5E+06	3E+07	4E+07
CL(70:3)	3E+07	3E+07	2E+07	5E+06	2E+07	2E+07
CL(70:4)	1E+07	2E+07	1E+07	2E+07	2E+07	2E+07
CL(71:3)	9E+05	4E+05	2E+05	0	0	0
CL(71:4)	0	3E+05	2E+05	0	0	0
CL(72:2)	2E+06	4E+05	3E+06	9E+05	4E+05	3E+06
CL(72:3)	3E+06	2E+06	3E+06	7E+05	3E+06	1E+06
CL(72:4)	2E+06	2E+06	2E+06	1E+06	6E+05	1E+06
PA(34:1)	2E+07	4E+06	1E+07	7E+06	2E+06	1E+06
PA(35:2)	1E+08	6E+07	2E+08	4E+07	6E+06	1E+07
PA(36:2)	2E+07	6E+06	1E+07	3E+05	2E+06	4E+05
PE(16:1)	5E+07	2E+07	1E+07	2E+07	2E+06	4E+07
PE(18:1)	6E+06	2E+06	1E+07	6E+07	9E+07	6E+07
PE(32:0)	8E+07	4E+07	3E+07	1E+07	9E+06	6E+07
PE(32:1)	1E+09	7E+08	1E+09	9E+08	1E+09	2E+09
PE(32:2)	2E+08	2E+08	2E+08	2E+08	3E+08	2E+08
PE(33:1)	2E+06	1E+07	2E+07	2E+06	3E+06	2E+06

**Table 15 Continued**

Phospholipid Species	2-Cyclopentenone			Formaldehyde		
PE(33:2)	3E+08	4E+08	3E+08	4E+08	2E+08	6E+07
PE(34:0)	2E+06	3E+07	1E+06	8E+06	2E+06	2E+07
PE(34:1)	8E+08	7E+08	8E+08	6E+08	7E+08	1E+09
PE(34:2)	1E+09	7E+08	1E+09	8E+08	1E+09	1E+09
PE(36:0)	81389	0	0	0	0	0
PE(36:1)	6E+07	5E+07	4E+07	3E+06	3E+06	1E+07
PE(36:2)	2E+08	2E+08	2E+08	2E+08	2E+08	3E+08
PE(37:2)	0	0	1E+05	0	0	2E+05
PE(38:1)	0	1E+05	63629	0	0	0
PE(38:2)	2E+06	3E+06	2E+06	2E+05	0	1E+06
PG(30:0)	2E+05	5E+05	5E+05	7E+05	0	3E+06
PG(30:1)	4E+06	7E+06	9E+06	2E+07	5E+06	1E+07
PG(32:0)	1E+06	2E+06	8E+06	6E+06	0	2E+07
PG(32:1)	8E+08	1E+09	2E+09	3E+09	7E+08	2E+09
PG(32:2)	3E+07	5E+07	6E+07	2E+08	1E+08	2E+08
PG(33:0)	2E+06	0	1E+05	7E+06	0	4E+05
PG(33:1)	1E+08	1E+08	1E+08	1E+08	6E+06	3E+07
PG(33:2)	1E+07	2E+07	2E+07	3E+07	4E+06	1E+07
PG(34:0)	90624	0	0	0	0	8E+05
PG(34:1)	7E+08	1E+09	1E+09	2E+09	3E+08	1E+09
PG(34:2)	1E+09	8E+08	7E+08	4E+09	1E+09	4E+06
PG(34:3)	5E+05	1E+06	5E+05	2E+06	4E+05	3E+06
PG(35:1)	1E+06	8E+05	3E+06	5E+05	0	1E+06
PG(35:2)	1E+08	1E+08	2E+08	1E+08	8E+06	4E+07
PG(36:0)	1E+06	3E+06	2E+06	1E+07	2E+06	5E+06
PG(36:1)	3E+07	5E+07	3E+07	1E+08	2E+07	1E+08
PG(36:2)	3E+08	4E+08	5E+08	8E+08	2E+08	5E+08
PG(37:2)	1E+06	6E+05	5E+05	2E+05	0	0
PG(38:1)	5E+05	8E+05	3E+05	6E+05	0	1E+06
PG(38:2)	4E+06	6E+06	6E+06	1E+07	2E+06	9E+06
PS(34:1)	6E+06	1E+06	2E+06	2E+06	5E+05	1E+06
PS(34:2)	0	0	84021	0	0	0
PS(35:1)	3E+07	2E+07	5E+07	2E+07	5E+06	8E+06
PS(35:2)	2E+06	4E+06	3E+06	4E+07	8E+06	1E+07
PS(36:2)	1E+05	2E+05	0	0	0	0
PS(O-35:1)	3E+06	3E+06	6E+05	0	0	0



**Table 15 Continued**

Phospholipid Species	2-Cyclopentenone			Formaldehyde		
PS(P-33:0)	6E+07	5E+07	8E+07	7E+05	1E+07	7E+05

**Table 16. Compiled master list of phospholipid species validated by MS2 spectra in LIQUID with MZmine-aligned peak areas in *P. putida* EM42 samples grown in *p*-cresol and sodium acetate.**

Phospholipid Species	<i>p</i> -Cresol			Sodium acetate		
CL(64:1)	5E+06	1E+07	6E+06	3E+05	0	0
CL(64:2)	5E+07	9E+06	5E+06	5E+06	2E+06	7E+06
CL(64:3)	4E+05	0	0	0	0	3E+05
CL(65:1)	4E+06	0	0	0	0	0
CL(65:2)	1E+07	2E+06	5E+05	3E+06	6E+06	2E+07
CL(66:2)	2E+08	1E+07	7E+06	1E+07	8E+05	4E+06
CL(66:3)	1E+08	2E+07	1E+07	5E+07	3E+07	5E+06
CL(67:2)	2E+07	5E+06	1E+06	3E+07	1E+06	6E+07
CL(67:3)	2E+07	3E+06	1E+06	7E+07	3E+07	1E+08
CL(67:4)	1E+06	0	0	7E+06	6E+06	4E+06
CL(68:0)	8E+05	4E+06	8E+06	5E+05	0	0
CL(68:1)	4E+07	2E+07	7E+06	6E+06	0	4E+06
CL(68:2)	3E+07	1E+07	1E+07	5E+06	2E+07	1E+07
CL(68:3)	2E+08	5E+07	3E+07	9E+07	3E+07	2E+08
CL(68:4)	8E+07	3E+07	1E+07	1E+08	5E+07	1E+08
CL(69:3)	1E+07	2E+06	4E+05	6E+07	3E+07	3E+07
CL(69:4)	1E+07	2E+06	4E+05	9E+07	2E+07	6E+07
CL(70:2)	6E+06	9E+06	3E+06	8E+06	6E+05	4E+06
CL(70:3)	3E+07	9E+06	3E+06	2E+07	3E+07	9E+07
CL(70:4)	2E+07	6E+06	2E+06	5E+07	2E+07	1E+08
CL(71:3)	0	0	9E+05	6E+06	4E+06	2E+06
CL(71:4)	1E+06	0	0	2E+07	9E+06	4E+07
CL(72:2)	8E+05	3E+06	3E+06	3E+06	2E+06	2E+06
CL(72:3)	4E+06	4E+05	0	2E+06	6E+05	7E+06
CL(72:4)	1E+06	0	0	5E+06	2E+06	1E+07
PA(34:1)	6E+07	1E+08	6E+07	6E+07	2E+07	1E+07
PA(35:2)	3E+07	3E+07	5E+07	3E+08	4E+07	2E+08
PA(36:2)	2E+06	3E+06	4E+06	7E+07	2E+07	4E+07
PE(16:1)	5E+07	4E+07	5E+07	2E+08	5E+06	1E+08
PE(18:1)	3E+08	5E+08	4E+08	6E+08	2E+08	5E+08
PE(32:0)	3E+07	5E+08	3E+08	2E+07	1E+06	1E+07
PE(32:1)	6E+08	5E+08	7E+08	1E+09	5E+08	6E+08
PE(32:2)	2E+08	5E+07	3E+07	1E+08	5E+07	2E+08
PE(33:1)	3E+07	6E+06	2E+07	3E+08	9E+07	4E+07
PE(33:2)	5E+08	5E+07	9E+07	1E+08	3E+07	6E+07

Table 16 Continued

Phospholipid Species	<i>p</i> -Cresol			Sodium acetate		
PE(34:0)	9E+06	2E+08	1E+08	1E+07	2E+06	7E+06
PE(34:1)	7E+08	1E+09	1E+09	1E+09	3E+08	4E+08
PE(34:2)	6E+08	7E+08	6E+08	2E+09	8E+08	1E+09
PE(36:0)	9E+06	1E+07	7E+06	0	0	0
PE(36:1)	1E+08	2E+08	2E+08	1E+07	1E+07	3E+07
PE(36:2)	1E+08	1E+08	1E+08	5E+08	2E+08	4E+08
PE(37:2)	5E+05	0	0	4E+06	0	3E+06
PE(38:1)	0	1E+06	3E+05	4E+05	0	0
PE(38:2)	1E+06	7E+05	4E+05	4E+06	0	3E+06
PG(30:0)	2E+07	3E+06	2E+06	3E+07	3E+06	2E+07
PG(30:1)	0	0	4E+05	3E+06	2E+06	2E+06
PG(32:0)	1E+08	8E+07	9E+07	0	1E+06	2E+06
PG(32:1)	5E+08	4E+08	4E+08	8E+08	5E+08	5E+08
PG(32:2)	3E+06	0	0	7E+07	5E+07	5E+07
PG(33:0)	9E+06	3E+06	1E+06	3E+07	3E+07	2E+07
PG(33:1)	9E+07	8E+07	8E+07	5E+08	3E+08	4E+08
PG(33:2)	1E+07	4E+06	2E+06	2E+08	1E+08	1E+08
PG(34:0)	2E+06	3E+06	3E+06	0	0	0
PG(34:1)	7E+08	7E+08	6E+08	1E+09	7E+08	9E+08
PG(34:2)	5E+08	5E+08	4E+08	2E+09	2E+09	2E+09
PG(34:3)	0	0	0	2E+07	4E+06	1E+07
PG(35:1)	9E+06	1E+07	1E+07	3E+05	0	2E+08
PG(35:2)	4E+07	4E+07	4E+07	2E+09	1E+09	1E+09
PG(36:0)	6E+06	3E+06	4E+06	5E+06	7E+06	1E+07
PG(36:1)	1E+08	1E+08	9E+07	5E+07	6E+07	1E+08
PG(36:2)	1E+08	1E+08	1E+08	1E+09	6E+08	8E+08
PG(37:2)	0	5E+05	4E+05	4E+07	0	4E+07
PG(38:1)	7E+06	9E+06	6E+06	2E+06	2E+06	2E+06
PG(38:2)	6E+06	7E+06	7E+06	3E+07	2E+07	2E+07
PS(34:1)	9E+05	0	0	6E+07	1E+07	5E+07
PS(34:2)	7E+06	1E+07	1E+07	0	2E+05	2E+05
PS(35:1)	8E+05	6E+05	1E+06	1E+08	2E+07	7E+07
PS(35:2)	0	2E+06	1E+06	1E+08	5E+07	9E+07
PS(36:2)	0	0	0	7E+07	3E+07	6E+07
PS(O-35:1)	0	3E+06	3E+06	0	0	0
PS(P-33:0)	5E+06	3E+07	2E+07	8E+06	6E+06	0

**Table 17. Compiled master list of phospholipid species validated by MS2 spectra in LIQUID with MZmine-aligned peak areas in *P. putida* EM42 samples grown in vanillin and the mock wastewater solution.**

Phospholipid Species	Vanillin			Mock Wastewater		
CL(64:1)	3E+05	0	3E+05	5E+05	5E+05	7E+05
CL(64:2)	2E+07	2E+07	2E+07	8E+06	6E+06	3E+06
CL(64:3)	2E+06	4E+05	6E+06	1E+06	8E+05	3E+05
CL(65:1)	0	0	0	0	0	0
CL(65:2)	6E+05	1E+06	7E+05	2E+05	0	0
CL(66:2)	4E+07	4E+06	4E+06	1E+05	0	4E+05
CL(66:3)	1E+08	8E+07	9E+07	2E+07	2E+07	8E+06
CL(67:2)	6E+05	3E+05	3E+05	0	0	0
CL(67:3)	7E+06	1E+07	5E+06	6E+05	4E+05	0
CL(67:4)	3E+06	7E+05	2E+06	0	0	0
CL(68:0)	3E+06	1E+06	3E+06	4E+05	2E+06	0
CL(68:1)	4E+06	6E+06	6E+06	2E+06	6E+05	2E+06
CL(68:2)	5E+06	4E+06	4E+06	7E+06	9E+06	4E+06
CL(68:3)	1E+08	2E+08	1E+08	2E+07	2E+07	8E+06
CL(68:4)	1E+08	1E+08	1E+08	2E+07	2E+07	8E+06
CL(69:3)	7E+05	4E+06	3E+05	0	0	0
CL(69:4)	6E+06	9E+06	6E+06	3E+05	3E+05	0
CL(70:2)	7E+06	3E+06	8E+06	6E+06	9E+06	3E+05
CL(70:3)	1E+07	3E+07	3E+07	4E+06	5E+06	1E+06
CL(70:4)	4E+07	5E+07	4E+07	4E+06	4E+06	1E+06
CL(71:3)	0	0	0	0	0	0
CL(71:4)	0	4E+05	0	0	0	0
CL(72:2)	2E+06	3E+06	2E+06	1E+06	0	0
CL(72:3)	2E+06	3E+06	2E+06	4E+05	0	0
CL(72:4)	2E+06	6E+06	2E+06	1E+05	1E+05	0
PA(34:1)	2E+06	4E+05	1E+06	3E+05	0	6E+05
PA(35:2)	4E+06	1E+06	3E+06	4E+07	6E+07	4E+05
PA(36:2)	2E+06	6E+05	5E+05	7E+05	3E+05	7E+05
PE(16:1)	2E+08	2E+08	2E+08	7E+07	6E+07	5E+07
PE(18:1)	7E+08	4E+08	9E+08	8E+07	7E+07	3E+07
PE(32:0)	3E+07	7E+06	6E+06	2E+07	2E+07	2E+07
PE(32:1)	1E+09	5E+08	8E+08	3E+08	3E+08	3E+08
PE(32:2)	1E+08	3E+08	2E+08	9E+07	5E+07	1E+07
PE(33:1)	2E+06	4E+06	3E+06	1E+06	1E+06	4E+05
PE(33:2)	8E+07	5E+08	2E+08	2E+06	5E+07	7E+06

**Table 17 Continued**

Phospholipid Species	Vanillin			Mock Wastewater		
PE(34:0)	2E+07	1E+07	1E+07	2E+06	1E+06	3E+06
PE(34:1)	8E+08	3E+08	7E+08	2E+08	2E+08	2E+08
PE(34:2)	2E+09	2E+09	2E+09	4E+08	4E+08	5E+08
PE(36:0)	0	0	0	0	0	0
PE(36:1)	9E+06	1E+07	5E+06	7E+06	1E+07	7E+06
PE(36:2)	4E+08	3E+08	4E+08	5E+07	6E+07	6E+07
PE(37:2)	4E+05	3E+05	0	0	0	0
PE(38:1)	0	0	2E+05	0	0	0
PE(38:2)	2E+06	1E+06	1E+06	3E+05	0	0
PG(30:0)	5E+06	8E+06	3E+06	1E+05	6E+05	0
PG(30:1)	6E+06	8E+06	7E+06	1E+06	1E+06	6E+05
PG(32:0)	2E+06	2E+06	6E+05	0	1E+06	0
PG(32:1)	1E+09	1E+09	1E+09	3E+08	4E+08	2E+08
PG(32:2)	1E+08	2E+08	1E+08	3E+06	2E+07	6E+05
PG(33:0)	1E+06	3E+06	3E+06	0	3E+05	0
PG(33:1)	4E+07	5E+07	4E+07	7E+06	1E+07	6E+06
PG(33:2)	3E+07	4E+07	3E+07	1E+06	5E+06	6E+06
PG(34:0)	0	0	0	0	0	0
PG(34:1)	1E+09	1E+09	1E+09	2E+08	3E+08	2E+08
PG(34:2)	2E+09	3E+09	3E+09	5E+08	6E+08	5E+08
PG(34:3)	3E+06	4E+06	4E+06	0	0	2E+05
PG(35:1)	2E+06	6E+05	1E+06	0	0	0
PG(35:2)	7E+07	1E+08	8E+07	6E+06	1E+07	7E+06
PG(36:0)	4E+06	2E+06	4E+06	8E+05	2E+06	1E+06
PG(36:1)	3E+07	2E+07	3E+07	2E+07	2E+07	2E+07
PG(36:2)	2E+06	8E+08	7E+08	7E+07	1E+08	8E+07
PG(37:2)	2E+05	8E+05	5E+05	0	0	0
PG(38:1)	8E+05	1E+06	1E+06	0	0	0
PG(38:2)	1E+07	1E+07	1E+07	1E+06	2E+06	1E+06
PS(34:1)	3E+05	2E+06	2E+06	0	1E+05	0
PS(34:2)	0	0	0	0	1E+05	0
PS(35:1)	8E+06	1E+07	8E+06	9E+05	1E+06	0
PS(35:2)	7E+05	2E+06	2E+07	9E+05	2E+06	8E+05
PS(36:2)	0	0	0	0	0	0
PS(O-35:1)	0	0	0	0	0	0
PS(P-33:0)	1E+07	2E+06	1E+07	2E+05	7E+05	6E+05

## Results and Discussion

### *The lipids of the gene-reduced strain Pseudomonas putida EM42 align similarly to the commonly researched strain P. putida KT2440*

Figure 42 shows the phospholipid composition of the major observed species within cultures grown only in glucose and to mid and late exponential phase. In general, the phospholipid trends are in line with reported values for *P. putida* phospholipid profiles, but there is a distinct difference in phospholipid speciation between mid and late exponential phase cultures with respect to PE to PG ratio. Studies on eukaryotic organisms show that growth phase was linked to increases in PG and PE species and decreases in PC [362], though studies on *E. coli* and *B. subtilis* indicated that exponential growth did not induce drastic shifts in phospholipid composition, though stationary phase and sporulation could involve mild changes [218]. Still, specific changes between each phase do not appear to be well reported [17].

Table 18 shows a selection of previous reports on *P. putida* lipidomics, with reported ratios of the three main expected phospholipid species PE, PG, and CL, as well as a representative sample of the closely related *P. aeruginosa*. Unlike with *B. subtilis*, *P. putida* membranes are usually dominated by PE (as is to be expected in most Gram-negative bacteria [186]), with PG occupying a lower fraction of the overall lipidome and cardiolipin existing in a similar low percentage as with other bacteria. As can be seen in Figure 43, there are no genes present in *P. putida* KT2440 that encode specifically for production of PC, which is a known component of the closely related *P. aeruginosa*, but genes do exist for synthesis of PE (4.1.1.65), PG (3.1.3.27), and cardiolipin (ClsA/B/C).

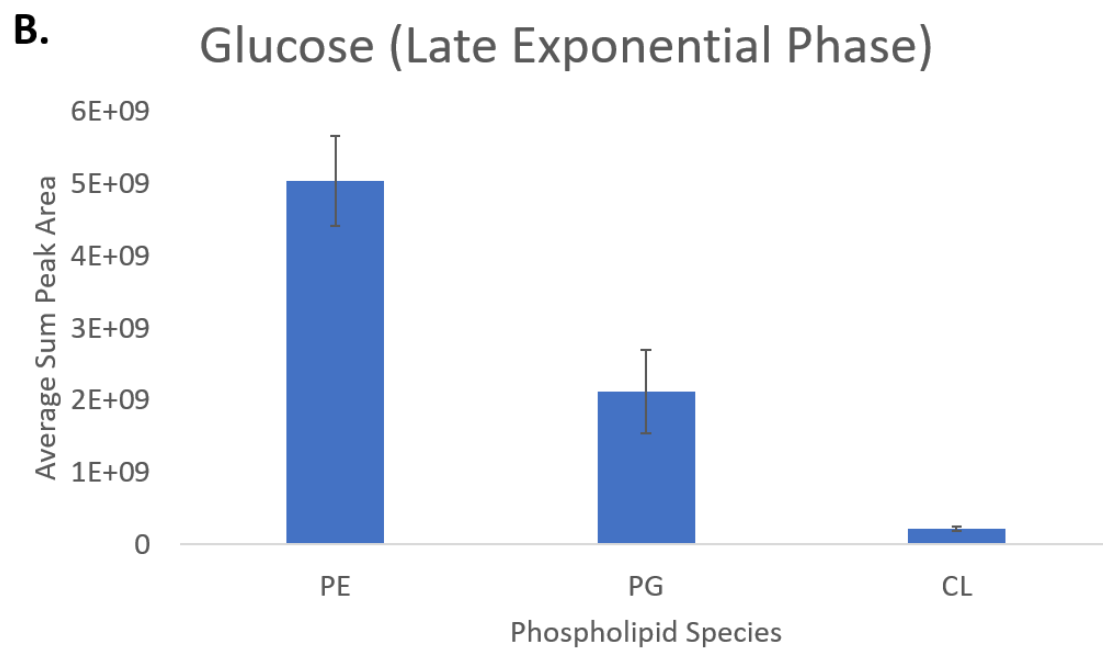
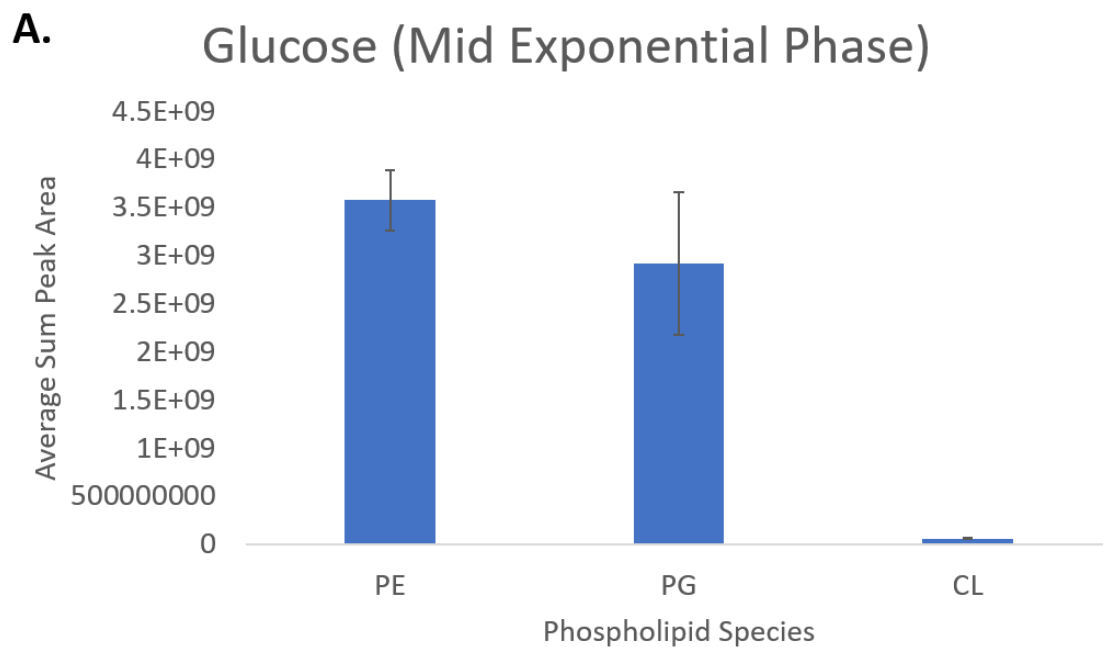


**Figure 42. Phospholipid composition by peak area of *P. putida* EM42 cultures grown in glucose to A) mid exponential phase and B) late exponential phase**

**Table 18. Previous phospholipid profiling studies performed on several strains of *Pseudomonas putida*, as well as representative *P. aeruginosa* profiles to exemplify the differences within a genus.**

<b>Previously Reported <i>P. putida</i> Phospholipid Ratios</b>				
<b>Source</b>	<b>PE</b>	<b>PG</b>	<b>CL</b>	<b>Other (if reported)</b>
Pinkart & White, 1997 [363] Strains: MW1200 and Idaho Mole percentage	MW1200: 55.97%	MW1200: 28.79%	MW1200: 11.24%	MW1200: PA: 2.4%; PS: 1.56%
	Idaho: 73.93%	Idaho: 14.21%	Idaho: 6.6%	Idaho: PA: 1.12%; PS: 0.78%
Rühl, et al, 2012 [172] Strains: KT2440, DOT-T1E, S12, VLB120 Ratio of peak area of species to overall area	KT2440: 62%	KT2440: 33%	KT2440: 4%	N/A
	DOT-T1E: 64%	DOT-T1E: 33%	DOT-T1E: 3%	
	S12: 59%	S12: 38%	S12: 3%	
	VLB120: 72%	VLB120: 24%	VLB120: 4%	
Wang, et al, 2015 [364] Strains: KT2442 Comparison of standard peak areas to tested samples	79.9%	12.7%	7.4%	N/A
Hancock & Meadow, 1969 [365] Strains: <i>P. aeruginosa</i> 8602 Molar composition by phosphorus assay	6 hr.: 83.2% 8 hr.: 80.6% 14 hr.: 71.8% 24 hr.: 70.8%	6 hr.: 14% 8 hr.: 17.8% 14 hr.: 12.1% 24 hr.: 11.8%	NA	For bis-PG: 6 hr.: 2.8% 8 hr.: 1.5% 14 hr.: 8.1% 24 hr.: 8.4%
Tashiro, et al, 2011 [366] Han, et al, 2018 [367] Deschamps, et al, 2021 [368] <i>P. aeruginosa</i>	No defined proportions, but presence of PG, PE, and CL confirmed, as well as the <i>P. aeruginosa</i> -exclusive PC			





Table 18 also shows that there is infrequent reporting of PA and PS species within *P. putida*. While those are not inherent species being produced as a part of the membrane, PA is a generic phospholipid precursor produced from glycerol 3-phosphate (1.1.1.91) or the phosphorylation of diacylglycerol (2.3.1.51 & 2.7.1.107), and PS is specifically synthesized (2.7.8.8) as a direct precursor and intermediate in the production of PE (4.1.1.65), so while observation of these phospholipid species is not necessarily expected, it is not surprising either.

While there are published studies on the lipid profile of the parent strain *P. putida* KT2440, there currently are no lipid profiling studies on the gene-reduced form of *P. putida* EM42. While none of the gene deletions present in *P. putida* EM42 explicitly influence any part of phospholipid synthesis and recycling, the loss of the flagella gene and flagella as a major structural component embedded within the membrane could theoretically cause changes in membrane composition. Indeed, there have been studies reporting on the differences in membrane content between the region surrounding the mounting point of the flagella and the rest of the cell membrane, indicating PG was depleted in the flagellar membrane region and PE was enriched [370]. There are also reports that decreased flagellar formation could be linked to cellular deficiencies in PG and CL [371], which was supported by observation of increased levels of cardiolipin in the flagellar sheath [372]. With that in mind, while removal of the flagella does not constitute a massive shift in the composition of the cell membrane, it still stands to reason those observable shifts in the overall lipid profile of the cell might be evident as a result.

Despite a significant difference in cellular construction, the Gram-negative *P. putida* and Gram-positive *B. subtilis* largely share the same genes encoding for fatty acid biosynthesis (Figure 44), with *P. putida* expressing FabA and FabB, which are historically only observed in Gram-negative species such as *P. putida* or the commonly researched *E. coli* [373]. Similarly, FabI and FabL are not observed in *P. putida*, as they are genes specific to *B. subtilis* [374], and the Gram-negative counterpart in FabV is what is observed here [375]. While not necessarily odd observations, it is intriguing to see how simultaneously similar and different two species can be within the same pathway.

#### ***A high-level view of P. putida phospholipid speciation and characteristics***

To begin, general information about the composition and variance across phospholipid inventories in each of the sampling conditions was collected. First, given prior information about the major phospholipid components of *P. putida* being PE and PG, the ratio of PE to PG across each of the sampling conditions was examined (Figure 45). While all samples generally conformed to previous studies [172], several samples stood out. The samples grown in the mock wastewater solution as well as *p*-cresol showed noticeably elevated amounts of PE within their lipidomes. The *p*-cresol and mock wastewater solution trending together may not be completely unexpected, given the mock wastewater solution contains several cresol isomers as well as other aromatic molecules (Table 13). Given previous studies indicating that Gram-negative bacteria exhibit a higher sensitivity to *p*-cresol than Gram-positive species [376], this could possibly be indicative of the cresol species being highly influential on how the lipidome of *P. putida* adapts within the mock wastewater solution.



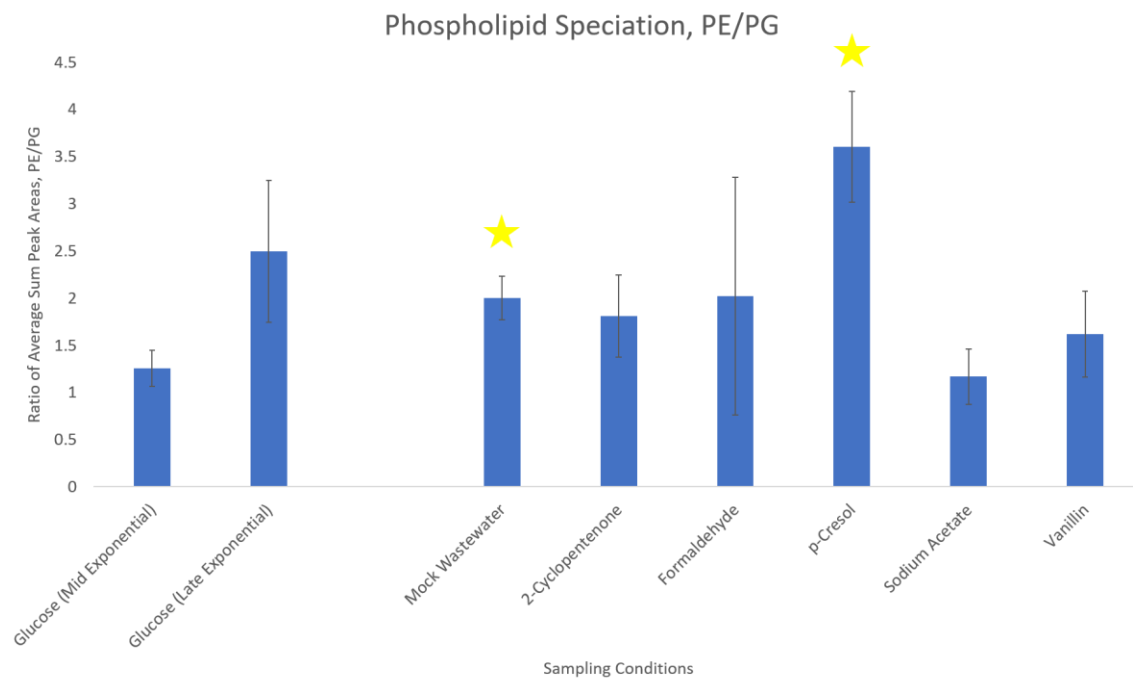


**Figure 45. Ratio of PE to PG across all sampling conditions of *P. putida* EM42. Stars indicate species deemed significantly different from the mid exponential glucose control by the Student's t-test.**

Next, the composition of the fatty acid portion of the phospholipid inventory was examined, with an examination of average fatty acid chain length (Figure 46) as well as average degree of unsaturation (Figure 47). When compared to the mid exponential glucose control, two samples were determined to contain, on average, significantly longer fatty acids – the samples grown in sodium acetate and vanillin. Both of those samples also contained higher degrees of unsaturation, as well as the other glucose sample, grown to late exponential phase.

With this information in hand, statistics showed that the samples grown in sodium acetate, vanillin, and *p*-cresol demonstrated significant differences in lipidome composition, and as such, further examination of each condition was explored to try to elucidate if specific phospholipids drove those changes, as well as the biological implications of those shifts in phospholipid profile. Additionally, given the mock wastewater composition is composed of molecules derived from similar chemical classes, the changes in phospholipid profile in the mock wastewater solution were also examined.

#### ***p*-Cresol shows notable relative increases in fully saturated fatty acid content**

To begin, the sample showing the most variance in average phospholipid ratio between PE and PG was examined (Figure 48). Interestingly enough, upon closer inspection of the phospholipids that varied the most between sample and control (as determined by a p-value cutoff of 0.05 or less), there was not an obvious trend within the *p*-cresol samples of the presence of more PE species. Both the glucose control and *p*-cresol samples contained specific PE species that showed significant fold change increases compared to the other condition.

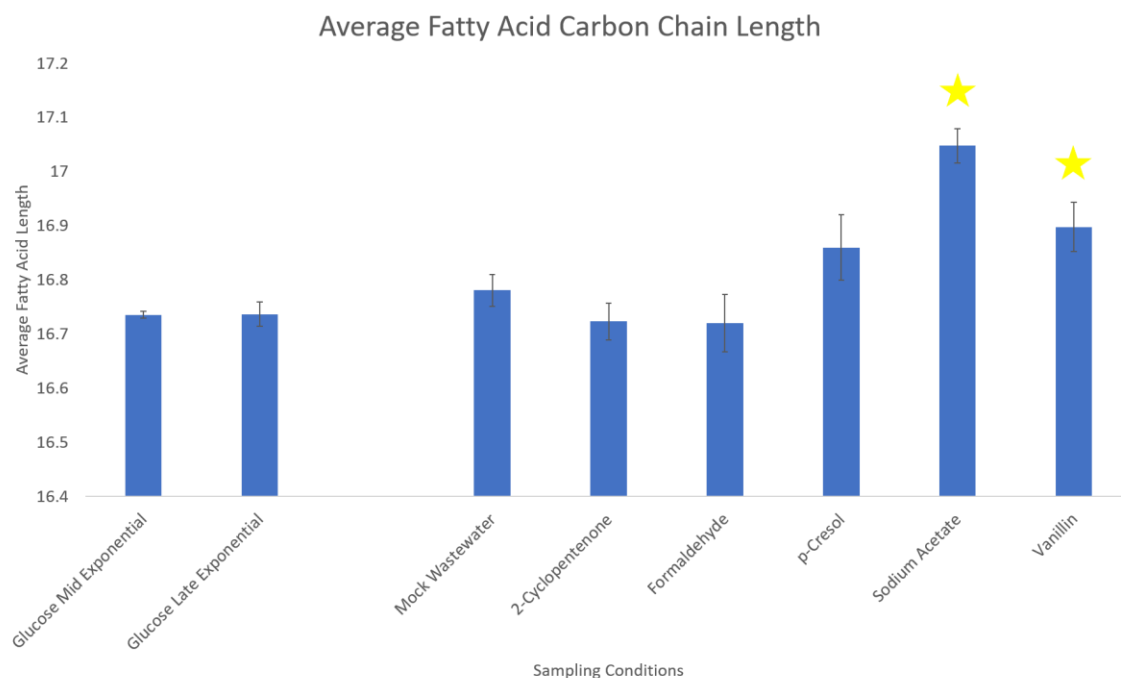


**Figure 46. Average fatty acid chain length of phospholipids across all sampling conditions of *P. putida* EM42. Stars indicate species deemed significantly different from the mid exponential glucose control by the Student's t-test.**

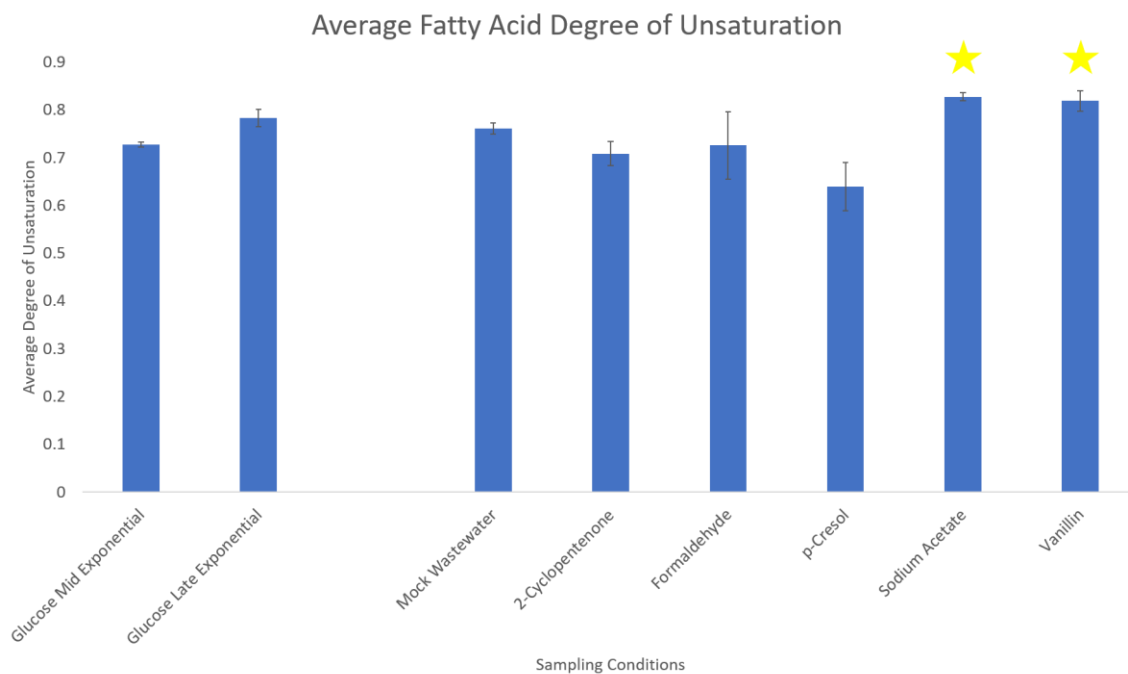


**Figure 47. Average degree of unsaturation of phospholipids across all sampling conditions of *P. putida* EM42. Stars indicate species deemed significantly different from the mid exponential glucose control by the Student's t-test.**



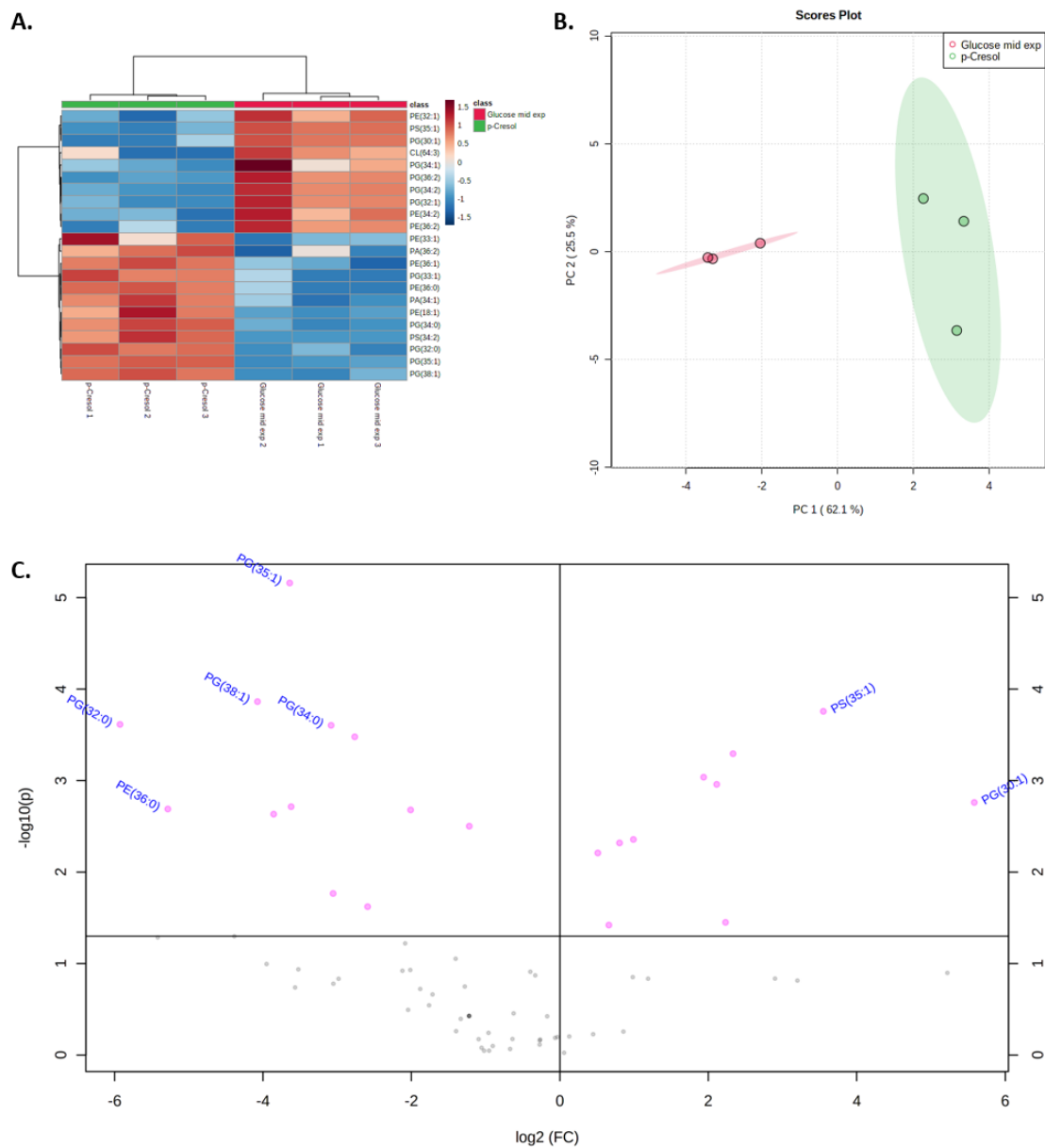


**Figure 48. A) Heatmap, B) PCA plot (with 95% confidence regions), and C) volcano plot (left indicating preference to the control and right indicating preference to the sampling condition) comparing the lipid profiles of p-cresol to the mid exponential glucose control in *P. putida* EM42.**

What might be more curious is relative increases in the *p*-cresol samples of several PG and PE species containing fully saturated fatty acid chains, as well as a relative increase in phospholipids containing longer fatty acids (Figure 48A). This was in line with previous studies that have investigated the influence of exposure to *p*-cresol and other phenolic species on the fluidity of the bacterial membrane. It was found that the ratio of saturated to unsaturated fatty acids being produced and incorporated into the cell membrane increased as the concentration of *p*-cresol that the bacteria was exposure was also increased [378]; other phenols were found to induce similar activity as well [379]. An overall lengthening of phospholipid fatty acids as well as a decrease in unsaturation would indicate an overall increase in the rigidity of the cell membrane. Closer examination of the fully saturated phospholipids compared between the glucose control and *p*-cresol further confirmed this (Figure 49), with most of the selected phospholipids showing significantly increased presence in the *p*-cresol samples.

***The mystery of odd-numbered fatty acids appearing within P. putida phospholipids within sodium acetate-grown cultures***

Next, sodium acetate was examined, noted earlier as having phospholipids with significantly longer fatty acids and higher degrees of unsaturation (Figure 50). Compared to *p*-cresol, sodium acetate contained a wide variety of phospholipids that significantly differed from the glucose control samples (Figure 50A), and variance supported the (Figure 50B & C). Upon examination of the lipidome of the sodium acetate samples, a feature that stood out was the notable increase of phospholipid species containing odd-numbered fatty acids.

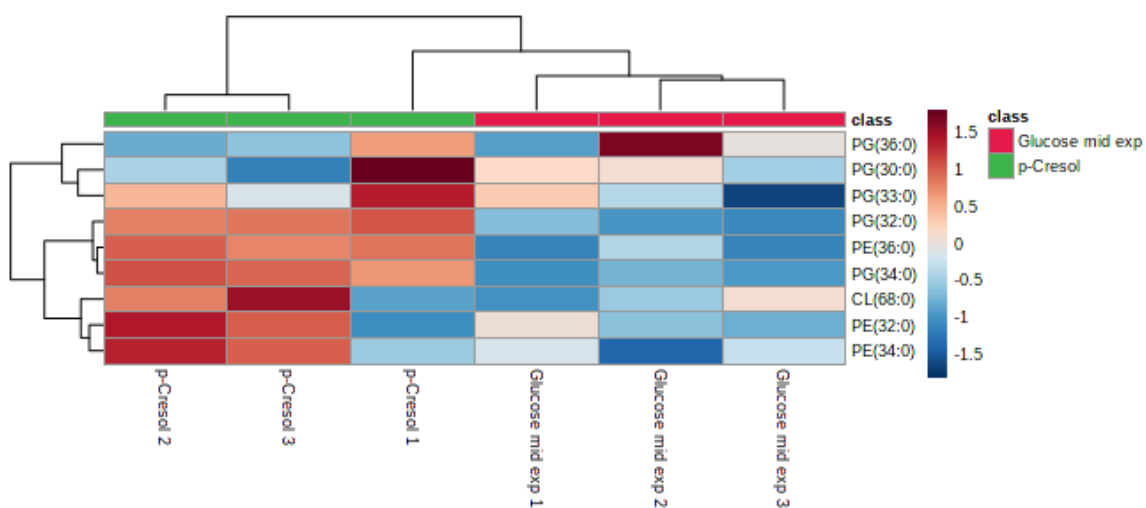


**Figure 49. Heatmap of the fully saturated phospholipids compared between the glucose control and *p*-cresol samples in *P. putida* EM42**

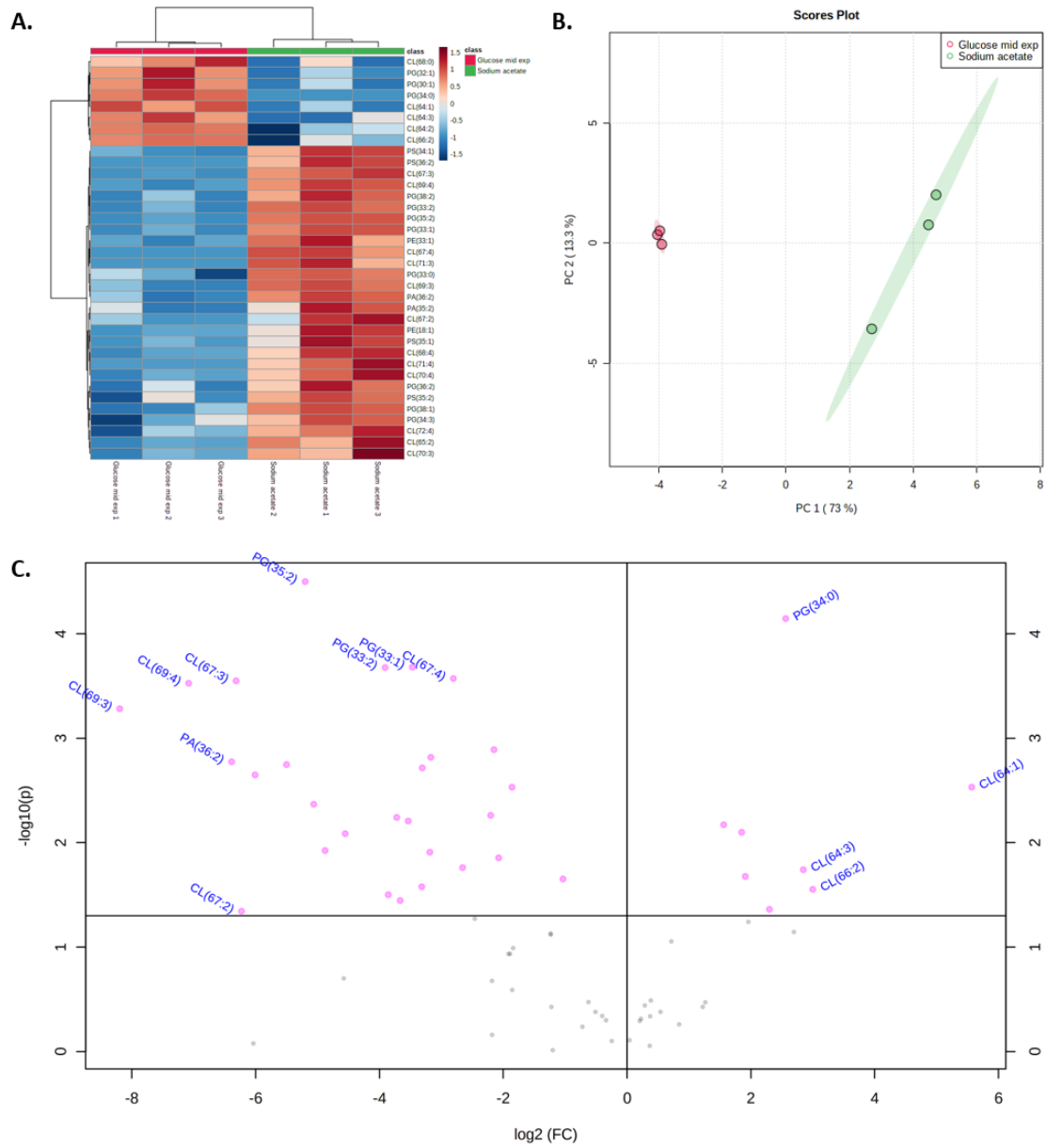
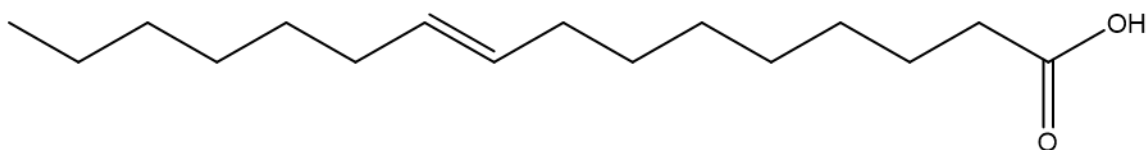


**Figure 50. A) Heatmap, B) PCA plot (with 95% confidence regions), and C) volcano plot (left indicating preference to the sampling condition and right indicating preference to the control) comparing the lipid profiles of sodium acetate to the mid exponential glucose control in *P. putida* EM42.**

In general, bacteria are unlikely to produce odd-numbered fatty acids as a part of normal metabolism. Even concerted efforts to force bacteria to produce odd-numbered fatty acids result in very moderate improvements in overall proportion of even- to odd-numbered fatty acids [380]. Typical fatty acid metabolism in most organisms is driven by the sequential addition of two carbons onto fatty acid precursors [381], which in bacteria almost always contain even numbers of carbon, such as is the case with *P. putida* [172], and as shown earlier (Figure 44) fatty acid precursors are often constructed as even-numbered chains. There have been reports that incorporation of specific amino acids, such as valine, leucine, and isoleucine, can result in the genesis of odd-numbered fatty acid chains [382], but that is not widely reported as a prevalent phenomenon in bacteria.

An alternative explanation might help to deconvolute this - bacteria are well known for incorporating modifications into phospholipid fatty acids [383]. These modifications can include the addition of short, branched chains [384] and conversion of double bonds to cyclopropane [385] or hydroxyl groups [172, 386]. While hydroxyl groups would be relatively easy to spot as a distinct feature using mass spectrometry, the simple addition or movement of carbons resulting from branching or double bond conversion to cyclopropane could be much more subtle. The modification of a fatty acid to contain a cyclopropane (Figure 51) or a branched chain (Figure 52) can easily masquerade as a more basic fatty acid.



Monoisotopic mass: 254.2246 Da

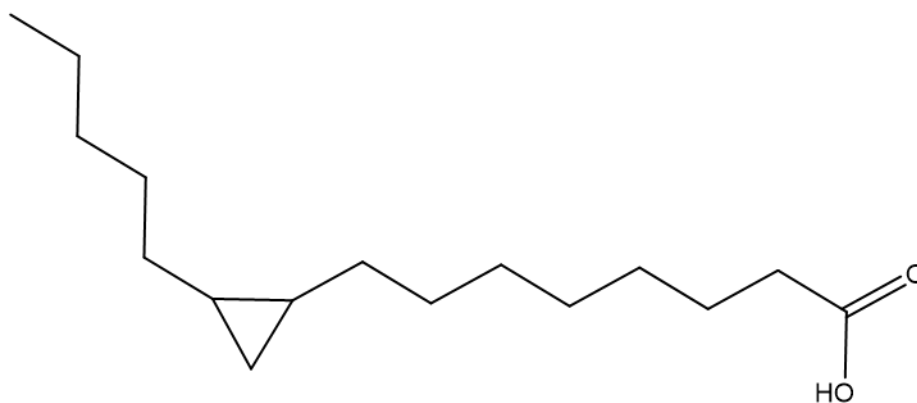
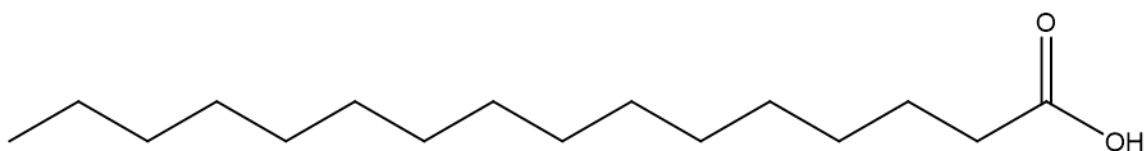


**Figure 51. Comparison of the mass-equal palmitoleic acid (top) and the cyclopropane variant 8-(2-pentylcyclopropyl)octanoic acid (bottom).**



Monoisotopic mass: 256.2402 Da

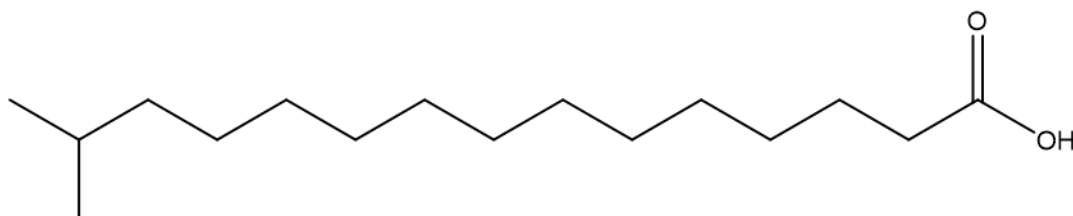


**Figure 52. Comparison of the mass-equal palmitic acid (top) and the branched fatty acid 14-methylpentadecanoic acid (bottom).**

This creates unique scenarios in mass spectrometry where fatty acid modifications are often overlooked due to a lack of required measurement depth needed to definitively characterize phospholipids with cyclopropane modifications to fatty acid chains. Often, specialized detection methods are necessary to characterize these variants, such as GC/MS [387, 388], NMR [389], or ultraviolet photodissociation mass spectrometry [390]. Indeed, GC/MS analysis on *P. putida* EM42 revealed the presence of branched chain fatty acids, though it is worth mentioning that the method used was not optimized to detect cyclopropane fatty acids and therefore were not represented in the results (Table 19). However, they have been shown to exist within *P. putida*, with their synthesis having been linked to environmental stress conditions [391-393].

Cardiolipin species also appear to be – both the glucose control and sodium acetate samples have cardiolipin species that were significantly more abundant in each sample. Further examination of the cardiolipin species revealed similar trends to those observed within the fatty acid profiles (Figure 53) – the cardiolipin species within the sodium acetate samples had notably longer fatty acids with high degrees of unsaturation. Previous studies have shown that CL content within the membrane can be affected by osmotic shock, often with reciprocal effects on the relative proportion of PE [394]. While there were no conditions applied that specifically simulated the effects of osmotic shock on *P. putida*, the presence of sodium acetate as a salt theoretically would have some level of effect on the ionic product of water, and as such, it stands to reason that the ratio of PE to CL might shrink compared to the glucose control samples, which not only was confirmed but also visible across several other samples (Figure 54).

**Table 19. GC-MS data of the fatty acid composition of *Pseudomonas putida* EM42**

<b>Fatty Acid Detected</b>	<b>Percentage</b>		
	<b>Run 1</b>	<b>Run 2</b>	<b>Run 3</b>
Capric acid (10:0)	1.28%	0.42%	0.88%
Lauric acid (12:0)	35.41%	13.31%	20.83%
Myristic acid (14:0)	0.55%	0.34%	0.42%
Palmitic acid (16:0)	14.68%	24.47%	20.46%
Palmitelaidic acid (16:1; <i>trans</i> -7)	11.66%	11.58%	10.53%
Palmitelaidic acid (16:1; <i>cis</i> -9)	0.81%	0.33%	0.49%
Palmitoleic acid (16:1; <i>cis</i> -7)	9.71%	6.96%	7.04%
Margaric acid, iso (i17:0)	16.50%	21.09%	22.55%
Stearic acid (18:0)	0.00%	0.95%	0.77%
Vaccenic acid (18:1, <i>trans</i> -7)	2.41%	6.90%	4.91%
Vaccenic acid (18:1, <i>cis</i> -7)	6.99%	13.64%	11.13%



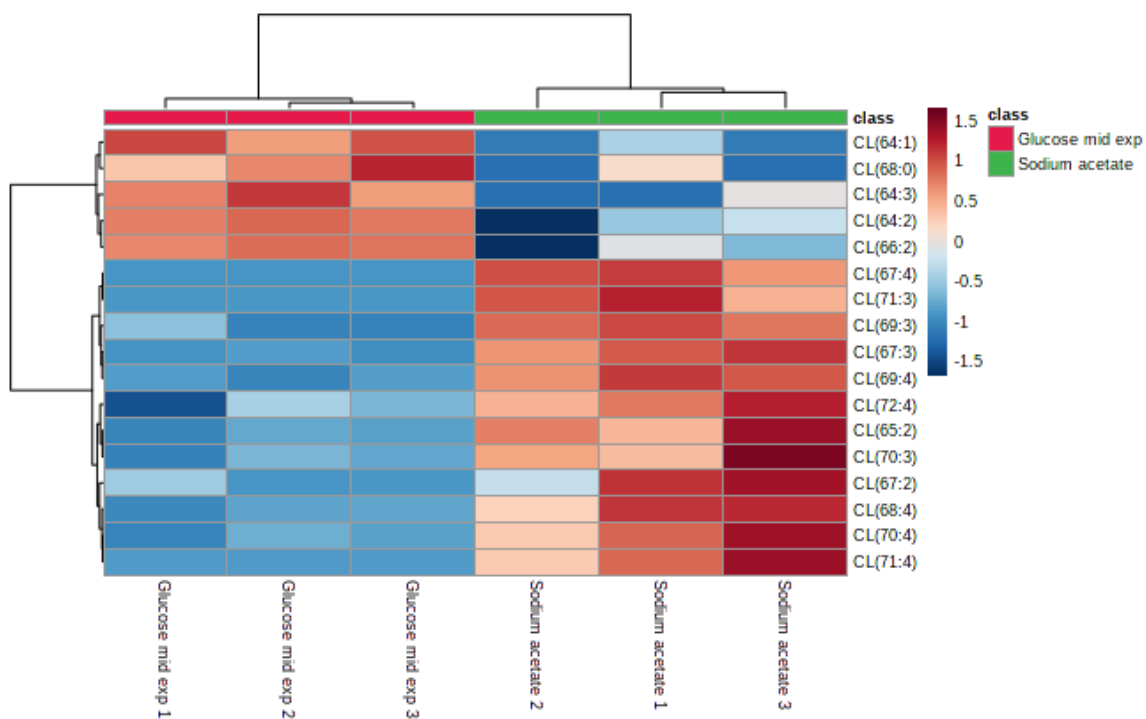


**Figure 53.** Heatmap of the cardiolipin species compared between the glucose control and *p*-cresol samples in *P. putida* EM42.

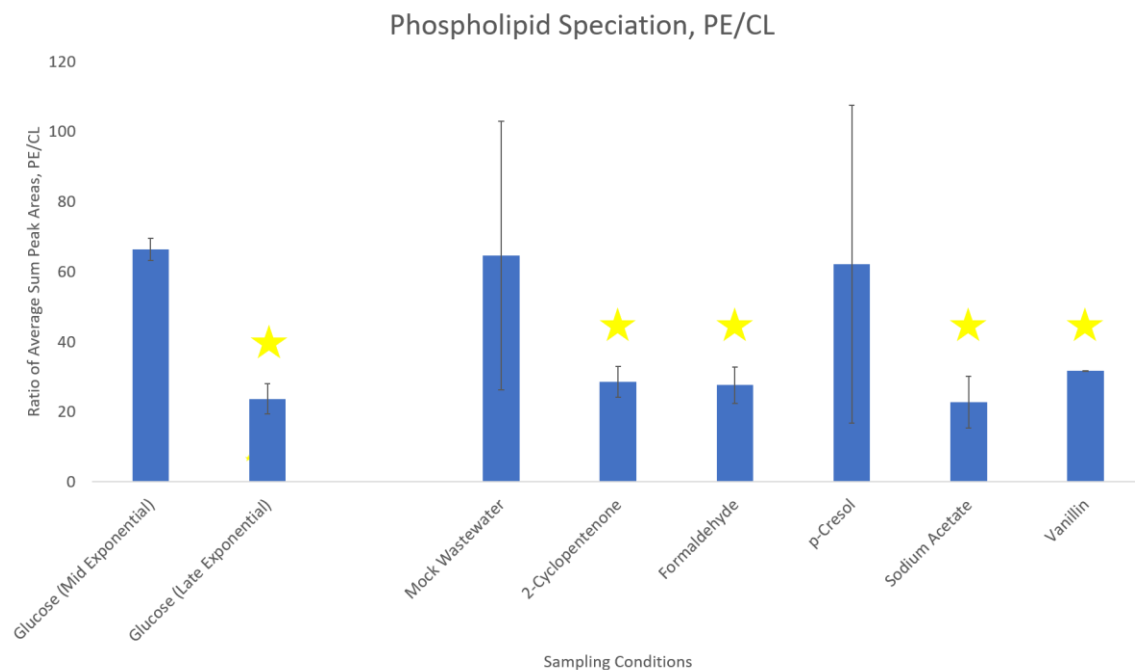


**Figure 54. Ratio of PE to CL across all sampling conditions of *P. putida* EM42. Stars indicate species deemed significantly different from the mid exponential glucose control by the Student's t-test.**

### ***Vanillin reveals increased presence of lysophospholipids***

The other growth condition found to contain notably increased levels of phospholipids with longer, more unsaturated fatty acids was the vanillin-grown cultures. However, upon investigation of the significantly differing phospholipids compared to glucose, the changes induced by the presence of vanillin are much more subtle (Figure 55). Surprisingly, the phospholipid profile of vanillin-grown *P. putida* cells resembled those of the control cells grown to late exponential phase, though one significant difference stands out. The vanillin-grown *P. putida* cells appeared to contain noticeably elevated levels of lysophospholipids. The role of lysophospholipids within bacteria is somewhat unclear, with the only known major function in bacteria being an intermediate in phosphatidic acid synthesis, which itself is a precursor to most other phospholipids; they also have a role in the biosynthesis of lipid A as well as reduction of stress induced by membrane curvature [395]. However, there have been studies that have shown that accumulation of lysophospholipids within the membrane have a negative impact on membrane rigidity, increasing permeability, as well as being a major player in bacterial membrane remodeling [396]. Likewise, the effect of vanillin on cell membranes is also poorly understood, with only very general reports that the presence of vanillin leads to elevated melting points of the membrane [397]. Vanillin is a known toxin to bacteria that have been engineered to produce it and numerous proteins have been identified that exhibit changes in the presence of vanillin [398].

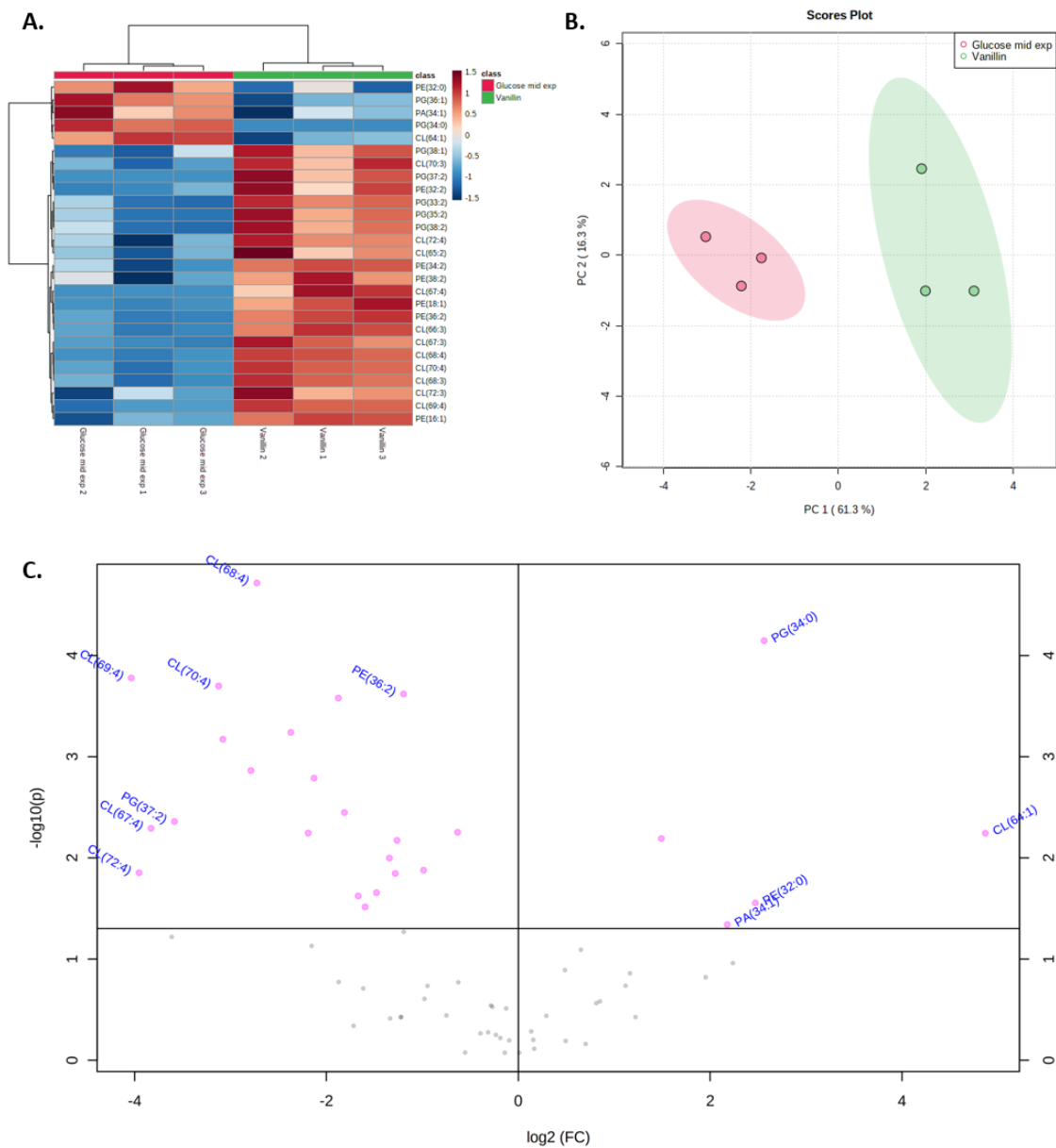


**Figure 55. A) Heatmap, B) PCA plot (with 95% confidence regions), and C) volcano plot (left indicating preference to the sampling condition and right indicating preference to the control) comparing the lipid profiles of vanillin to the mid exponential glucose control in *P. putida* EM42.**

Lysophospholipids have also been shown to have significant influence on membrane fluidity. Because of the shape of lysophospholipids and the presence of only a singular fatty acid tail, lysophospholipids often present themselves within the membrane as having a conical shape, as opposed to many traditional two-tail phospholipids which are often more cylindrical in shape [399]. This is not universal – both PA and PE have headgroups that are small enough to still invoke a conical shape (with the thin part of the cone being the headgroup), even with two fatty acids, while other phospholipids such as PG, PS, PC, and PI all have rather large headgroups that result in more cylindrical shapes. A shift towards lysophospholipids results in a net shift towards inverted cones, where the thin part of the cone actually lies with the fatty acid tail [400]. This modulation of cylindrical and conical phospholipids in the membrane has an obvious effect on membrane curvature [401, 402], but what might not be so obvious is the effect on lipid packing. In *P. putida*, a rod-shaped phospholipid with a PE-dominated membrane, significant introduction of lyso-PE species, which would likely be more cylindrical in shape, into the membrane would likely force changes in both membrane curvature and alter the fluidity of the membrane.

Outside of the lysophospholipids observed, most of the trends observed within the vanillin phospholipids were echoed from the profiles of the sodium acetate samples – there was a noticeable uptick in longer, more unsaturated fatty acids in line with prior observations of fatty acid character, with cardiolipin species representing a significant portion of those phospholipids. Odd-numbered fatty acids appearing within phospholipids also continued to be observed.

### ***A brief examination of the lipid profiles of the mock wastewater solution***

Finally, a broader look at the general influence of the mock wastewater on *P. putida* was performed (Figure 56), though the response of the mock wastewater solution was noticeably poor compared to the other samples. This could be indicative of impaired cell growth, but it is more likely that elements of the complex mock wastewater were extracted along with the lipids, causing issues with detection via LC-MS. Therefore, the lipid profiles may not be that helpful, and the general observations of phospholipid character become more important, as well as consideration of the influences of individual growth conditions that are representative of larger chemical categories.

### ***A brief look across all phospholipid profiles***

Examination of all conditions revealed further emphasis of previously observed trends, as well as some new observations (Figure 57). Formaldehyde, which was not discussed due to no appreciable differences compared to the control sample, was notable because of how variable the spread across replicates was. While this might be due to sampling or instrumentation error, the known toxicity of formaldehyde towards bacteria [403] would mean that lack of any appreciable differences would be highly unexpected. The wide variance across replicates could be indicative of more generalized issues within the cell (Figure 57B) – the . Additionally, relatively even ratios of PE and PG could be indicative that significant membrane remodeling is occurring as a result of the presence of the small and simple formaldehyde, which can easily penetrate through relatively rigid membranes thanks to its chemical structure, and the variance between replicates could be a visual representation of a changing membrane construction.

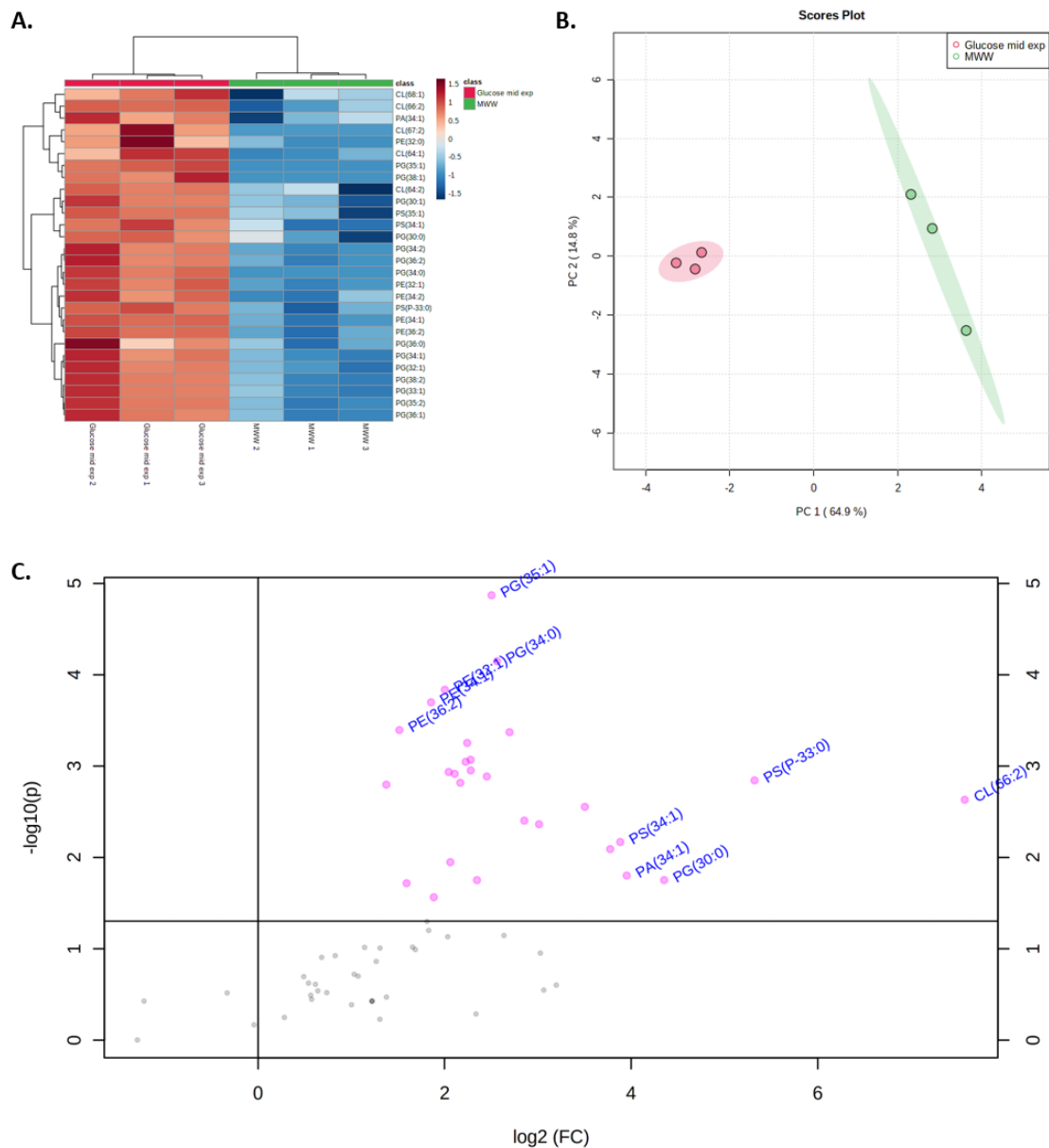


**Figure 56. A) Heatmap, B) PCA plot (with 95% confidence regions), and C) volcano plot (left indicating preference to the sampling condition and right indicating preference to the control) comparing the lipid profiles of the mock wastewater solution to the mid exponential glucose control in *P. putida* EM42**

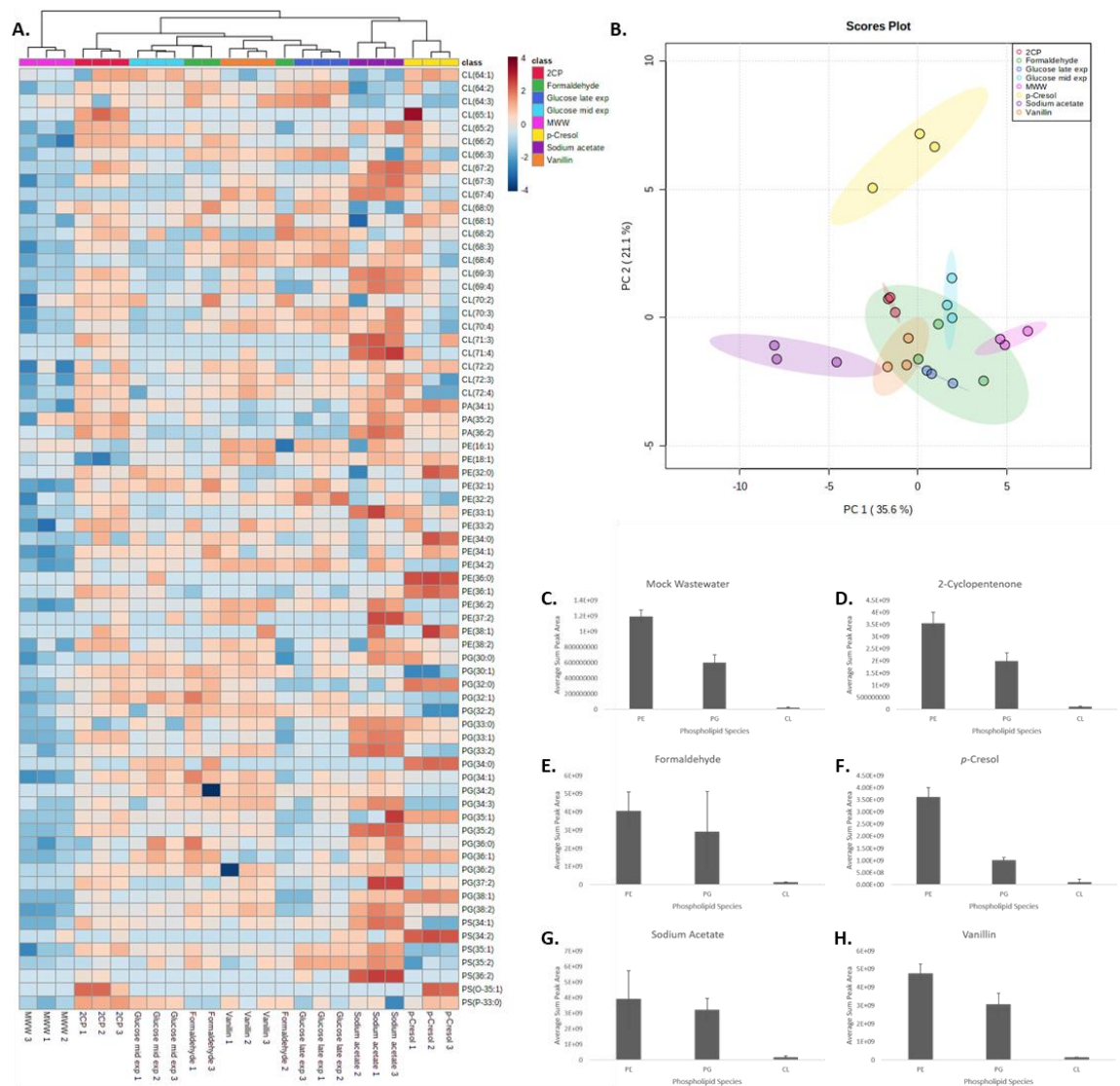


**Figure 57. Full comparison of the phospholipid profiles across all conditions. A) Heatmap. B) PCA plot. General phospholipid profiles for C) the mock wastewater solution, D) 2- cyclopentenone, E) formaldehyde, F) p-cresol, G) sodium acetate, and H) vanillin in *P. putida* EM42.**



## Phospholipid derivatives and other lipid species

### *Aminoacylated phospholipids*

Unlike in *B. subtilis*, *P. putida* is much more limited in the reported presence and abundance of aminoacylated phospholipids within the membrane. While *B. subtilis* is known to have phospholipids with lysine and alanine head group modifications, *P. putida* has only been reported to contain alanylated phosphatidylglycerol (Ala-PG) and at much lower proportions, with Ala-PG only representing 0.5-5% of the total lipid pool [92].

Indeed, upon extraction of expected Ala-PG species, using trends on expected fatty acid lengths within the samples described here, a very limited pool of Ala-PG species was observed (Figure 58). Previous studies on the parent species KT2440 [172] and earlier data suggested that normal fatty acid chains within *P. putida* PG species would be of length 16 and 18, with 17 showing a mild presence potentially under stress, and a range of zero to two double bonds per phospholipid. Upon analysis, this was limited to only alanylated derivatives of PG(32:2) and PG(32:1) - no other species were detected above the noise threshold set while analyzing within MZmine. This is important to note because it bears mentioning that Ala-PG species were reported to be a much smaller overall component of the *P. putida* lipidome, compared to rates that were 3-34% higher for just one of the two aminoacylated species observed in *B. subtilis* samples. It is entirely possible that data processing could have artificially modified and reduced the effective analysis-accessible pool of Ala-PG. Of the samples that did show some level of Ala-PG, the 2-cyclopentenone samples were the only ones to have significantly elevated levels of Ala-PG.

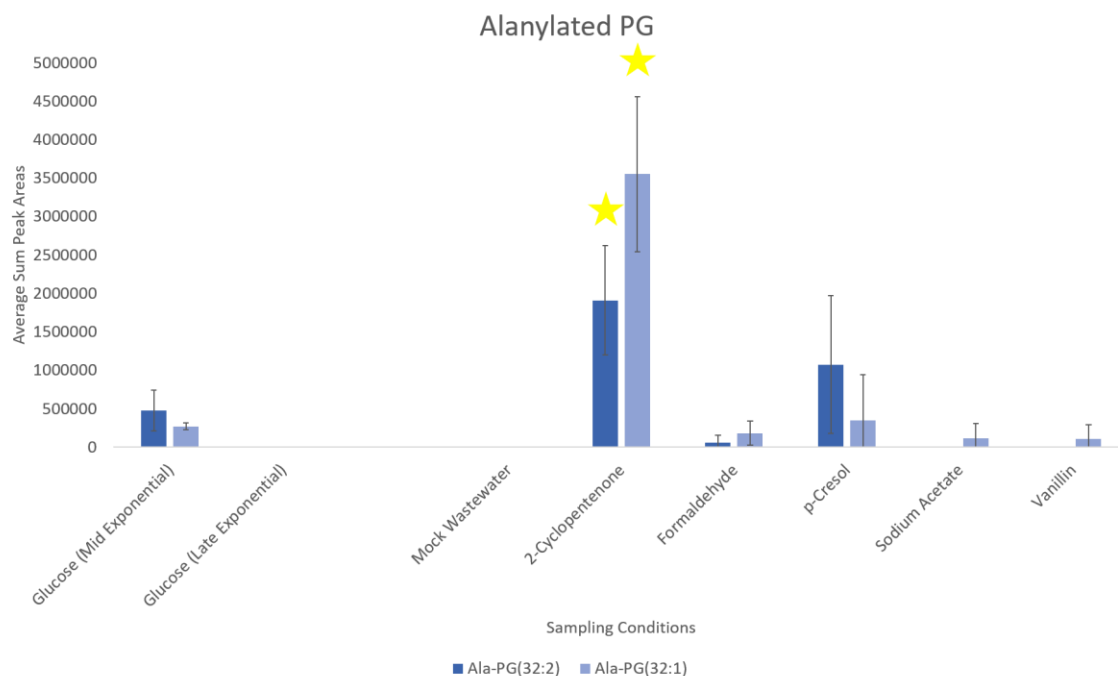


**Figure 58. Ala-PG species observed within *P. putida* EM42 strains inoculated with different wastewater simulated conditions. Stars indicate species deemed significantly different from the mid exponential glucose control by the Student's t-test.**

There are limited studies on Ala-PG as it pertains to what can induce changes of it within the membrane. Arendt et al examined the relative proportion of Ala-PG across several different bacteria and conditions, including *P. putida*. That experiment found that acidic conditions were often linked to elevated levels of Ala-PG within the membrane [22]. Curiously, the exact opposite trend was observed here – the two sampling conditions either directly fed acetic acid (sodium acetate) or the mock wastewater solution containing both acetic and formic acid were found to contain nearly no Ala-PG.

### **Discussion/Conclusions**

Growth of *P. putida* within several compounds commonly found within various wastewater streams and subsequent analysis of the lipid profiles of the cultures allowed probing of the differences that arose within the microbial cell membrane. While the comprehensive mock wastewater solution was not very informative in isolation, several of the individual solvent growth conditions indicated changes in the cell membrane indicative of shifts in fatty acid composition of the phospholipids or the genesis of cyclopropane fatty acids as an indicator of increased chemical tolerance.

One critical area that could act as a complementary study to the above research is a focused analysis of the fatty acid content of these samples. Given preliminary evidence that fatty acid saturation and cyclopropane fatty acids could have a significant effect on the action of *P. putida* to protect itself from chemical toxicity, GC-MS FAME analysis could yield even more information about the relative proportions of specific fatty acid properties, such as chain length, saturation, and presence of chain modifications.

Additionally, future strains of *P. putida* that push the boundaries of what can be modified within the cell membrane are still of interest (Figure 59). The ability to control expression of genes controlling specific phospholipid production or modifications to the fatty acid content of phospholipids could enable the creation of elegant custom strains of *P. putida* designed to withstand specific conditions through the customization of cell membrane production, with preliminary work having already been undertaken to that effect [404]. Indeed, strains of various bacteria have been produced that can have elevated production of phospholipids and/or variations of fatty acids (through overexpression of specific genes), such as PS/PE species (*pssA*) [405, 406], cardiolipin (*clsA*) [407, 408], cis double bonds (*FabA* and *FabB*) [409, 410], trans double bonds (*Cti*) [411, 412], and cyclopropane fatty acids (*cfaB*) [393, 413].

The results shown here indicate that those could be a viable route for future strain development. Observation of specific shifts in PE/PG ratios in both the mock wastewater and *p*-cresol samples (as well as PE/CL ratio shifts across all other sampling conditions) could point towards manipulation of PE biosynthesis as a potential route for increased durability in *P. putida*. Additionally, the observation of moderately strange trends in fatty acid length in several sampling conditions opens up further studies probing the exact composition of phospholipid fatty acid content could mean that better understanding of the links between *P. putida* fatty acid biosynthesis under certain conditions could lead to membrane optimization through manipulation of fatty acid biosynthesis.



Presented here was a comprehensive lipidomics experiment examining the effects of various known wastewater contaminants on the composition of the phospholipid membrane of *P. putida*. Analysis revealed that individual contaminants resulted in increased amounts of lyso-phospholipids and phospholipids with odd-chain fatty acids, theorized to be cyclopropane fatty acids, while the mock wastewater sample resulted in overall decreased phospholipid yields. Key shifts in phospholipid speciation, fatty acid chain length, and degree of unsaturation tied to specific pollutants could be incredibly informative moving forward to help with future *P. putida* strains that can be applied to various wastewater bioremediation applications.

## **CHAPTER 6: OVERVIEW AND OUTLOOK ON UTILIZATION OF LIPIDOMICS IN BIOLOGICAL RESEARCH**

## **Dissertation in summary**

Current approaches to comprehensive cellular analyses have proven to be capable of excellent coverage of a wide range of cell-bound molecules that provide information on cellular function and survival, but there is still plenty of work to be done in order to fully leverage the data to the fullest. While access to efficient cell preparation techniques and extraction methods and state of the art instrumentation is key to quality omics research, recognition of the limitations within data analysis and informatics is equally important, and proper utilization of every pool of potential extractable analytes is still an ongoing challenge for researchers wishing to understand or optimize biological systems. Lipidomics is not immune to those struggles, requiring high level instrumentation to generate rich data sets and no small amount of guesswork and manual interpretation to begin to pull apart the intricacies of the data contained within.

Still, if a more comprehensive approach to analysis of a system's lipidome can be constructed, lipidomics can be an incredibly powerful analysis tool for beginning to understand the cell's primary response to the environment. Understanding those considerations, this dissertation was constructed with two primary questions in mind. The first related to basic analytical chemistry – is it possible to construct a HILIC-MS/MS lipidomics platform that can detect bacterial phospholipids and other related molecules with high levels of sensitivity and reproducibility? The second is more biological in nature – what can be inferred about cell health and membrane fluidity from observation of changes, trends, and modifications in the cell membrane and lipidome of bacterial species exposed to fluctuating growth environments?



Chapter 1 laid out a brief overview on the state of the field of lipidomics and where the strengths and weaknesses currently lie, as well as introducing the outline of the dissertation. Chapters 2 and 3 focused on method development and rigorous testing of extraction methodologies, proper use of a HILIC-MS/MS platform, and exploration of informatics packages to fully understand and interpret data sets. The platform was optimized via consideration of feasible techniques for extraction, analysis, and informatics, with validation being performed through the use of standards and test samples. Selection of extractions was carefully performed with both lipid extraction efficiency, ease of use, and potential future applications in multiomics experiments. The choice of stationary phase was strongly driven by compatibility with lipid extracts and the balancing act of elution and mobile phase construction, with HILIC proving to be the easier than RP in terms of bulk elution of lipids. Similarly, negative mode ionization was preferred over positive mode because of the expected phospholipids present in bacterial sample sets. With use of nano-electrospray tandem mass spectrometry on the rise, that particular platform was utilized for increased sensitivity and the ability to validate phospholipids with high quality fragmentation data. Finally, a number of lipidomics informatics packages and approaches were considered, and a custom approach utilizing software with processing capabilities as well as efficient utilization of the MS2 fragmentation data was crafted. While MTBE lipid extractions and use of HILIC, nanoscale chromatography, and nano-electrospray ionization are not necessarily novel techniques for lipidomics, the simultaneous application of all four techniques to bacterial

lipidomes and mock reactor/wastewater conditions is an exciting prospect for future studies.

Chapters 4 and 5 took advantage of the methods formulated in Chapters 2 and 3 and applied them to real life datasets. Chapter 4 examined the Gram-positive microbe *Bacillus subtilis*, specifically examining lipid profile shifts as a function of limited and controlled fatty acid access as well as the effects of growth in solvents simulating the conditions of a biofuel reactor, while Chapter 5 was an examination of the effects of wastewater components, as well as a composite solution of chemicals found within wastewater, on the lipidome of the Gram-negative microbe *Pseudomonas putida*. Distinct trends in how phospholipid speciation and fatty acid composition changed in direct relation to not only distinguished specific solvents were connected to specific solvents, as well as inferences about how more general chemical classes might influence those same bacteria. The influence of lipid modifications was also made apparent, with aminoacylated phospholipids being a significant contributor to both *B. subtilis* and *P. putida* as well as observation of lipoteichoic acids in the former and potential fatty acid modifications in the latter. As a whole, the shifts and trends in phospholipid speciation as a function of changing growth environment were incredibly valuable, potentially enabling development of better bacterial strains that can be beneficial to real world industrial or experimental applications.

### **What challenges remain in lipidomics?**

Many of the unsolved issues within lipidomics are technical points that are shared across all variations of omics analyses. Ensuring a robust analysis from start to finish

through the use of specific extractions, separations, and mass detection is key, and optimization of each of those parameters helps to shape future experiments. Back-end validity is also necessary, with accurate annotation of features within a class of molecules and the ability to predict or detect potential modifications or unknown variants of critical importance. That being said, the biggest challenges currently facing lipidomics are limitations within informatics as well as proper utilization and interpretation of data.

As mentioned in Chapters 2-3, informatics within omics datasets can be a tricky problem to solve. Between filtering through the many different program options available and trying to assess the depth with which to analyze sample sets, it can be difficult, if not impossible, to locate a singular program that fulfills every desire on the checklist of a given experiment. For most omics experiments utilizing a LC-MS/MS approach, a basic wish list for an informatics package likely includes an entry level ease of use, proper utilization of MS1 scans, the ability to process MS2 fragmentation data, some level of data processing and consolidation, and depending on the experiment, utilization of isomer and retention time data.

It becomes quickly apparent that this is not something that is not easy to find. Even here, it was necessary to research numerous programs and use two, which did not even completely fulfill the needs of the experiment and required further manual interpretation of the spectra in order to probe further. Many programs available are extremely efficient at specific tasks – some are wonderful for basic data manipulation and file consolidation and alignment; others are specialized to handle the processing of very specific datasets or classes of molecules. There is also the issue of programs being locked

behind either a vendor paywall or only being compatible with files that come from a certain type of instrument – many of those might be applicable to the needs of a specific experiment but it is impossible to assess them.

So where does that leave lipidomics informatics? Even though the field is slowly growing, it is still very much a field built on the back of metabolomics, and as such, comprehensive libraries of lipids are still hard to come by, and those that do exist focus mainly on variations in head group or fatty acid chain length/saturation. Modifications to head groups or the fatty acid chains themselves are well reported in literature but not well represented within databases as of the time of writing, and those variables might be just as, if not more informative, to many biological questions as simple variation in chains or headgroups. To keep lipidomics advancing in a positive direction, there needs to be a concerted effort to consolidate all of these into one place, programs that can not only do basic data manipulation but also have truly comprehensive libraries as well as algorithms that can use known lipid modifications and predict their presence or absence based on high quality mass spectra.

The other important advancement that needs to be done in lipidomics is proper utilization of data. That does not mean that current and past lipidomics studies are incorrect or invalid, but there could be a case to be made, with the described informatics challenges in mind, that lipidomics studies have not fully utilized their data sets. While current lipidomics pipelines can generate incredibly relevant and useful observations (as described in detail in this dissertation), the depth of those measurements is limited by time investment and the power of whatever informatics platform is selected. That often

results in a decision between topical comparisons across general phospholipid and fatty acid categories and delving into specific lipid variants and/or modifications that require specialized approaches or manual interpretation; taking on both can quickly escalate into a massive time investment. Balancing expected results and potential unknown sample pools of interest can always convolute this, and the best way to help solve these issues is advancement of informatics technology to the point where much of this process can be automated where currently methods require multiple different programs and approaches to even approach a complete analysis.

As for sample preparation, Chapters 4 and 5 highlighted one of the big challenges of current lipidomics studies as it pertains to examination of lipidomes from organisms that could be industrially relevant given the right circumstances and properties in that not all organic solvents induce equal changes within organisms. It is important to keep in mind that even within a specific chemical category, rather drastic differences can be observed in the general lipidome profile. Chapter 4 showed that bacterial growth within butanol and isobutanol, two relatively similar molecules whose only difference is the location of a singular  $\text{CH}_3$  group within the molecule, resulted in rather drastically different lipid profiles, while isobutanol and THF, which share very little in terms of molecular shape and chemical properties, resulted in relatively similar lipid profiles. Chapter 5 further explored this from a slightly different angle and showed solvents spanning a wide range of molecular classes induced changes in a number of areas, including fatty acid chain length, head group speciation, and the possible presence of modified lipids. All of these factors point towards deep dives into specific solvent

conditions as potentially being very useful moving forward, especially when examining field samples for what might be the main driver behind changes in the organisms present.

### **Where does lipidomics go from here?**

The power of lipidomics lies in answering very simple questions that arise from broader observations of systems biology – in simpler organisms, lipids help to identify how cells react to changing environmental states, while the lipids of plants and animals are not as limited to just the cell and can be more broadly applicable to the health of the organism as a whole. While there may not be as many discrete ways to infer changes as fields such as genomics, proteomics, and metabolomics, where modifications are more readily identifiable at the core of the organism or through biomarker observation, the ability to monitor the composition of lipids within the membrane of the cell is uniquely applicable. Not only is it possible to actively monitor changes in phospholipid composition and infer how those changes relate back to the environment of the cell, but the more exciting prospect is being able to leverage knowledge of beneficial and detrimental changes in the composition of the phospholipid membrane and use that to engineer organisms to produce more optimal cell membranes. The uses of such organisms are widespread, with the beginnings of such approaches shown throughout this dissertation.

Lipidomics has an incredible well of untapped potential as a diagnostic technique as well. Many biochemical studies utilize gene mutations, protein modifications, and the genesis of unique biomarkers to detect when something within a system has changed or gone wrong, but there is a case to be made for utilization of lipids, a class of molecules

that is easily extracted within a solvent layer most discard for other omics measurements and one that is potentially more diagnostic than any of those other detection methods because of the proximity of lipids to the outside world. Currently, utilization of every part of a biological system is still not fully realized, and it is only a matter of time before scientists fully understand the ramifications of properly using all parts of the cell. Related to that, in a broader sense, the rising interest of single pot multiomics analysis platforms plays very well into that. The full utilization of DNA, proteins, metabolites, and lipids, accessible with one singular extraction, sounds like the correct and optimal way to approach biochemistry from an analytical standpoint, but research has not quite caught up to that.

Finally, a more general note on informatics is appropriate. As mentioned in the previous section, lipidomics appears to present much more serious challenges than other disciplines in terms of comprehensive reporting of basic lipids. Every omics discipline has long struggled with detection, reporting, and accessibility of modifications and novel species within their given field because of how transient and inconsistent they can be within samples, but lipidomics still has the feel of a field that has only begun to scratch the surface of potential, only really having widespread access to the most common lipids. Lipidomics needs to advance informatics specifically to fully take advantage of MS2 data for discrimination of overlapping masses between lipid classes as well as use relatively predictable modifications (amino acids, sugars, proteins, etc.) for additional search algorithms. MS3 measurements may also become the norm for lipidomics as well to be able to examine fatty acid chain composition for double bonds, double bond location, and

areas of oxidation or acylation, though this does come with the stipulation of having access to instrumentation that can process samples at that level of fragmentation. With these considerations in mind, there is strong hope for lipidomics to become more widely spread applicable to a variety of analyses that may currently only utilize a specific part of the cell, as well as taking advantage of using comprehensive measurements of all extractable parts of a sample to characterize biological systems in a more complete manner.



## REFERENCES

1. Karahalil, B., *Overview of Systems Biology and Omics Technologies*. Current Medicinal Chemistry, 2016. **23**(37): p. 4221-4230.
2. Breitling, R., *What is systems biology?* Frontiers in physiology., 2010. **1**.
3. Wang, Z., M. Gerstein, and M. Snyder, *RNA-Seq: a revolutionary tool for transcriptomics*. Nature Reviews Genetics, 2009. **10**(1): p. 57-63.
4. Lowe, R., et al., *Transcriptomics technologies*. PLOS Computational Biology, 2017. **13**(5): p. e1005457.
5. Baggerman, G., et al., *Peptidomics*. Journal of Chromatography B, 2004. **803**(1): p. 3-16.
6. Dallas, D.C., et al., *Current peptidomics: Applications, purification, identification, quantification, and functional analysis*. PROTEOMICS, 2015. **15**(5-6): p. 1026-1038.
7. Molinaro, R.J., et al., *Shotgun glycomics: a microarray strategy for functional glycomics*. Nature methods, 2011. **8**(1): p. 85-90.
8. Mechref, Y., et al., *Quantitative Glycomics Strategies*. Molecular & cellular proteomics, 2013. **12**(4): p. 874-884.
9. Nidenführ, S., W. Wiechert, and K. Nöh, *How to measure metabolic fluxes: a taxonomic guide for <sup>13</sup>C fluxomics*. Current opinion in biotechnology, 2015. **34**: p. 82-90.
10. Winter, G. and J.O. Krömer, *Fluxomics - connecting 'omics analysis and phenotypes*. Environmental Microbiology, 2013. **15**(7): p. 1901-1916.
11. Santos, A.L. and G. Preta, *Lipids in the cell: organisation regulates function*. Cellular and molecular life sciences : CMLS, 2018. **75**(11): p. 1909-1927.
12. Kenar, J.A., *The use of lipids as phase change materials for thermal energy storage*. Lipid Technology, 2014. **26**(7): p. 154-156.
13. Welte, M.A. and A.P. Gould, *Lipid droplet functions beyond energy storage*. Biochimica et Biophysica Acta (BBA) - Molecular and Cell Biology of Lipids, 2017. **1862**(10): p. 1260-1272.
14. Kretschmer, S., et al., *Synthetic cell division via membrane-transforming molecular assemblies*. BMC Biology, 2019. **17**(1).
15. Atilla-Gokcumen, G.E., et al., *Dividing Cells Regulate Their Lipid Composition and Localization*. Cell, 2014. **156**(3): p. 428-439.
16. Storck, E.M., C. Özbacı, and U.S. Eggert, *Lipid Cell Biology: A Focus on Lipids in Cell Division*. Annual review of biochemistry., 2018. **87**(1): p. 839-869.
17. Barák, I. and K. Muchová, *The Role of Lipid Domains in Bacterial Cell Processes*. International Journal of Molecular Sciences, 2013. **14**(2): p. 4050-4065.
18. Pichler, H. and A. Emmerstorfer-Augustin, *Modification of membrane lipid compositions in single-celled organisms – From basics to applications*. Methods, 2018. **147**: p. 50-65.
19. Haucke, V. and G. Di Paolo, *Lipids and lipid modifications in the regulation of membrane traffic*. Current Opinion in Cell Biology, 2007. **19**(4): p. 426-435.

20. Chandler, C.E. and R.K. Ernst, *Bacterial lipids: powerful modifiers of the innate immune response*. F1000Research, 2017. **6**: p. 1334.
21. Yusupov, M., et al., *Effect of head group and lipid tail oxidation in the cell membrane revealed through integrated simulations and experiments*. Scientific Reports, 2017. **7**(1).
22. Arendt, W., et al., *Resistance Phenotypes Mediated by Aminoacyl-Phosphatidylglycerol Synthases*. Journal of Bacteriology, 2012. **194**(6): p. 1401-1416.
23. Geiger, O., et al., *Amino acid-containing membrane lipids in bacteria*. Progress in lipid research, 2010. **49**(1): p. 46-60.
24. Wahle, K.W.J., *Fatty acid modification and membrane lipids*. Proceedings of the Nutrition Society, 1983. **42**(2): p. 273-287.
25. Züllig, T., M. Trötz Müller, and H.C. Köfeler, *Lipidomics from sample preparation to data analysis: a primer*. Analytical and Bioanalytical Chemistry, 2020. **412**(10): p. 2191-2209.
26. Hill, J., et al., *Environmental, economic, and energetic costs and benefits of biodiesel and ethanol biofuels*. Proceedings of the National Academy of Sciences, 2006. **103**(30): p. 11206-11210.
27. Li, Q., et al., *Treatment of high-salinity chemical wastewater by indigenous bacteria – bioaugmented contact oxidation*. Bioresource technology, 2013. **144**: p. 380-386.
28. Ruggiero, C.E., et al., *Actinide and metal toxicity to prospective bioremediation bacteria*. Environmental microbiology, 2005. **7**(1): p. 88-97.
29. Brooijmans, R.J.W., M.I. Pastink, and R.J. Siezen, *Hydrocarbon-degrading bacteria: the oil-spill clean-up crew*. Microbial Biotechnology, 2009. **2**(6): p. 587-594.
30. Zhong, C., *Industrial-Scale Production and Applications of Bacterial Cellulose*. Frontiers in bioengineering and biotechnology., 2020. **8**.
31. Pham, J.V., et al., *A Review of the Microbial Production of Bioactive Natural Products and Biologics*. Frontiers in microbiology, 2019. **10**.
32. Smith, D.R. and M.R. Chapman, *Economical Evolution: Microbes Reduce the Synthetic Cost of Extracellular Proteins*. mBio, 2010. **1**(3): p. e00131-10-e00131.
33. Adrio, J.-L. and A.L. Demain, *Recombinant organisms for production of industrial products*. Bioengineered Bugs, 2010. **1**(2): p. 116-131.
34. Crater, J.S. and J.C. Lievens, *Scale-up of industrial microbial processes*. FEMS Microbiology Letters, 2018. **365**(13).
35. Pieper, D.H. and W. Reineke, *Engineering bacteria for bioremediation*. Current opinion in biotechnology., 2000. **11**(3): p. 262-270.
36. Ojuederie, O. and O. Babalola, *Microbial and Plant-Assisted Bioremediation of Heavy Metal Polluted Environments: A Review*. International Journal of Environmental Research and Public Health, 2017. **14**(12): p. 1504.
37. Wang, J., W. Ma, and X. Wang, *Insights into the structure of Escherichia coli outer membrane as the target for engineering microbial cell factories*. Microbial Cell Factories, 2021. **20**(1).

38. Chwastek, G., et al., *Environmentally Induced Lipidome Adaptation in the Bacterial Model Organism M. extorquens*. SSRN Electronic Journal, 2019.
39. Baeshen, N.A., et al., *Cell factories for insulin production*. Microbial Cell Factories, 2014. **13**(1).
40. Akinosho, H., et al., *Toxicological challenges to microbial bioethanol production and strategies for improved tolerance*. Ecotoxicology, 2015. **24**(10): p. 2156-2174.
41. Elshahed, M.S., *Microbiological aspects of biofuel production: Current status and future directions*. Journal of advanced research., 2010. **1**(2): p. 103-111.
42. Jeong, S.W. and Y.J. Choi, *Extremophilic Microorganisms for the Treatment of Toxic Pollutants in the Environment*. Molecules, 2020. **25**(21): p. 4916.
43. Igiri, B.E., et al., *Toxicity and Bioremediation of Heavy Metals Contaminated Ecosystem from Tannery Wastewater: A Review*. Journal of Toxicology, 2018. **2018**: p. 1-16.
44. Murínová, S. and K. Dercová, *Response Mechanisms of Bacterial Degraders to Environmental Contaminants on the Level of Cell Walls and Cytoplasmic Membrane*. International Journal of Microbiology, 2014. **2014**: p. 1-16.
45. Chikere, C.B., G.C. Okpokwasili, and B.O. Chikere, *Monitoring of microbial hydrocarbon remediation in the soil*. 3 Biotech, 2011. **1**(3): p. 117-138.
46. Parsons, J.B. and C.O. Rock, *Bacterial lipids: Metabolism and membrane homeostasis*. Progress in Lipid Research, 2013. **52**(3): p. 249-276.
47. Li, J., T. Vosegaard, and Z. Guo, *Applications of nuclear magnetic resonance in lipid analyses: An emerging powerful tool for lipidomics studies*. Progress in Lipid Research, 2017. **68**: p. 37-56.
48. Schiller, J., *MALDI-TOF MS in lipidomics*. Frontiers in Bioscience, 2007. **12**(1): p. 2568.
49. Han, X. and R.W. Gross, *Electrospray ionization mass spectroscopic analysis of human erythrocyte plasma membrane phospholipids*. Proceedings of the National Academy of Sciences, 1994. **91**(22): p. 10635-10639.
50. Brugger, B., et al., *Quantitative analysis of biological membrane lipids at the low picomole level by nano-electrospray ionization tandem mass spectrometry*. Proceedings of the National Academy of Sciences, 1997. **94**(6): p. 2339-2344.
51. Hsu, F., *Mass spectrometry-based shotgun lipidomics – a critical review from the technical point of view*. Analytical and Bioanalytical Chemistry, 2018. **410**(25): p. 6387-6409.
52. Bhaskar, A.K., et al., *A high throughput lipidomics method using scheduled multiple reaction monitoring*. 2021, Cold Spring Harbor Laboratory.
53. Forest, A., et al., *Comprehensive and Reproducible Untargeted Lipidomic Workflow Using LC-QTOF Validated for Human Plasma Analysis*. Journal of Proteome Research, 2018. **17**(11): p. 3657-3670.
54. Ghaste, M., R. Mistrik, and V. Shulaev, *Applications of Fourier Transform Ion Cyclotron Resonance (FT-ICR) and Orbitrap Based High Resolution Mass Spectrometry in Metabolomics and Lipidomics*. International Journal of Molecular Sciences, 2016. **17**(6): p. 816.

55. Schuhmann, K., et al., *Bottom-Up Shotgun Lipidomics by Higher Energy Collisional Dissociation on LTQ Orbitrap Mass Spectrometers*. Analytical chemistry., 2011. **83**(14): p. 5480-5487.
56. Schuhmann, K., et al., *Shotgun lipidomics on a LTQ Orbitrap mass spectrometer by successive switching between acquisition polarity modes*. Journal of mass spectrometry., 2012. **47**(1): p. 96-104.
57. Sohlenkamp, C. and O. Geiger, *Bacterial membrane lipids: diversity in structures and pathways*. FEMS Microbiology Reviews, 2016. **40**(1): p. 133-159.
58. Epand, R.M. and R.F. Epand, *Lipid domains in bacterial membranes and the action of antimicrobial agents*. Biochimica et biophysica acta, 2009. **1788**(1): p. 289-294.
59. Pham, T.H., et al., *Targeting Modified Lipids during Routine Lipidomics Analysis using HILIC and C30 Reverse Phase Liquid Chromatography coupled to Mass Spectrometry*. Scientific Reports, 2019. **9**(1).
60. Yamaguchi, T., et al., *Effects of pH on Membrane Fluidity of Human Erythrocytes*. The journal of biochemistry, 1982. **91**(4): p. 1299-1304.
61. Gianotti, A., et al., *Effect of acidic conditions on fatty acid composition and membrane fluidity of Escherichia coli strains isolated from Crescenza cheese*. Annals of Microbiology, 2009. **59**(3): p. 603-610.
62. Angelova, M.I., et al., *pH sensing by lipids in membranes: The fundamentals of pH-driven migration, polarization and deformations of lipid bilayer assemblies*. Biochimica et Biophysica Acta (BBA) - Biomembranes, 2018. **1860**(10): p. 2042-2063.
63. McElhaney, R.N. and K.A. Souza, *The relationship between environmental temperature, cell growth and the fluidity and physical state of the membrane lipids in Bacillus stearothermophilus*. Biochimica et biophysica acta., 1976. **443**(3): p. 348-359.
64. Leach, M.D. and L.E. Cowen, *Membrane fluidity and temperature sensing are coupled via circuitry comprised of Ole1, Rsp5, and Hsf1 in Candida albicans*. Eukaryotic cell, 2014. **13**(8): p. 1077-1084.
65. Santhosh, P.B., et al., *Influence of nanoparticle–membrane electrostatic interactions on membrane fluidity and bending elasticity*. Chemistry and physics of lipids, 2014. **178**: p. 52-62.
66. Galassi, V.V. and N. Wilke, *On the Coupling between Mechanical Properties and Electrostatics in Biological Membranes*. Membranes, 2021. **11**(7): p. 478.
67. Lande, M.B., J.M. Donovan, and M.L. Zeidel, *The relationship between membrane fluidity and permeabilities to water, solutes, ammonia, and protons*. Journal of General Physiology, 1995. **106**(1): p. 67-84.
68. Khaware, R.K., A. Koul, and R. Prasad, *High membrane fluidity is related to NaCl stress in Candida membranefaciens*. Biochem Mol Biol Int, 1995. **35**(4): p. 875-80.
69. Chapman, D. and P.J. Quinn, *A method for the modulation of membrane fluidity: homogeneous catalytic hydrogenation of phospholipids and phospholipids and*

- phospholipid-water model biomembranes*. Proceedings of the National Academy of Sciences, 1976. **73**(11): p. 3971-3975.
70. Kurita, K., F. Kato, and D. Shiomi, *Alteration of Membrane Fluidity or Phospholipid Composition Perturbs Rotation of MreB Complexes in Escherichia coli*. Frontiers in molecular biosciences, 2020. **7**.
  71. Hac-Wydro, K. and P. Wydro, *The influence of fatty acids on model cholesterol/phospholipid membranes*. Chem Phys Lipids, 2007. **150**(1): p. 66-81.
  72. Mondal, D., et al., *Modulation of Membrane Fluidity Performed on Model Phospholipid Membrane and Live Cell Membrane: Revealing through Spatiotemporal Approaches of FLIM, FAIM, and TRFS*. Analytical chemistry, 2019. **91**(7): p. 4337-4345.
  73. Siliakus, M.F., J. Van Der Oost, and S.W.M. Kengen, *Adaptations of archaeal and bacterial membranes to variations in temperature, pH and pressure*. Extremophiles, 2017. **21**(4): p. 651-670.
  74. Fox, M.H. and T.M. Delohery, *Membrane fluidity measured by fluorescence polarization using an EPICS V cell sorter*. Cytometry, 1987. **8**(1): p. 20-25.
  75. Kaneko, T., et al., *Cellular membrane fluidity measurement by fluorescence polarization in indomethacin-induced gastric cellular injury in vitro*. Journal of gastroenterology, 2007. **42**(12): p. 939-946.
  76. Noutsi, P., E. Gratton, and S. Chaieb, *Assessment of Membrane Fluidity Fluctuations during Cellular Development Reveals Time and Cell Type Specificity*. PLOS ONE, 2016. **11**(6): p. e0158313.
  77. Ballweg, S., et al., *Regulation of lipid saturation without sensing membrane fluidity*. Nature Communications, 2020. **11**(1).
  78. Silhavy, T.J., D. Kahne, and S. Walker, *The Bacterial Cell Envelope*. Cold Spring Harbor Perspectives in Biology, 2010. **2**(5): p. a000414-a000414.
  79. Bramkamp, M. and D. Lopez, *Exploring the Existence of Lipid Rafts in Bacteria*. Microbiology and Molecular Biology Reviews, 2015. **79**(1): p. 81-100.
  80. Knittelfelder, O.L., et al., *A versatile ultra-high performance LC-MS method for lipid profiling*. Journal of chromatography, 2014. **951-952**: p. 119-128.
  81. Quehenberger, O., A.M. Armando, and E.A. Dennis, *High sensitivity quantitative lipidomics analysis of fatty acids in biological samples by gas chromatography–mass spectrometry*. Biochimica et Biophysica Acta (BBA) - Molecular and Cell Biology of Lipids, 2011. **1811**(11): p. 648-656.
  82. Pang, D., et al., *Destruction of the cell membrane and inhibition of cell phosphatidic acid biosynthesis in Staphylococcus aureus : an explanation for the antibacterial mechanism of morusin*. Food & function, 2019. **10**(10): p. 6438-6446.
  83. May, K.L. and M. Grabowicz, *The bacterial outer membrane is an evolving antibiotic barrier*. Proceedings of the National Academy of Sciences, 2018. **115**(36): p. 8852-8854.
  84. Malanovic, N. and K. Lohner, *Antimicrobial Peptides Targeting Gram-Positive Bacteria*. Pharmaceuticals, 2016. **9**(3): p. 59.

85. Nickels, J.D., et al., *The in vivo structure of biological membranes and evidence for lipid domains*. PLOS Biology, 2017. **15**(5): p. e2002214.
86. Kinnun, J.J., et al., *Biomembrane Structure and Material Properties Studied With Neutron Scattering*. Frontiers in chemistry, 2021. **9**.
87. Qian, S., V.K. Sharma, and L.A. Clifton, *Understanding the Structure and Dynamics of Complex Biomembrane Interactions by Neutron Scattering Techniques*. Langmuir, 2020. **36**(50): p. 15189-15211.
88. Poger, D. and A.E. Mark, *A Ring to Rule Them All: The Effect of Cyclopropane Fatty Acids on the Fluidity of Lipid Bilayers*. The journal of physical chemistry, 2015. **119**(17): p. 5487-5495.
89. Catalá, Á., *Lipid peroxidation modifies the assembly of biological membranes "The Lipid Whisker Model"*. Frontiers in physiology., 2015. **5**.
90. Roach, C., et al., *Comparison of Cis and Trans Fatty Acid Containing Phosphatidylcholines on Membrane Properties*. Biochemistry, 2004. **43**(20): p. 6344-6351.
91. Loffeld, B. and H. Keweloh, *cis/trans isomerization of unsaturated fatty acids as possible control mechanism of membrane fluidity in Pseudomonas putida P8*. Lipids., 1996. **31**(8): p. 811-815.
92. Slavetinsky, C., S. Kuhn, and A. Peschel, *Bacterial aminoacyl phospholipids – Biosynthesis and role in basic cellular processes and pathogenicity*. Biochimica et biophysica acta, 2017. **1862**(11): p. 1310-1318.
93. Roy, H., K. Dare, and M. Ibba, *Adaptation of the bacterial membrane to changing environments using aminoacylated phospholipids*. Molecular Microbiology, 2009. **71**(3): p. 547-550.
94. Kehelpannala, C., et al., *A comprehensive comparison of four methods for extracting lipids from Arabidopsis tissues*. Plant Methods, 2020. **16**(1).
95. Alvarez-Jarreta, J., et al., *LipidFinder 2.0: advanced informatics pipeline for lipidomics discovery applications*. 2020, Cold Spring Harbor Laboratory.
96. Herzog, R., et al., *LipidXplorer: A Software for Consensual Cross-Platform Lipidomics*. PLoS ONE, 2012. **7**(1): p. e29851.
97. Goracci, L., et al., *Lipostar, a Comprehensive Platform-Neutral Cheminformatics Tool for Lipidomics*. Analytical chemistry., 2017. **89**(11): p. 6257-6264.
98. Kyle, J.E., et al., *LIQUID: an-open source software for identifying lipids in LC-MS/MS-based lipidomics data*. Bioinformatics, 2017. **33**(11): p. 1744-1746.
99. Pluskal, T., et al., *MZmine 2: Modular framework for processing, visualizing, and analyzing mass spectrometry-based molecular profile data*. BMC Bioinformatics, 2010. **11**(1): p. 395.
100. Smith, C.A., et al., *XCMS: Processing Mass Spectrometry Data for Metabolite Profiling Using Nonlinear Peak Alignment, Matching, and Identification*. Analytical chemistry, 2006. **78**(3): p. 779-787.
101. Clasquin, M.F., E. Melamud, and J.D. Rabinowitz, *LC-MS Data Processing with MAVEN: A Metabolomic Analysis and Visualization Engine*. Current Protocols in Bioinformatics, 2012.

102. Percy, M.G. and A. Gründling, *Lipoteichoic Acid Synthesis and Function in Gram-Positive Bacteria*. Annual review of microbiology, 2014. **68**(1): p. 81-100.
103. O'Brien, J.P., et al., *193 nm Ultraviolet Photodissociation Mass Spectrometry for the Structural Elucidation of Lipid A Compounds in Complex Mixtures*. Analytical Chemistry, 2014. **86**(4): p. 2138-2145.
104. Li, L., et al., *Recent development on liquid chromatography-mass spectrometry analysis of oxidized lipids*. Free radical biology & medicine, 2019. **144**: p. 16-34.
105. Shortreed, M.R., et al., *Global Identification of Protein Post-translational Modifications in a Single-Pass Database Search*. Journal of Proteome Research, 2015. **14**(11): p. 4714-4720.
106. Mahieu, N.G. and G.J. Patti, *Systems-Level Annotation of a Metabolomics Data Set Reduces 25 000 Features to Fewer than 1000 Unique Metabolites*. Analytical Chemistry, 2017. **89**(19): p. 10397-10406.
107. Sellers, K.F. and J.C. Miecznikowski, *Feature Detection Techniques for Preprocessing Proteomic Data*. International Journal of Biomedical Imaging, 2010. **2010**: p. 1-9.
108. Lu, W., et al., *Improved Annotation of Untargeted Metabolomics Data through Buffer Modifications That Shift Adduct Mass and Intensity*. Analytical Chemistry, 2020. **92**(17): p. 11573-11581.
109. Chaleckis, R., et al., *Challenges, progress and promises of metabolite annotation for LC-MS-based metabolomics*. Current Opinion in Biotechnology, 2019. **55**: p. 44-50.
110. Schrimpe-Rutledge, A.C., et al., *Untargeted Metabolomics Strategies—Challenges and Emerging Directions*. Journal of the American Society for Mass Spectrometry, 2016. **27**(12): p. 1897-1905.
111. Reeves, G.A., D. Talavera, and J.M. Thornton, *Genome and proteome annotation: organization, interpretation and integration*. Journal of The Royal Society Interface, 2009. **6**(31): p. 129-147.
112. Folch, J., M. Lees, and G.H.S. Stanley, *A SIMPLE METHOD FOR THE ISOLATION AND PURIFICATION OF TOTAL LIPIDES FROM ANIMAL TISSUES*. Journal of Biological Chemistry, 1957. **226**(1): p. 497-509.
113. Bligh, E.G. and W.J. Dyer, *A RAPID METHOD OF TOTAL LIPID EXTRACTION AND PURIFICATION*. Canadian journal of biochemistry and physiology., 1959. **37**(8): p. 911-917.
114. Matyash, V., et al., *Lipid extraction by methyl-tert-butyl ether for high-throughput lipidomics*. Journal of Lipid Research, 2008. **49**(5): p. 1137-1146.
115. Wong, M.W.K., et al., *Comparison of Single Phase and Biphasic Extraction Protocols for Lipidomic Studies Using Human Plasma*. Frontiers in neurology, 2019. **10**.
116. Schaechter, M., *Escherichia coli and Salmonella 2000: the View From Here*. Microbiology and Molecular Biology Reviews, 2001. **65**(1): p. 119-130.
117. *Storage & Handling of Lipids*. Available from: <https://avantilipids.com/tech-support/storage-handling-of-lipids>.

118. Lam, S.M., H. Tian, and G. Shui, *Lipidomics, en route to accurate quantitation*. Biochimica et Biophysica Acta (BBA) - Molecular and Cell Biology of Lipids, 2017. **1862**(8): p. 752-761.
119. Li, P., et al., *Quantification of total lipids based on the characteristic absorption of tetra- $\beta$ -(2-octanyloxy)-substituted nickel phthalocyanine*. Analytical Methods, 2019. **11**(43): p. 5629-5637.
120. Elmer-Dixon, M.M. and B.E. Bowler, *Rapid quantification of vesicle concentration for DOPG/DOPC and Cardiolipin/DOPC mixed lipid systems of variable composition*. Analytical Biochemistry, 2018. **553**: p. 12-14.
121. Mantovani, D., et al., *Lipid Concentration Profile across the Wall of Pseudoatherosclerotic Synthetic Arterial Prostheses Using FTIR Microspectroscopy*. Analytical Chemistry, 1998. **70**(5): p. 1041-1044.
122. Derenne, A., O. Vandersleyen, and E. Goormaghtigh, *Lipid quantification method using FTIR spectroscopy applied on cancer cell extracts*. Biochimica et biophysica acta. Molecular and cell biology of lipids, 2014. **1841**(8): p. 1200-1209.
123. Shapaval, V., et al., *Biochemical profiling, prediction of total lipid content and fatty acid profile in oleaginous yeasts by FTIR spectroscopy*. Biotechnology for Biofuels, 2019. **12**(1).
124. Khoury, S., et al., *Quantification of Lipids: Model, Reality, and Compromise*. Biomolecules, 2018. **8**(4): p. 174.
125. Amiel, A., et al., *Proton NMR Enables the Absolute Quantification of Aqueous Metabolites and Lipid Classes in Unique Mouse Liver Samples*. Metabolites, 2019. **10**(1): p. 9.
126. Chen, J., K.B. Green, and K.K. Nichols, *Quantitative Profiling of Major Neutral Lipid Classes in Human Meibum by Direct Infusion Electrospray Ionization Mass Spectrometry*. Investigative Ophthalmology & Visual Science, 2013. **54**(8): p. 5730.
127. Patel, A., et al., *Lipids detection and quantification in oleaginous microorganisms: an overview of the current state of the art*. BMC Chemical Engineering, 2019. **1**(1).
128. Coskun, O., *Separation Techniques: CHROMATOGRAPHY*. Northern Clinics of Istanbul, 2016.
129. Hoes, I., et al., *Comparison between capillary and nano liquid chromatography–electrospray mass spectrometry for the analysis of minor DNA–melphalan adducts*. Journal of chromatography, 2000. **748**(1): p. 197-212.
130. Gama, M.R., C.H. Collins, and C.B.G. Bottoli, *Nano-Liquid Chromatography in Pharmaceutical and Biomedical Research*. Journal of Chromatographic Science, 2013. **51**(7): p. 694-703.
131. Fanali, C., et al., *Capillary-liquid chromatography (CLC) and nano-LC in food analysis*. TrAC Trends in Analytical Chemistry, 2013. **52**: p. 226-238.
132. Karlsson, K.E. and M. Novotny, *Separation efficiency of slurry-packed liquid chromatography microcolumns with very small inner diameters*. Analytical Chemistry, 1988. **60**(17): p. 1662-1665.



133. Szumski, M. and B. Buszewski, *State of the Art in Miniaturized Separation Techniques*. Critical Reviews in Analytical Chemistry, 2002. **32**(1): p. 1-46.
134. *ZIC-pHILIC HPLC Column General Instructions for Care and Use*, SeQuant, Editor. 2020.
135. Liigand, J., R. de Vries, and F. Cuyckens, *Optimization of flow splitting and make-up flow conditions in liquid chromatography/electrospray ionization mass spectrometry*. Rapid communications in mass spectrometry, 2019. **33**(3): p. 314-322.
136. Meiring, H.D., et al., *Nanoscale LC–MS(n): technical design and applications to peptide and protein analysis*. Journal of Separation Science, 2002. **25**(9): p. 12.
137. Li, Z., J. Tatlay, and L. Li, *Nanoflow LC–MS for High-Performance Chemical Isotope Labeling Quantitative Metabolomics*. Analytical Chemistry, 2015. **87**(22): p. 11468-11474.
138. Luo, X. and L. Li, *Metabolomics of Small Numbers of Cells: Metabolomic Profiling of 100, 1000, and 10000 Human Breast Cancer Cells*. Analytical Chemistry, 2017. **89**(21): p. 11664-11671.
139. Taylor, G., *Disintegration of water drops in an electric field*. Proceedings of the Royal Society of London. Series A. Mathematical and Physical Sciences, 1964. **280**(1382): p. 383-397.
140. Dole, M., et al., *Molecular Beams of Macroions*. The Journal of Chemical Physics, 1968. **49**(5): p. 2240-2249.
141. Fenn, J., et al., *Electrospray ionization for mass spectrometry of large biomolecules*. Science, 1989. **246**(4926): p. 64-71.
142. Ho, C.S., et al., *Electrospray ionisation mass spectrometry: principles and clinical applications*. The Clinical biochemist, 2003. **24**(1): p. 3-12.
143. Siuzdak, G., *An Introduction to Mass Spectrometry Ionization: An Excerpt from The Expanding Role of Mass Spectrometry in Biotechnology, 2nd ed.; MCC Press: San Diego, 2005*. JALA: Journal of the Association for Laboratory Automation, 2004. **9**(2): p. 50-63.
144. Meher, A.K. and Y. Chen, *Electrospray Modifications for Advancing Mass Spectrometric Analysis*. Mass Spectrometry, 2017. **6**(2): p. S0057-S0057.
145. Sanders, K.L. and J.L. Edwards, *Nano-liquid chromatography-mass spectrometry and recent applications in omics investigations*. Analytical Methods, 2020. **12**(36): p. 4404-4417.
146. Juraschek, R., T. Dülcks, and M. Karas, *Nanoelectrospray—More than just a minimized-flow electrospray ionization source*. Journal of the American Society for Mass Spectrometry, 1999. **10**(4): p. 300-308.
147. Schmidt, A., M. Karas, and T. Dülcks, *Effect of different solution flow rates on analyte ion signals in nano-ESI MS, or: when does ESI turn into nano-ESI?* Journal of the American Society for Mass Spectrometry, 2003. **14**(5): p. 492-500.
148. El-Faramawy, A., K.W.M. Siu, and B.A. Thomson, *Efficiency of nano-electrospray ionization*. Journal of the American Society for Mass Spectrometry, 2005. **16**(10): p. 1702-1707.

149. Karas, M., U. Bahr, and T. Dülcks, *Nano-electrospray ionization mass spectrometry: addressing analytical problems beyond routine*. Fresenius' journal of analytical chemistry, 2000. **366**(6-7): p. 669-676.
150. *Orbitrap Velos Pro Hardware Manual*, T.F. Scientific, Editor. 2011.
151. Kingdon, K.H., *A Method for the Neutralization of Electron Space Charge by Positive Ionization at Very Low Gas Pressures*. Physical Review, 1923. **21**(4): p. 408-418.
152. Perry, R.H., R.G. Cooks, and R.J. Noll, *Orbitrap mass spectrometry: Instrumentation, ion motion and applications*. Mass Spectrometry Reviews, 2008. **27**(6): p. 661-699.
153. Makarov, A., *Electrostatic Axially Harmonic Orbital Trapping: A High-Performance Technique of Mass Analysis*. Analytical Chemistry, 2000. **72**(6): p. 1156-1162.
154. Makarov, A., et al., *Performance Evaluation of a Hybrid Linear Ion Trap/Orbitrap Mass Spectrometer*. Analytical Chemistry, 2006. **78**(7): p. 2113-2120.
155. Drotleff, B. and M. Lämmerhofer, *Guidelines for Selection of Internal Standard-Based Normalization Strategies in Untargeted Lipidomic Profiling by LC-HR-MS/MS*. Analytical chemistry, 2019. **91**(15): p. 9836-9843.
156. Koelmel, J.P., et al., *Software tool for internal standard based normalization of lipids, and effect of data-processing strategies on resulting values*. BMC Bioinformatics, 2019. **20**(1).
157. Ladd, M.P., et al., *Untargeted Exometabolomics Provides a Powerful Approach to Investigate Biogeochemical Hotspots with Vegetation and Polygon Type in Arctic Tundra Soils*. Soil Systems, 2021. **5**(1): p. 10.
158. Fischler, M.A. and R.C. Bolles, *Random sample consensus*. Communications of the ACM, 1981. **24**(6): p. 381-395.
159. Korf, A., et al., *Digging deeper - A new data mining workflow for improved processing and interpretation of high resolution GC-Q-TOF MS data in archaeological research*. Scientific Reports, 2020. **10**(1).
160. Polpitiya, A.D., et al., *DAnTE: a statistical tool for quantitative analysis of -omics data*. Bioinformatics, 2008. **24**(13): p. 1556-1558.
161. Pang, Z., et al., *MetaboAnalyst 5.0: narrowing the gap between raw spectra and functional insights*. Nucleic Acids Research, 2021. **49**(W1): p. W388-W396.
162. Karki, S., et al., *Direct Analysis of Proteins from Solutions with High Salt Concentration Using Laser Electrospray Mass Spectrometry*. Journal of the American Society for Mass Spectrometry, 2018. **29**(5): p. 1002-1011.
163. Ohta, Y., et al., *Salt Tolerance Enhancement of Liquid Chromatography-Matrix-Assisted Laser Desorption/Ionization-Mass Spectrometry Using Matrix Additive Methylenediphosphonic Acid*. Mass Spectrometry, 2014. **3**(1): p. A0031-A0031.
164. Myers, J.N., P.V. Rekhadevi, and A. Ramesh, *Comparative Evaluation of Different Cell Lysis and Extraction Methods for Studying Benzo(a)pyrene Metabolism in HT-29 Colon Cancer Cell Cultures*. Cellular Physiology and Biochemistry, 2011. **28**(2): p. 209-218.

165. Patra, M., et al., *Under the Influence of Alcohol: The Effect of Ethanol and Methanol on Lipid Bilayers*. Biophysical Journal, 2006. **90**(4): p. 1121-1135.
166. Starke, R., et al., *Incomplete cell disruption of resistant microbes*. Scientific Reports, 2019. **9**(1).
167. Lee, I. and J. Han, *Simultaneous treatment (cell disruption and lipid extraction) of wet microalgae using hydrodynamic cavitation for enhancing the lipid yield*. Bioresource technology, 2015. **186**: p. 246-251.
168. Balasundaram, B. and A.B. Pandit, *Significance of location of enzymes on their release during microbial cell disruption*. Biotechnology and bioengineering, 2001. **75**(5): p. 607-614.
169. Shehadul Islam, M., A. Aryasomayajula, and P. Selvaganapathy, *A Review on Macroscale and Microscale Cell Lysis Methods*. Micromachines, 2017. **8**(3): p. 83.
170. Wang, J., et al., *Importance of mobile phase and injection solvent selection during rapid method development and sample analysis in drug discovery bioanalysis illustrated using convenient multiplexed LC-MS/MS*. Analytical methods, 2010. **2**(4): p. 375.
171. Bernat, P., et al., *Lipid composition in a strain of Bacillus subtilis, a producer of iturin A lipopeptides that are active against uropathogenic bacteria*. World Journal of Microbiology and Biotechnology, 2016. **32**(10).
172. Rühl, J., et al., *The glycerophospholipid inventory of Pseudomonas putida is conserved between strains and enables growth condition-related alterations*. Microbial Biotechnology, 2012. **5**(1): p. 45-58.
173. Cajka, T. and O. Fiehn, *Comprehensive analysis of lipids in biological systems by liquid chromatography-mass spectrometry*. Trends in Analytical Chemistry, 2014. **61**: p. 192-206.
174. Cajka, T. and O. Fiehn, *Increasing lipidomic coverage by selecting optimal mobile-phase modifiers in LC-MS of blood plasma*. Metabolomics, 2016. **12**(2).
175. Ulmer, C.Z., et al., *A Robust Lipidomics Workflow for Mammalian Cells, Plasma, and Tissue Using Liquid-Chromatography High-Resolution Tandem Mass Spectrometry*, in *Methods in Molecular Biology*. 2017, Springer New York. p. 91-106.
176. George, A.D., et al., *Untargeted lipidomics using liquid chromatography-ion mobility-mass spectrometry reveals novel triacylglycerides in human milk*. Scientific Reports, 2020. **10**(1).
177. Cai, X. and R. Li, *Concurrent profiling of polar metabolites and lipids in human plasma using HILIC-FTMS*. Scientific Reports, 2016. **6**(1): p. 36490.
178. Matich, E.K., et al., *Time-series lipidomic analysis of the oleaginous green microalga species Ettlia oleoabundans under nutrient stress*. Biotechnology for Biofuels, 2018. **11**(1).
179. Lange, M. and M. Fedorova, *Evaluation of lipid quantification accuracy using HILIC and RPLC MS on the example of NIST® SRM® 1950 metabolites in human plasma*. Analytical and Bioanalytical Chemistry, 2020. **412**(15): p. 3573-3584.

180. Rampler, E., et al., *Simultaneous non-polar and polar lipid analysis by on-line combination of HILIC, RP and high resolution MS*. The Analyst, 2018. **143**(5): p. 1250-1258.
181. Li, A., K.M. Hines, and L. Xu, *Lipidomics by HILIC-Ion Mobility-Mass Spectrometry*, in *Methods in Molecular Biology*. 2020, Springer US. p. 119-132.
182. Riley, N.M., et al., *The Negative Mode Proteome with Activated Ion Negative Electron Transfer Dissociation (AI-NETD)*. Molecular & cellular proteomics, 2015. **14**(10): p. 2644-2660.
183. Lei, Z., D.V. Huhman, and L.W. Sumner, *Mass Spectrometry Strategies in Metabolomics*. Journal of Biological Chemistry, 2011. **286**(29): p. 25435-25442.
184. Breitkopf, S.B., et al., *A relative quantitative positive/negative ion switching method for untargeted lipidomics via high resolution LC-MS/MS from any biological source*. Metabolomics, 2017. **13**(3).
185. Schwaiger, M., et al., *Merging metabolomics and lipidomics into one analytical run*. The Analyst, 2019. **144**(1): p. 220-229.
186. Bogdanov, M., et al., *Phospholipid distribution in the cytoplasmic membrane of Gram-negative bacteria is highly asymmetric, dynamic, and cell shape-dependent*. Science advances, 2020. **6**(23): p. eaaz6333-eaaz6333.
187. Hsu, F. and J. Turk, *Studies on phosphatidylglycerol with triple quadrupole tandem mass spectrometry with electrospray ionization: Fragmentation processes and structural characterization*. Journal of the American Society for Mass Spectrometry, 2001. **12**(9): p. 1036-1043.
188. Pi, J., X. Wu, and Y. Feng, *Fragmentation patterns of five types of phospholipids by ultra-high-performance liquid chromatography electrospray ionization quadrupole time-of-flight tandem mass spectrometry*. Analytical methods, 2016. **8**(6): p. 1319-1332.
189. Chagovets, V.V., et al., *Endometriosis foci differentiation by rapid lipid profiling using tissue spray ionization and high resolution mass spectrometry*. Scientific Reports, 2017. **7**(1).
190. Hsu, F., et al., *Structural characterization of cardiolipin by tandem quadrupole and multiple-stage quadrupole ion-trap mass spectrometry with electrospray ionization*. Journal of the American Society for Mass Spectrometry, 2005. **16**(4): p. 491-504.
191. Ong, S., et al., *Stable Isotope Labeling by Amino Acids in Cell Culture, SILAC, as a Simple and Accurate Approach to Expression Proteomics*. Molecular & Cellular Proteomics, 2002. **1**(5): p. 376-386.
192. Rune, M., S. Pan, and R. Aebersold, *Quantitative Proteomics by Stable Isotope Labeling and Mass Spectrometry*. Mass Spectrometry Data Analysis in Proteomics: p. 209-218.
193. Klein, S. and E. Heinzle, *Isotope labeling experiments in metabolomics and fluxomics*. Wiley Interdisciplinary Reviews: Systems Biology and Medicine, 2012. **4**(3): p. 261-272.
194. Triebl, A. and M. Wenk, *Analytical Considerations of Stable Isotope Labelling in Lipidomics*. Biomolecules, 2018. **8**(4): p. 151.

195. Chokkathukalam, A., et al., *Stable isotope-labeling studies in metabolomics: new insights into structure and dynamics of metabolic networks*. Bioanalysis, 2014. **6**(4): p. 511-524.
196. Kim, J., et al., *Deuterium Oxide Labeling for Global Omics Relative Quantification: Application to Lipidomics*. Analytical chemistry, 2019. **91**(14): p. 8853-8863.
197. Kostyukevich, Y., et al., *Hydrogen/Deuterium Exchange Aiding Compound Identification for LC-MS and MALDI Imaging Lipidomics*. Analytical chemistry (Washington), 2019. **91**(21): p. 13465-13474.
198. Neubauer, C., et al., *Towards measuring growth rates of pathogens during infections by D 2 O-labeling lipidomics*. Rapid Communications in Mass Spectrometry, 2018. **32**(24): p. 2129-2140.
199. Lattova, E. and H. Perreault, *Labelling saccharides with phenylhydrazine for electrospray and matrix-assisted laser desorption–ionization mass spectrometry*. Journal of chromatography, 2003. **793**(1): p. 167-179.
200. Han, J., et al., *An isotope-labeled chemical derivatization method for the quantitation of short-chain fatty acids in human feces by liquid chromatography–tandem mass spectrometry*. Analytica chimica acta, 2015. **854**: p. 86-94.
201. Peng, B., et al., *LipidCreator workbench to probe the lipidomic landscape*. Nature Communications, 2020. **11**(1).
202. Mohamed, A., J. Molendijk, and M.M. Hill, *lipidr: A Software Tool for Data Mining and Analysis of Lipidomics Datasets*. Journal of proteome research, 2020. **19**(7): p. 2890-2897.
203. Kind, T., et al., *LipidBlast in silico tandem mass spectrometry database for lipid identification*. Nature Methods, 2013. **10**(8): p. 755-758.
204. Errington, J. and L.T.V.D. Aart, *Microbe Profile: Bacillus subtilis: model organism for cellular development, and industrial workhorse*. Microbiology, 2020. **166**(5): p. 425-427.
205. Lee, S., et al., *Bacterial Valorization of Lignin: Strains, Enzymes, Conversion Pathways, Biosensors, and Perspectives*. Frontiers in bioengineering and biotechnology, 2019. **7**.
206. Sun, Z., et al., *Bright Side of Lignin Depolymerization: Toward New Platform Chemicals*. Chemical Reviews, 2018. **118**(2): p. 614-678.
207. Dyrda, G., et al., *The effect of organic solvents on selected microorganisms and model liposome membrane*. Molecular Biology Reports, 2019. **46**(3): p. 3225-3232.
208. Huffer, S., et al., *Role of Alcohols in Growth, Lipid Composition, and Membrane Fluidity of Yeasts, Bacteria, and Archaea*. Applied and Environmental Microbiology, 2011. **77**(18): p. 6400-6408.
209. Han, X., *Lipidomics for studying metabolism*. Nature reviews, 2016. **12**(11): p. 668-679.
210. Yang, K. and X. Han, *Lipidomics: Techniques, Applications, and Outcomes Related to Biomedical Sciences*. Trends in Biochemical Sciences, 2016. **41**(11): p. 954-969.

211. Saito, Y., *Lipid peroxidation products as a mediator of toxicity and adaptive response – The regulatory role of selenoprotein and vitamin E*. Archives of biochemistry and biophysics, 2021. **703**: p. 108840.
212. Zhang, L., X. Han, and X. Wang, *Is the clinical lipidomics a potential goldmine?* Cell Biology and Toxicology, 2018. **34**(6): p. 421-423.
213. Appala, K., et al., *Recent applications of mass spectrometry in bacterial lipidomics*. Analytical and Bioanalytical Chemistry, 2020. **412**(24): p. 5935-5943.
214. Singh, A. and M. Del Poeta, *Sphingolipidomics: An Important Mechanistic Tool for Studying Fungal Pathogens*. Frontiers in microbiology, 2016. **7**.
215. Afzal, F., et al., *Technological Platforms to Study Plant Lipidomics*. 2016, Springer International Publishing: Cham. p. 477-492.
216. Shulaev, V. and K.D. Chapman, *Plant lipidomics at the crossroads: From technology to biology driven science*. Biochimica et biophysica acta, 2017. **1862**(8): p. 786-791.
217. den Kamp, J.A., I. Redai, and L.L. van Deenen, *Phospholipid Composition of Bacillus subtilis*. Journal of Bacteriology, 1969. **99**(1): p. 298-303.
218. Gidden, J., et al., *Lipid compositions in Escherichia coli and Bacillus subtilis during growth as determined by MALDI-TOF and TOF/TOF mass spectrometry*. International Journal of Mass Spectrometry, 2009. **283**(1-3): p. 178-184.
219. Rigomier, D., J.P. Bohin, and B. Lubochinsky, *Effects of Ethanol and Methanol on Lipid Metabolism in Bacillus subtilis*. Microbiology, 1980. **121**(1): p. 139-149.
220. Tsvetanova, F., P. Petrova, and K. Petrov. *MICROBIAL PRODUCTION OF 1-BUTANOL RECENT ADVANCES AND FUTURE PROSPECTS ( Review )*. 2018.
221. Birgen, C., et al., *Butanol production from lignocellulosic biomass: revisiting fermentation performance indicators with exploratory data analysis*. Biotechnology for Biofuels, 2019. **12**(1).
222. Zheng, Y.-N., et al., *Problems with the microbial production of butanol*. Journal of Industrial Microbiology & Biotechnology, 2009. **36**(9): p. 1127-1138.
223. Nawab, S., et al., *Genetic engineering of non-native hosts for 1-butanol production and its challenges: a review*. Microbial cell factories, 2020. **19**(1): p. 79-79.
224. Visioli, L.J., et al., *Recent advances on biobutanol production*. Sustainable Chemical Processes, 2014. **2**(1): p. 15.
225. Chen, C.-T. and J.C. Liao, *Frontiers in microbial 1-butanol and isobutanol production*. FEMS Microbiology Letters, 2016. **363**(5): p. fnw020.
226. Smith, M.D., et al., *Cosolvent pretreatment in cellulosic biofuel production: effect of tetrahydrofuran-water on lignin structure and dynamics*. Green Chemistry, 2016. **18**(5): p. 1268-1277.
227. Cai, C.M., et al., *THF co-solvent enhances hydrocarbon fuel precursor yields from lignocellulosic biomass*. Green chemistry, 2013. **15**(11): p. 3140-3145.
228. Yao, Y., et al., *Assessment of toxicity of tetrahydrofuran on the microbial community in activated sludge*. Bioresource technology, 2010. **101**(14): p. 5213-5221.

229. Yao, Y., et al., *The effect of tetrahydrofuran on the enzymatic activity and microbial community in activated sludge from a sequencing batch reactor*. Ecotoxicology, 2012. **21**(1): p. 56-65.
230. Korf, A., et al., *Lipid Species Annotation at Double Bond Position Level with Custom Databases by Extension of the MZmine 2 Open-Source Software Package*. Analytical chemistry, 2019. **91**(8): p. 5098-5105.
231. Nickels, J.D., et al., *Impact of Fatty-Acid Labeling of Bacillus subtilis Membranes on the Cellular Lipidome and Proteome*. Frontiers in microbiology, 2020. **11**: p. 914-914.
232. Clejan, S., et al., *Membrane lipid composition of obligately and facultatively alkalophilic strains of Bacillus spp.* Journal of Bacteriology, 1986. **168**(1): p. 334-340.
233. Bartlett, G.R., *Phosphorus Assay in Column Chromatography*. Journal of Biological Chemistry, 1959. **234**(3): p. 466-468.
234. Kawai, F., et al., *Cardiolipin Domains in Bacillus subtilis Marburg Membranes*. Journal of Bacteriology, 2004. **186**(5): p. 1475-1483.
235. Matsuoka, H., K. Hirooka, and Y. Fujita, *Organization and Function of the YsiA Regulon of Bacillus subtilis Involved in Fatty Acid Degradation*. Journal of Biological Chemistry, 2007. **282**(8): p. 5180-5194.
236. Burkholder, P.R. and N.H. Giles, *INDUCED BIOCHEMICAL MUTATIONS IN BACILLUS SUBTILIS*. American journal of botany, 1947. **34**(6): p. 345-348.
237. Zhang, Z., et al., *Parallel isotope differential modeling for instationary <sup>13</sup>C fluxomics at the genome scale*. Biotechnol Biofuels, 2020. **13**: p. 103.
238. Zhu, Y., et al., *Polymyxins Bind to the Cell Surface of Unculturable Acinetobacter baumannii and Cause Unique Dependent Resistance*. Adv Sci (Weinh), 2020. **7**(15): p. 2000704.
239. Zullig, T., M. Trotzmuller, and H.C. Kofeler, *Lipidomics from sample preparation to data analysis: a primer*. Anal Bioanal Chem, 2020. **412**(10): p. 2191-2209.
240. Schujman, G.E., et al., *Response of Bacillus subtilis to Cerulenin and Acquisition of Resistance*. Journal of Bacteriology, 2001. **183**(10): p. 3032-3040.
241. Bajerski, F., D. Wagner, and K. Mangelsdorf, *Cell Membrane Fatty Acid Composition of Chryseobacterium frigidisoli PB4T, Isolated from Antarctic Glacier Forefield Soils, in Response to Changing Temperature and pH Conditions*. Frontiers in microbiology, 2017. **8**.
242. Paulucci, N.S., et al., *Growth Temperature and Salinity Impact Fatty Acid Composition and Degree of Unsaturation in Peanut-Nodulating Rhizobia*. Lipids, 2011. **46**(5): p. 435-441.
243. Fozo, E.M. and R.G. Quivey, *The fabM Gene Product of Streptococcus mutans Is Responsible for the Synthesis of Monounsaturated Fatty Acids and Is Necessary for Survival at Low pH*. Journal of Bacteriology, 2004. **186**(13): p. 4152-4158.
244. Guo, Q., L. Liu, and B.J. Barkla, *Membrane Lipid Remodeling in Response to Salinity*. International Journal of Molecular Sciences, 2019. **20**(17): p. 4264.

245. Muthusamy, S., et al., *Comparative proteomics reveals signature metabolisms of exponentially growing and stationary phase marine bacteria*. Environ Microbiol, 2017. **19**(6): p. 2301-2319.
246. Furusawa, C., T. Horinouchi, and T. Maeda, *Toward prediction and control of antibiotic-resistance evolution*. Current opinion in biotechnology, 2018. **54**: p. 45-49.
247. Nomanbhay, S. and M. Ong, *A Review of Microwave-Assisted Reactions for Biodiesel Production*. Bioengineering, 2017. **4**(2): p. 57.
248. Li, W., et al., *Fractionation and characterization of lignin streams from unique high-lignin content endocarp feedstocks*. Biotechnology for Biofuels, 2018. **11**(1).
249. Pingali, S.V., et al., *Deconstruction of biomass enabled by local demixing of cosolvents at cellulose and lignin surfaces*. Proceedings of the National Academy of Sciences, 2020. **117**(29): p. 16776-16781.
250. Figueirêdo, M.B., et al., *A Two-Step Approach for the Conversion of Technical Lignins to Biofuels*. Advanced Sustainable Systems, 2020. **4**(10): p. 1900147.
251. Ingram, L.O., *Ethanol Tolerance in Bacteria*. Critical reviews in biotechnology, 1989. **9**(4): p. 305-319.
252. Bohin, J.P. and B. Lubochinsky, *Alcohol-resistant sporulation mutants of Bacillus subtilis*. Journal of Bacteriology, 1982. **150**(2): p. 944-955.
253. Wilbanks, B. and C.T. Trinh, *Comprehensive characterization of toxicity of fermentative metabolites on microbial growth*. Biotechnology for Biofuels, 2017. **10**(1).
254. Jeucken, A., et al., *Control of n-Butanol Induced Lipidome Adaptations in E. coli*. Metabolites, 2021. **11**(5): p. 286.
255. Kanno, M., et al., *Isolation of Butanol- and Isobutanol-Tolerant Bacteria and Physiological Characterization of Their Butanol Tolerance*. Applied and Environmental Microbiology, 2013. **79**(22): p. 6998-7005.
256. Guo, J., et al., *Bacterial lipopolysaccharide core structures mediate effects of butanol ingress*. Biochimica et biophysica acta. Biomembranes, 2020. **1862**(2): p. 183150.
257. Barry, J.A. and K. Gawrisch, *Direct NMR Evidence for Ethanol Binding to the Lipid-Water Interface of Phospholipid Bilayers*. Biochemistry, 1994. **33**(26): p. 8082-8088.
258. Ly, H.V. and M.L. Longo, *The Influence of Short-Chain Alcohols on Interfacial Tension, Mechanical Properties, Area/Molecule, and Permeability of Fluid Lipid Bilayers*. Biophysical journal, 2004. **87**(2): p. 1013-1033.
259. Vaňousová, K., et al., *Membrane fluidization by alcohols inhibits DesK-DesR signalling in Bacillus subtilis*. Biochimica et biophysica acta, 2018. **1860**(3): p. 718-727.
260. Espinosa, G., et al., *Shear rheology of lipid monolayers and insights on membrane fluidity*. Proceedings of the National Academy of Sciences, 2011. **108**(15): p. 6008-6013.
261. Unsay, J.D., et al., *Cardiolipin Effects on Membrane Structure and Dynamics*. Langmuir, 2013. **29**(51): p. 15878-15887.



262. Cartwright, C.P., et al., *Ethanol Dissipates the Proton-motive Force across the Plasma Membrane of Saccharomyces cerevisiae*. Microbiology, 1986. **132**(2): p. 369-377.
263. Peschel, A., et al., *Staphylococcus aureus Resistance to Human Defensins and Evasion of Neutrophil Killing via the Novel Virulence Factor MprF Is Based on Modification of Membrane Lipids with l-Lysine*. Journal of Experimental Medicine, 2001. **193**(9): p. 1067-1076.
264. Klein, S., et al., *Adaptation of Pseudomonas aeruginosa to various conditions includes tRNA-dependent formation of alanyl-phosphatidylglycerol*. Molecular Microbiology, 2009. **71**(3): p. 551-565.
265. Vinuesa, P., et al., *Genetic Analysis of a pH-Regulated Operon from Rhizobium tropici CIAT899 Involved in Acid Tolerance and Nodulation Competitiveness*. Molecular Plant-Microbe Interactions®, 2003. **16**(2): p. 159-168.
266. Ernst, C.M., et al., *The Bacterial Defensin Resistance Protein MprF Consists of Separable Domains for Lipid Lysinylation and Antimicrobial Peptide Repulsion*. PLoS Pathogens, 2009. **5**(11): p. e1000660.
267. Custer, J.E., et al., *The Relative Proportions of Different Lipid Classes and their Fatty Acid Compositions Change with Culture Age in the Cariogenic Dental Pathogen Streptococcus mutans UA159*. Lipids, 2014. **49**(6): p. 543-554.
268. Griffiths, K.K. and P. Setlow, *Effects of modification of membrane lipid composition on Bacillus subtilis sporulation and spore properties*. Journal of Applied Microbiology, 2009. **106**(6): p. 2064-2078.
269. Atila, M. and Y. Luo, *Profiling and tandem mass spectrometry analysis of aminoacylated phospholipids in Bacillus subtilis*. F1000Research, 2016. **5**: p. 121.
270. Atila, M., et al., *Characterization of N-Succinylation of L-Lysylphosphatidylglycerol in Bacillus subtilis Using Tandem Mass Spectrometry*. Journal of the American Society for Mass Spectrometry, 2016. **27**(10): p. 1606-1613.
271. Zhang, Z., et al., *Identification of lysine succinylation as a new post-translational modification*. Nature Chemical Biology, 2011. **7**(1): p. 58-63.
272. Rashid, R., et al., *Comprehensive analysis of phospholipids and glycolipids in the opportunistic pathogen Enterococcus faecalis*. PLOS ONE, 2017. **12**(4): p. e0175886.
273. Young, S.A., et al., *Characterisation of Staphylococcus aureus lipids by nanoelectrospray ionisation tandem mass spectrometry (nESI-MS/MS)*. 2019, Cold Spring Harbor Laboratory.
274. Song, D., H. Jiao, and Z. Liu, *Phospholipid translocation captured in a bifunctional membrane protein MprF*. Nature Communications, 2021. **12**(1).
275. Smith, A.M., et al., *A Conserved Hydrolase Responsible for the Cleavage of Aminoacylphosphatidylglycerol in the Membrane of Enterococcus faecium*. Journal of Biological Chemistry, 2013. **288**(31): p. 22768-22776.
276. Sohlenkamp, C., et al., *The Lipid Lysyl-Phosphatidylglycerol Is Present in Membranes of Rhizobium tropici CIAT899 and Confers Increased Resistance to*

- Polymyxin B Under Acidic Growth Conditions*. Molecular Plant-Microbe Interactions®, 2007. **20**(11): p. 1421-1430.
277. Kilelee, E., et al., *Lysyl-Phosphatidylglycerol Attenuates Membrane Perturbation Rather than Surface Association of the Cationic Antimicrobial Peptide 6W-RP-1 in a Model Membrane System: Implications for Daptomycin Resistance*. Antimicrobial Agents and Chemotherapy, 2010. **54**(10): p. 4476-4479.
  278. Haest, C.W.M., et al., *Changes in permeability of Staphylococcus aureus and derived liposomes with varying lipid composition*. Biochimica et biophysica acta, 1972. **255**(3): p. 720-733.
  279. Matias, V.R.R.F. and T.J. Beveridge, *Lipoteichoic Acid Is a Major Component of the Bacillus subtilis Periplasm*. Journal of Bacteriology, 2008. **190**(22): p. 7414-7418.
  280. Swoboda, J.G., et al., *Wall Teichoic Acid Function, Biosynthesis, and Inhibition*. ChemBioChem, 2009. **11**(1): p. 35-45.
  281. Armstrong, J.J., et al., *Teichoic Acids from Bacterial Walls: Composition of Teichoic Acids from a Number of Bacterial Walls*. Nature, 1959. **184**(4682): p. 247-248.
  282. Brown, S., J.P. Santa Maria, and S. Walker, *Wall Teichoic Acids of Gram-Positive Bacteria*. Annual Review of Microbiology, 2013. **67**(1): p. 313-336.
  283. Ginsburg, I., *Role of lipoteichoic acid in infection and inflammation*. The Lancet infectious diseases, 2002. **2**(3): p. 171-179.
  284. Deininger, S., et al., *Presentation of lipoteichoic acid potentiates its inflammatory activity*. Immunobiology, 2008. **213**(6): p. 519-529.
  285. Claes, I.J., et al., *Lipoteichoic acid is an important microbe-associated molecular pattern of Lactobacillus rhamnosus GG*. Microbial Cell Factories, 2012. **11**(1): p. 161.
  286. Mizuno, H., et al., *Lipoteichoic Acid Is Involved in the Ability of the Immunobiotic Strain Lactobacillus plantarum CRL1506 to Modulate the Intestinal Antiviral Innate Immunity Triggered by TLR3 Activation*. Frontiers in immunology, 2020. **11**.
  287. Reichmann, N.T. and A. Gründling, *Location, synthesis and function of glycolipids and polyglycerolphosphate lipoteichoic acid in Gram-positive bacteria of the phylum Firmicutes*. FEMS Microbiology Letters, 2011. **319**(2): p. 97-105.
  288. Neuhaus, F.C. and J. Baddiley, *A Continuum of Anionic Charge: Structures and Functions of d-Alanyl-Teichoic Acids in Gram-Positive Bacteria*. Microbiology and Molecular Biology Reviews, 2003. **67**(4): p. 686-723.
  289. Fischer, W., H.U. Koch, and R. Haas, *Improved Preparation of Lipoteichoic Acids*. European Journal of Biochemistry, 1983. **133**(3): p. 523-530.
  290. Morath, S., A. Geyer, and T. Hartung, *Structure–Function Relationship of Cytokine Induction by Lipoteichoic Acid from Staphylococcus aureus*. Journal of Experimental Medicine, 2001. **193**(3): p. 393-398.

291. Villéger, R., et al., *Characterization of lipoteichoic acid structures from three probiotic Bacillus strains: involvement of d-alanine in their biological activity*. Antonie van Leeuwenhoek, 2014. **106**(4): p. 693-706.
292. Luo, Y., *Alanylated lipoteichoic acid primer in Bacillus subtilis*. F1000Research, 2016. **5**: p. 155.
293. Coley, J., M. Duckworth, and J. Baddiley, *Extraction and purification of lipoteichoic acids from gram-positive bacteria*. Carbohydrate research, 1975. **40**(1): p. 41-52.
294. Nelson, K.E., et al., *Complete genome sequence and comparative analysis of the metabolically versatile Pseudomonas putida KT2440*. Environmental microbiology, 2002. **4**(12): p. 799-808.
295. Belda, E., et al., *The revisited genome of Pseudomonas putida KT2440 enlightens its value as a robust metabolic chassis*. Environmental Microbiology, 2016. **18**(10): p. 3403-3424.
296. Puchalka, J., et al., *Genome-Scale Reconstruction and Analysis of the Pseudomonas putida KT2440 Metabolic Network Facilitates Applications in Biotechnology*. PLoS Computational Biology, 2008. **4**(10): p. e1000210.
297. Nogales, J., et al., *High-quality genome-scale metabolic modelling of Pseudomonas putida highlights its broad metabolic capabilities*. Environmental Microbiology, 2020. **22**(1): p. 255-269.
298. Poblete-Castro, I., et al., *Industrial biotechnology of Pseudomonas putida and related species*. Applied Microbiology and Biotechnology, 2012. **93**(6): p. 2279-2290.
299. Raghavan, P.U.M. and M. Vivekanandan, *Bioremediation of oil-spilled sites through seeding of naturally adapted Pseudomonas putida*. International biodeterioration & biodegradation, 1999. **44**(1): p. 29-32.
300. Sunar, N.M., et al., *The Effectiveness of Pseudomonas putida Atcc 49128 as Biodegradable Agent in Biodiesel Soil Contamination*. 2014, Springer Singapore. p. 817-823.
301. Maia, M., A. Capão, and L. Procópio, *Biosurfactant produced by oil-degrading Pseudomonas putida AM-b1 strain with potential for microbial enhanced oil recovery*. Bioremediation journal, 2019. **23**(4): p. 302-310.
302. Mardani, G., et al., *Application of Genetically Engineered Dioxygenase Producing Pseudomonas putida on Decomposition of Oil from Spiked Soil*. Jundishapur journal of natural pharmaceutical products, 2017. **In Press**(In Press).
303. Wang, X., J. Atencia, and R.M. Ford, *Quantitative analysis of chemotaxis towards toluene by Pseudomonas putida in a convection-free microfluidic device*. Biotechnology and bioengineering, 2015. **112**(5): p. 896-904.
304. Izmalkova, T.Y., et al., *The organization of naphthalene degradation genes in Pseudomonas putida strain AK5*. Research in microbiology, 2013. **164**(3): p. 244-253.
305. Samuel, M.S., A. Sivaramakrishna, and A. Mehta, *Bioremediation of p-Nitrophenol by Pseudomonas putida 1274 strain*. Journal of Environmental Health Science and Engineering, 2014. **12**(1): p. 53.

306. Samin, G., et al., *A Pseudomonas putida Strain Genetically Engineered for 1,2,3-Trichloropropane Bioremediation*. Applied and Environmental Microbiology, 2014. **80**(17): p. 5467-5476.
307. Gong, T., et al., *Metabolic Engineering of Pseudomonas putida KT2440 for Complete Mineralization of Methyl Parathion and  $\gamma$ -Hexachlorocyclohexane*. ACS synthetic biology, 2016. **5**(5): p. 434-442.
308. John, R. and A.P. Rajan, *Pseudomonas putida APRRJVITS11 as a potent tool in chromium (VI) removal from effluent wastewater*. Preparative biochemistry & biotechnology, 2021: p. 1-8.
309. Cabral, L., et al., *Methylmercury degradation by Pseudomonas putida VI*. Ecotoxicol Environ Saf, 2016. **130**: p. 37-42.
310. Khraisheh, M., M.A. Al-Ghouti, and F. AlMomani, *P. putida as biosorbent for the remediation of cobalt and phenol from industrial waste wastewaters*. Environmental technology & innovation, 2020. **20**: p. 101148.
311. Khashei, S., Z. Etemadifar, and H.R. Rahmani, *Immobilization of Pseudomonas putida PT in resistant matrices to environmental stresses: a strategy for continuous removal of heavy metals under extreme conditions*. Annals of Microbiology, 2018. **68**(12): p. 931-942.
312. Nakazawa, T., *Travels of a Pseudomonas, from Japan around the world*. Environmental microbiology, 2002. **4**(12): p. 782-786.
313. Zhou, Z., et al., *Enhancing Bioremediation Potential of Pseudomonas putida by Developing Its Acid Stress Tolerance With Glutamate Decarboxylase Dependent System and Global Regulator of Extreme Radiation Resistance*. Frontiers in microbiology, 2019. **10**.
314. Xu, Y., et al., *Nitrogen Removal Characteristics of Pseudomonas putida Y-9 Capable of Heterotrophic Nitrification and Aerobic Denitrification at Low Temperature*. BioMed Research International, 2017. **2017**: p. 1-7.
315. Salvachúa, D., et al., *Outer membrane vesicles catabolize lignin-derived aromatic compounds in Pseudomonas putida KT2440*. Proceedings of the National Academy of Sciences, 2020. **117**(17): p. 9302-9310.
316. Weisburger, E.K., *Carcinogenicity studies on halogenated hydrocarbons*. Environmental health perspectives, 1977. **21**: p. 7-16.
317. Włodarczyk-Makuła, M. and E. Wiśniowska, *Halogenated Organic Compounds in Water and in Wastewater*. Civil and Environmental Engineering Reports, 2019. **29**(4): p. 236-247.
318. Burleson, G.R., M.J. Caulfield, and M. Pollard, *Ozonation of mutagenic and carcinogenic polyaromatic amines and polyaromatic hydrocarbons in water*. Cancer research (Chicago, Ill.), 1979. **39**(6 Pt 1): p. 2149.
319. Villegas, L.G.C., et al., *A Short Review of Techniques for Phenol Removal from Wastewater*. Current Pollution Reports, 2016. **2**(3): p. 157-167.
320. Ayanda, O.S., et al., *Phenols, flame retardants and phthalates in water and wastewater – a global problem*. Water Science and Technology, 2016. **74**(5): p. 1025-1038.

321. Anku, W.W., M.A. Mamo, and P.P. Govender, *Phenolic Compounds in Water: Sources, Reactivity, Toxicity and Treatment Methods*. 2017, InTech.
322. Chang, S.E., et al., *Consequences of oil spills: a review and framework for informing planning*. Ecology and Society, 2014. **19**(2).
323. Barron, M.G., et al., *Long-Term Ecological Impacts from Oil Spills: Comparison of Exxon Valdez , Hebei Spirit , and Deepwater Horizon*. Environmental science & technology, 2020. **54**(11): p. 6456-6467.
324. Shin, D., Y. Kim, and H.S. Moon, *Fate and toxicity of spilled chemicals in groundwater and soil environment I: strong acids*. Environmental Health and Toxicology, 2018. **33**(4): p. e2018019.
325. Thomasson, E.D., et al., *Acute Health Effects After the Elk River Chemical Spill, West Virginia, January 2014*. Public Health Reports, 2017. **132**(2): p. 196-202.
326. Nogales, J., B.Ø. Palsson, and I. Thiele, *A genome-scale metabolic reconstruction of Pseudomonas putida KT2440: iJN746 as a cell factory*. BMC Systems Biology, 2008. **2**(1): p. 79.
327. Nikel, P.I. and V. De Lorenzo, *Robustness of Pseudomonas putida KT2440 as a host for ethanol biosynthesis*. New Biotechnology, 2014. **31**(6): p. 562-571.
328. Franden, M.A., et al., *Engineering Pseudomonas putida KT2440 for efficient ethylene glycol utilization*. Metabolic engineering, 2018. **48**: p. 197-207.
329. Martínez-García, E., et al., *Pseudomonas 2.0: genetic upgrading of P. putida KT2440 as an enhanced host for heterologous gene expression*. Microbial Cell Factories, 2014. **13**(1).
330. Martínez-García, E., et al., *The metabolic cost of flagellar motion in Pseudomonas putida KT2440*. Environmental Microbiology, 2014. **16**(1): p. 291-303.
331. Martínez-García, E., et al., *Freeing Pseudomonas putida KT2440 of its proviral load strengthens endurance to environmental stresses*. Environmental Microbiology, 2015. **17**(1): p. 76-90.
332. Jekel, M. and W. Wackernagel, *The periplasmic endonuclease I of escherichia coli has amino-acid sequence homology to the extracellular DNases of Vibrio cholerae and Aeromonas hydrophila*. Gene, 1995. **154**(1): p. 55-59.
333. Smith, E. and A. Badawy, *Bacteria survival experiment for assessment of wastewater reuse in agriculture*. Water science and technology, 2010. **61**(9): p. 2251-2258.
334. Calero, P. and P.I. Nikel, *Chasing bacterial chassis for metabolic engineering: a perspective review from classical to non-traditional microorganisms*. Microbial Biotechnology, 2019. **12**(1): p. 98-124.
335. Borchert, A.J., W.R. Henson, and G.T. Beckham, *Challenges and opportunities in biological funneling of heterogeneous and toxic substrates beyond lignin*. Current opinion in biotechnology, 2022. **73**: p. 1-13.
336. Tan, Z., et al., *Engineering Escherichia coli membrane phospholipid head distribution improves tolerance and production of biorenewables*. Metabolic engineering, 2017. **44**: p. 1-12.

337. Bale, N.J., et al., *Lipidomics of Environmental Microbial Communities. I: Visualization of Component Distributions Using Untargeted Analysis of High-Resolution Mass Spectrometry Data*. Frontiers in microbiology, 2021. **12**.
338. Mahfouz, S., et al., *Dioxin impacts on lipid metabolism of soil microbes: towards effective detection and bioassessment strategies*. Bioresources and Bioprocessing, 2020. **7**(1).
339. Jung, J.W., H.S. Lee, and K.-J. Kim, *Purification of Acetic Acid Wastewater using Layer Melt Crystallization*. Separation science and technology, 2008. **43**(5): p. 1021-1033.
340. Vaiopoulou, E., P. Melidis, and A. Aivasidis, *Process control, energy recovery and cost savings in acetic acid wastewater treatment*. Journal of hazardous materials, 2011. **186**(2-3): p. 1141-1146.
341. Ubukata, Y., *The Role of Particulate Organic Matter and Acetic Acid in the Removal of Phosphate in Anaerobic/Aerobic Activated Sludge Processes*. Engineering in life sciences, 2007. **7**(1): p. 61-66.
342. Huang, L., et al., *Modeling of acetate-type fermentation of sugar-containing wastewater under acidic pH conditions*. Bioresource technology, 2018. **248**: p. 148-155.
343. Yu, L., et al., *Recovery of acetic acid from dilute wastewater by means of bipolar membrane electrodialysis*. Desalination., 2000. **129**(3): p. 283-288.
344. Andrews, J., et al., *Acetic acid recovery from a hybrid biological–hydrothermal treatment process of sewage sludge – a pilot plant study*. Water science and technology, 2015. **71**(5): p. 734-739.
345. Liu, X., et al., *Treatment of m -Cresol Wastewater in an Anaerobic Fluidized Bed Microbial Fuel Cell Equipped with Different Modified Carbon Cloth Cathodes*. Energy & fuels, 2020. **34**(8): p. 10059-10066.
346. Iliuta, I. and M.C. Iliuta, *Intensified phenol and p-cresol biodegradation for wastewater treatment in countercurrent packed-bed column bioreactors*. Chemosphere, 2022. **286**: p. 131716.
347. Fang, H.H.P. and G.-M. Zhou, *Degradation of phenol and p-cresol in reactors*. Water Science and Technology, 2000. **42**(5-6): p. 237-244.
348. Zheng, D., et al., *Multistage A-O Activated Sludge Process for Paraformaldehyde Wastewater Treatment and Microbial Community Structure Analysis*. Journal of chemistry, 2016. **2016**: p. 1-7.
349. Lotfy, H.R. and I.G. Rashed, *A method for treating wastewater containing formaldehyde*. Water research, 2002. **36**(3): p. 633-637.
350. Moussavi, G., A. Yazdanbakhsh, and M. Heidarizad, *The removal of formaldehyde from concentrated synthetic wastewater using O<sub>3</sub>/MgO/H<sub>2</sub>O<sub>2</sub> process integrated with the biological treatment*. Journal of hazardous materials, 2009. **171**(1-3): p. 907-913.
351. Di Blasi, C., A. Galgano, and C. Branca, *Influences of the Chemical State of Alkaline Compounds and the Nature of Alkali Metal on Wood Pyrolysis*. Industrial & engineering chemistry research, 2009. **48**(7): p. 3359-3369.

352. Alvarez, J., et al., *Sewage sludge valorization by flash pyrolysis in a conical spouted bed reactor*. Chemical engineering journal, 2015. **273**: p. 173-183.
353. Di Palma, L., et al., *Biological Treatment of Wastewater from Pyrolysis Plant: Effect of Organics Concentration, pH and Temperature*. Water, 2019. **11**(2): p. 336.
354. Voss, R.H., *Neutral organic compounds in biologically treated bleached kraft mill effluents*. Environmental science & technology, 1984. **18**(12): p. 938-946.
355. Kovacs, T.G., et al., *Kraft mill effluent survey: Progress toward best management practices for reducing effects on fish reproduction*. Environmental toxicology and chemistry, 2011. **30**(6): p. 1421-1429.
356. Kıpçak, E. and M. Akgün, *Oxidative gasification of olive mill wastewater as a biomass source in supercritical water: Effects on gasification yield and biofuel composition*. The Journal of supercritical fluids, 2012. **69**: p. 57-63.
357. Gao, K., O.A. Sahraei, and M.C. Iliuta, *Development of residue coal fly ash supported nickel catalyst for H<sub>2</sub> production via glycerol steam reforming*. Applied catalysis, 2021. **291**: p. 119958.
358. Shamsuri, A.A. and D.K. Abdullah, *A Preliminary Study of Oxidation of Lignin from Rubber Wood to Vanillin in Ionic Liquid Medium*. arXiv: Chemical Physics, 2013.
359. Fache, M., B. Boutevin, and S. Caillol, *Vanillin Production from Lignin and Its Use as a Renewable Chemical*. ACS sustainable chemistry & engineering, 2016. **4**(1): p. 35-46.
360. Zirbes, M., et al., *High-Temperature Electrolysis of Kraft Lignin for Selective Vanillin Formation*. ACS sustainable chemistry & engineering, 2020. **8**(19): p. 7300-7307.
361. Sadler, J.C. and S. Wallace, *Microbial synthesis of vanillin from waste poly(ethylene terephthalate)*. Green Chemistry, 2021. **23**(13): p. 4665-4672.
362. Vítová, M., et al., *The biosynthesis of phospholipids is linked to the cell cycle in a model eukaryote*. Biochimica et Biophysica Acta (BBA) - Molecular and Cell Biology of Lipids, 2021. **1866**(8): p. 158965.
363. Pinkart, H.C. and D.C. White, *Phospholipid biosynthesis and solvent tolerance in Pseudomonas putida strains*. Journal of Bacteriology, 1997. **179**(13): p. 4219-4226.
364. Wang, Y., et al., *Structure Characterization of Phospholipids and Lipid a of Pseudomonas Putida KT2442*. European journal of mass spectrometry, 2015. **21**(5): p. 739-746.
365. Hancock, I.C. and P.M. Meadow, *The extractable lipids of Pseudomonas aeruginosa*. Biochimica et biophysica acta, 1969. **187**(3): p. 366-379.
366. Tashiro, Y., et al., *Characterization of Phospholipids in Membrane Vesicles Derived from Pseudomonas aeruginosa*. Bioscience, Biotechnology, and Biochemistry, 2011. **75**(3): p. 605-607.
367. Han, M.-L., et al., *Alterations of Metabolic and Lipid Profiles in Polymyxin-Resistant Pseudomonas aeruginosa*. Antimicrobial Agents and Chemotherapy, 2018. **62**(6): p. AAC.02656-17.

368. Deschamps, E., et al., *Membrane phospholipid composition of Pseudomonas aeruginosa grown in a cystic fibrosis mucus-mimicking medium*. Biochimica et biophysica acta., 2021. **1863**(1): p. 183482.
369. Santos, A.L. and G. Preta, *Lipids in the cell: organisation regulates function*. Cell Mol Life Sci, 2018. **75**(11): p. 1909-1927.
370. Serricchio, M., et al., *Flagellar membranes are rich in raft-forming phospholipids*. Biology Open, 2015. **4**(9): p. 1143-1153.
371. Nishino, T., et al., *Flagellar Formation Depends on Membrane Acidic Phospholipids in Escherichia coli*. Bioscience, biotechnology, and biochemistry, 1993. **57**(10): p. 1805-1808.
372. Chu, J.K., et al., *Loss of a Cardiolipin Synthase in Helicobacter pylori G27 Blocks Flagellum Assembly*. Journal of Bacteriology, 2019. **201**(21).
373. Wang, H. and J.E. Cronan, *Functional Replacement of the FabA and FabB Proteins of Escherichia coli Fatty Acid Synthesis by Enterococcus faecalis FabZ and FabF Homologues*. Journal of Biological Chemistry, 2004. **279**(33): p. 34489-34495.
374. Heath, R.J., et al., *The Enoyl-[acyl-carrier-protein] Reductases FabI and FabL from Bacillus subtilis*. Journal of Biological Chemistry, 2000. **275**(51): p. 40128-40133.
375. Massengo-Tiassé, R.P. and J.E. Cronan, *Vibrio cholerae FabV Defines a New Class of Enoyl-Acyl Carrier Protein Reductase*. Journal of Biological Chemistry, 2008. **283**(3): p. 1308-1316.
376. Passmore, I.J., et al., *Para-cresol production by Clostridium difficile affects microbial diversity and membrane integrity of Gram-negative bacteria*. PLOS Pathogens, 2018. **14**(9): p. e1007191.
377. Dyrda, G., et al., *The effect of organic solvents on selected microorganisms and model liposome membrane*. Mol Biol Rep, 2019. **46**(3): p. 3225-3232.
378. Keweloh, H., R. Diefenbach, and H.J. Rehm, *Increase of phenol tolerance of Escherichia coli by alterations of the fatty acid composition of the membrane lipids*. Archives of microbiology, 1991. **157**(1): p. 49-53.
379. Heipieper, H.J., H. Keweloh, and H.J. Rehm, *Influence of phenols on growth and membrane permeability of free and immobilized Escherichia coli*. Applied and Environmental Microbiology, 1991. **57**(4): p. 1213-1217.
380. Park, Y., R. Ledesma-Amaro, and J. Nicaud, *De novo Biosynthesis of Odd-Chain Fatty Acids in Yarrowia lipolytica Enabled by Modular Pathway Engineering*. Frontiers in bioengineering and biotechnology, 2020. **7**.
381. Beld, J., et al., *Probing fatty acid metabolism in bacteria, cyanobacteria, green microalgae and diatoms with natural and unnatural fatty acids*. Molecular bioSystems, 2016. **12**(4): p. 1299-1312.
382. Poudel, S., et al., *Integrated omics analyses reveal the details of metabolic adaptation of Clostridium thermocellum to lignocellulose-derived growth inhibitors released during the deconstruction of switchgrass*. Biotechnology for Biofuels, 2017. **10**(1).



383. Cronan, J., *Phospholipid modifications in bacteria*. Current opinion in microbiology, 2002. **5**(2): p. 202-205.
384. Kaneda, T., *Iso- and anteiso-fatty acids in bacteria: biosynthesis, function, and taxonomic significance*. Microbiological Reviews, 1991. **55**(2): p. 288-302.
385. Chang, Y. and J.E. Cronan, *Membrane cyclopropane fatty acid content is a major factor in acid resistance of Escherichia coli*. Molecular Microbiology, 1999. **33**(2): p. 249-259.
386. Kim, K. and D. Oh, *Production of hydroxy fatty acids by microbial fatty acid-hydroxylation enzymes*. Biotechnology advances, 2013. **31**(8): p. 1473-1485.
387. Caligiani, A., et al., *Development of a Quantitative GC–MS Method for the Detection of Cyclopropane Fatty Acids in Cheese as New Molecular Markers for Parmigiano Reggiano Authentication*. Journal of agricultural and food chemistry, 2016. **64**(20): p. 4158-4164.
388. Okada, S., et al., *Producing Cyclopropane Fatty Acid in Plant Leafy Biomass via Expression of Bacterial and Plant Cyclopropane Fatty Acid Synthases*. Frontiers in plant science, 2020. **11**.
389. Lolli, V., et al., *Determination of Cyclopropane Fatty Acids in Food of Animal Origin by <sup>1</sup>H NMR*. Journal of Analytical Methods in Chemistry, 2018. **2018**: p. 1-8.
390. Blevins, M.S., D.R. Klein, and J.S. Brodbelt, *Localization of Cyclopropane Modifications in Bacterial Lipids via 213 nm Ultraviolet Photodissociation Mass Spectrometry*. Analytical Chemistry, 2019.
391. Muñoz-Rojas, J.S., et al., *Involvement of Cyclopropane Fatty Acids in the Response of Pseudomonas putida KT2440 to Freeze-Drying*. Applied and Environmental Microbiology, 2006. **72**(1): p. 472-477.
392. Pini, C., et al., *Regulation of the cyclopropane synthase cfaB gene in Pseudomonas putida KT2440*. FEMS microbiology letters., 2011. **321**(2): p. 107-114.
393. Pini, C., et al., *Cyclopropane fatty acids are involved in organic solvent tolerance but not in acid stress resistance in Pseudomonas putida DOT-T1E*. Microbial Biotechnology, 2009. **2**(2): p. 253-261.
394. Romantsov, T., Z. Guan, and J.M. Wood, *Cardiolipin and the osmotic stress responses of bacteria*. Biochimica et biophysica acta, 2009. **1788**(10): p. 2092-2100.
395. Zheng, L., et al., *Biogenesis, transport and remodeling of lysophospholipids in Gram-negative bacteria*. Biochimica et Biophysica Acta (BBA) - Molecular and Cell Biology of Lipids, 2017. **1862**(11): p. 1404-1413.
396. Lin, Y., et al., *Substrate Selectivity of Lysophospholipid Transporter LplT Involved in Membrane Phospholipid Remodeling in Escherichia coli*. Journal of Biological Chemistry, 2016. **291**(5): p. 2136-2149.
397. Wargenau, A., et al., *Evaluating the Cell Membrane Penetration Potential of Lipid-Soluble Compounds Using Supported Phospholipid Bilayers*. Analytical Chemistry, 2018. **90**(19): p. 11174-11178.

398. Pattrick, C.A., et al., *Proteomic Profiling, Transcription Factor Modeling, and Genomics of Evolved Tolerant Strains Elucidate Mechanisms of Vanillin Toxicity in Escherichia coli*. mSystems, 2019. **4**(4).
399. Ailte, I., et al., *Addition of lysophospholipids with large head groups to cells inhibits Shiga toxin binding*. Scientific Reports, 2016. **6**(1): p. 30336.
400. Zhukovsky, M.A., et al., *Phosphatidic acid in membrane rearrangements*. FEBS Letters, 2019. **593**(17): p. 2428-2451.
401. Sreekumari, A. and R. Lipowsky, *Lipids with bulky head groups generate large membrane curvatures by small compositional asymmetries*. The Journal of Chemical Physics, 2018. **149**(8): p. 084901.
402. Kamal, M.M., et al., *Measurement of the membrane curvature preference of phospholipids reveals only weak coupling between lipid shape and leaflet curvature*. Proceedings of the National Academy of Sciences, 2009. **106**(52): p. 22245-22250.
403. Chen, N.H., et al., *Formaldehyde Stress Responses in Bacterial Pathogens*. Frontiers in microbiology, 2016. **7**.
404. Henson, W.R., et al., *Biological upgrading of pyrolysis-derived wastewater: Engineering Pseudomonas putida for alkylphenol, furfural, and acetone catabolism and (methyl)muconic acid production*. Metabolic engineering, 2021. **68**: p. 14-25.
405. Bartoli, J., et al., *The Long Hunt for pssR —Looking for a Phospholipid Synthesis Transcriptional Regulator, Finding the Ribosome*. Journal of Bacteriology, 2017. **199**(14): p. JB.00202-17.
406. Mutalik, V.K., et al., *Dual-barcoded shotgun expression library sequencing for high-throughput characterization of functional traits in bacteria*. Nature Communications, 2019. **10**(1).
407. Tan, B.K., et al., *Discovery of a cardiolipin synthase utilizing phosphatidylethanolamine and phosphatidylglycerol as substrates*. Proceedings of the National Academy of Sciences, 2012. **109**(41): p. 16504-16509.
408. Douglass, M.V., F. Cl  on, and M.S. Trent, *Cardiolipin aids in lipopolysaccharide transport to the gram-negative outer membrane*. Proceedings of the National Academy of Sciences of the United States of America, 2021. **118**(15): p. e2018329118.
409. Dodge, G.J., et al., *Structural and dynamical rationale for fatty acid unsaturation in Escherichia coli*. Proceedings of the National Academy of Sciences, 2019. **116**(14): p. 6775-6783.
410. Hayashi, S., et al., *Control Mechanism for Carbon-Chain Length in Polyunsaturated Fatty-Acid Synthases*. Angewandte Chemie : international edition, 2019. **58**(20): p. 6605-6610.
411. Kondakova, T., S. Kumar, and J.E. Cronan, *A novel synthesis of trans-unsaturated fatty acids by the Gram-positive commensal bacterium Enterococcus faecalis FA2-2*. Chemistry and physics of lipids, 2019. **222**: p. 23-35.
412. Neumann, G., N. Kabelitz, and H.J. Heipieper, *The regulation of the cis-trans isomerase of unsaturated fatty acids in Pseudomonas putida: correlation between*

- cti* activity and  $K^+$ -uptake systems. European Journal of Lipid Science and Technology, 2003. **105**(10): p. 585-589.
413. Taylor, F.R. and J.E. Cronan, *Cyclopropane fatty acid synthase of Escherichia coli. Stabilization, purification, and interaction with phospholipid vesicles.* Biochemistry, 1979. **18**(15): p. 3292-3300.
414. Wolrab, D., et al., *Oncolipidomics: Mass spectrometric quantitation of lipids in cancer research.* TrAC Trends in Analytical Chemistry, 2019. **120**.

## VITA

David Thomas Reeves was born and raised in Knoxville, Tennessee, where he graduated from Knoxville Catholic High School. He obtained a Bachelor of Science degree, double majoring in Chemistry and Japanese, from the University of Notre Dame in South Bend, Indiana in 2013. He then obtained a Masters of Arts in Japanese Language, Literature, and Culture from the University of Massachusetts, Amherst in Amherst, Massachusetts in 2015, publishing a thesis on the translation and interpretation of the works of Aoki Rosui, an author of ghost tales written in classical Japanese. In 2015, he applied for and was accepted for a competitive fellowship with the Bredesen Center for Interdisciplinary Research and Graduate Education as a graduate research fellow, and in the following year, he joined Dr. Robert Hettich's biological mass spectrometry group at Oak Ridge National Laboratory, studying the metabolite and lipid profiles of environmentally and industrially relevant bacterial species by liquid chromatography-mass spectrometry. He is graduating with a Doctor of Philosophy in Energy Science and Engineering in December 2021.